Pilvax- a novel peptide antigen delivery strategy for the generation of vaccines

Dasun Dinidu Wagachchi

A thesis submitted in fulfilment of the requirements for the degree of

Doctor of Philosophy

Department of Molecular Medicine and Pathology

Faculty of Medical and Health Sciences

The University of Auckland

2016

Abstract

There has been a shift in vaccine development from being based on killed or attenuated whole microorganisms to smaller, more specific subunit vaccines, including peptides. However, peptides by themselves are often poorly immunogenic, necessitating the need for an adjuvant or a specialised delivery system. A novel peptide delivery strategy, Pilvax, was developed in this thesis by expressing peptides within the serotype M1 group A streptococcus (GAS) pilus structure on the surface of *Lactococcus lactis*.

In GAS, each fully assembled pilus structure consists of approximately 50-100 Spy0128 pilin subunits that are covalently linked by isopeptide bond formation. Genetically engineering a peptide into the Spy0128 subunit will result in the expression of hundreds of repeated copies of the peptide on a single pilus and thousands of copies across the surface of the bacterium. The complete GAS pilus structure can be expressed and assembled on the surface of *L. lactis*, a non-pathogenic bacterium which has generally recognised as safe (GRAS) status. *L. lactis* is a promising antigen delivery vehicle, having been used to deliver numerous vaccine candidate antigens to both mucosal and systemic sites.

Six loop regions and the N-terminus of the Spy0128 pilin were selected as possible sites where a peptide could be engineered into. However, peptides could only be engineered into two of the loop regions without affecting the polymerisation of the pilus on the surface of *L. lactis*. To show proof of principle, a peptide consisting of ovalbumin from positions 323 to 339 ($OVA_{323-339}$) was engineered between the β_E and β_F loop of Spy0128 and the peptide-linked pilus was expressed on the surface of *L. lactis*. Incorporation of $OVA_{323-339}$ into the pilus structure was demonstrated by Western blot analyses of cell wall proteins and by flow cytometry. Intranasal immunisation of mice with *L. lactis* expressing pilus-linked $OVA_{323-339}$ results in production of both a systemic and mucosal antibody response against ovalbumin.

The feasibility of using Pilvax to deliver a structural epitope was then investigated. The J14 peptide, a chimeric peptide derived from the carboxy-terminal C-repeat region of the GAS M protein, was chosen to be engineered into Pilvax. The peptide contains a conformationally restricted B cell epitope fused to coil-promoting moieties from the yeast GCN4 protein to maintain the original coiled-coil structure. The J14 peptide engineered between the β_E and β_F loop of Spy0128 showed incorporation of J14 into pili, expressed on the surface of *L. lactis,* as demonstrated by Western blot analyses of cell wall proteins. However, intranasal immunisation of mice with *L. lactis* expressing pilus-linked J14 only induced a weak J14-specific antibody response and the antibodies elicited could not recognise and bind the native M protein. This suggests that the alpha-helical conformation of J14, required for the peptide to be an effective vaccine candidate, is disrupted when it is engineered into a loop region of Spy0128.

Thus, Pilvax may provide an alternative strategy to allow safe and effective delivery of vaccine peptides to mucosal sites, but may be limited to conformation-independent peptides.

Acknowledgements

I would like to thank my supervisor Associate Professor Thomas Proft for giving me the opportunity to work on this project and also for his guidance throughout my PhD. A special thank you to my co supervisor Dr. Jacelyn Loh for being the best mentor one could hope for. You were always willing to help me no matter how busy you were and I really appreciate it.

A very special thank you to my fellow lab members Nazneen Adenwalla and Catherine Tsai for being there for me, especially during the first 11 months of my PhD when all my cloning experiments failed and I had absolutely no results. Your encouragement and support really helped me persevere with my project and for that you have my deepest gratitude.

To the rest of the Proft lab, a big thank you for all your assistance and guidance. I would like to thank Mrs. Adrina Khemlani for teaching me the basics of cloning and for proof reading my thesis. I would also like to thank Dr. John Steemson for his advice on protein purification and for cheering me up with his singing in the lab. To the past and present members: Sam Blanchett, Lisa Zheng, Stefan Erdelt, Martin Bach, Angela Chan, Ann Chang, and the honorary member Jay Choi, thank you for making the lab a very welcoming and lively place to be in.

I would like to thank Dr Fiona Radcliff and Ms Fiona Clow for their advice and for letting me borrow reagents whenever I needed them. I would also like to thank Mr. Stephen Edgar for helping me with any questions I had about flow cytometry.

Lastly, Mum and Dad, thank you with all of my heart for always being there for me. I know you have sacrificed a lot for my education and I hope I can convey through this thesis the appreciation I have for all that you have done for me.

Table of Contents

Chapter 2

Materials and Methods

List of Figures

List of Tables

Abbreviations

SI prefixes

µ	micro (10^{-6})
m	milli (10^{-3})

SI units

s	second
min	minute
M	molar
g	gram
L	litre

Other units and abbreviations

^{o}C	Degrees Celcius
AP1	Ancillary protein 1
AP2	Ancillary protein 2
APC	Antigen-presenting cells
APS	Ammonium persulphate
BALF	Bronchoalveolar lavage fluid
BCG	Bacillus Calmette-Guerin
BCR	B cell receptor
BHI	Brain Heart Infusion Broth
BP	Backbone protein
bp	Base pairs
CFA	Complete Freund's adjuvant
CFU	Colony forming unit

CIP	Calf intestinal alkaline phosphatase
CMIS	Common mucosal immune system
CRR	Conserved C-repeat region
CTL	Cytotoxic T lymphocyte
CV	Column volume
DTaP	Diphtheria, tetanus, and acellular pertussis
DTwP	Diphtheria, tetanus, and whole-cell pertussis
ELISA	Enzyme-linked immunosorbent assay
FCT	Fibronectin- and collagen-binding protein and T-antigen
FFluc	Firefly luciferase
FIM 2/3	Fimbriae 2/3
FHA	Filamentous haemagglutinin
fw	Forward
GAS	Group A streptococcus
GBS	Group B streptococcus
GRAS	Generally Recognized As Safe
GI	Gastro-intestinal
GSH	Glutathione
GST	Glutathione-S-transferase
HBsAg	Hepatitis B surface antigen
HBV	Hepatitis B virus
HCV	Hepatitis C virus
HIV	Human immunodeficiency virus
HPV	Human papilloma virus
IFA	Incomplete Freund's adjuvant
i.n.	Intranasally

ISCOM	Immunostimulating complex
LAB	lactic acid bacterium
LB	Luria-Bertani broth
LPS	Lipopolysaccharide
MALT	Mucosa-associated lymphoid tissue
MHC	Major histocompatibility complex
MDP	Muramyl dipeptide
MMR	Measles, mumps, and rubella
NALT	Nasopharynx-associated lymphoid tissue
NICE	Nisin-controlled expression system
OPV	Oral polio vaccine
OVA	Ovalbumin
PAMP	Pathogen-associated molecular pattern
PBS	Phosphate-buffered Saline
PCR	Polymerase chain reaction
PLGA	Poly (lactic/glycolic) acid
PRN	Pertactin
PRR	Pathogen recognition receptor
PspA	Pneumococcal surface protein A antigen
PT	Pertussis toxin
RPMI	Roswell Park Memorial Institute media
RT	Room temperature
rw	Reverse
SDS	Sodium dodecyl sulfate
SDS-PAGE	Sodium dodecyl sulfate-polyacrylamide gel electrophoresis
subQ	Subcutaneous

TB	Tuberculosis
TCA	Trichloroacetic acid
Th	Helper T cell
TMB	3’,5,5’-Tetramethylbenzidine
TNF	Tumor necrosis factor
TLR	Toll-like receptor
TSST-1	Toxic shock syndrome toxin 1
TTFC	Tetanus fragment C
UV	Ultraviolet
VAPP	Vaccine-associated paralytic poliomyelitis
VLP	Virus-like particle
v/v	Volume per volume
w/v	Weight per volume

Chapter 1

Introduction

1.1 Overview

Vaccination has been one of the most successful health initiatives, having a major effect on mortality and population growth throughout the world (Ehreth, 2003). The term “vaccine” is derived from the Latin word *vacca*, which means “cows”. Its origin lies in the discovery by Dr. Edward Jenner that deliberate inoculation with cowpox virus could protect individuals against smallpox disease. Following on from Dr. Jenner’s discovery, the exponential growth in vaccine research and development has led to the eradication or control of a number of major diseases (Plotkin, 2005).

Vaccines function by using whole or part of a pathogen to induce an immune response that will provide protection against subsequent disease. Vaccines can generally be classified into three broad groups: live attenuated vaccines, subunit vaccines, and genetic vaccines. Vaccine development has progressed from being based on attenuated or killed microorganisms, towards carefully designed subunit vaccines, including peptide immunogens. However, a limitation of using peptides to design vaccines is that they are often poorly immunogenic, requiring administration with an adjuvant or specialised delivery system (Moingeon, et al., 2002).

This thesis concerns the development of a novel peptide delivery system for the generation of vaccines, by using the pilus of group A streptococcus (GAS), expressed on the surface of *Lactococcus lactis*, as a carrier of peptide antigens.

1.2 Vaccines

The ideal characteristics of a vaccine would include the ability to elicit a long-lived protective immune response, without the need for multiple doses, and to have a high safety profile in all population groups. The vaccine should also ideally be cost effective, producible in large scale, and be free from strict storage requirements (Levine & Sztein, 2004). Many different vaccine strategies have been invented, each with a number of advantages and disadvantages as shown in table 1.1.

Table 1.1 A comparison of different vaccine strategies

Vaccine type	Diseases	Advantages	Disadvantages
Live, attenuated vaccines	Measles, mumps, rubella, polio, yellow fever	Strong and usually long-lived immune responses with 1 or 2 doses	Possible reversion back to virulence, needs cold storage
Inactivated or killed vaccines	Cholera, influenza, hepatitis A, plague, polio, rabies	Safer than live vaccines, more easily stored	Weaker immune response, often requiring multiple doses
Subunit vaccines	Hepatitis B, pertussis, pneumonia	Fewer adverse reactions as only specific parts of the pathogen are used	Generally require strong adjuvants, lower immune response, mainly B cell responses
Conjugate vaccines	Haemophilus influenza type B	Enhances the immune responses to weakly immunogenic antigens	Usually requires booster shots every few years to remain effective
DNA vaccines	HIV, malaria, influenza, hepatitis B	Relatively stable, cheap, can elicit both T and B cell responses	Possible incorporation into host genome

1.2.1 Live attenuated vaccines and inactivated vaccines

Live attenuated vaccines consist of pathogens that have been weakened in some way, either through in vitro passaging or by genetically knocking out key pathogenic genes (Plotkin, 2014). Two of the most successful vaccines that have been created are the live attenuated vaccines for small pox and yellow fever. The most widely used vaccine for smallpox has been the vaccinia

virus and the use of the vaccine led to the global eradication of small pox (Bhattacharya, 2008). The yellow fever vaccine consists of the live attenuated strain 17D, derived from the wild-type strain Asibi. The original 17D strain was developed following 176 passages of the wild-type strain in mouse and chicken tissue and has been administered to more than 400 million people (Wilson, et al., 2004).

Another attenuated vaccine, licensed for use against a bacterial pathogen, is the Bacillus Calmette-Guerin (BCG) vaccine against *Mycobacterium tuberculosis*, the causative agent of tuberculosis (TB). The vaccine was developed by culturing *Mycobacterium bovis* on bile-containing medium and has been one of the most commonly used vaccines. It was estimated that over 100 million BCG vaccinations were given to infants in 2002 and the vaccine had consistently high efficacy against childhood tuberculosis. The vaccine, costing US$2–3 per dose at the time, was also a highly cost-effective intervention (Calmette, 1931; Trunz, et al., 2006).

A number of live attenuated vaccines are also currently recommended as part of the U.S. Childhood Immunisation Schedule, such as the vaccine against measles, mumps, and rubella (via the combined MMR vaccine), varicella (chickenpox), and influenza (in the nasal spray version of the seasonal flu vaccine) (Byington, et al., 2015).

One of the main reasons for the success of live attenuated vaccines is the ability to elicit strong and usually long-lived immune responses. Taking the small pox vaccine as an example, after a single dose of the vaccine, the antiviral antibody responses remained stable between 1−75 years after vaccination and the antiviral T cell responses only declined slowly, with a half-life of 8−15 years (Hammarlund, et al., 2003).

However, a limitation of using live attenuated strains as vaccines is the possibility of reversion of the strain back to virulence. Such reversion may occur as a result of back-mutation of the attenuating mutations, compensatory mutations elsewhere in the genome, or recombination between viral genomes. One vaccine with a propensity to revert back to virulence is the oral

polio vaccine (OPV). Following vaccination, the incidence of paralytic poliomyelitis from OPV is approximately one case per 500,000 first doses of OPV administered and approximately one case per 12 million subsequent doses administered (Nkowane, et al., 1987).

Poliovirus isolates from immunocompetent Vaccine-associated paralytic poliomyelitis (VAPP) cases showed that key substitutions causing the attenuated phenotype had often reverted, leading to virulence (Georgescu, et al., 1997). Reversion to virulence may have also been caused by recombination, since many isolates from VAPP cases were detected with both intertypic vaccine/vaccine and vaccine/non-vaccine recombinants (Furione, et al., 1993).

One method to overcome the problem of reversion of live vaccines back to virulence is to use inactivated or killed whole-cell vaccines. Inactivated pathogens can no longer replicate or revert back to their pathogenic form. The use of the inactivated polio vaccine, for example, has resulted in the discontinuation of vaccination with OPV in the USA (Sutter, et al., 2000).

However, there are still certain pathogens for which a whole cell vaccine would be difficult to create. These include pathogens that mutate rapidly (such as HIV), those that exist as multiple serotypes (such as dengue virus), and those that cause persistent or latent infection (such as HIV and hepatitis C virus).

1.2.2 Subunit vaccines

Subunit vaccines are similar to inactivated vaccines in that they do not contain live components of the pathogen. However, the difference is that subunit vaccines only contain the microbial components necessary to elicit a protective immune response. They often contain whole proteins or carbohydrates, but can also be reduced down to the smaller peptide level. Subunit vaccines can also be made from detoxified toxins. Subunit vaccines usually function by eliciting humoral immune responses, but when administered with certain adjuvants can produce cytotoxic T lymphocyte (CTL) responses (Ellis, 1999).

The first protein-based subunit vaccines relied on a natural source of antigen. The hepatitis B vaccine, for example, consisted of the hepatitis B surface antigen (HBsAg) which was originally purified from the plasma of human carriers of hepatitis B virus (HBV) (Szmuness, et al., 1980). However, advances in recombinant DNA technology have meant that this plasma-derived vaccine has now largely been replaced by the production of recombinant HBsAg by *Saccharomyces cerevisiae* (Valenzuela, et al., 1982).

Using subunit vaccines reduces the chance of adverse reactogenic, allergenic, or autoimmune responses as the vaccines only require the minimal microbial components needed to elicit an effective immune response. Furthermore, the use of recombinant DNA technology means that the pathogen itself is not used as the source. Therefore, the current focus of vaccine development has shifted from whole cell vaccines to subunit vaccines. An excellent example of the shift towards subunit vaccines can be demonstrated by the vaccine against diphtheria, tetanus, and pertussis in the childhood immunisation schedule.

Originally the diphtheria, tetanus, and whole-cell pertussis (DTwP) vaccine was formulated using a combination of diphtheria and tetanus toxoids with suspensions of inactivated *Bordetella pertussis*. This vaccine had been in widespread use since the 1940s, but there has been some concern about the safety of the vaccine. In a study to characterise the reactogenicity of licensed DTwP vaccines available in the U.S.A, only 7% of the 1232 children included in the study had reported no reaction to the vaccine. 27.3% of children reported a mild reaction, 58.6% reported a moderate reaction, and 7.1% reported severe reactions (Pichichero, 1996). In a subsequent larger study, some of the severe reactions included hypotonic-hyporesponsive episodes, fevers greater than 40.5 °C, seizures, acute encephalopathy, and permanent neurological defects (Cody, et al., 1981).

Due to the safety concerns of the DTwP vaccine, during the past two decades, several subunit vaccines consisting of acellular pertussis components combined with diphtheria and tetanus toxoids (DTaP) have been licensed for use in the United States and most European countries.

The acellular pertussis fraction consists of a combination of purified pertussis antigens: pertussis toxin (PT), filamentous haemagglutinin (FHA), pertactin (PRN), and fimbriae (FIM 2/3) (Decker, et al., 1995).

The DTaP vaccine was first used in Japan in 1981 and completely replaced the whole cell vaccine. From the records of Government surveillance of pertussis in Japan, a dramatic decrease in pertussis has been recorded over the past 23 years. Furthermore, incidences of encephalopathy, febrile seizures, and sudden deaths were significantly lower with acellular pertussis vaccination than with whole cell pertussis vaccination (Kuno-Sakai & Kimura, 2004). Other trials have also demonstrated that the DTaP vaccine is less reactogenic than the DTwP vaccine. In a clinical trial to compare safety and immunogenicity of a fifth dose of DTaP in children who had received 4 previous doses of the same DTaP product, the results suggested that the overall safety profile for the DTaP vaccine was better than that of the DTwP vaccine (Pichichero, et al., 2000). The same pattern was also observed in a study conducted by Greco *et al*, where the acellular vaccines were much less likely to cause adverse reactions than the whole-cell vaccine (Greco, et al., 1996).

While using proteins eliminates the unnecessary antigenic load in vaccines, proteins themselves contain a multitude of antigenic epitopes, some of which may have harmful side-effects. For example, the M-protein, an extensively studied virulence factor on the surface of GAS, has been investigated as a possible vaccine candidate for GAS. However, laboratory studies with vaccines containing M protein epitopes revealed that these vaccines elicited antibodies that cross-reacted with human heart, brain, kidney, or joint cartilage (Baird, et al., 1991; Bronze & Dale, 1993; Dale & Beachey, 1982). Such problems have evoked an interest in creating peptide vaccines containing only epitopes capable of inducing the desired immune response.

1.2.3 Peptide-based vaccines

Peptide-based vaccines have been made possible by the ability to map specific B cell and T cell epitopes capable of eliciting immune responses. The peptide epitopes are usually short (8-20

amino acids) and can be easily created by cost effective, organic peptide synthesis methods (Celis, 2002). Peptide antigens that contain B cell epitopes are recognised by B cell surface receptors (BCRs) (McHeyzer-Williams, et al., 2012). Co-stimulation with helper T cells (Th) results in B cell activation, antibody secretion, and memory B cell generation. B cells can also be activated in a T cell-independent manner through clustering of BCRs by antigens with multiple copies of an epitope, although memory B cells are generally not formed when this happens (McHeyzer-Williams, et al., 2012).

Antigens may also contain epitopes that are recognized by CD8+ and CD4+ T cells. These peptide epitopes are processed by antigen-presenting cells (APCs), loaded onto major histocompatibility complex (MHC) molecules and presented on the cell surface (Trombetta & Mellman, 2005). Antigens found outside of cells (exogenous) are phagocytised and presented to CD4+ T cells by MHC class II molecules on the cell surface (Kaufmann, 2007). The CD4+ T cells then activate various cells of the immune system (B cells and CD8+ T cells) and coordinate the immune response by the secretion of cytokines and chemokines. Antigens produced inside cells (endogenous) are processed and presented on MHC I to CD8+ T cells which function to kill infected or damaged cells (Foged, et al., 2012; Kaufmann, 2007).

Using specific peptide epitopes in vaccines allows for the elicitation of the desired cellular and humoral responses while reducing the risk of side effects and autoimmune responses. Furthermore, using multiple immunodominant epitopes or epitopes conserved between multiple serotypes of a pathogen can result in a vaccine with broad-spectrum immunity.

To date, there are many peptide vaccines under development, including vaccines for human immunodeficiency virus (HIV) (Liu, et al., 2007), hepatitis C virus (HCV) (Kolesanova, et al., 2013), malaria (Nardin, 2010), influenza (Stanekova, et al., 2011), anthrax (Jon, et al., 2010), human papilloma virus (HPV) (Solares, et al., 2011), and therapeutic anti-cancer vaccines for certain cancers (Bernhardt, et al., 2006; Brunsvig, et al., 2006; Kyte, et al., 2009). While no

peptide vaccine has been approved for human use by the U.S. Food and Drug Administration, many have been successful enough to progress to clinical trials (Li, et al., 2014).

The disadvantage of using peptides as vaccines is that, owing to their relatively small size, peptides by themselves are usually poorly immunogenic. This necessitates delivery with immune-stimulatory adjuvants or conjugation to carrier proteins in order to elicit an immune response (Black, et al., 2010).

1.3 Adjuvants

Adjuvants are compounds that can provoke an immune response against co-inoculated antigens (Vogel, 1998). Adjuvants can also be used to reduce the amount of antigen used in a vaccine, reduce the number of immunisations required, improve the efficacy of vaccines in certain population groups, and allow the uptake of antigens by mucosal immune cells (Douce, et al., 1995; Marx, et al., 1993; McElrath, 1995).

Ideally, adjuvants should be stable with a long shelf life, cheap to produce, immunologically inert, and promote an appropriate immune response (Edelman, 1980). Many types of vaccine adjuvants have been created to date, but only a few have been approved for human use (O'Hagan & De Gregorio, 2009) (table 1.2). However, significant advances in the engineering of adjuvants have resulted in a number of novel adjuvants being created.

Table 1.2 Licensed adjuvants

Adjuvant name	Adjuvant class	Components	Disease
Alum (various companies)	Mineral salts	Aluminium phosphate or aluminium hydroxide	Various
MF59 (Novartis)	Oil-in-water emulsion	Squalene, Span85, Tween 80, citrate buffer	Fluad (seasonal influenza), Focetria (pandemic influenza), Aflunov (pre-pandemic influenza)
AS03 (GlaxoSmithKline)	Oil-in-water emulsion	Squalene, Tween 80, α-tocopherol	Pandremix (pandemic influenza), Prepandrix (pre-pandemic influenza)
Virosomes (Berna Biotech)	Liposomes	Lipids, hemagglutinin	Inflexal (seasonal influenza), Epaxal (hepatitis A)
AS04 (GlaxoSmithKline)	Alum-absorbed TLR4 agonist	Aluminium hydroxide, MPL	Fendrix (hepatitis B), Cervarix (human papilloma virus)
AF03 (Sanofi)	Oil-in-water emulsion	Squalene,Montane 80, Eumulgin B1-PH	Humenza (pandemic influenza)

1.3.1 Adjuvant categories

1.3.1.1 Mineral salt adjuvants

Aluminium salt (Alum) based adjuvants, such as aluminium phosphate and aluminium hydroxide, have been the most widely used human adjuvants (Vogel & Powell, 1995). The ability of aluminium compounds to be used as adjuvants was first demonstrated in 1926 with diphtheria toxoid absorbed to alum (Glenny & Barr, 1931). Since then, alum adjuvants have been routinely used in childhood vaccines such as the DTP vaccine (Baylor, et al., 2002).

Studies suggest that alum adjuvants work by enhancing antigen uptake, producing danger signals, and recruiting various types of immune cells (Reed, et al., 2013). Due to their particulate nature, they are also taken up by APCs and cause increased MHC class II expression and antigen presentation (Ulanova, et al., 2001).

However, despite being one of the few licensed adjuvants, there are limitations associated with its use. A significant limitation is the inability to provoke CD8+ T cell responses that are required to eliminate intracellular pathogens such as malaria and *M. tuberculosis* (Marrack, et al., 2009). Alum salts are also ineffective when administered by the oral or nasal route and can induce granulomas when administered via the subcutaneous route, a problem for vaccines requiring frequent boosts (Alpar, et al., 1992; Bordet, et al., 2001). Alum-associated pathology and vaccine-specific IgE production have also been reported (Gupta & Relyveld, 1991). Storage of alum-containing vaccines is also problematic as freezing alum leads to a loss of potency (Diminsky, et al., 1999)

1.3.1.2 Emulsions

Adjuvant emulsions include oil in water or water in oil emulsions. Two well-known water-in-oil emulsions are complete Freund's adjuvant (CFA), which consists of paraffin oil mixed with killed Mycobacteria, and incomplete Freund's adjuvant (IFA) consisting of only the water-in-oil emulsion. The mechanism of action involves the formation of an antigen depot at the injection site, allowing for a slow release of the antigen (Freund, 1956). However, these adjuvants are too toxic for use in humans. The discovery of oil-induced neoplasms and Arlacel-A (emulsifying agent in IFA) induced carcinogenesis in mice, meant that the use of IFA in humans was discontinued (Murray, et al., 1972; Potter & Boyce, 1962).

A new emulsion, named MF-59, consisting of a squalene-based oil in water nano-emulsion has been used in Europe as an adjuvant in influenza vaccines (Fang & Hora, 2000). M59 has an acceptable safety profile and both humoral/cellular immune responses were enhanced with its use (Ott, et al., 1995).

1.3.1.3 Tensoactive adjuvants

Saponins are tensoactive adjuvants isolated from plants. Saponins are triterpene glycosides that induce strong cytotoxic $CD8^+$ lymphocyte responses and provoke responses towards mucosal antigens (Kensil, 1996). Quil-A, extracted from the bark of the Quillaja saponaria tree, is a saponin that has been used successfully for veterinary applications (Dalsgaard, 1974). However, Quil-A has not been approved in humans due to its side effects of haemolysis and local inflammation (Gupta, et al., 1993).

1.3.1.4 Microorganism-derived adjuvants

There are a number of adjuvants that have been derived from bacteria and fungi. Some of these adjuvants are not highly immunogenic but act through the activation of Toll-like receptors (TLRs) which can provoke an immune response (F. M. Audibert & Lise, 1993). Muramyl dipeptide (MDP) is an adjuvant sourced from different species of bacteria including: *Mycobacterium* spp., *Corynebacterium parvum*, *Streptococcus mutans* and *Corynebacterium diphtheria* (Kotani, et al., 1975). MDP, incorporated in liposomes, can induce strong cellular responses, whilst it enhances humoral immunity in aqueous solutions (F. Audibert, et al., 1976). MDP is required for the adjuvant properties of CFA, but the use of CFA in humans has been banned due to the high toxicity of MDP (Gupta et al., 1993).

Another adjuvant, derived from the cell wall of Gram-negative bacteria, is Lipopolysaccharide (LPS) (Johnson, et al., 1956). Lipid A, the structural element of LPS, is responsible for the adjuvant effect and can activate APCs (Rietschel, et al., 1982). However, lipid A shows high toxicity and is not licensed for use in humans (Gupta et al., 1993).

1.4 Antigen delivery systems

In addition to using adjuvants, specialised delivery systems can also be used to improve the immunogenicity of antigens. Vaccine delivery systems are generally particulate and mainly function to target associated antigens into APCs like macrophages and dendritic cells (DCs).

Particulate delivery systems include liposomes, polymeric microspheres, virus-like particles (VLPs), and immunostimulating complexes (ISCOMs) (Bramwell & Perrie, 2005).

1.4.1 Liposomes

Liposomes are *in vitro* generated spheres, consisting of phospholipid bilayers separated by aqueous compartments, which can encapsulate antigens and act as adjuvants (Allison & Gregoriadis, 1974). The potency of liposomes as adjuvants depends on the number of lipid layers (Shek, et al., 1983), electric charge (Allison & Gregoriadis, 1974), and composition (Heath, et al., 1976).

Liposomes can enhance both antibody production and cellular immunity to the antigen it carries (Amidi, et al., 2012). Liposomes can also extend the half-life of antigens in blood to allow a higher antigen exposure to APCs after vaccination (Kramp, et al., 1982). These properties are useful for antigen delivery and a number of protein and peptide antigens, trapped in liposomes or coupled to liposomal membranes, have been investigated for their ability to stimulate immune responses (Felnerova, et al., 2004). However, stability, manufacturing, and quality assurance problems have hampered the use of liposomes in humans (Katre, 2004).

1.4.2 Microspheres

Microspheres are biodegradable and biocompatible polymers, usually composed of poly (lactic/glycolic) acid (PLGA), that have been used safely as drug delivery vehicles in humans (Morris, et al., 1994; Shive & Anderson, 1997). Microspheres have also been used as protein and peptide antigen delivery systems (Eldridge, et al., 1991; Esparza & Kissel, 1992). A water-oil emulsion technique is generally used for encapsulation of substances into microspheres.

The advantage of microspheres is the ability to control the release rates of the encapsulated substance by selecting varying polymers that have different degradation kinetics (Cohen, et al., 1991). Microspheres can also transfer exogenous antigens into the MHC class I pathway but the CTL responses have been weak. However, Potent CTL responses have been generated when

used in conjunction with other novel vaccine approaches such as VLPs (Boisgerault, et al., 2005; Tabata & Ikada, 1988).

1.4.3 Virus-like particles

VLPs are empty capsids or viruses that do not contain DNA or RNA and, thus, lack the associated risk of infection. VLPs have been investigated as subunit vaccine carriers, where antigens have been fused to the surface loops of VLPS (Garcea & Gissmann, 2004; Lechmann, et al., 2001). Antigens displayed on VLPs are processed by DCs and elicit potent immune responses. Since VLPs are particulates, they can be internalised by APCs and have been observed in the cytoplasm (Charpilienne, et al., 2001). The effects on APCs appear to be TLR-mediated (Yokota, et al., 2003).

VLPs of different viruses have proved very immunogenic and have been developed as vaccines. Immunisation of young healthy women with Human papillomavirus 16 VLPs, composed of the major structural protein L1, induced high titre neutralising antibodies and protected the patients from HPV infection and associated cervical dysplasia (Koutsky, et al., 2002). A new VLPs-based formulation, called NASVAC, has also been developed for chronic hepatitis B therapy and is based on the surface and core HBV antigens. It is a nasal vaccine that has shown safety and immunogenicity in clinical trials (Betancourt, et al., 2007).

1.4.4 ISCOMs®

ISCOMs® are 40 nm particles created with saponins, lipids, cholesterol, and the selected antigen. Cholesterol binds to saponin, forming rings, and the rings are fixed together by lipids to form spherical nanoparticles. Hydrophobic or amphipathic antigens can be incorporated into this complex. ISCOMs® increase the efficiency of antigen presentation to B cells and uptake by the APCs (Sjolander, et al., 1998).

1.5 Using the pilus of *Streptococcus pyogenes* as a peptide antigen delivery system

1.5.1 *Streptococcus pyogenes*

S. pyogenes, also known as GAS, is a Gram-positive, facultative anaerobic bacterium that is a strictly human pathogen (Bessen, 2009). Streptococcal species can be separated into different groups based on their haemolytic-activity and antigenic differences in their cell wall carbohydrate composition (Lancefield, 1933). *S. pyogenes* grown on blood-agar plates completely lyses the erythrocytes. Thus, *S. pyogenes* is a β-haemolytic streptococcus (Pichichero, 1998). Dr. Rebecca Lancefield created another classification based on the immunological test for a group-specific carbohydrate (Lancefield, 1933), N-acetyl-glucosamine linked to a rhamnose polymer (McCarty, 1956). This defines *S. pyogenes* as a group A streptococcus.

A method to further classify GAS into different serotypes, based on the immunological differences of two surface components, the M protein and the T antigen, was also developed by Dr. Lancefield (Lancefield, 1940). The M type marker, the highly variable M protein, gives rise to more than 100 M serotypes that are identified using standardised antisera (Cunningham, 2000). Alternatively, sequencing of the M protein (*emm*) gene has led to the recognition of a vast number of new *emm* types that were previously nontypable by serotyping (Podbielski, et al., 1991; Steer, et al., 2009). In high-income countries, such as USA and Canada, the M1/*emm1* type accounts for almost 20 % of all isolates, whereas there is higher diversity in Africa or in the Pacific region (Steer, et al., 2009).

1.5.2 Epidemiology of GAS infections

GAS is a strictly human pathogen and it colonises epithelial surfaces, mainly of the throat and skin, but can also colonise other surfaces such as the vagina and rectum. GAS is responsible for a wide variety of diseases ranging from non-invasive, mild infections, such as pharyngitis and

impetigo, to life-threatening, invasive conditions, such as bacteraemia, pneumonia, necrotizing fasciitis (NF), and streptococcal toxic shock syndrome (STSS). In addition, GAS is responsible for nonsuppurative sequelae of infection specifically acute rheumatic fever (ARF) and post streptococcal glomerulonephritis. The global impact of disease has been estimated to be >500,000 deaths per year, primarily due to rheumatic fever, rheumatic heart disease, and invasive GAS infection. In 2005, the WHO reported a global estimate of 18.1 million cases of severe GAS disease, with 1.78 million new cases of severe disease. In addition, there were >111 million prevalent cases of GAS pyoderma and >616 million incident cases of GAS pharyngitis per year (Carapetis, et al., 2005).

In industrialised societies, a significant percentage of GAS isolates belong to a few *emm* types, for example *emm* types 1, 3, 12, and 28, which account for approximately 40% of disease in these countries. However, these *emm* types are less likely to be isolated from cases of human disease in Africa, the Pacific region and the Indian subcontinent (Steer, et al., 2009).

In New Zealand, a study which investigated the circulating pharyngeal GAS *emm* types in Auckland found that, while there was substantial diversity in *emm* types, only a few types predominated. The three predominant *emm* types in the region (*emm*1; *emm*89 and *emm*12) were similar to those described from GAS pharyngeal isolates in other developed countries (Williamson, et al., 2014).

Additionally, some *emm* types are associated with the post infectious sequelae of GAS disease such as ARF (e.g., *emm* types 1, 3, 5, 6, 11, 12, 14, 17, 18, 19, 24, 27, 29, 30, 32, and 41), and post streptococcal glomerulonephritis (e.g., *emm* types 1, 4, 12, 49, 55, 57, and 60) (Metzgar & Zampolli, 2011).

1.5.3 Burden of Immune Sequelae

ARF is a systemic disorder that can follow untreated GAS pharyngeal infection. It can result in inflammation of the joints (arthritis) (60 to 80% of cases), inflammation of the heart (carditis) (30 to 45% of cases), and/or neurological symptoms (e.g., Sydenham chorea) (10% of cases). Less common manifestations of the skin include erythema marginatum (2% of cases) or, rarely, subcutaneous nodules. ARF is a major source of morbidity and mortality worldwide, particularly as it may result in long-term damage to the heart, termed Rheumatic Heart Disease, which is the most common cause of pediatric heart disease worldwide (Lee, et al., 2009).

ARF is a particularly serious problem in indigenous populations and developing nations, where the highest rates of disease are observed. In a 2005 study, the highest rates of ARF were found in sub-Saharan Africa (5.7 cases per 1,000), in the Pacific Islander and indigenous minority populations of Australia and New Zealand (3.5 cases per 1,000), and south central Asia (2.2 cases per 1,000) (Carapetis, et al., 2005).

ARF is especially significant in New Zealand as it is intensely concentrated in children (5- to 14-year-olds). For this age group, the average annual incidence rate across all ethnic groups over the period 2000–2009 was 17.2 per 100 000. Incidence rates for Maori and Pacific children were also about 20-fold and 40-fold higher than those for non-Maori/Pacific children, even though Maori and Pacific children comprise only 30% of NZ's 5- to 14- year olds. Therefore there is an ethnic disparity in children being affected by ARF as well. Incidence rates for Pacific and Maori children 5 to 14 years of age have increased by more than 70% since 1993, while rates have declined by about 70% for non-Maori/Pacific children. The absence of progress since 1993 in the control of ARF for Maori and Pacific peoples appears to be linked to socioeconomic disparity. The ARF incidence rates in New Zealand are associated with household crowding at the neighbourhood level. Access to health care for Maori and Pacific ethnic groups has been shown to be inadequate as well. Rheumatic fever, therefore, is an important public health issue for NZ with the burden falling on disadvantaged Maori and Pacific children (Milne, et al., 2012).

A second immune sequaelae is Acute Poststreptococcal Glomerulonephritis. It is an immune complex-mediated disorder of the kidneys, resulting in symptoms such as edema, hypertension, urinary sediment abnormalities, and decreased levels of complement components in the serum (Shulman & Tanz, 2010). The disease rates are highest in children in less developed countries, with incidence rates as high as 94.3/1,000 being reported in the Northern Territory of Australia (Marshall, et al., 2011).

1.5.4 Pili of *S. pyogenes*

Pili (or fimbriae) are hair-like, filamentous protein appendages found on the surface of several bacteria which mainly mediate adhesion and enable colonisation of host tissues (Proft & Baker, 2009).The presence of pili were first reported in Gram-negative bacteria (Duguid, et al., 1955) and a few Gram-positive strains of corynebacteria (Yanagawa & Otsuki, 1970). Afterwards, the presence of pili on the surface of Gram-positive pathogenic bacteria such as *S. pyogenes* was also reported (Mora, et al., 2005).

The pili from Gram-positive bacteria are usually assembled from two to three subunits (pilins) by covalent polymerisation, as was first elucidated by Ton-That *et al*. in *C. diphtheria* (Ton-That & Schneewind, 2003). This is in contrast to Gram-negative bacteria where the pilin subunits are linked through non-covalent interactions (Proft & Baker, 2009).

In *S. pyogenes*, the pili consist of a backbone protein (BP), which forms the pilus shaft, and either 1 or 2 ancillary proteins (AP1, localised to the pilus tip, and AP2, the cell wall anchor of the pilus) covalently assembled and linked to the cell wall by a series of sortase-mediated transpeptidase reactions. The pilus subunits and the pilus-specific sortase are encoded together in a highly variable pathogenic island called the fibronectin- and collagen-binding protein and T-antigen (FCT) region (Falugi, et al., 2008).

In *S. pyogenes*, the BP is generally known as FctA, the AP1 as Cpa, and the AP2 as FctB. However, in the M1 strain SF370, used in this thesis, the gene locus tags Spy0128, Spy0125 and

Spy0130 are used for the BP, AP1, and AP2 respectively (figure 1.1). Furthermore, the BP is also the T-antigen of *S. pyogenes* (Mora, et al., 2005), which was discovered by Dr. Lancefield and established as a typing system for *S. pyogenes* (Lancefield, 1940).

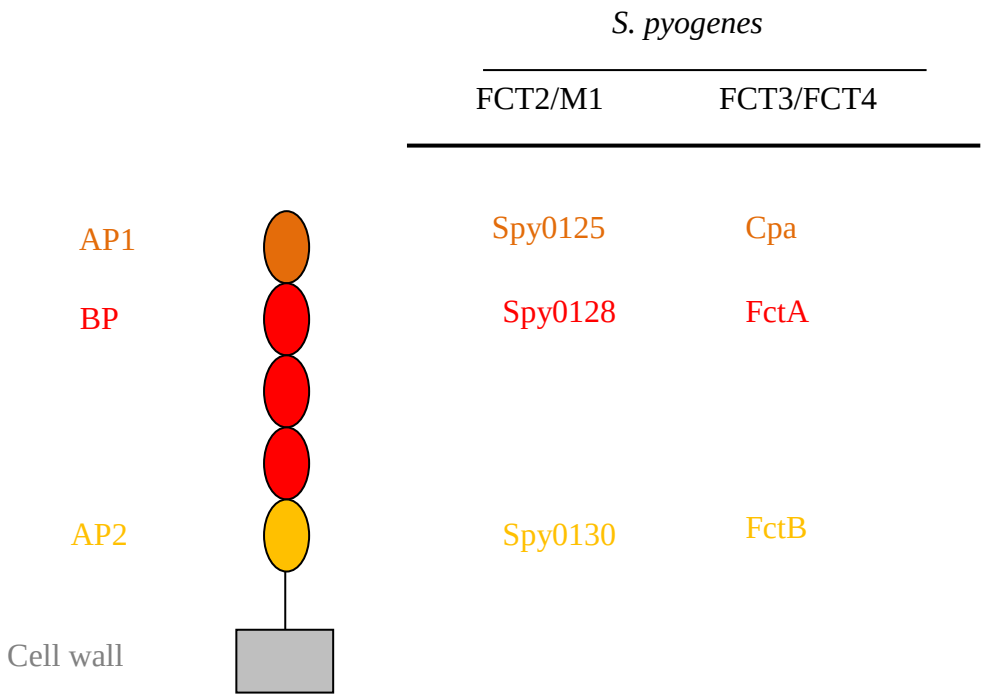

Figure 1.1 Structure and subunits of the pili from *S. pyogenes*

The shaft of the pilus is formed from multiple BP subunits. The nomenclature is given for *S. pyogenes* pili of two common types (FCT2 and FCT3/FCT4). Abbreviations: BP, backbone protein; AP1, ancillary protein 1; AP2, ancillary protein 2; FCT, fibronectin and collagen-binding protein and T-antigen (Falugi, et al., 2008; Mora, et al., 2005; Smith, et al., 2010).

Currently, nine types of FCT islands have been identified (Bessen & Kalia, 2002; Kratovac, et al., 2007). Of these, the FCT2, 3, and 4 islets are more closely related to each other, as all 3 BP have 2-domain folds (figure 1.2), and FCT types 7 and 8 are derived from the FCT4 islets. Other FCT islets are the result of horizontal gene transfer, such as the AP1 and AP2 subunits of the FCT6 islet which has an ~ 90 % sequence identity with the pilus islet PI-1 from *S. Agalactiae* (Falugi, et al., 2008; Kratovac, et al., 2007).

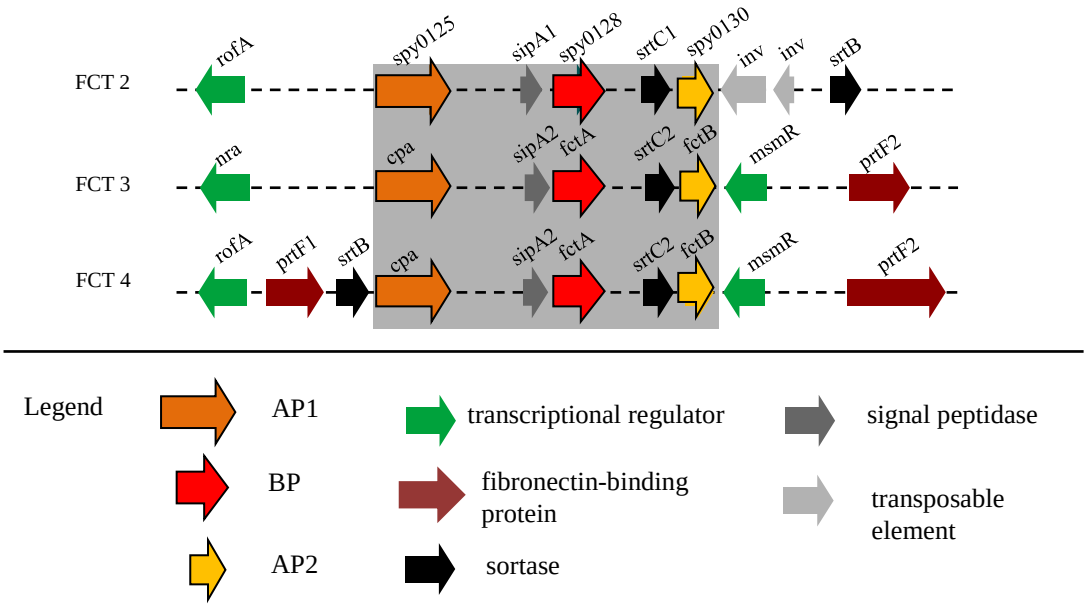

Figure 1.2 Genetic organisation of pilus islands from *S. pyogenes*

Presented are the *S. pyogenes* FCT islet 2 (strain SF370, serotype M1, NC 002737), 3 (MGAS315, M3, NC 004070) and 4 (MGAS6180, M28, NC 007296). The pilus genes of FCT region 2–4 are highlighted with a grey box. The length of the genes is rendered in scale. Abbreviations: AP1, ancillary protein 1; BP, backbone protein; AP2, ancillary protein 2; FCT, fibronectin-and collagen-binding protein and T-antigen (Falugi, et al., 2008).

The pilus from the FCT2 type M1 strain SF370, which was used in this thesis, has been well characterised (Manetti, et al., 2007). Five genes from the FCT region are essentially needed for the formation of functional pili at the cell surface. The *spy0128* gene encodes the backbone pilin which forms the shaft, the *spy0129* gene encodes the sortase C1 that generate the covalent linkages between the pilin subunits, the *spy0125* gene encodes the pilus-presented adhesin, the *spy0130* gene encodes a cell wall linker protein, and the *SipA* gene encodes the SipA protein

whose function is unknown (Linke, et al., 2010; Mora, et al., 2005; W. D. Smith, et al., 2010; Young, et al., 2014). Deletion of *SipA*, *spy0128*, or *spy0129* from the chromosome abrogates pilus assembly, while deletion of *spy0125* or *spy0130* produces polymerised pili that were not functional (Abbot, et al., 2007; Young, et al., 2014).

The crystal structure of Spy0128 has been solved and it consists of 2 domains that have irregular all-β structures that are modified variants of the immunoglobulin fold (Kang, et al., 2007). The N-terminal domain, residues 18 to 171, forms a β sandwich while the C-terminal domain, residues 173 to 307, comprises 11 β strands whose core is a β sandwich in which a five-stranded β sheet packs against a four-stranded β sheet. The two domains are only separated by two residues, $Ser^{172}$and T^{173} (figure 1.3). The Spy0128 structure explained the trypsin resistance of the T-antigen. A result of two intra-molecular isopeptide bonds cross-linking the side chains of a lysine and an asparagine (Lys^{36}-Asn^{168} in the N domain; Lys^{179}-Asn^{303} in the C domain), which confers high stability on the domains. Recombinant Spy0128 containing point mutations which abrogated intra-molecular bond formation were shown to be much more susceptible to protease degradation and heating when compared to the native protein (Kang, et al., 2007).

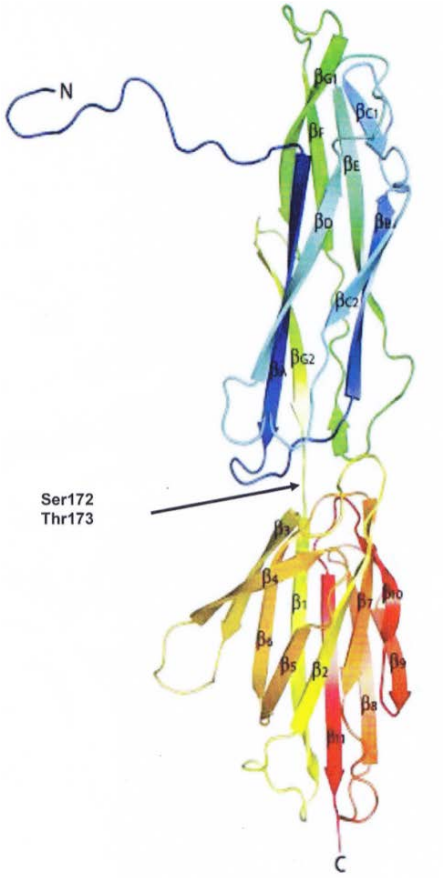

Figure 1.3 Structural model of the BP Spy0128 from *S. pyogenes*

Computer generated structure of Spy0128 from *S. pyogenes*, generated using the protein structure homology-modelling server SWISS-MODEL.

Furthermore, the crystal structure and mass spectral analysis helped elucidate a model for pilus fibre assembly. Spy0128 is formed with a C-terminal membrane anchor and the sortase-recognition motif EVPTG. Spy0129 cleaves between threonine and glycine of the EVPTG motif to form a sortase-pilin intermediate. The carboxyl group of the C-terminal threonine of Spy0128 is then linked, via an isopeptide bond, to the ε-amino group of the side-chain of a conserved lysine (K161) in the N-terminal domain of the next Spy0128 subunit (Kang, et al., 2007) (figure 1.4). Approximately 50-100 Spy0128 subunits are assembled through homopolymerisation before the Spy0130 subunit is added to stop pilus assembly and link the pilus structure to the cell wall (Linke, et al., 2010).

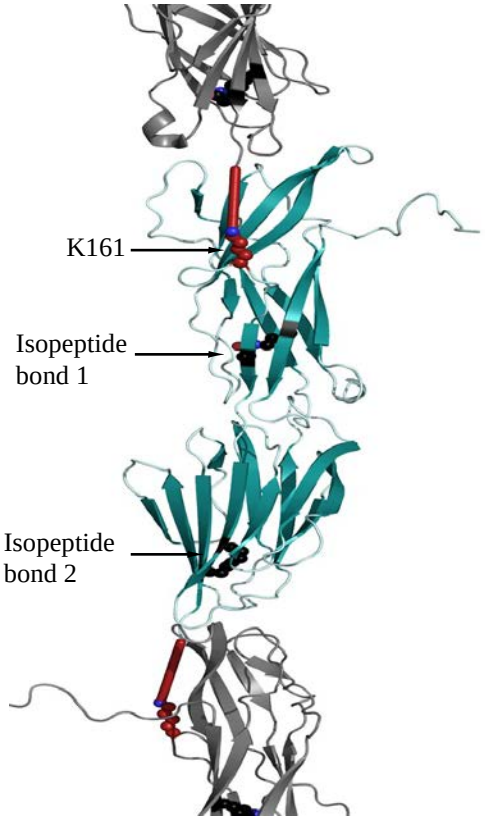

Figure 1.4 Homopolymerisation of Spy0128 pilin subunits

A Spy0128 monomer (cyan) is shown as part of the *S. pyogenes* pilus shaft with two adjacent subunits (grey), as suggested by the Spy0128 crystal packing. The sidechain of Lys-161, essential for the covalent pilus polymerisation, is drawn as red spheres (Linke, 2010). 50–100 Spy0128 subunits form the pilus shaft in both bacteria. All pilins are covalently joined by pilus-specific sortases, and the pilus polymer is attached to the cell wall by the housekeeping sortase (Kang, et al., 2007; Linke, et al., 2010)

1.5.5 Potential use of the pilus of GAS as a vaccine peptide carrier

The homopolymerisation of the Spy0128 subunits to form a pilus shaft enables the potential use of the pilus as a vaccine peptide carrier. As each pilus structure consists of 50-100 Spy0128 subunits covalently linked together, genetically engineering a vaccine peptide into the Spy0128 subunit would result in the expression of 50-100 repeated copies of the peptide along the pilus extension. Since each bacterium is believed to express several peritrichous pili on the cell surface, thousands of copies of a given peptide would be produced on the bacterial cell surface. The proteins that form the pilus are also immunogenic. Vaccination of adult CD1 mice with recombinant Spy0128, Spy0130, and Spy0125 conferred strain-specific protection to a lethal

challenge with a mouse-adapted M1 strain (Mora, et al., 2005). This multimeric presentation of a vaccine peptide in the pilus structure would likely increase the immunogenicity of the peptide. Furthermore, the pilus subunits possess a rigid protease-resistant structure which might provide increase stability to the peptide.

However, to allow the multimeric presentation of a vaccine peptide integrated into the Spy0128 subunit, the peptide-linked pilus has to be expressed on the surface of a bacterium. One possibility is to use *L. lactis*, a non-pathogenic relative of GAS, as the delivery vehicle for the peptide-linked pilus. *L. lactis* has been used successfully to develop a pilus-based vaccine carrier, using the native tip protein (Cpa) of the T3 pilus from *S. pyogenes.* In a proof of concept study, the *Escherichia coli* maltose-binding protein was fused to the C-terminal region of Cpa and the recombinant pilus was successfully expressed on the surface of *L. lactis* (Quigley, et al., 2010). Furthermore, the wild-type pilus from M1 strain SF370 has been successfully expressed on the surface of *L. lactis* using an *E. coli* – GAS shuttle vector pLZ12, containing the lactococcal promoter P23. Immunoblot analyses shows that the assembly of the pilus on the surface of *L. lactis* is similar to that of the wild-type SF370 strain (unpublished data).

1.6 Using *L. lactis* as a mucosal delivery vehicle for the peptide-linked pilus

1.6.1 The mucosal immune response

The mucosal immune system is the first line of immunological defence against invading pathogens. Antigen specific immune responses are initiated at regions which compromise Microfold cells located in the epithelium overlying follicles of the mucosa-associated lymphoid tissue (MALT). These regions contain all the immunocompetent cells that are required for the initiation of an immune response (that is, T cells, B cells, and antigen-presenting cells). Peyer's patches, in the gut, and nasopharynx-associated lymphoid tissue (NALT) are the two main components of the MALT. These are the inductive tissue for the generation of mucosal

immunity, through recognition of antigens in the intestinal and respiratory tracts respectively. The common mucosal immune system (CMIS) connects the Peyer's patches and NALT with effector sites, such as the lamina propria of the intestinal or respiratory tracts and glandular tissue, for the generation of antigen specific immune responses (Yuki & Kiyono, 2003).

The initial response towards a pathogen involves non-specific mechanisms produced by the innate immune response (the most conserved elements of the immune system). Innate responses require no previous exposure but rely on recognition of evolutionarily conserved structures on pathogens, termed pathogen-associated molecular patterns (PAMPs), through a limited number of germ line-encoded pattern recognition receptors (PRRs). PAMPs are conserved products of microbial metabolism that are generally unique to microorganisms (examples include lipopolysaccharides, lipoproteins, peptidoglycan, lipoteichoic acids, DNA, and RNA) (Akira, et al., 2006). PAMPS are often needed for microbial survival, preventing the generation of escape mutants, and are invariant between microorganisms of a given class, allowing a limited number of germ-line-encoded PRRs to detect nearly any microbial infection. Although the target molecule may contain differences between microbial species, common molecular patterns can be found in all. For example, the lipid-A portion of LPS is invariant and serves as a PAMP; in contrast, the O-antigen varies between species and is not a strong activator of the innate immune system (Mogensen, 2009).

PRRs that recognise PAMP include mannose receptors (that bind to terminal mannose groups on microbial glycoproteins, facilitating their endocytosis), nucleotide-binding oligomerization domain proteins (NODs, that promote intracellular recognition of microbial peptidoglycans), and the Toll-like receptors (TLRs). The TLRs have been the most extensively studied PRRs. TLRs are found both on the cell surface and within the cell, where they facilitate recognition of and response to PAMPs, such as endotoxin [TLR-4], bacterial flagellin [TLR-5], viral RNA, [TLR-3, -7, -8], and bacterial DNA [TLR-9] (Mogensen, 2009).

Upon PAMP recognition, PRRs present at the cell surface or intracellularly signal to the host the presence of infection and trigger proinflammatory and antimicrobial responses by activating numerous intracellular signaling pathways, including adaptor molecules, kinases, and transcription factors (Akira & Takeda, 2004). PRR-induced signal transduction pathways result in the activation of gene expression and synthesis of a broad range of molecules, including cytokines, chemokines, cell adhesion molecules, and immunoreceptors which stimulate the early host response to infection and at the same time represent an important link to the adaptive immune response (Akira, et al., 2006).

A highly specific response towards the pathogen occurs afterwards facilitated by the adaptive immune response (Czerkinsky, et al., 1999). Dendritic cells provide an important link between the innate and adaptive immune system. When the pattern recognition receptors on DCs are stimulated, immature DCs participate in the innate immune response. After activation, DCs initiate an adaptive and antigen-specific immune response by processing antigens and presenting those to naive T cells in the lymph nodes (Chaplin, 2010).

Two components of adaptive immunity contribute to the elimination of pathogens, the cellular cytotoxic responses and antibody production both of which involve CD8+ and CD4+ T cells (Purcell, et al., 2003). $CD8^+$ T cells primarily recognize antigenic peptides derived from cytosolic proteins expressed on the MHC class-I complex. Recognition of foreign cytosolic peptides of the target cell in the context of MHC-I by the T cell receptor on $CD8^+$ T cells leads to the creation of a conjugate with an immunologic synapse (IS) thereby activating apoptotic cell death in the target cell. This process is mediated by rapid mobilisation of granules to the IS, where the granule membranes fuse with the plasma membrane, resulting in exocytosis of the granule contents, including granzymes and perforin. It is through these cytotoxic T lymphocyte responses that virally infected cells, tumour cells and sometimes even normal healthy cells are destroyed, clearing the virus or eradicating tumour cells from the host (Lieberman, 2010).

Combined with the cytotoxic response, the generation of antibodies are essential to the clearance of many pathogens. Antibodies also recognise and bind to relatively short peptide sequences but in this case the peptides need to maintain conformational integrity for binding. Therefore, unless a relatively short peptide sequence can be assembled into a conformation that resembles that of the corresponding sequence in the native protein, antigenic activity will be lost. Antibody production is controlled by contact between CD4+ T helper cells and antigen specific B cells that express immunoglobulin on their cell surface.

CD4+ T helper cells recognise the MHC class II complexes that are expressed constitutively on specialized antigen presenting cells (APC) such as B cells, DCs and macrophages (Purcell, et al., 2003). The CD4+ T helper cells that are involved in the adaptive immune response differentiate into functionally different subsets, two main subsets being the T helper 2 (Th2) and T helper 1 (Th1) cells. Cytokines playing a critical role in T helper cell polarization, the two pivotal cytokines that control Th1 and Th2 differentiation are IL-12 and IL-4, respectively. The balance of inflammatory and anti-inflammatory cytokine production in DCs is also crucial in determining the type of Th cell response (Neurath, et al., 2002).

Following DC-mediated stimulation, Th2 cells induce IgA committed B cells in the germinal centre of the lymphoid follicle. These Th2 and IgA+ B cells migrate to effector sites, including the nasal passages, through the thoracic ducts and blood circulation. In these effector sites, the IgA+ B cells enter into the final differentiation stage to become IgA-producing plasma cells in the presence of cytokines such as IL-5 and IL-6 which are produced by Th2 cells for the subsequent production of dimeric or polymeric forms of IgA (Yuki & Kiyono, 2009). Th2 cells also control immunity to extracellular parasites and the allergic inflammatory immune responses (Paul & Zhu, 2010).

Th1 cells are characterized by their ability to produce cytokines such as IL-2 and IFN-γ, along with TNF-α and TNF-β, to stimulate immune responses. The Th1 response results in the activaction of macrpahges to kill intracellular parasites, in delayed type hypersensitivity, and in

IgG2a, but not IgE, synthesis (Romagnani, 1992). Th1 cells are important in protection of the host from intracellular pathogens and virally infected targets; however control is essential as too great a pro-inflammatory response by Th1 cells can cause tissue damage and elicit unwanted inflammatory and autoimmune diseases (Davidson, et al., 1996, Leung et al, 2000).

1.6.2 *L. lactis*

L. lactis is a Gram-positive lactic acid bacterium (LAB) that is commonly used in the dairy industry. It is homofermentative and has the ability to produce L-lactic acid; hence, it is used as a starter culture for dairy fermentation (Casalta & Montel, 2008). *L. lactis* ssp. *cremoris*, the strain used in this study, is the dominant strain in 'Caspian Sea yogurt' which is a fermented milk circulated in Japan. The milk contains *L. lactis* at 10^8 to 10^9 CFU per gram (Uchida, et al., 2009). *L. lactis* is also used to create different flavours and textures of cheese through the production of aroma compounds (Kieronczyk, et al., 2003).

Based on its history of use in food fermentation, *L. lactis* has generally recognised as safe (GRAS) status by the US Food and Drug Administration and is included in the European Food Safety Authority list of microorganisms with "Qualified Presumption of Safety". However, despite being a non-pathogenic bacterium, *L. lactis* strains exhibit adjuvant properties and are able to stimulate various immune responses.

1.6.3 *In vitro* immunostimulatory effects of *L. lactis*

The immunostimulatory effects of *L. lactis* have been investigated *in vitro* through co-incubation of *L. lactis* with different immune cells. *In vitro* co-incubation of a macrophage-like cell line with various strains of *L. Lactis* induced the production of cytokines IL-12, IL-6, and TNFα (Kimoto, et al., 2004; Suzuki, et al., 2008).

In vitro co-incubation of *L. lactis*, with immortalized bone marrow macrophages from B10A.Bcgr congenic strains of mice also induced the transcription of various chemokines, including CCL3/MIP-1α and CCL4/MIP-1β which are ligands of the CCR5 chemokine receptor

that is preferentially expressed on Th1 cells (Yam, et al., 2008). *L. lactis* was also able to induce expression of a Th2 stimulating chemokine, CCL2/MCP-1 (Yam, et al., 2008).

The ability of *L. lactis* to induce the maturation of murine DCs, detected by the increased surface expression of MHC-II and CD86, has also been reported and implies that *L. lactis* is able to elicit adaptive immunes responses (Niers, et al., 2007; Yam, et al., 2008). Co-incubation of DCs with *L. lactis* also induced the expression of proinflammatory cytokines IL-1β and IL-12 which suggests that *L. lactis* exhibits adjuvant properties (Yam, et al., 2008).

1.6.4 *In vivo* immunostimulatory effects of *L. lactis*

Since *L. lactis* has GRAS status and can be safely consumed, the effects of *L .lactis in vivo*, particularly after oral ingestion, have been well researched. Unlike certain other LAB, *L. lactis* does not colonise the human gastro-intestinal (GI) tract. Following oral administration with live *L. lactis* in healthy human volunteers, only 1% of the initial bacterial inoculum was detected in the ileal aspirates at 4 hours, and no bacteria were detected after 5 hours (Vesa, et al., 2000). Similarly, the transit time of *L. lactis* through the GI tract of mice was less than 24 hours (Gruzza, et al., 1994).

Despite the short transit time through the GI tract, oral administration with *L. lactis* can stimulate various *in vivo* immune responses. Mice fed with four daily doses of live *L. lactis* (strain MG1363) demonstrated a slight increase in IFN-γ production in the intestinal mucosa (Pavan, et al., 2003), suggesting that *L. lactis* can stimulate Th1 immune responses *in vivo.* Splenocytes from mice given seven daily doses of live *L. Lactis* (strain G50) showed increased production of Th1 cytokines IL-12 and IFN-γ and a reduction in the Th2 cytokine IL-4 (Kimoto, et al., 2004). When *L. lactis* (strain G50) was co-administered with antigen administered intraperitoneally, there was a reduction in the levels of antigen-specific IgE and IgG1 antibodies in the serum which suggest that *L. lactis* (strain G50) is able to reduce the Th2 immune response while enhancing the Th1-type immune response (Kimoto, et al., 2004). *L. lactis* (strain NZ9000) is also capable of recruiting leukocytes, mainly neutrophils, into murine air-pouches *in vivo*. The

amount of leukocytes recruited by *L. lactis* is similar to *E. coli* and *Salmonella typhimurium* (Yam, et al., 2008).

Oral administration of *L. lactis* (strain NZ9000) has also been shown to improve resistance to *Streptococcus pneumoniae* respiratory infection (Villena, et al., 2008). Mice administered with *L. lactis* and challenged with *S. pneumoniae* demonstrated increased clearance of the pathogen from the lungs, reduced tissue damage, and enhanced production of TNFα in bronchoalveolar lavage fluid. The mice also had increased survival after infection. These effects were due to increased recruitment of neutrophils into the lungs and increased activation of alveolar macrophages. Mice that ingested *L. lactis* also had an enhanced mucosal immune response, demonstrating an increase in the number of cells positive for IgA in the small intestines and bronchus during infection (Villena, et al., 2008).

In addition to the many studies demonstrating the immunostimulating properties of *L. lactis*, as mentioned previously, it is a safe bacterium for human consumption. Given these reasons, a practical application for this bacterium is its use as a live antigen delivery vector.

1.6.5 Using *L. lactis* as a mucosal delivery vector of antigens

Mucosal routes for vaccine delivery have gained an increased interest in modern vaccinology. Mucosal surfaces represent a major entry site of many pathogens. Hence, the ability of a vaccine to induce a local mucosal immune response is an efficient prophylactic strategy. Mucosal vaccination also has an advantage over parenterally administered vaccines in that it can elicit both mucosal and systemic immune responses, generally with reduced adverse side effects (Bermudez-Humaran, et al., 2005). Additionally, mucosal vaccines can be administered without needles and syringes, eliminating the need for trained personnel (Yuki & Kiyono, 2009).

Protective antigens can be delivered to mucosal sites through the use of attenuated pathogenic microorganisms. However, these organisms have the potential to recover their pathogenic potential. Therefore, *L. lactis* has been investigated as a possible alternative to attenuated

pathogens. In addition to its established safety profile and immunostimulating properties, *L. lactis* is a Gram-positive bacterium and, therefore, does not contain endotoxic lipopolysaccharides. *L. lactis* also expresses fewer native exoproteins that can potentially contaminate samples when it is used as a live antigen carrier (Bermudez-Humaran, et al., 2002). Furthermore, *L. lactis* elicits only a weak immune response against itself even though it has immunostimulating properties (K. Robinson, et al., 1997). This is advantageous as immunity against the carrier can lessen the immune response against the expressed vaccine antigens (Sevil Domenech, et al., 2007).

Several expression signals are available for the heterologous protein production in *L. lactis*. Thirty-eight lactococcal promoters that can induce varying amount of protein expression have been analysed and found to be constitutive (de Vos, 1999). Controlled expression of heterologous proteins has also been achieved using inducible promoters. The best-characterised controllable expression systems are the *L. lactis lac* operon encoding the lactose phosphotransferase system and the food grade nisin-controlled expression (NICE) system (de Vos, 1999).

Using a variety of protein expression systems, numerous studies have shown that recombinant *L. lactis* strains heterologously expressing bacterial, viral, or protozoal antigens are able to successfully elicit mucosal and systemic immunes response against the expressed antigen (Bermudez-Humaran, et al., 2011).

1.6.5.1 Delivery of bacterial antigens by *L. lactis*

The first reported use of *L. lactis* as a live vaccine delivery vector utilised recombinant *L. lactis* expressing the tetanus fragment C (TTFC). Subcutaneous immunisation with the recombinant *L. lactis* protected mice against lethal challenge with tetanus toxin (Wells, et al., 1993). Afterwards, the effect of oral and nasal immunisation using *L. lactis* expressing TTFC was evaluated. Oral immunisation in mice elicited lower serum IgG and mucosal IgA antibody responses compared to nasal immunisation, however, both immunisation routes protected mice

against lethal challenge with tetanus toxin (Norton, et al., 1997; K. Robinson, et al., 1997). Interestingly, oral administration of UV-killed *L. lactis* expressing TTFC elicited a protective serum antibody response as well, indicating that colonisation or invasion of the mucosa by recombinant *L. lactis* is not necessary to provide protection. This suggests that *L. lactis* functions as an antigen-loaded microparticle and does not require further expression of the antigen after oral administration (Grangette, et al., 2002).

Live vaccines against *S. pneumoniae* have also been developed using *L. lactis* as the delivery vector. Intranasal immunisation with live *L. lactis* expressing the pneumococcal surface protein A (PspA) antigen was able to protect mice against respiratory pneumococcal challenge. The *L. lactis* vaccine repeatedly elicited protection that was significantly better than that obtained by vaccination of recombinant PspA mixed with alum. In contrast to the recombinant protein vaccine which mainly elicited antigen-specific IgG_1 isotype antibodies, the lactococcal vaccine elicited similar titers of IgG_1 and IgG_{2a} isotype antibodies. This suggests that the protection elicited by the lactococcal vaccine correlated with a shift towards a Th1 immune response (Hanniffy, et al., 2007).

The conserved C-repeat region (CCR) of M protein from *S. pyogenes* serotype 6 has also been expressed in *L. lactis* for use as a live vaccine. Mice were immunised either subcutaneously or intranasally and, while both routes protected mice against the lethal effects of *S. pyogenes* M serotype 14, only intranasal immunisation could protect mice against pharyngeal infection. Protection may be mediated by antigen-specific salivary IgA, which was only produced by intranasal immunisation with the lactococcal vaccine, and this shows the importance of the route of immunisation in generating a mucosal antibody response (Mannam, et al., 2004).

Another vaccine that has been created against group B streptococcus (GBS) utilises *L. lactis* expressing the pilin island 1 from GBS. The efficacy of the vaccine was tested by immunising female mice with recombinant *L. lactis* and then analysing the survival of their offspring after GBS challenge. Significant protection was obtained in the offspring of mice immunised

intranasally with the vaccine. In intranasally vaccinated mice, IgG and IgA antibodies were present in both nasal and vaginal lavages, which is advantageous as the genital tract is the primary site of GBS colonisation in humans (Buccato, et al., 2006).

A multitude of other bacterial vaccine antigens have also been expressed in *L. lactis* to create live vaccines; some of which are listed in table 1.3. These studies support the use of *L. lactis* to deliver bacterial antigens to mucosal sites in order to elicit a protective immune response.

Table 1.3 Bacterial proteins heterologously expressed in *L. lactis*

Protein	Origin	Reference
TTFC	*Clostridium tetani*	(K. Robinson, et al., 1997)
Cag7	*Helicobacter pylori*	(Kim, et al., 2009)
UreB	*Helicobacter pylori*	(M. H. Lee, et al., 2001)
CPS	*Streptococcus pneumonie*	(Gilbert, et al., 2000)
PppA	*Streptococcus pneumoniae*	(Medina, et al., 2008)
PspA	*Streptococcus pneumoniae*	(Hanniffy, et al., 2007)
EspA	Enterhemorrhagic *Escherichia coli*	(Luan, et al., 2010)
FaeG	Enterotoxigenic *Escherichia coli*	(Hu, et al., 2009)
L7/L12	*Brucella abortus*	(Pontes, et al., 2003)
LcrV	*Yersinia pseudotuberculosis*	(Daniel, et al., 2009)
LLO	*Listeria monocytogenes*	(Bahey-El-Din, et al., 2008)
MrpA	*Proteus mirabilis*	(Scavone, et al., 2007)
SpaA	*Erysipelothrix rhusiopathiae*	(Cheun, et al., 2004)

1.6.5.2 Delivery of viral antigens by *L. lactis*

In addition to *L. lactis* expressing TTFC, a seminal study on the feasibility of *L. lactis* as a live vaccine used *L. lactis* expressing human papillomavirus type 16 E7 antigen. The nisin-inducible system was used to express the E7 antigen within the cytoplasm, secreted from the cell using

the Usp45 secretion signal, or anchored on the cell surface using the cell wall anchor domain of the M6 protein of *S. pyogenes*. The intracellular expression of E7 antigen led to its degradation in the cytoplasm. However, the secreted and cell wall-anchored forms did not undergo proteolysis and produced a higher level of E7 in *L. lactis* (Bermudez-Humaran, et al., 2002; Cortes-Perez, et al., 2003). Intranasal immunisation of mice with *L. lactis* expressing E7 as a cell wall-anchored form elicited the highest amount the antigen-specific antibodies in the serum and the highest amount of antigen specific IL-2 and IFN-γ production in re-stimulated splenocytes (Bermudez-Humaran, et al., 2004).

The envelope protein of HIV has also been expressed on the surface of *L. lactis* in an attempt to create a live vaccine for HIV. Oral immunisation of mice with recombinant *L. lactis* elicited high levels of HIV-specific serum IgG and fecal IgA antibodies. Cell-mediated responses were also generated in both the regional lymph nodes and the spleen. *L. lactis* was shown to infect DCs which may be responsible for the development of the immune responses. In addition, vaccinated mice were protected against intraperitoneal challenge with HIV Env-expressing vaccinia virus, producing viral loads which were 350 fold less than the load from control mice (Xin, et al., 2003).

Other viral antigens that were expressed on *L. lactis* to create live vaccines include antigens from severe acute respiratory syndrome (Pei, et al., 2005), rotavirus (Perez, et al., 2005) and dengue virus (Sim, et al., 2008). These studies give further evidence for the use of *L. lactis* to deliver vaccine antigens to mucosal sites.

1.6.5.3 Delivery of parasitic antigens by *L. lactis*

L. lactis live vaccines have also been created against protozoan parasites. The merozoite surface protein-1 protein of *Plasmodium yoelii* was expressed within the cytoplasm of *L. lactis* and oral immunisation of mice with the recombinant *L. lactis* vaccine induced protection against malaria challenge. The immunised mice displayed reduced parasitemia in the blood as well as increased survival following infection (Zhang, et al., 2005).

The merozoite surface antigen-2 of *Plasmodium falciparum* has also been expressed on the cell surface of *L. lactis*. Oral or intranasal immunisation of rabbits with recombinant *L. lactis* elicited antigen-specific IgG antibodies in the serum and IgA antibodies in the intestines (Ramasamy, et al., 2006). Similarly, combined intranasal and oral immunisation of mice with recombinant *L. lactis* also induced antigen-specific IgG antibodies in the serum and IgA antibodies in faecal pellets. MSA2-specific IFN-γ-secreting cells were also detected in the spleens of these immunised mice, which is indicative of a Th1 type immune response (Moorthy & Ramasamy, 2007).

1.6.5.4 Delivery of cytokines by *L. lactis*

In addition to vaccine antigens, *L. lactis* can also be engineered to secrete fully active cytokines. A strain of *L. lactis* engineered to constitutively secrete murine IL-10 was successfully used to treat a mouse model of inflammatory bowel disease. Mice treated with dextran sulfate sodium (DSS) or lacking the IL-10 gene will develop colitis. Oral administration with live *L. lactis* expressing IL-10 was able to reverse DSS–induced colitis in wild-type mice and delay the onset of colitis in IL-10–deficient mice (Steidler, et al., 2000).

L. lactis expressing IL-10 was also used to prevent allergic responses to food. The delivery of *L. lactis* expressing IL-10 into the gut of mice before sensitisation to a common food allergen, β-lactoglobulin, was able to decrease the severity of food-induced anaphylaxis and almost completely abrogate the Th2 responses associated with allergic reaction in mice through the inhibition of antigen-specific IgE and IgG_1 antibodies (Frossard, et al., 2007).

In contrast to using *L. lactis* to down-regulate immune responses with IL-10, *L. lactis* has also been used as an immune stimulator by expressing IL-12, which is a pro-inflammatory cytokine that can stimulate a Th1 type immune response. Co-administration of *L. lactis* expressing IL-12 with a live vaccine strain of *L. lactis* expressing the E7 antigen of HPV-16 increased antigen-specific production of IL-2 and IFN-γ in restimulated splenocytes, in comparison to the

administration of the vaccine strain alone (Bermudez-Humaran, et al., 2003). Furthermore, when challenged with lethal levels of the tumor cell line TC-1, derived from primary lung epithelial cells of C57BL/6 mice, expressing E7, the growth of tumors was prevented in immunised mice, even after a second challenge, suggesting that this prophylactic immunisation can provide long-lasting immunity (Bermudez-Humaran, et al., 2005).

1.6.6 Recombinant *L. lactis* in a clinical trial

The successful use of *L. Lactis* expressing IL-10 to treat colitis in mice raised the possibility of using the engineered *L. lactis* in humans. However, the recombinant strains of *L. lactis* used in mice contained extra-chromosomal plasmids with antibiotic resistance genes for selection. These strains cannot be used in humans due to safety issues such as the possible transfer of antibiotic resistance genes to other bacteria. To overcome this problem, Steidler *et al*. created a bio-containable strain of *L. lactis* by replacing the chromosomal thymidylate synthase (*thyA*) gene with the gene for IL-10 (*thyA* LL-IL10 strain) (Steidler, et al., 2003). The *thyA* gene is needed for the synthesis of thymidine which is essential for bacterial growth. Without thymidine supplementation, the *thyA* LL-IL10 strain will undergo DNA fragmentation and cell death. If the bio-containable strain acquires a functional *thyA* gene by homologous recombination, the IL-10 transgene will be excised. In the absence of thymidine or thymine, the viability of the *thyA* LL-IL10 strain was reduced by several orders of magnitude and the strain exhibited a 20-fold decrease in its viability through the GI tract of pigs in comparison to wild-type *L. lactis* (Steidler, et al., 2003).

The bio-containable strain of *L. lactis* secreting human IL-10 was used to treat patients with Crohn's disease in a phase I clinical trial (Braat, et al., 2006). Ten patients were given capsules containing 10 x 10^{10}colony forming units (CFU) of lyophilized *L. Lactis* twice a day for seven days. To improve bacterial viability in the gut, patients were also treated with a proton pump inhibitor to inhibit the production of gastric acids. The administration of live bacteria was well tolerated and did not induce systemic or long-term side effects. Eight of the ten patients

experienced benefits to the treatment and five of the ten patients went into complete clinical remission, although the lack of a control group prevents conclusions being drawn regarding clinical efficacy (Braat, et al., 2006).

The seminal work done on creating a bio-containable *L. lactis* strain and the approval for its use in a phase I clinical trial shows promise for the application of live recombinant *L. lactis* as a therapeutic tool in humans. Combined with the fact that *L. lactis* provides a genetically tractable carrier in which vaccine antigens can be expressed and delivered, it makes *L. lactis* the ideal carrier for the proposed peptide delivery system using the pilus of GAS.

1.7 Research aim and objectives

The overall aim of this thesis was to develop a novel peptide delivery system by expressing peptide antigens within the group A streptococcus pilus structure on the surface of *Lactococcus lactis* - Pilvax.

This is based on the hypothesis that the presentation of antigens as part of the pilus structure will have several advantages:

1. The pilus subunits have a rigid protease-resistant structure which will provide increased stability to the peptide.
2. Because the backbone pilus subunit homopolymerises, natural amplification of the antigenic peptide engineered within it will occur.
3. Multiple pili are expressed on the surface of *L. lactis* resulting in further amplification of the antigenic peptide.
4. The vaccine antigens will be expressed outside the bacterium and will be exposed to host immune cells.
5. *L. lactis* has adjuvant properties, is biocompatible, and lacks toxicity
6. No chemical coupling is necessary, which saves time and cost of production.
7. *L. lactis* can also be lyophilized which means the vaccine can have a long shelf life.

The first objective of this project was to determine if a peptide can be successfully expressed within the GAS pilus structure on the surface of *L. lactis*. Since the homopolymerisation of the Spy0128 subunits is essential for the amplification of the peptide, it was imperative to engineer peptides into regions of the Spy0128 that will not affect the structure or integrity of the pilus. It was hypothesised that the loop regions connecting the core β strands of Spy0128 may be possible sites for peptide insertion. The model B cell peptide epitope, consisting of ovalbumin (OVA) from positions 323 to 339 ($OVA_{323-339}$), was chosen to be engineered into Spy0128 by replacing selected loop regions with the $OVA_{323-339}$ peptide.

The second objective was to demonstrate if this vaccine strategy was able to induce an OVA-specific mucosal and systemic immune response in an *in vivo* mouse model.

The third objective was to determine if a structural epitope can be presented by this vaccine strategy. The peptide chosen was the J14 peptide, a chimeric peptide that contains 14 amino acids from the conserved C-region of the GAS M-protein. The J14 peptide is known to require presentation as a coiled-coil structure in order to generate protective antibodies against GAS.

Chapter 2

Materials and Methods

Materials

2.1 Molecular biology reagents

If not declared otherwise, buffer constituents and solvents were purchased from BD, Scharlau and Sigma-Aldrich. All buffers, solutions and media were prepared using Type I/18 M-ohm/cm MilliQ water unless otherwise stated.

2.1.1 Common buffers

Phosphate-buffered Saline (PBS)	120 mM NaCl, 2.7 mM KCl, 10 mM phosphate salts, pH 7.4
TAE	2 mM EDTA, 0.1 % (v/v) glacial acetic acid (Merck), 40 mM Tris pH 8.0

2.1.2 DNA

a) Reagents

DNA Loading buffer (6x)	30 % (v/v) glycerol (Labserv), 0.25 % (w/v) bromophenol blue, 0.25 % (w/v) xylene cyanol (Serva), 50 mM Tris pH 7.6
PCR buffer (10x)	500 mM KCl, 0.1 % (v/v) Triton-X 100, 100 mM Tris pH 8.3

b) Plasmids

Table 2.1 Plasmid vectors used for DNA manipulation and protein expression

Name	Selection marker	Source	Details
pBlueScript	Ampicillin	Stratagene	Cloning Vector
pET32a-3C	Ampicillin	Dr. Ries Langley (University of Auckland, New Zealand)	A modified version of pET32a (Novagen) with the 2T trypsin cleavage site replaced by a 3C protease cleavage site
pGEX-3c	Ampicillin	Dr. Thomas Proft (University of Auckland, New Zealand)	A modified version of pGEX-2T (Pharmacia) with the 2T trypsin cleavage site replaced by a 3C protease cleavage site.

Table 2.2 Plasmid vector used for heterogeneous expression of the GAS M1 pilus on the surface of *L. lactis*

Name	Selection marker	Source	Details
pLZ12-Km2:P23R	Kanamycin	Dr. Jacelyn Loh (University of Auckland, New Zealand)	An *E. coli* – GAS shuttle vector containing the lactococcal promoter P23

c) Synthetic oligonucleotides

Table 2.3 Primers used for single colony PCR. Custom made oligonucleotides were purchased from Sigma

Primer name	Description	Sequence 5'-3'
Spy0125 fw	Binds to the *spy0125* gene of the GAS M1 pilus	GGATCCAAGACTGTTTTTGGTTTAG
Spy0130 rv	Binds to the *spy0130* gene of the GAS M1 pilus	GAATTCTTAACCATTACGTTTTTTCTG
Spy0127 fw	Binds to the *spy0127* gene of the GAS M1 pilus	CTATTAACGGGAGCAGCC
Spy0128 fw	Binds to the *spy0128* gene of the GAS M1 pilus	GGAGCAGCCCTAACTAGTTTTGC
Spy0128 rv	Binds to the *spy0128* gene of the GAS M1 pilus	GAGCTCCACCAACTGCTACAATTC
OVA fw	Binds to the $ova_{323-339}$ DNA sequence	GCTGTTCATGCTGCACATGC
J14 fw	Binds to the J14 DNA sequence	CGGGATCCCTCGAGAAACAAGCTG

***Streptococcus pyogenes SF370 (serotype M1) was used as the reference genome for primer design**

Table 2.4 Primer pairs used to insert an XhoI site into a region of Spy0128. Custom made oligonucleotides were purchased from Sigma

Primer Name	Description	Sequence
Spy0128_ β_B -Xho -F,R	Replaces the β_B-β_{C1} loop region with an XhoI site	F:5'-GAGAGAGACTCGAGGGAAA TAAGTTTAAAGGTGTAGC- 3' (XhoI) R:5'-GAGAGAGACTCGAGAGTATC AGGTTCGATTTTAAATG- 3' (XhoI)
Spy0128_ β_2-Xho -F,R	Replaces the β_2-β_3 loop region with an XhoI site	F: 5'-GAGAGAGACTCGAGTCAGAA AAAGTCATGATTGAG- 3' (XhoI) R:5'-GAGAGAGACTCGAGTGCTTT TAAAGTCAGACC- 3' (XhoI)
Spy0128_ β_3-Xho -F,R	Replaces the β_3-β_4 loop region with an XhoI site	F: 5'-GAGAGAGACTCGAGCCTGTT CAAACAGAGGCTAG- 3' (XhoI) R: 5'- GAGAGAGACTCGAGAGTTG TCTTCTCAATCATGAC- 3' (XhoI)

Spy0128_ β_D -Xho -F,R	Replaces the β_D-β_E loop region with an XhoI site	F: 5'- GAGAGAGACTCGAGGGTG TTTATTATTACAAAG- 3' (XhoI) R: 5'- GAGAGAGACTCGAGAAAA TCAAATTCTGCAG- 3' (XhoI)
Spy0128_β_E-Xho -F,R	Replaces the β_E-β_F loop region with an XhoI site	F:5'- GAGAGAGACTCGAGGGTGT TTCTTATGATACAAC- 3' (XhoI) R:5'- GAGAGAGACTCGAGCTCCT CAGTTACTTTG- 3' (XhoI)
Spy0128_β_9-Xho -F,R	Replaces the β_9-β_{10} loop region with an XhoI site	F:5'- GAGAGAGACTCGAGAAAAA TATCGCAGGTAATTC- 3' (XhoI) R:5'- GAGAGAGACTCGAGTTGAG GACTAACTTCCACG- 3' (XhoI)
Spy0128_N29-Xho -F,R	Inserts an XhoI site at amino acid position 29 of Spy0128	F:5'- CCCGCTCGAGGGAGCCAAAC TAACAGTTAC- 3' (XhoI) R:5'- CCCGCTCGAGGTTTACAACA GTCTCCCC- 3' (XhoI)

Restriction sites are underlined

2.2 Bacterial culture reagents

2.2.1 Media

Luria-Bertani (LB) broth	2.5 % (w/v) LB powder (HiMedia)
GM17 broth	3.725 % (w/v) M17 powder (BD), 0.5 % (w/v) glucose
Brain Heart Infusion Broth (BHI)	3.7% (w/v) BHI powder
Agar plates	Media broth containing 1.5% Bacto agar

2.2.2 Selective antibiotics

All antibiotics were purchased from Sigma

Kanamycin (Kan)	Used at a final concentration of 50 µg/mL (*E. coli* culture)
	Used at a final concentration of 200 µg/mL (*L. lactis* culture)
Ampicillin (Amp)	Used at a final concentration of 50 µg/mL
Chloramphenicol (Cm)	Used at a final concentration of 30 µg/mL

2.2.3 Bacterial Strains

Table 2.5 List of bacterial strains used

Bacterial Strain	Characteristics	Source
DH5α	Escherichia coli with genotype F– Φ80*lac*ZΔM15 Δ(*lac*ZYA-*arg*F) U169 *rec*A1 *end*A1 *hsd*R17 (rK–, mK+) *pho*A *sup*E44 λ– *thi*-1 *gyr*A96 *rel*A1	ATCC PTA-1789
AD494(DE3)pLysS	Escherichia coli with genotype F– *omp*T *hsd*SB(rB–, mB–) *gal dcm* (DE3) pLysS (CamR)	Novagen
L. lactis M1363	Strain used for heterogeneous expression of the GAS M1 pilus	Nicolas Heng, (University of Otago, New Zealand)
GAS M1 SF370	Wildtype GAS	ATCC 700249

2.2.4 Buffers for preparation of competent cells

TFB I (sterile filter)	30 mM potassium acetate, 50 mM $MgCl_2$, 100 mM RbCl, 5 mM $CaCl_2$, 15 % (v/v) glycerol. Adjusted to pH 5.8 with 1 M HCl, stored at -20°C
TFB II (sterile filter)	10 mM MOPS pH 7.0, 75 mM $CaCl_2$, 10 mM RbCl, 15 % (v/v) glycerol, stored at -20°C

2.3 Protein expression and functional analysis

2.3.1 Reagents

Protoplast buffer	40 % (w/v) sucrose, 100 mM K_2HPO_4, 10 mM $MgCl_2$, 2 mg lysozyme, 40 U mutanolysin, 1 tablet of cOmplete, Mini, EDTA-free protease inhibitor (Roche)
MCAC-0	20 mM Tris.HCl pH7.9, 0.5 M NaCl, l0% glycerol
MCAC-1000	20 mM Tris.HCl pH7.9, 0.5 M NaCl, 10% glycerol, 1M imidazole
GSH buffer l	25 mM Tris.HCl pH 7.4, 50 mM NaCl, 1 mM EDTA
GSH buffer 2	25 mM Tris.HCl pH 7.4, 500 mM NaCl, 1 mM EDTA
GSH buffer 3	25 mM Tris.HCl pH 7.4, 50 mM NaCl, 1 mM EDTA, 5 mM glutathione, 1 mM DTT
SDS-PAGE loading buffer	125 mM Tris pH 6.8, 20 % (v/v) glycerol, 0.3 M 2-mercaptoethanol, 4 % (w/v) SDS, $lxl0^{-4}$ % (w/v) bromophenol blue
SDS-PAGE gel solution A	30% (w/v) acrylamide, 0.8% (w/v) bisacrylamide (Carl Roth)
SDS-PAGE gel solution B	0.4% (w/v) SDS, 1.5 M Tris.HCl pH8.8
SDS-PAGE gel solution C	0.4% (w/v) SDS, 0.5 M Tris.HCl pH6.8
SDS-PAGE running buffer	0.1 % (w/v) SDS, 250 mM glycine, 25 mM Tris pH 8.0
Coomassie stain	0.06 % (w/v) Brilliant Blue R-250, 50 % (v/v) ethanol (Labserv), 7.5 % (v/v) acetic acid
Coomassie destain	25 % (v/v) ethanol, 8 % (v/v) acetic acid
ELISA Coating buffer	15 mM Na_2CO_3, 35 mM $NaHCO_3$, pH 9.6

PBS-T	PBS with 0.05% (v/v) Tween-20
Towbin transfer buffer	25 mM Tris.HCl pH8.3, 192 mM glycine, 0.375% (w/v) SDS, 20% (v/v) methanol (Merck)
TBS	10 mM Tris pH 8.0, 120 mM NaCl
TBS-T	TBS with 0.1 % (v/v) Tween 20
Blocking solution	TBS-T with 5% (w/v) non-fat dairy milk powder (Fonterra)
Probing solution	TBS-T with 2.5% (w/v) non-fat dairy milk powder

2.3.2 Antibodies

Table 2.6 Summary of commercial antibodies used

	Species	Source	Dilution
Anti-rabbit IgG:HRP	Goat	BD Biosciences	1:10,000
Anti-mouse IgG:HRP	Goat	BD Biosciences	1:8000
Anti-mouse IgG1:HRP	Goat	Life Technologies	1:1000
Anti-mouse IgG2a :HRP	Goat	Life Technologies	1:1000
Anti-mouse IgA:HRP	Goat	Life Technologies	1:10,000
Anti-mouse IgG:FITC	Goat	Abcam	1:50

2.3.3 Peptides

$OVA_{323-339}$ ISQAVHAAHAEINEAGR represents a peptide consisting of ovalbumin from positions 323 to 339. Synthesised by Peptide 2.0 inc.

2.4 Murine cell culture reagents

Complete RPMI	Roswell Park Memorial Institute media 1640 pH 7.4 supplemented with 50 U/mL penicillin, 50 μg/mL streptomycin, 2 mM L-glutamine, 110 μg/mL sodium pyruvate, and 10% fetal calf serum (FCS) that had been heat inactivated for 30 min at 56 °C (all from Life Technologies)
2-ME	$5x10^{-5}$ M 2-mercaptoethanol was added to complete RPMI before use

2.5 Mouse strains

The BALB/c, CD1, and FVB/n mouse strains used in this thesis were purchased from the animal resources unit (University of Auckland, New Zealand)

2.6 Methods for DNA work

2.6.1 Plasmid extraction from *E. coli* DH5α

Plasmid DNA was extracted using the QIAprep Spin Miniprep Kit (Qiagen). Briefly, 5 mL of LB media was inoculated with *E. coli* DH5α containing the plasmid of interest and the appropriate antibiotics were added. The culture was incubated overnight at 37 °C with shaking (200 rpm). The following day, the cells were harvested by centrifugation at 4,369 *g* for 15 min using a Heraeus® Multifuge® 3SR centrifuge with a TTH-750 swing bucket rotor (Thermo Scientific) and the plasmid DNA was purified according to the manufacturer's instructions provided with the kit. DNA was quantified by UV spectrophotometry using a Nanodrop ND-1000 Spectrophotometer (Thermo Scientific). Plasmid DNA was stored at -20 °C.

2.6.2 Agarose gel electrophoresis

Plasmid DNA was analysed using Agarose gel electrophoresis. Gels were prepared by dissolving 1% (w/v) agarose in TAE-buffer using a microwave. DNA samples were mixed with 6x DNA loading dye at a ratio of 6:1 and loaded into the wells of the gel. DNA was separated by applying an electric field of 100 V and 400 mA. Gels were stained in TAE buffer containing SYBR® Safe DNA gel stain (Life Technologies) at a dilution of 1:10,000 and visualized using a Gel Doc® EZ Imager (Bio-Rad).

2.6.3 Polymerase chain reaction (PCR)

PCR amplification of plasmid DNA was carried out in a MyCycler™ thermal cycler (Bio-Rad) with a reaction mix of 100 ng of plasmid DNA, 0.5 µM concentrations of specific primers, 200 µM of each deoxynucleoside triphosphate, 10X iProof HF Buffer and 2 U of iProof™ High-Fidelity DNA Polymerase (Bio-Rad). The plasmid DNA was amplified under the following conditions:

- Step 1 (single cycle)

  Initial denaturation: 98 ºC for 30 s

- Step 2 (25 cycles):

  Denaturation: 98 ºC for 10 s

  Annealing: 60 ºC for 30 s

  Extension: 72 ºC for 3 min 30 s

- Step 3 (single cycle):

  Final extension: 72 ºC for 5 min

Single colony PCR was carried out in a MyCycler™ thermal cycler (Bio-Rad) with a reaction mix of 2.5 U Taq polymerase (produced in *E. coli* by Prof. John Fraser, University of Auckland, New Zealand), 1× PCR buffer, 2.5 mM $MgCl_2$, 100 uM of each deoxynucleoside triphosphate, 0.2 µM concentrations of specific primers, in a total volume of 25 µL. The bacterial colonies were screened under the following conditions:

- Step 1 (single cycle)

  Initial denaturation: 95 ºC for 5 min

- Step 2 (15 cycles):

  Denaturation: 95 ºC for 30 s

  Annealing: 53 ºC for 1 min

  Extension: 72 ºC for 1 min

- Step 3 (single cycle):

  Final extension: 72 ºC for 10 min

2.6.4 Purification of PCR products

PCR products were purified using the QIAquick PCR Purification kit (Qiagen) following the manufacturer's instructions or through gel electrophoresis after SYBR® Safe staining. If gel electrophoresis was used, PCR products were extracted from the gel using the freeze-thaw method. The PCR product was excised from the gel using a razor blade and the gel slice was frozen at -80 ºC for 10 min. The slice was thawed at room temperature (RT) and grinded into small pieces. The pieces were flash frozen in dry ice/ethanol bath and transferred to the top of a filter pipette tip sitting in an Eppendorf tube. The gel pieces were allowed to thaw and the Eppendorf tube was centrifuged at 15,600 *g* for 1 min using a Spectrafuge™ 24D Micro Centrifuge (Labnet) to elute the DNA through the filter.

2.6.5 Restriction enzyme digestion of DNA and Phenol/Chloroform purification

Restriction enzymes (Roche) were used with the corresponding buffers according to the manufacturer's instructions. The total volume of enzymes added was no more than 10% of final reaction volume. If linearised plasmids were obtained, 5 U of calf intestinal alkaline phosphatase (CIP) was added for another 30 min at 37 ºC to prevent self-ligation. The reaction mix was purified using Phenol/Chloroform extraction and ethanol precipitation. Equivalent volume of chloroform and Tris-saturated phenol (1:1) was added to the DNA sample (with a minimum volume of 100 µL), vortexed for 20 s, and centrifuged at 15,600 *g* for 1 min. The upper aqueous phase was transferred into a new Eppendorf tube for ethanol precipitation. To precipitate DNA, sodium acetate at a concentration of 0.3 M and 2 volumes of 100% ethanol was added and the reaction mix was incubated on ice for 10 min. The Eppendorf tube was centrifuged for 10 min at 15,600 *g* and all the supernatant was removed. The precipitated DNA pellet was finally resuspended in milliQ water.

2.6.6 Ligation reaction

The linearised plasmid vector and DNA insert was mixed using an insert: vector ratio of 3:1 and ligated using the rapid DNA ligation kit (Roche) according to the instructions provided with the kit. The mixture was incubated for 30 min at RT before transformation into chemically competent *E. coli* DH5α.

2.6.7 Preparation of chemically competent DH5α

A single colony of *E. coli* DH5α from a freshly streaked plate was inoculated in 5 ml of LB, supplemented with 10 mM KCl and 20 mM $MgSO_4$, and incubated overnight at 37 °C with shaking (200 rpm). The following day, 100 ml of LB broth containing 10 mM KCl and 20 mM $MgSO_4$ was inoculated with 1ml of the overnight culture and incubated at 37°C with shaking until the optical density at a wavelength of 600 nm (OD_{600}) reached 0.4-0.6. The cells were harvested by centrifugation at 4,369 *g* for 10 min at 4 °C. The cell pellet was resuspended in 60 mL of ice-cold TFB I and chilled on ice for 10 min. The cells were then centrifuged at 4,000 *g* for 5 min at 4 °C and the cell pellet was carefully resuspended in 4 mL ice cold TFB II. Aliquots of 50 µl were flash frozen in a dry ice/ethanol bath and stored at -80 °C.

2.6.8 Transformation of chemically competent *E. coli*

50 µl aliquots of chemically competent cells were thawed on ice, and then incubated with 2 µL of the ligation mixture for 10 min at 4 °C. Bacteria were heat shocked in a water bath at 42 °C for 45 s, then immediately chilled on ice for 5 min. 500 µL of LB broth was added to the cells and incubated at 37 °C for 30 min. Bacteria were collected by centrifugation at 2,300 *g* for 5 min, then 400 µL of the supernatant was removed, and the bacteria were resuspended in the remaining 100 µL of LB broth. Bacteria were plated onto LB agar plates containing the appropriate antibiotics and grown overnight at 37 °C.

2.6.9 Preparation of electrocompetent *L. lactis*

A single colony of *L. lactis* MG1363 from a freshly streaked plate was inoculated in 1.5 ml of GM17 and grown overnight statically at 28 °C. The following day, 1 ml of overnight culture was used to inoculate 50 mL of fresh GM17 medium and this was incubated at 28 °C until an OD600 of 0.4 - 0.6 was reached. The cells were harvested by centrifugation at 4,369 g for 10 min at 4 °C. The cells were kept on ice or in a cooling centrifuge from this point onwards and all solutions used to create electrocompetent cells were chilled on ice before use. The cell pellet was washed twice with 4 mL of milliQ water, once with 2 mL of 50 mM EDTA and once with 2 mL of 0.3 M sucrose. All washing steps were done with centrifugation at 4,369 *g* for 5 min at 4 °C. After washing, the cell pellet was gently resuspended in 0.4 mL of 0.3 M sucrose and used immediately for electroporation.

2.6.10 Electroporation of electrocompetent *L. lactis*

1 μg of purified plasmid DNA was mixed with 50 μL of electrocompetent *L. lactis* cells and incubated on ice for 5 min. the mixture was transferred to a chilled electroporation cuvette (2 mm, Bio-rad) and electroporated using a Gene Pulser XCell (Bio-Rad) at 1.05 kV/mm, 25 μF capacitance and 200 Ω resistance. 1 ml of GM17 medium was added to the cuvette and the bacterial cells were transferred into an Eppendorf tube and incubated at 28 °C for 2 hours. Cells were collected by centrifugation at 4,369 *g* for 5 min and, after removing 950 μL of the supernatant, the cells were resuspended in the remaining 50 μL. The cells were then plated onto GM17 agar with appropriate antibiotics. Single colony PCR was used to confirm if the electroporation was successful.

2.7 Methods for protein work

2.7.1 Protein production

2.7.1.1 Inducing protein expression for purification in *E. coli*

LB broth (100 ml) containing the appropriate antibiotics were inoculated with bacteria carrying the plasmid of interest and left overnight at 37 °C, 200 rpm. The following day, the 100 mL culture was added to 900 mL of LB containing the same antibiotics and left shaking at 37 ºC for 1.5 hours. The culture was then cooled to approximately 30 ºC before inducing expression by adding 0.1 mM IPTG. Bacteria were incubated at the induction temperature for 4-5 hours with constant shaking. The bacteria were pelleted at 4,369 *g* for 20 min and then frozen at -20 ºC overnight.

2.7.1.2 Protein purification

Frozen bacterial pellets were resuspended (10% w/v) in the appropriate lysis buffer (GSH Buffer 1, 1% tritonX for the pGEX system, or MCAC-0, 1% tritonX for the pET system) containing 0.1 mM PMSF. The bacteria were sonicated using a Qsonica sonicator Q700 (Alpha Technologies Ltd) at an amplitude of 50 for two rounds of 1 min duration. Cell debris was pelleted by centrifugation at 8,000 g for l0 min at 4 ºC and lysate was retained for protein purification by GSH or Nickel affinity chromatography.

a) GSH affinity chromatography

GSH affinity chromatography was used with the pGEX expression system that produced recombinant proteins as a fusion with Glutathione-S-transferase (GST). GSH agarose was obtained from Ms. Fiona Clow (University of Auckland, New Zealand). A column containing the GSH agarose was equilibrated with l0 column volumes (CV) of GSH buffer I before cell lysate was passed through. The column was then washed with l0 CV of GSH buffer 2 and the fusion protein eluted with GSH buffer 3, with 1 ml fractions collected. The eluted fractions containing the fusion protein were pooled together and dialysed overnight into PBS at 4 °C.

b) Nickel affinity chromatography

Ni^{2+} affinity chromatography was used with the pET expression system that produced recombinant proteins as a fusion with Thioredoxin. A column was loaded with Profinity IMAC Ni-Charged Resin (Bio-Rad) and equilibrating with 10 column volumes (CVs) of MCAC-0. Cell lysate was passed over the column, and the column was then washed with l0 CV of MCAC-10 buffer. The fusion protein was then eluted in a step-wise process using MCAC-0 containing a range of imidazole concentrations (20 mM to 150 mM). The eluted fractions containing the fusion protein were pooled together and dialysed overnight into PBS at 4 °C.

2.7.2 Sodium Dodecyl Sulphate – Polyacrylamide Gel Electrophoresis (SDS-PAGE)

2.7.2.1 Preparation of SDS-PAGE

Protein samples were separated and analysed using denaturing SDS-PAGE in a Hoefer SE 245 dual gel caster unit (Amersham Biosciences). For a single 10 % running gel, 1.65 mL solution A, 1.25 mL solution B and 2.1 mL milliQ water were mixed. For a single 15 % running gel, 2.63 mL solution A, 1.25 mL solution B and 2.1 mL milliQ water were mixed. Polymerisation was catalysed by adding 4 μLs of TEMED and 30 μLs of 10 % ammonium persulphate (APS) and the gel was immediately poured into the gel caster unit. Water saturated butanol was added to level the surface. Butanol was removed after the gel solidified, and the stacker gel, containing 0.25 mL solution A, 0.415 mL solution C, 1.0 mL milliQ water, 1.65 μL TEMED, and 20 μL 10 % APS, was poured onto the running gel. A 10 well comb was inserted afterwards.

2.7.2.2 Protein separation by SDS-PAGE

Protein samples, mixed with an equal volume of 2x SDS-PAGE loading buffer were incubated at 95 ^{o}C for 5 min. Samples were loaded onto a polyacrylamide gel and run at 20 mA (100-200 V) in SDS-PAGE running buffer until the loading buffer was no longer visible.

2.7.2.3 Coomassie blue staining of SDS-PAGE gels

Proteins on SDS-PAGE gel were visualised by staining the gel with coomassie stain for at least 30 min at RT with shaking (~45 rpm). The gel was rinsed with deionised water and destained with shaking in destaining solution with tissue paper overlaid to absorb excess dye.

2.8 Analyses of recombinant *L. lactis*

2.8.1 Cell wall extract

A single colony of *L. lactis* containing the plasmid of interest was inoculated in 50 ml of GM17 medium and incubated statically at 28 °C overnight. The next day, the culture was centrifuged at 4,369 *g* for 10 min at 4 °C and the cell pellet washed once with PBS. The cell pellet was resuspended in 1ml of cold protoplast buffer and incubated for 3 hours at 37 °C. The supernatant was isolated by centrifugation at 15,600 *g* for 15 min at 4 °C and stored at -20 °C. To detect Spy0128 protein, the supernatant was mixed with an equal volume of 2x SDS-PAGE loading buffer before analyses by Western Blot. To detect OVA or J14 peptides expressed within the pilus, the cell wall extract was concentrated using Trichloroacetic acid (TCA) protein precipitation. Proteins in the 1 ml culture supernatant of *L. lactis* were precipitated with an equal volume of 20 % (v/v) ice cold TCA and incubated at 37 °C for 1 hour. The sample was centrifuged at 15,600 *g* for 15 min at 4 °C, washed once with ice cold ethanol and dried. The supernatant was discarded and the pellet was resuspended in SDS-PAGE loading buffer for analyses by Western Blot.

2.8.2 Western Blotting analyses

The cell wall extracts run on an SDS-PAGE gel were transferred to a nitrocellulose membrane (Pall Life Sciences) using a TE77 semi-dry transfer unit (Hoefer) at 50 mA/gel for 1 hour. Benchmark Prestained Ladder (Life Technologies) was used to determine if the transfer was successful. The membrane was blocked for 1 hour with 5% (w/v) milk powder /TBS-T at RT. The membrane was then probed with primary antibody at an optimised concentration in 2.5%

(w/v) milk powder /TBS-T and incubated overnight at 4 °C with shaking (50rpm). Unbound probe was removed by washing three times with TBS-T for 5 min each at RT with shaking. The membrane was then incubated with a secondary antibody coupled to horseradish peroxidase, diluted 1:10,000 in a probing solution of 2.5% (w/v) milk powder /TBST, for 1 hour with shaking and washed as above. Immobilised complexes were visualised using chemiluminescence achieved through the ECL western Blotting Detection Reagents (Amersham) and detected by the Fujifilm LAS-3000 developer (Alphatech).

2.8.3 Flow cytometry

A single colony of the bacterium of interest was inoculated in 1.5 ml of the appropriate medium and incubated overnight. The following day, 1 ml of the overnight culture was used to inoculate 15 mL of medium and the culture was incubated at the appropriate temperature until an OD600 of 0.4-0.6 was reached. The bacteria were washed twice with 1X PBS, resuspended in 2.5% BSA/PBS, and incubated for 30 min at RT on a rotator. The bacteria were again washed twice with 1X PBS and resuspended in 0.1%BSA /PBS at an OD600 of 0.15. 200 µL of the bacteria were taken and incubated in a 1:200 dilution of primary antibody for 30 min on ice. The bacteria were washed twice with 0.1% BSA/PBS and resuspended in 100 µL of 0.1% BSA /PBS, containing a 1:50 dilution of Goat Anti-Mouse IgG:FITC, for 30 min on ice. Incubation with Goat Anti-Mouse IgG:FITC without primary antibodies was performed to determine background fluorescence and incubation with primary antibody alone was performed to determine autoflourescence. Following incubation, the bacteria were washed twice in 0.1% BSA /PBS and resuspended in 4% paraformaldehyde/PBS for 15 min at RT to fix the cells. The bacteria were then washed twice with 0.1% BSA/PBS, resuspended in 0.5ml 0.1% BSA/PBS, and measured by flow cytometry using an LSR II (BD Biosciences) with FACS Diva v 6.1.3 software.The Laser used to detect FITC fluorescence was the 488 nm Laser at a voltage of 590 Volts. The filter set used were the 530/30 band pass filter and the 505LP Dichroic mirror.

2.9 Experimental animal models and techniques

Animals were housed and cared for under specific-pathogen-free conditions in accordance with the Animal Welfare Act (1999) and institutional guidelines provided by the University of Auckland Animal Ethics Committee, which reviewed and approved these experiments (AEC protocol number 001059).

2.9.1 Bioluminescent imaging (BLI)

Mice, under anesthesia, were administered with 50 µl of bioluminescent *L. lactis* (1×10^9 CFU) in PBS intranasally. Mice were imaged at the required time points, 5 min after intranasal administration of 25 µl luciferin (15 mg/ml), using the IVIS^R Kinetic optical imaging system (Caliper Life Sciences) with Living Image® 3.2 software.

2.9.2 Vaccine formulations

a) Pilvax and negative control (*L. Lactis*:pLZ12-Km2:P23R_PilM1)

The Pilvax and negative control strains were grown in GM17 media with kanamycin until an OD of 0.5 was reached. Cells were centrifuged and resuspended in 10% glycerol/PBS at an OD of 20. 0.5 ml aliquots were frozen at -80°C. Multiple samples were tested for bacterial enumeration. Western blot of cell wall extracts were confirmed for pilus expression. On a day of immunisation, the bacterial aliquots were thawed, washed in PBS and resuspended at $4x10^9$ or $4x10^{10}$ CFU/ml. Mice were immunised with $1x10^9$ CFU/mouse in a volume of 25 µl or 50 µl.

b) Cholera toxin B (CTB)

Antigens were diluted to 50 µg/ml in PBS and mixed with 10 µg/ml of CTB (Sigma) prior to immunising mice with a volume of 25 µl or 50 µl.

c) Incomplete Freund's adjuvant (IFA)

Antigens were diluted to 50 µg/ml in 125 µl of PBS and emulsified 1:1 in IFA (Sigma) prior to immunising mice with a volume of 250 µl.

2.9.3 Immunisations

2.9.3.1 Intranasal Immunisation

Female mice, 5-6 weeks old, were inoculated intranasally (i.n.) by administration of 50 µl of the vaccine formulation into the nostrils. The mice were inoculated once every two weeks for a total of 4 immunisations (i.e., the animals were vaccinated on days 1, 14, 28, and 42).

2.9.3.2 Subcutaneous immunisation

Female mice, 5-6 weeks old, were inoculated subcutaneously by injecting 250 µL of the vaccine formulation into the nape of the neck. Mice were inoculated once every two week for a total of four immunisations.

2.9.4 Collection of blood

Blood was collected from the tail vein prior to immunisation and 7 days after each immunisation. At the conclusion of the experiment (day 49), blood was collected by cardiac puncture from euthanised mice. Blood was collected in Microvette® 500 Z-Gel tubes (Sarstedt). Serum was separated from red blood cells by centrifugation at 10,000 g for 5 min and stored at -20 °C.

2.9.5 Collection of saliva

Saliva samples were obtained by rinsing the mouth of euthanised mice three to four times with 150 µl of PBS, pH 7.4. Saliva samples were stored at -20 °C for analysis.

2.9.6 Collection of bronchoalveolar lavage fluid

Bronchoalveolar lavage fluid (BALF) was collected by inserting a 1 ml syringe into the exposed trachea of euthanised mice and injecting and withdrawing 1 ml of PBS. The BALFs were then stored at -20 °C for analysis.

2.9.7 Immunological assays

2.9.7.1 Dot blot immunoassay

Proteins (2 μl) were spotted onto a nitrocellulose membrane and air dried. The membrane was blocked with 5% (w/v) milk powder/TBS-T for 1 hour at RT before being washed for 15 min with TBS-T. The membrane was then incubated for 1 hour with serum from immunised mice (1:100 dilution) in 2.5% (w/v) milk powder/TBS-T at RT with gentle shaking. Unbound probe was removed by washing three times with TBS-T for 5 min each at RT with shaking. Afterwards, the membrane was incubated with anti-mouse IgG-HRP (1:8,000) in 2.5% (w/v) milk powder /TBS-T for 1 hour with shaking and washed as above. Immobilised complexes were visualised using chemiluminescence achieved through the ECL western Blotting Detection Reagents (Amersham) and detected by the Fujifilm LAS-3000 developer (Alphatech).

2.9.7.2 Enzyme-Linked Immunosorbent Assay (ELISA)

Maxisorp microtitre plates (Nunc) were coated overnight at 4 °C with antigen (1 µg/well Spy0128 protein or M-protein, 10 µg/well ovalbumin or GST-J14) in carbonate coating buffer (100 µl/well). On the following day, the plates were washed 3 times with PBS-T (PBS with 0.05% Tween-20) and blocked with 3% BSA/PBS-T for 15 min. After blocking, the plates were washed 3 times with PBS-T. Serum from immunised mice was diluted 1:200 in PBS-T and added to the top row of the plates. The serum was then serially diluted 1:2 down the plates and the plates incubated for 3 hours at room temperature. Following incubation, the plates were washed 5 times with PBS-T. Secondary antibody was diluted to the appropriate concentration in PBS-T and applied to all the wells. The plates were then incubated for 90 min at room temperature. After 5 final washes, 3', 5, 5'-Tetramethylbenzidine (TMB) was added to the plates (100 µl/well) and the reaction was allowed to progress in the dark for 10-20 min. The reaction was stopped using 1 M HCl (100 µl/well). The absorbance of each well was measured at 450 nm using the EnSpire® Multimode Plate Reader (PerkinElmer). The endpoint titres were determined as the highest dilution producing a signal above the mean plus 3 standard deviations of the reading obtained from the negative control mice. Antibody responses from BALF and saliva were also determined by ELISA except that undiluted samples were used.

2.9.7.3 In vitro proliferation assays

Spleen cells were excised from immunised animals 7 days after the last immunisation (day 49). Single cell suspensions were prepared by forcing tissue through a Falcon® 70µm Cell Strainer (Corning). Lymph node cells were washed once in RPMI and resuspended at $2xl0^6$ cells/ml in RPMI/ 2-ME. The splenocytes were separated from red blood cells using Histopaque®-1083 (Sigma) following the manufacturer's instructions. The splenocytes were then washed once and resuspended at $2xl0^6$ cells/ml in RPMI/ 2-ME. Cells ($2x10^5$/well) were added into flat bottomed 96 well plates and stimulated with titrated antigen in a total volume of 200 µl. Each antigen

concentration was setup in triplicate. Plates were incubated at 37 ^{o}C in 5% CO_2 and proliferation was quantified by adding 0.25 µCi ^{3}H-thymidine (Amersham) per well on day three. Cells were harvested ~16 hours later onto printed fibreglass filter mats (Wallac), using a Mach III 96 well harvester (Tomtec). Filter mats were left to dry and then sealed in sample bags (Wallac) containing Betaplate scintillation fluid (Wallac). Radioactivity was measured using a Wallac Jet 1450 Microbeta Trilux liquid scintillation counter (Wallac). Proliferation was measured by the incorporation of ^{3}H-thymidine into the cell genome during replication.

2.10 Statistics

All plots were created and statistical analyses performed using GraphPad Prism® 5.02 (GraphPad Software, Inc.), with *p* values of <0.05 considered statistically significant. Details of the tests applied are in the figure legends.

Due to the small sample sizes used in the experiments, parametric tests were used to analyse statistical significance. The Analysis Of Variance was used in Chapter 4 as the antibody production in four different mice groups were compared: mice immunised with Pilvax, mice immunised with the negative control of *L. lactis* expressing wild-type pilus, mice immunised intranasally with synthetic OVA mixed with CTB, and mice immunised subcutaneously with synthetic OVA emulsified in IFA. There was only one factor being studied, the production of antibody (IgG or IgA), so one-way ANOVA was used. In order to compare the mean from each group to every other mean, the Bonferroni correction method was used. The Tukey post hoc test is usually used when testing large numbers of means so Bonferroni correction method was preferred. Since a scatter plot was used to display the data which gave an indication of the variability between individual mice of the group, the standard error of the mean was used to determine the deviation of the sampling distribution instead of standard deviation.

In Chapter five, when a graph showed that both the mice immunised with the negative control of *L. lactis* expressing wild-type pilus and mice immunised subcutaneously with Thioredoxin-J14 emulsified in IFA had only background activity, the t-test was used to determine the statistical significance between the group of mice immunised with Pilvax and the group of mice immunised with the *L. lactis* expressing wild-type pilus.

Chapter 3

Expressing a model peptide within the GAS pilus on the surface of *L. lactis*

3.1 Introduction

The backbone fibre of the M1 pilus of GAS is formed by the homopolymerisation of the Spy0128 pilin subunit. In the assembled pilus, Spy0128 subunits are stacked head to tail and linked covalently between the carboxyl group of threonine 311 and the ε-amino group of lysine 161 of the next subunit (Kang, et al., 2007). Approximately 50-100 Spy0128 subunits are linked together before an adaptor protein (Spy0130) is added to stop pilus assembly and connect the pilus structure to the cell wall (Linke, et al., 2010).

The homopolymerisation of Spy0128 is an important feature for vaccine design as it amplifies the engineered antigenic peptide within it. Therefore, it is imperative to engineer peptides into regions of the Spy0128 subunit that will not disrupt this homopolymerisation on the surface of *L. lactis*. After analysing the crystal structure of Spy0128, it was determined that the core β strands should not be modified. However, the loop regions connecting the β strands were seen as possible sites where peptides could be engineered into without affecting the structure or integrity of the pilus on the cell surface. For proof of concept, the model peptide consisting of OVA from positions 323 to 339 ($OVA_{323-339}$) was chosen to be engineered into Spy0128, by replacing selected loop regions with the $OVA_{323-339}$ peptide (figure 3.1).

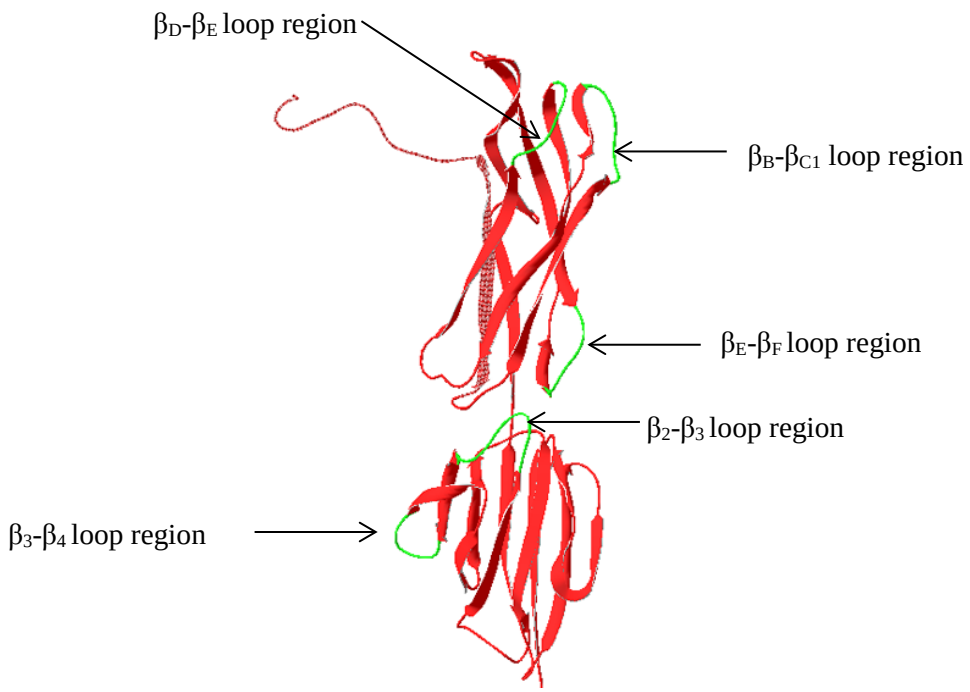

>Spy0128

```
  1 mklrhllltg aaltsfaatt vhgetvvnga kltvtknldl vnsnalipnt dftfkiepdt

 61 tvnedgnkfk gvalntpmtk vtytnsdkgg sntktaefdf sevtfekpgv yyykvteeki
    βB-βC1 loop                                  βD-βE loop
121 dkvpgvsydt tsytvqvhvl wneeqqkpva tyivgykegs kvpiqfknsl dsttltvkkk
    βE-βF loop
181 vsgtggdrsk dfnfgltlka nqyykasekv miekttkggq apvqteasid qlyhftlkdg
                          β2-β3 loop          β 3-β4 loop
241 esikvtnlpv gvdyvvtedd yksekyttnv evspqdgavk niagnsteqe tstdkdmtit

301 ftnkkdfevp tgvamtvapy ialgivavgg alyfvkkkna
```

Figure 3.1 Five loop regions selected to be replaced with the $OVA_{323-339}$ peptide

Computer generated structure (top), using the SWISS-MODEL web server, and the amino acid sequence (bottom) of the Spy0128 subunit highlighting the loop regions (in green) that were selected to be replaced with the $OVA_{323-339}$ peptide

3.2 Results

3.2.1 The strategy used to replace selected loop regions of Spy0128 with the $OVA_{323-339}$ peptide

3.2.1.1 The plasmid used for cloning

The complete M1 pilus structure has been successfully expressed on the surface of *L. lactis* using the *E. coli* – GAS shuttle plasmid pLZ12, containing the lactococcal promoter P23, a kanamycin selection marker (Km2), and the M1 pilus operon (PilM1). The plasmid pLZ12 is an E. coli/streptococcal shuttle vector that has been used for complementation analyses in *S. pyogenes* (Perez-Casal, et al., 1991). The pLZ12-Km2:P23R_PilM1 shuttle plasmid was kindly obtained from Dr. Jacelyn Loh (University of Auckland, New Zealand) and the XhoI site present in the plasmid was deleted, generating the pLZ12-Km2:P23R_PilM1 (-XhoI) plasmid which was used for cloning and expression of $OVA_{323-339}$ peptide-linked pili on the surface of *L. lactis*.

3.2.1.2 Construction of the pLZ12-Km2:P23R_PilM1_loop-*ova*$_{323-339}$ plasmids

A pBC vector containing the *ova*$_{323-339}$ DNA sequence flanked by a XhoI and a SalI restriction enzyme site was kindly obtained from Dr. Thomas Proft (University of Auckland, New Zealand). The XhoI and SalI digested overhangs are compatible; therefore, if a sequence encoding for a loop region in the *spy0128* gene, in pLZ12-Km2:P23R_PilM1 (-XhoI), is replaced with a XhoI restriction enzyme site, the XhoI/SalI digested *ova*$_{323-339}$ sequence from pBC: *ova*$_{323-339}$ can be directly cloned into that XhoI site, the end result being the replacement of the loop region sequence with the *ova*$_{323-339}$ sequence.

To replace a loop region sequence of Spy0128 with a XhoI site, the entire pLZ12-Km2:P23R_PilM1 (-XhoI) plasmid was PCR amplifying with a primer pair listed in Table 1. When a primer pair binds to the *spy0128* gene, the XhoI sequence will overlap the loop region sequence and the subsequent amplification of the entire plasmid, digestion with XhoI, and

ligation will result in the replacement of the loop region sequence with a XhoI site (figure 3.2). The resulting plasmid was digested with XhoI and the XhoI/SalI digested *ova*$_{323-339}$ DNA sequence was ligated into the XhoI site, generating a pLZ12-Km2:P23R_PilM1_loop-*ova*$_{323-339}$ plasmid (figure 3.3).

The pLZ12-Km2: P23R_PilM1_loop-*ova*$_{323-339}$ plasmid was then electroporated into *L. lactis* and the cell wall proteins were analysed by Western blot to determine if replacing the loop region with the peptide affects pilus polymerisation on the surface of *L. lactis*.

Table 3.1 Primer pairs used to replace a loop region sequence of *spy0128* with a XhoI site

Name	Description	Sequence
Spy0128_ β_B -Xho -F, R	Replaces the β_B-β_{C1} loop region with a XhoI site	F:5'-GAGAGAGACTCGAGGGAAA TAAGTTTAAAGGTGTAGC-3' (XhoI) R:5'-GAGAGAGACTCGAGAGTAT CAGGTTCGATTTTAAATG- 3' (XhoI)
Spy0128_ β_2-Xho -F, R	Replaces the β_2-β_3 loop region with a XhoI site	F:5'-GAGAGAGACTCGAGTCAGA AAAAGTCATGATTGAG- 3' (XhoI) R:5'-GAGAGAGACTCGAGTGCTT TTAAAG TCAGACC -3'(XhoI)
Spy0128_ β_3-Xho -F, R	Replaces the β_3-β_4 loop region with a XhoI site	F: 5'-GAGAGAGA CTC GAGCCTG TTCAAACAGAGGCTAG-3' (XhoI) R: 5'- GAGAGAGACTCGAGAGTTG TCTTCTCAATCATGAC-3' (XhoI)
Spy0128_ β_D -Xho -F, R	Replaces the β_D-β_E loop region with a XhoI site	F: 5'- GAGAGAGACTCGAGGGTGT TTATTATTACAAA G -3'(XhoI) R: 5'- GAGAGAGACTCGAGAAAAT CAAATTCTGCAG -3'(XhoI)
Spy0128_β_E-Xho -F, R	Replaces the β_E-β_F loop region with a XhoI site	F:5'- GAGAGAGACTCGAGGGTGT TTCTTATGATACAAC -3' (XhoI) R:5'- GAGAGAGACTCGAGCTCCT CAGTTACTTTG - 3' (XhoI)

Restriction sites are underlined

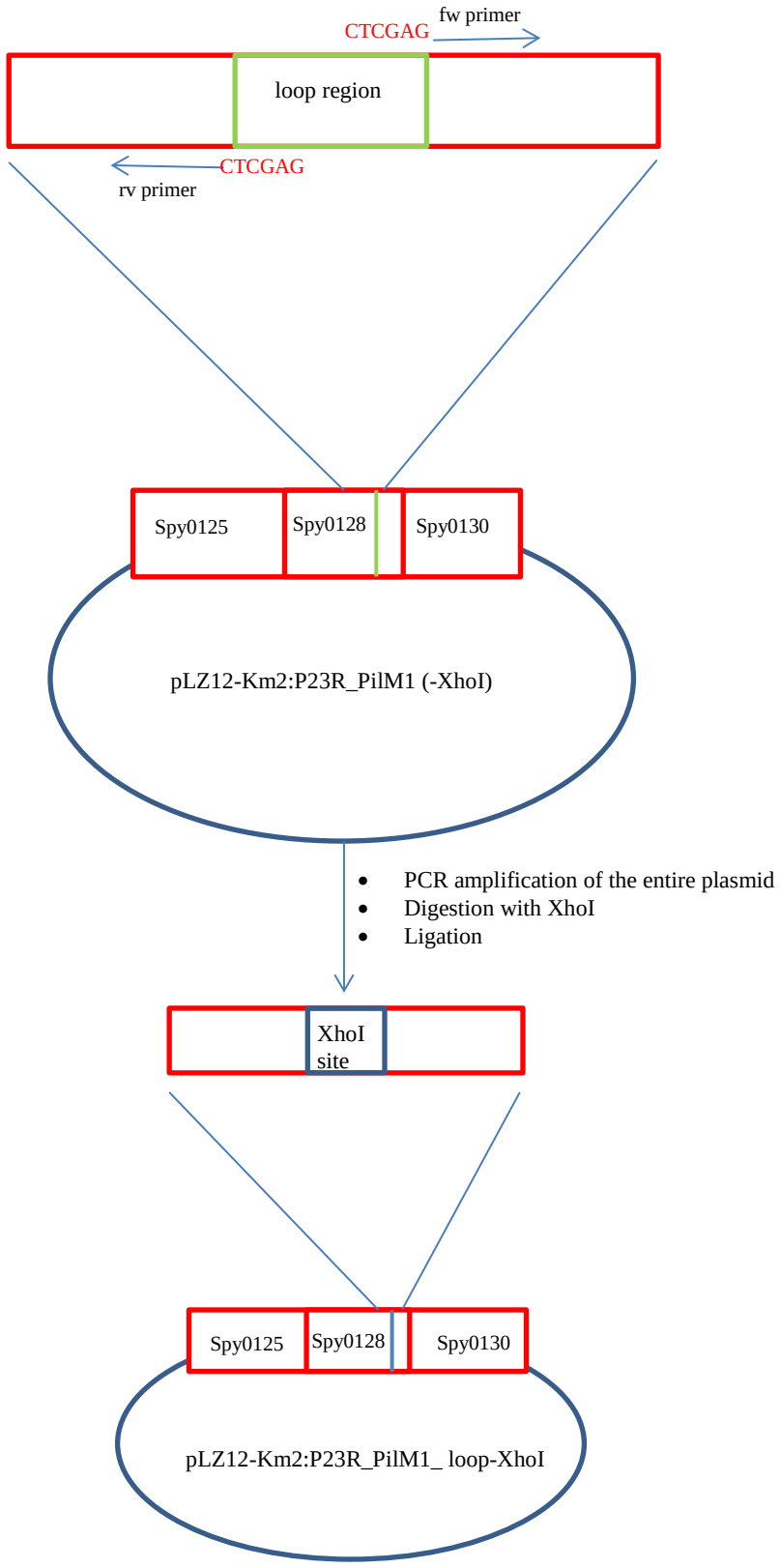

Figure 3.2 Replacing a loop region sequence of the *spy0128* gene with a XhoI site

A specific loop region sequence of the *spy0128* gene in the pLZ12-Km2:P23R_PilM1 (-XhoI) plasmid was replaced with a XhoI site by PCR amplifying the entire plasmid using a primer pair listed in table 3.1, followed by digestion with XhoI, and ligation.

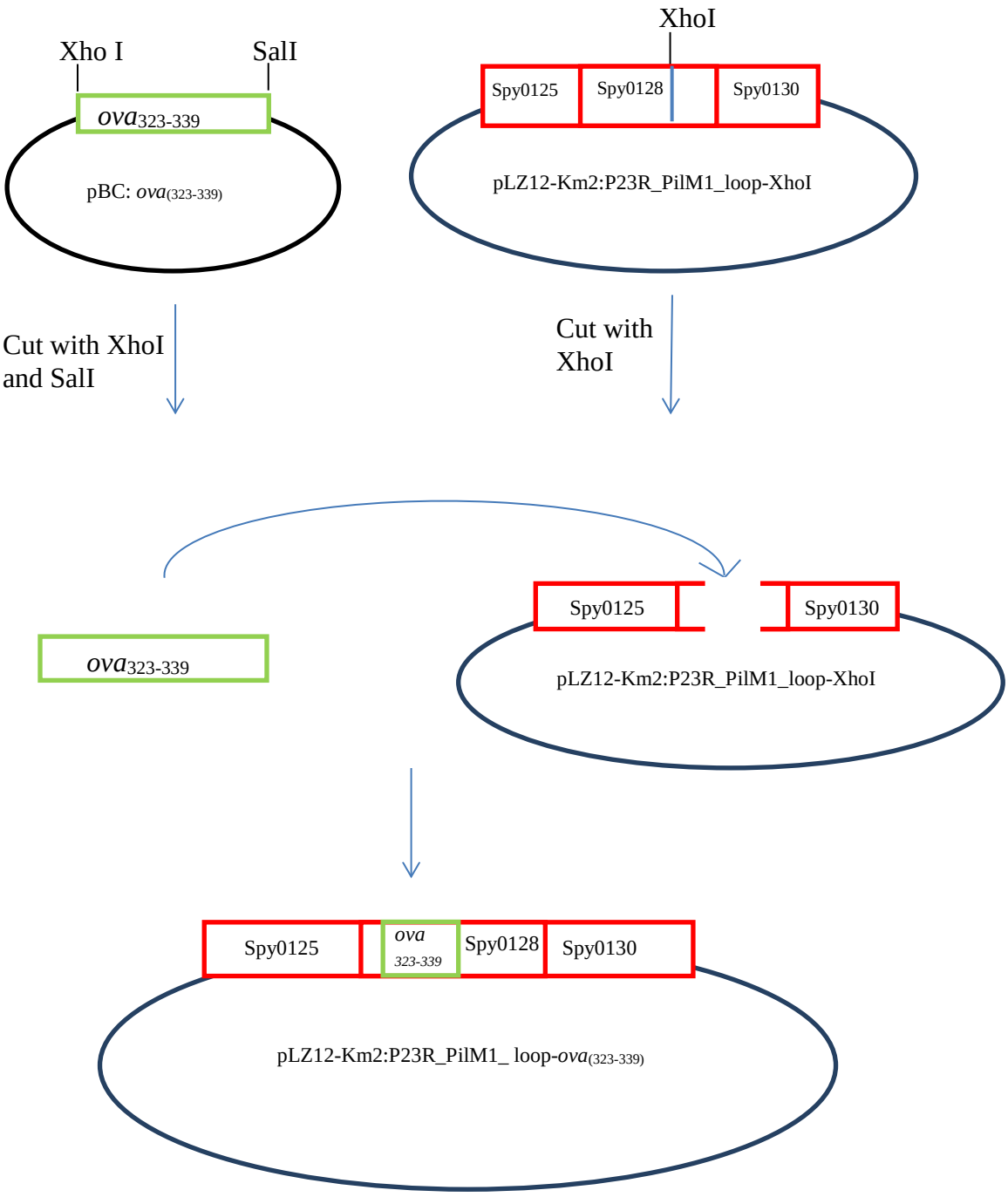

Figure 3.3 Construction of the pLZ12-Km2:P23R_PilM1_loop-*ova*$_{323\text{-}339}$ plasmids

A pLZ12-Km2:P23R_PilM1_loop-XhoI plasmid was digested with XhoI and the XhoI/SalI digested *ova*$_{323\text{-}339}$ DNA sequence from pBC:*ova*$_{\mathbf{323\text{-}339}}$ was cloned in by ligation using an insert to vector ratio of 3:1.

3.2.2 Replacing the β_B-β_{C1} loop region of Spy0128 with the $OVA_{323-339}$ peptide affects the polymerisation of the pilus on the surface of *L. lactis*

3.2.2.1 Replacing the β_B-β_{C1} loop region with a XhoI site

The first loop region selected to be replaced with the $OVA_{323-339}$ peptide was the loop region between the β_B and β_{C1} strands of Spy0128. A 15 base pair (bp) sequence encoding for the β_B-β_{C1} loop region was replaced with a XhoI restriction enzyme site by PCR amplifying the entire pLZ12-Km2:P23R_PilM1 (-XhoI) plasmid with the Spy0128_β_B-Xho fw and rv primers. The resulting plasmid, pLZ12-Km2:P23R_PilM1_β_B_XhoI, was transformed into *E. coli* DH5α and a positive colony was selected by single colony PCR using the Spy0125 fw and Spy0130 rv primers to ensure the entire pilus operon was present in the plasmid (figure 3.4). To confirm the presence of the XhoI site between the β_B and β_{C1} strands, the *spy0128* gene was PCR amplified using the Spy0127 fw/Spy0128 rv primer pair and digested overnight with XhoI. After visualising the digested and undigested *spy0128* gene on an agarose gel, the presence of two bands at ~ 650 and 800 bp confirms that the β_B-β_{C1} loop region has been replaced with a XhoI site (figure 3.5).

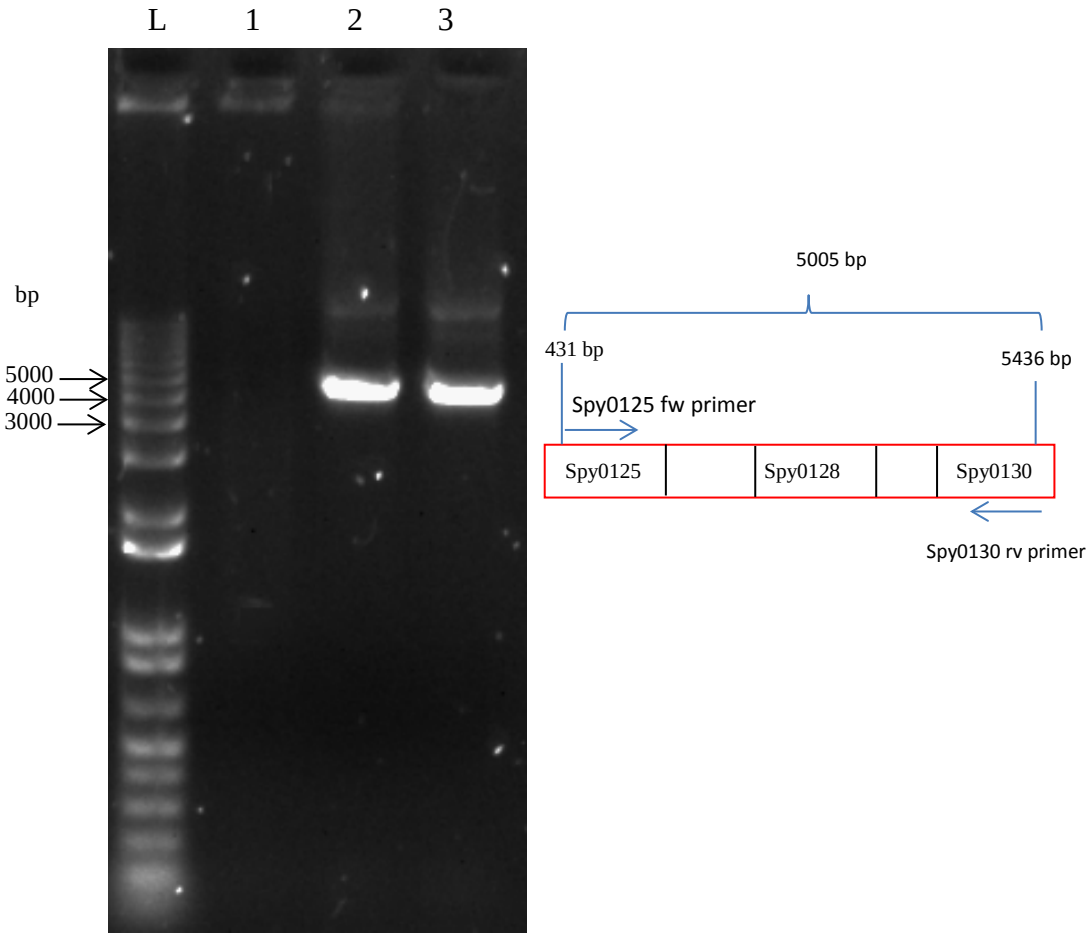

Figure 3.4 Screening of *E. coli* DH5α transformed with pLZ12-Km2:P23R_PilM1_ β_B_XhoI.

The Spy0125 fw and Spy0130 rv primers were used to select an *E. coli* DH5α colony containing the pLZ12-Km2:P23R_PilM1_ β_B_XhoI plasmid. Schematic diagram on the right shows primer binding sites and the expected size of the PCR product if positive. The image on the left features 1% agarose gel electrophoresis. Lane L: the 1 kb molecular weight marker. Lane 1: the negative control (*E. coli* DH5α containing pLZ12-Km2:P23R). Lane 2: the *E. coli* DH5α colony containing pLZ12-Km2:P23R_PilM1_ β_B_XhoI. Lane 3: the positive control (*E. coli* DH5α containing pLZ12-Km2:P23R_PilM1).

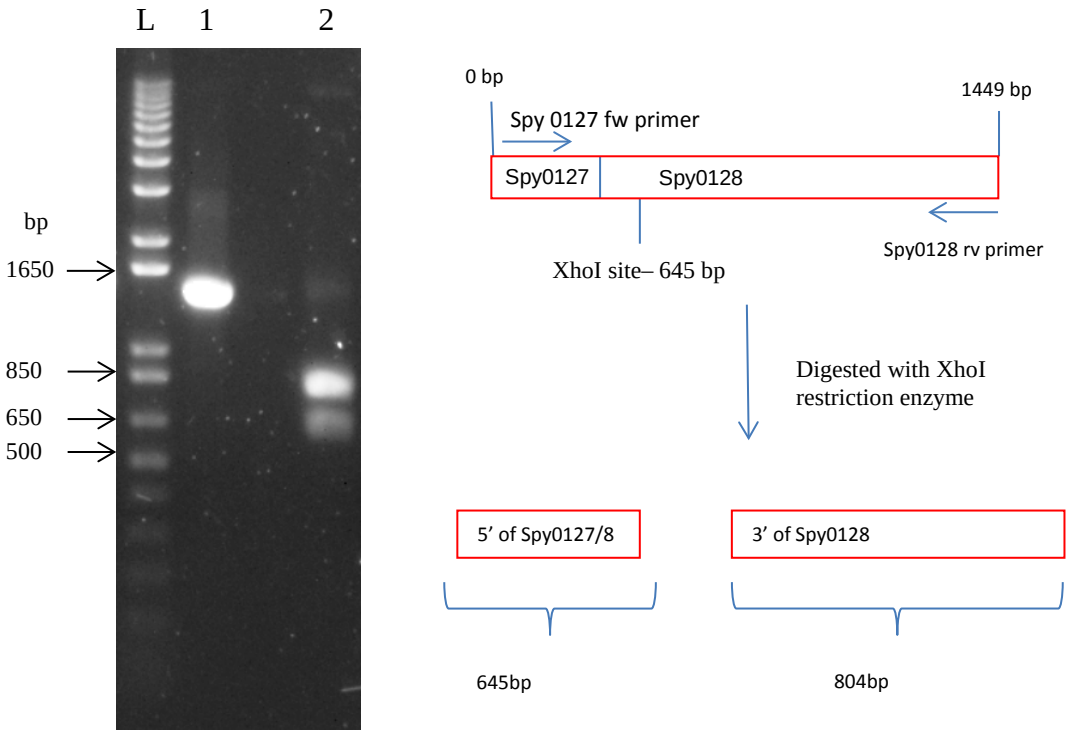

Figure 3.5 Confirming the presence of the XhoI site between the β_B and β_{C1} strands of Spy0128

The *spy0128* gene was PCR amplified from pLZ12-Km2:P23R_PilM1_ β_B_XhoI using the Spy0127 fw/Spy0128 rv primers and digested overnight with XhoI. Schematic diagram on the right shows the location of the XhoI site and the expected sizes of the digested PCR product. The image on the left features 1% agarose gel electrophoresis. Lane L: the 1 kb molecular weight marker. Lane 1: undigested *spy0128* gene. Lane 2: *spy0128* gene digested overnight with XhoI.

To determine if replacing the loop region with a XhoI site affects the polymerisation of the pilus on the surface of *L. lactis*, the pLZ12-Km2:P23R_PilM1_β_B_XhoI plasmid was electroporated into *L. lactis* and cell wall extracts were analysed by Western blot with rabbit antiserum specific for Spy0128. In the extract from *L. lactis*:pLZ12-Km2:P23R_PilM1_ β_B_XhoI, a ladder of high-molecular-mass bands was visible which suggests that the pilus structure was successfully assembled on the cell surface. The ladder pattern is formed due to varying numbers of covalently linked Spy0128 molecules in pilus fibres and has been previously observed in other GAS serotypes (Mora, et al., 2005). The pattern formed is comparable to that from the cell wall extract of *L. Lactis* expressing wild-type M1 pilus. In contrast, no bands were visible in the cell wall extract from *L. Lactis* containing the empty vector pLZ12-Km2:P23R as expected (figure 3.6).

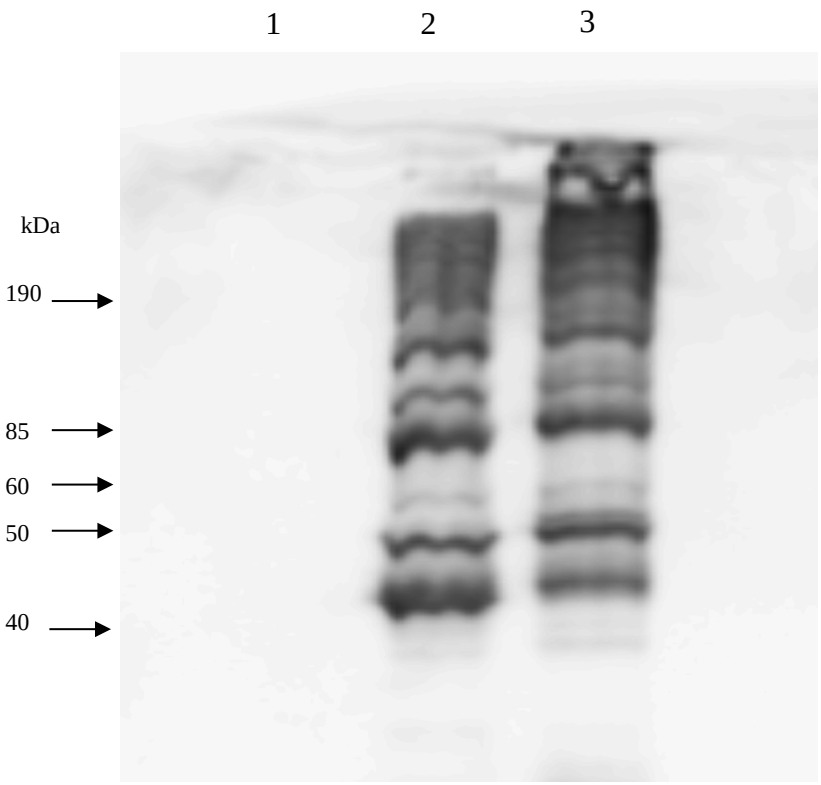

Figure 3.6 Western blot analyses of pLZ12-Km2:P23R_PilM1_ β_B_XhoI expressed in *L. lactis*

Cell wall extracts analysed by Western blot with rabbit anti-Spy0128 antiserum. Lane 1: the negative control (*L. lactis*:pLZ12-Km2:P23R). Lane 2: *L. lactis*:pLZ12-Km2:P23R_PilM1_β_B_XhoI. Lane 3: the positive control (*L. lactis*:pLZ12-Km2:P23R_ PilM1). A high molecular weight laddering pattern is observed in the cell wall extract from *L. lactis*:pLZ12-Km2:P23R_PilM1_β_B_XhoI, inferring that replacing the loop region with a XhoI site does not impair pilus polymerisation on the surface of *L. lactis.*

3.2.2.2 Cloning the $ova_{323-339}$ sequence into the XhoI site

The XhoI/SalI digested $ova_{323-339}$ DNA sequence from pBC:$ova_{(323-339)}$ was cloned into the XhoI digested pLZ12-Km2:P23R_PilM1_ β_B_XhoI and the resulting plasmid, pLZ12-Km2:P23R_PilM1_ β_B _ $ova_{323-339}$, was transformed into *E. coli* DH5α. A positive colony was selected using the OVA forward primer and Spy0128 reverse primers. These primers were used to ensure that the positive colony would have the DNA sequence ligated in the correct orientation. After visualising the PCR products on an agarose gel, the presence of a band at 850 bp confirms the ligation of the $ova_{323-339}$ sequence into the XhoI site (figure 3.7).

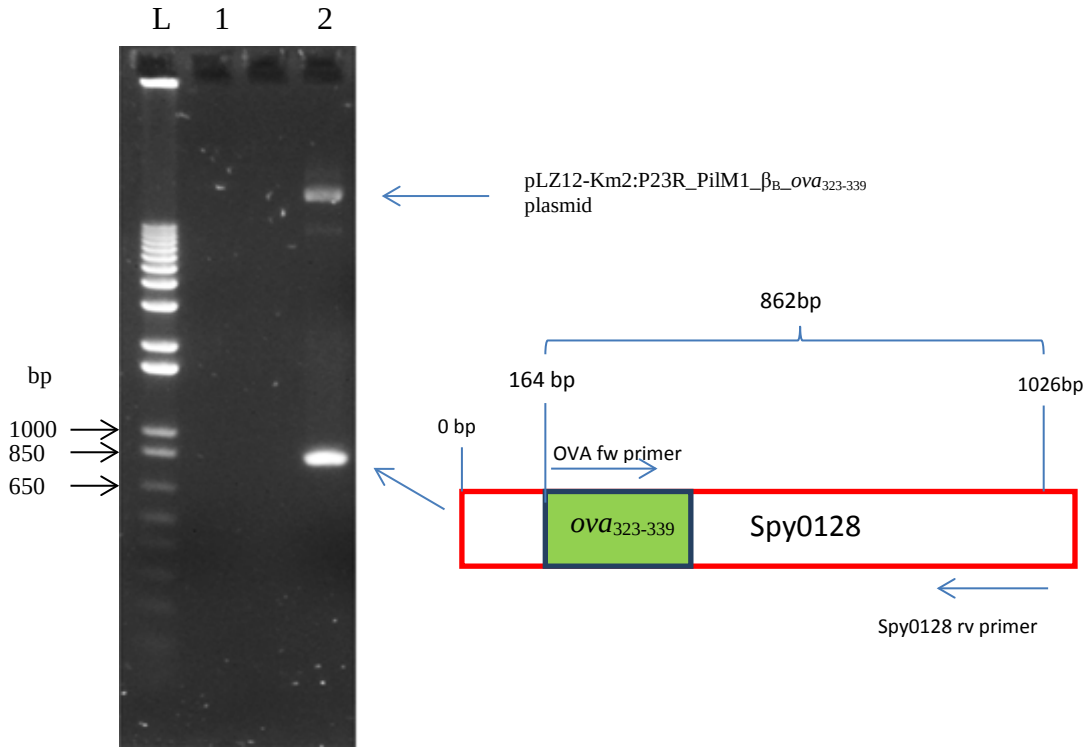

Figure 3.7 Cloning the *ova*$_{323-339}$ sequence into the XhoI site between the β_B and β_{C1} strands

The OVA fw and Spy0128 rv primers were used to select an *E. coli* DH5α colony containing the pLZ12-Km2:P23R_PilM1_β_B_*ova*$_{323-339}$ plasmid. Schematic diagram on the right shows primer binding sites and the expected size of the PCR product if positive. The image on the left features 1% agarose gel electrophoresis. Lane L: the 1 kb molecular weight marker. Lane 1: the negative control (*E. coli* DH5α containing pLZ12-Km2:P23R_PilM1). Lane 2: the *E. coli* DH5α colony containing pLZ12-Km2:P23R_PilM1_ β_B_*ova*$_{323-339}$.

3.2.2.3 The OVA$_{323-339}$ peptide disrupts the polymerisation of pilus on the cell surface

The most important aspect for the success of this vaccine delivery strategy is the assembly of the OVA$_{323-339}$ peptide-linked pilus on the surface of *L. lactis.* To determine whether replacing the β_B-β_{C1} loop region with the OVA$_{323-339}$ peptide affects pilus assembly on the cell surface, the pLZ12-Km2:P23R_PilM1_β_B_*ova*$_{323-339}$ plasmid was extracted from DH5α, electroporated into *L. lactis* (figure 3.8), and cell wall extracts from the recombinant *L. lactis* were analysed by Western blot using rabbit antiserum specific for Spy0128. In the extract from *L. lactis*:pLZ12-Km2:P23R_PilM1_β_B_*ova*$_{323-339}$, rabbit anti-Spy0128 antiserum did not recognise the ladder of high molecular weight bands which is characteristic of pilus formation. Some bright bands were

visible between ~40 and 85 kDa and this suggests that only shorter forms of the polymeric structure were being assembled (figure 3.9).

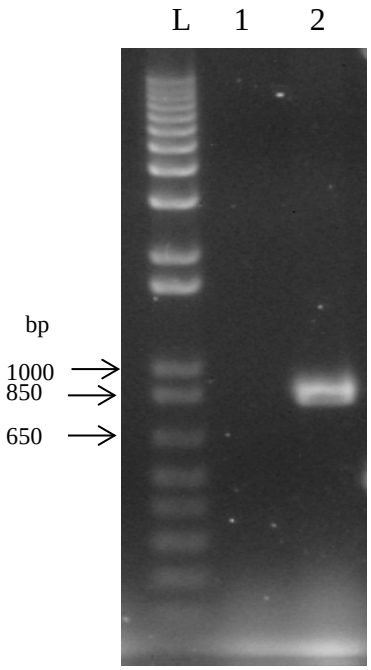

Figure 3.8 The pLZ12-Km2:P23R_PilM1_β_B_*ova*$_{323-339}$ plasmid was successfully electroporated into *L. lactis*

OVA fw and Spy0128 rv primers were used to select an *L. lactis* colony containing the pLZ12-Km2:P23R_PilM1_ β_B _ *ova*$_{323-339}$ plasmid. Lane L: the 1 kb molecular weight marker, lane 1: the negative control (*L. lactis*:pLZ12-Km2:P23R_PilM1), lane 2: *L. lactis*:pLZ12-Km2:P23R_PilM1_β_B _ *ova*$_{323-339}$, all electrophoresed on a 1% agarose gel.

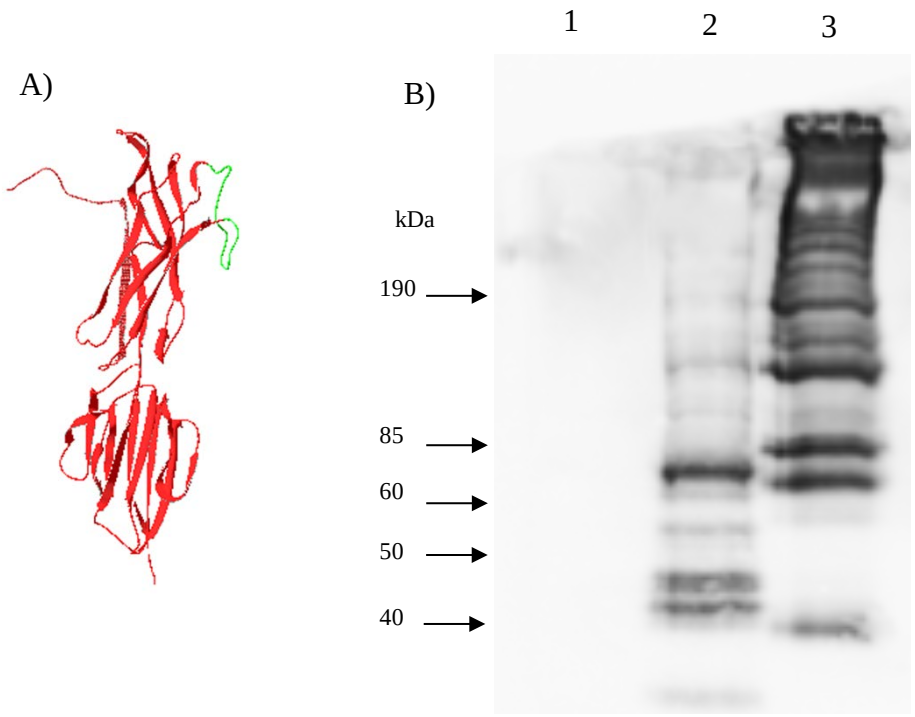

Figure 3.9 Western blot analyses of pLZ12-Km2:P23R_PilM1_ β_B_ *ova*$_{323-339}$ expressed in *L. lactis*

A) Computer generated structure, using the SWISS-MODEL web server, showing the $OVA_{323-339}$ peptide (in green) between the β_B and β_{C1} strands of Spy0128.

B) Cell wall extracts analysed by Western blot with rabbit anti-Spy0128 antiserum. Lane 1: the negative control (*L. lactis*:pLZ12-Km2:P23R). Lane 2: *L. lactis*:pLZ12-Km2:P23R_PilM1_ β_B_*ova*$_{323-339}$. Lane 3: the positive control (*L. lactis*:pLZ12-Km2:P23R_PilM1). The absence of a ladder of high molecular weight bands above 85 kDa in the extract from *L .lactis*:pLZ12-Km2: P23R_PilM1_ β_B _ *ova*$_{323-339}$ suggests that the assembly of long pili is affected by the $OVA_{323-339}$ peptide.

3.2.3 Replacing the β_2-β_3 loop region of Spy0128 with the $OVA_{323-339}$ peptide disrupts the polymerisation of pilus on the cell surface

Since replacing the β_B-β_{C1}loop region of Spy0128 with the $OVA_{323-339}$ peptide affected pilus polymerisation on the surface of *L. lactis*, the second loop region selected to be replaced with the peptide was between the β_2 and β_3 strands of Spy0128. An 18 bp sequence encoding for the β_2-β_3 loop region was replaced with a XhoI restriction enzyme site by PCR and the resulting plasmid, pLZ12-Km2:P23R_PilM1_β_2_XhoI, was transformed into *E. coli* DH5α. Correct

insertion of the XhoI site was verified by the presence of two bands at ~ 400 and 1000 bp when the PCR amplified *spy0128* gene was digested overnight with XhoI (figure 3.10).

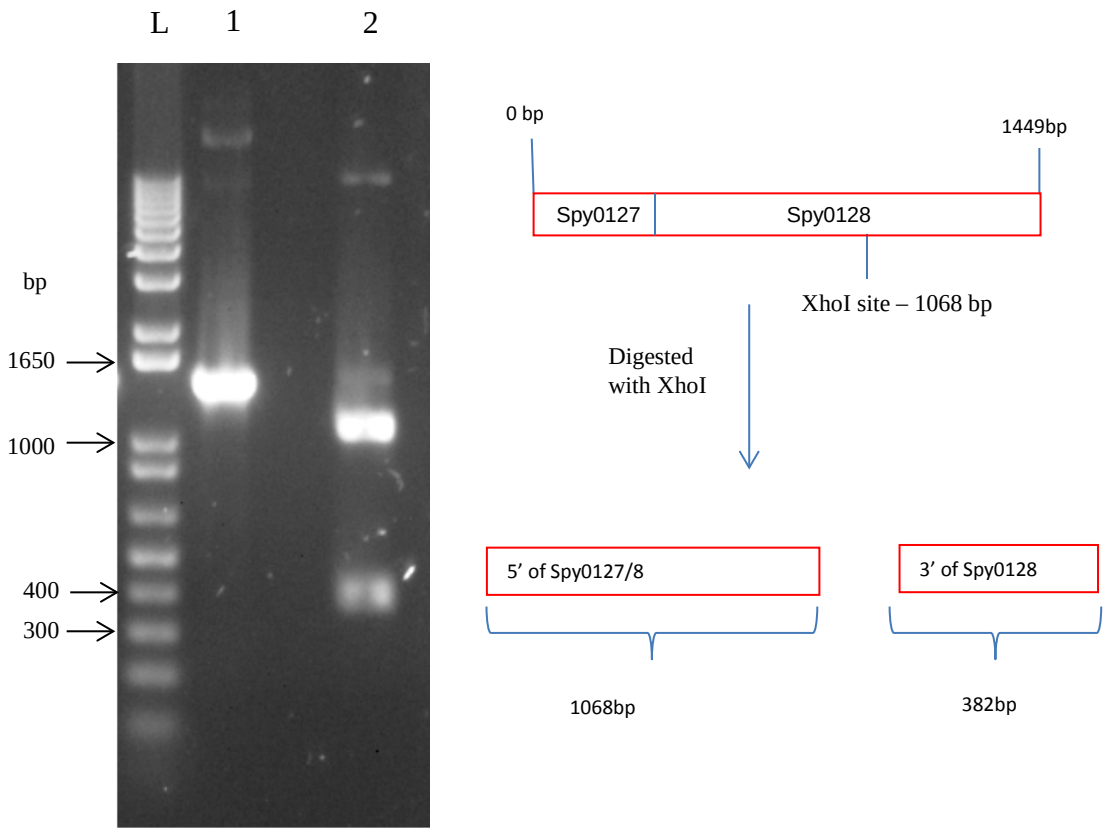

Figure 3.10 Confirming the presence of the XhoI site between the β_2 and β_3 strands of Spy0128

The *spy0128* gene fragment was PCR amplified from pLZ12-Km2:P23R_PilM1_ β_2 _XhoI using the Spy0127 fw and Spy0128 rv primers and digested overnight with XhoI. Schematic diagram on the right shows the location of the XhoI site and the expected sizes of the digested PCR product. The image on the left features the 1% agarose gel electrophoresis. Lane L: the 1 kb molecular weight marker. Lane 1: undigested *spy0128* gene. Lane 2: *spy0128* gene digested overnight with XhoI.

The pLZ12-Km2:P23R_PilM1_β_2_XhoI plasmid was electroporated into *L. lactis* and the cell wall proteins were analysed by Western blot with rabbit antiserum specific for Spy0128. A ladder of high molecular weight bands, characteristic of pilus formation, was visible (figure 3.11), therefore, the *ova*$_{323\text{-}339}$ DNA sequence was cloned into the XhoI site and the resulting plasmid, pLZ12-Km2:P23R_PilM1_β_2_*ova*$_{323\text{-}339,}$ was transformed into *E. coli* DH5α. Following confirmation of a positive colony using the OVA fw and Spy0128 rv primers, the plasmid was extracted from the DH5α and electroporated into *L. lactis* (figure 3.12).

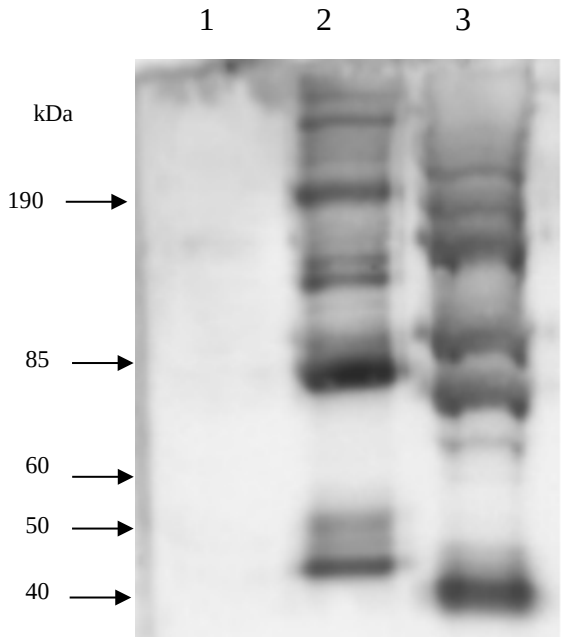

Figure 3.11 Western blot analyses of pLZ12-Km2:P23R_PilM1_β_2_XhoI expressed in *L. lactis*

Cell wall extracts analysed by Western blot with rabbit anti-Spy0128 antiserum. Lane 1: the negative control (*L. lactis*:pLZ12-Km2:P23R). Lane 2: *L. lactis*:pLZ12-Km2:P23R_PilM1_β_2_XhoI. Lane 3: the positive control (*L. lactis*:pLZ12-Km2:P23R_PilM1). A high molecular weight laddering pattern is observed in the cell wall extract from both *L. lactis*:pLZ12-Km2:P23R_PilM1_β_2_XhoI and the positive control.

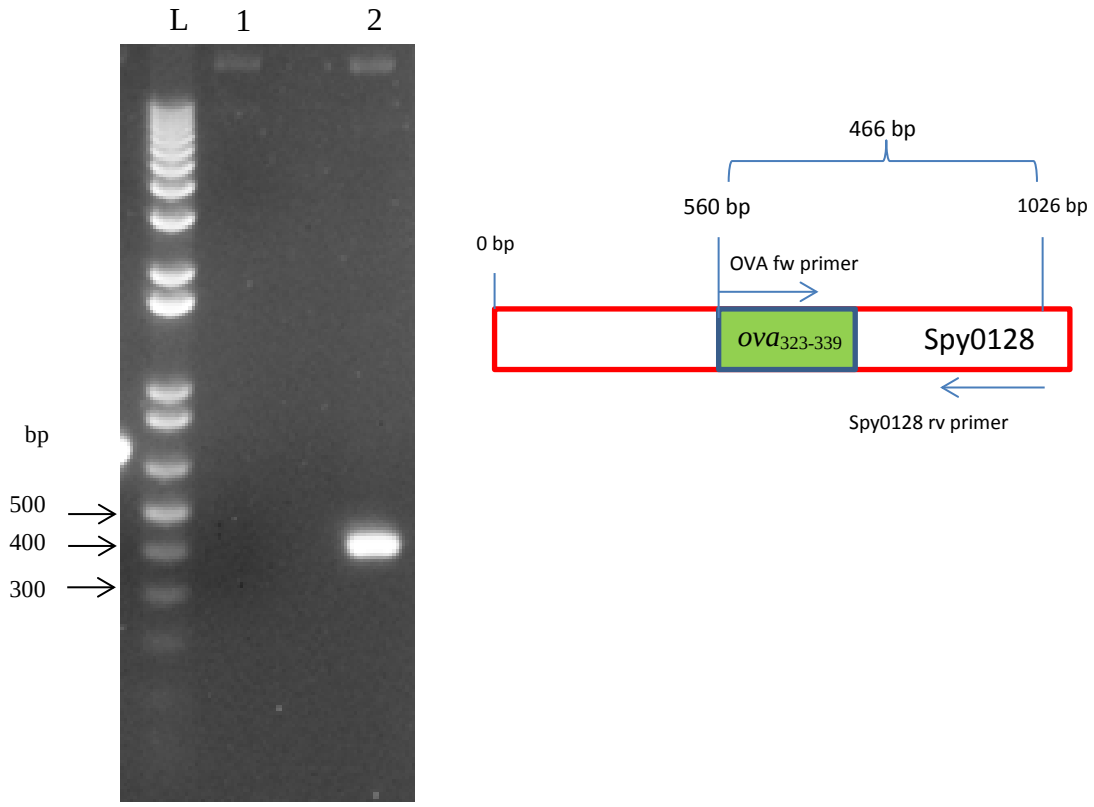

Figure 3.12 The pLZ12-Km2:P23R_PilM1_β_2_*ova*$_{323\text{-}339}$ plasmid was successfully electroporated into *L. lactis*

OVA fw and Spy0128 rv primers were used to select an *L. lactis* colony containing the pLZ12-Km2:P23R_PilM1_β_2_*ova*$_{323\text{-}339}$ plasmid. Schematic diagram on the right shows primer binding sites and the expected size of the PCR product if positive. The image on the left features 1% agarose gel electrophoresis. Lane L: the 1 kb molecular weight marker. Lane 1: negative control (*L. lactis:*pLZ12-Km2:P23R_PilM1 plasmid). Lane 2: the *L. lactis:*pLZ12-Km2:P23R_PilM1_β_2_*ova*$_{323\text{-}339}$ colony.

Western blot analyses of the cell wall extract from *L. lactis*:pLZ12-Km2:P23R_PilM1_β_2_*ova*$_{323\text{-}339}$, using rabbit anti-Spy0128 antiserum, revealed that the ladder of high molecular bands, indicative of pilus expression, is absent. Only molecular weight bands between ~ 50 and 85 kDa are present, similar to when the peptide was incorporated between the β_B and β_{C1} strands, which suggests that the OVA$_{323\text{-}339}$ peptide is interfering with the formation of long pilus structures on the surface of *L. lactis* (figure 3.13).

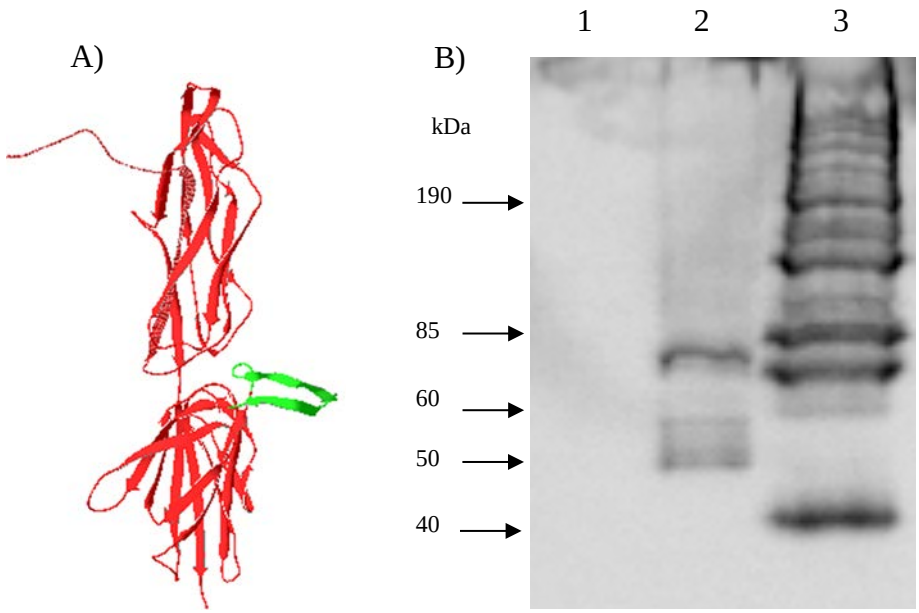

Figure 3.13 Western blot analyses of pLZ12-Km2:P23R_PilM1_β_2_*ova*$_{323-339}$ expressed in *L. lactis*

A) Computer generated structure, using the SWISS-MODEL web server, showing the $OVA_{323-339}$ peptide (in green) between the β_2 and β_3 strands of Spy0128.

B) Cell wall extracts analysed by Western blot with rabbit anti-spy0128 antiserum. Lane 1: Negative control (*L. lactis*:pLZ12-Km2:P23R). Lane 2: *L. lactis*:pLZ12-Km2:P23R_PilM1_β_2_*ova*$_{323-339}$. Lane 3: Positive control (*L. lactis*:pLZ12-Km2:P23R_PilM1). Laddering pattern for *L. lactis*:pLZ12-Km2:P23R_PilM1_β_2_*ova*$_{323-339}$ reveals that long pili are not polymerised.

3.2.4 Replacing the β_3-β_4 loop region of Spy0128 with the $OVA_{323-339}$ peptide eliminates pilus polymerisation on the cell surface

Since replacing the β_2-β_3 loop region with the $OVA_{323-339}$ peptide affected pilus polymerisation on the surface of *L. lactis*, the third loop region selected to be replaced with the peptide was between the β_3 and β_4 strands of Spy0128. A 15 bp sequence encoding for the β_3-β_4 loop region was replaced with a XhoI restriction enzyme site by PCR and the resulting plasmid, pLZ12-Km2:P23R_PilM1_ β_3_XhoI, was transformed into *E. coli* DH5α. Correct insertion of the XhoI site was verified by the presence of two bands at ~ 350 and 1100 bp when the PCR amplified *spy0128* gene was digested overnight with XhoI (figure 3.14). The pLZ12-Km2:P23R_PilM1_β_3_XhoI plasmid was electroporated into *L. lactis* and Western blot analyses of a cell wall extract, using rabbit antiserum specific for Spy0128, displayed a ladder of high molecular weight bands which indicated that pilus assembly was unaffected by the replacement of the loop region (figure 3.15). Therefore, the $ova_{323-339}$ DNA sequence was cloned into the XhoI site and the resulting plasmid, pLZ12-Km2:P23R_PilM1_β_3_$ova_{323-339}$, was transformed into *E.coli* DH5α. Following confirmation of a positive colony using the OVA fw and Spy0128 rv primers, the plasmid was extracted from the DH5α and electroporated into *L. lactis* (figure 3.16).

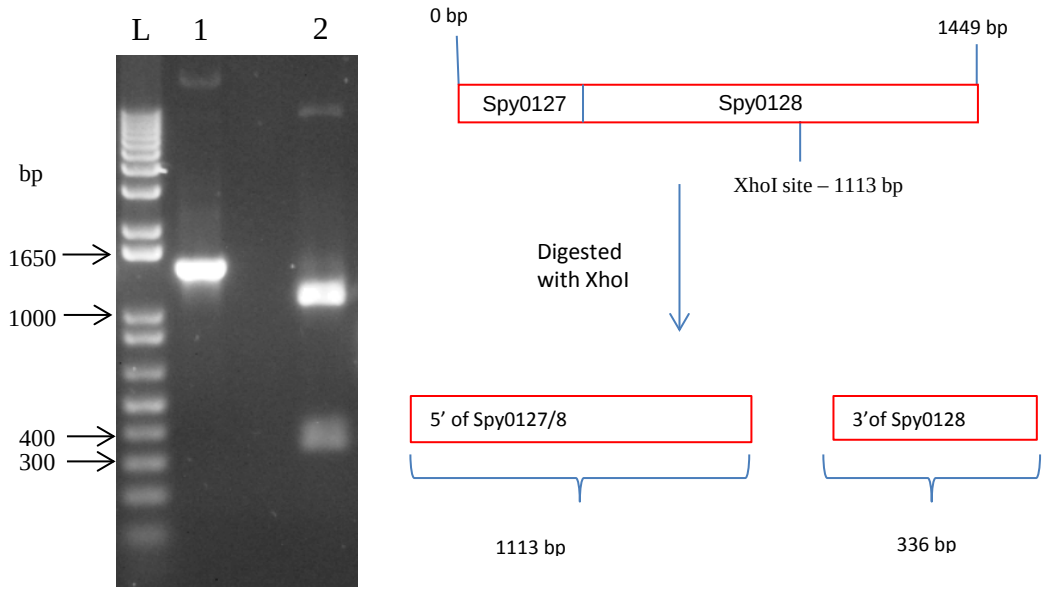

Figure 3.14 Confirming the presence of the XhoI site between the β_3 and β_4 strands of Spy0128

The *spy0128* gene fragment was PCR amplified from pLZ12-Km2:P23R_ PilM1_ β_3_XhoI using the Spy0127 fw and Spy0128 rv primers and digested overnight with XhoI. Schematic diagram on the right shows the location of the XhoI site and the expected sizes of the digested PCR product. The image on the left features 1% agarose gel electrophoresis. Lane L: the 1 kb molecular weight marker. Lane 1: undigested *spy0128* gene. Lane 2: *spy0128* gene digested overnight with XhoI.

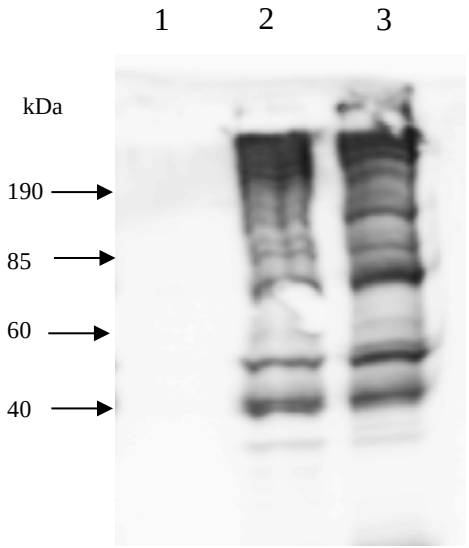

Figure 3.15 Western blot analyses of pLZ12-Km2: P23R_PilM1_ β_3_XhoI expressed in *L. lactis*

Cell wall extracts analysed by Western blot with rabbit anti-Spy0128 antiserum. Lane 1: the negative control (*L. lactis*:pLZ12-Km2:P23R). Lane 2: *L. lactis*:pLZ12-Km2:P23R_ PilM1_ β_3_XhoI. Lane 3: the positive control (*L. lactis*:pLZ12-Km2:P23R_ PilM1). A high molecular weight laddering pattern is observed in the cell wall extract from both *L. lactis*:pLZ12-Km2:P23R_ PilM1_ β_3_XhoI and the positive control.

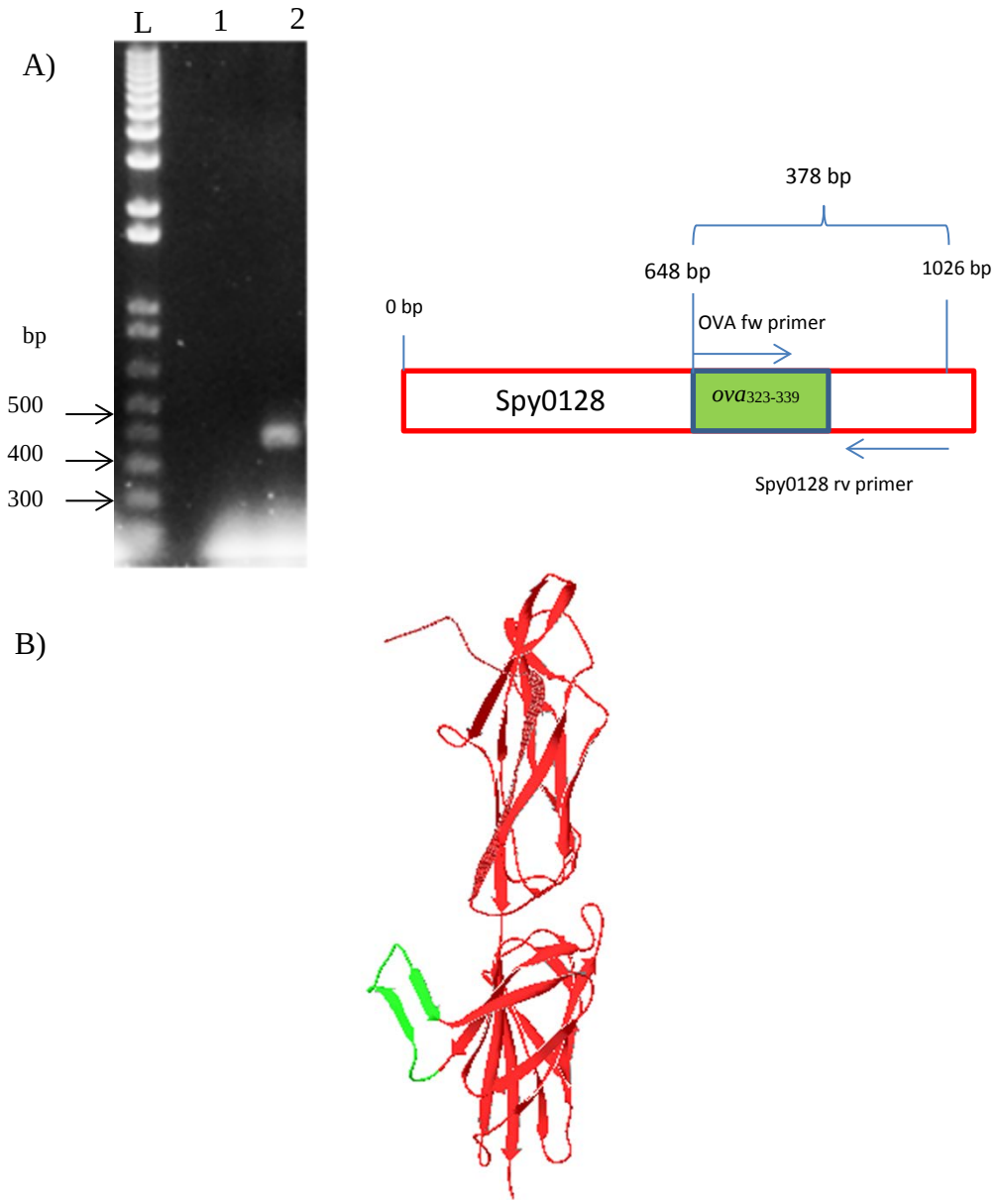

Figure 3.16 The pLZ12-Km2:P23R_PilM1_β3_*ova*323-339 plasmid was successfully electroporated into *L. lactis*

A) The OVA fw and Spy0128 rv primers were used to select an *L. lactis* colony containing with the pLZ12-Km2:P23R_PilM1_β3_*ova*323-339. Schematic diagram on the right shows primer binding sites and the expected size of the PCR product if positive. The image on the left features 1% agarose gel electrophoresis. Lane L: the 1 kb molecular weight marker. Lane 1: the negative control (*L. lactis*:pLZ12-Km2:P23R_PilM1 plasmid). Lane 2: *L. lactis*:pLZ12-Km2:P23R_PilM1_β3_*ova*323-339.

B) Computer generated structure, using the SWISS-MODEL web server, showing the OVA323-339 peptide (in green) between the β3 and β4 strands of Spy0128.

In a Western blot of the cell wall extract from *L. lactis*:pLZ12-Km2:P23R _PilM1_β_3_*ova*$_{323-339}$, rabbit antiserum specific for Spy0128 did not recognise any bands, in contrast to the extract from *L. lactis* expressing wild-type pilus where a laddering pattern was visible (figure 3.17). This suggests that integrating the peptide into Spy0128 likely prevented pilus assembly on the cell surface.

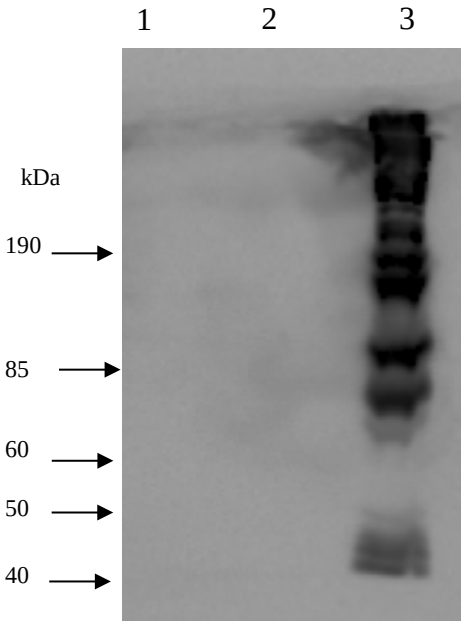

Figure 3.17 Western blot analyses of pLZ12-Km2: P23R_PilM1_β_3_*ova*$_{323-339}$ expressed in *L. lactis*

Representative Western blot, out of three independent experiments, of cell wall extracts analysed with rabbit anti-spy0128 antiserum. Lane 1: the negative control (*L. lactis*:pLZ12-Km2:P23R). Lane 2: *L. lactis*:pLZ12-Km2:P23R_PilM1_β_3_*ova*$_{323-339}$. Lane 3: the positive control (*L. lactis*:pLZ12-Km2: P23R_PilM1). No laddering pattern was visible in the cell wall extract from *L. lactis*:pLZ12-Km2: P23R_PilM1_β_3_*ova*$_{323-339}$.

3.2.5 Replacing the β_D-β_E loop region of Spy0128 with a XhoI site eliminates pilus polymerisation on the cell surface

Engineering the $OVA_{323-339}$ peptide between the β_3 and β_4 strands likely affected pilus polymerisation on the surface of *L. Lactis*, so a fourth loop region, the β_D-β_E loop, was replaced with a XhoI site by PCR and the resulting plasmid, pLZ12-Km2:P23R_PilM1_β_D _XhoI, was transformed into *E. coli* DH5α. Correct insertion of the site was confirmed by the presence of two bands at ~ 300 and 680 bp when the PCR amplified *spy0128* gene was digested overnight with XhoI and visualised on an agarose gel (figure 3.18).

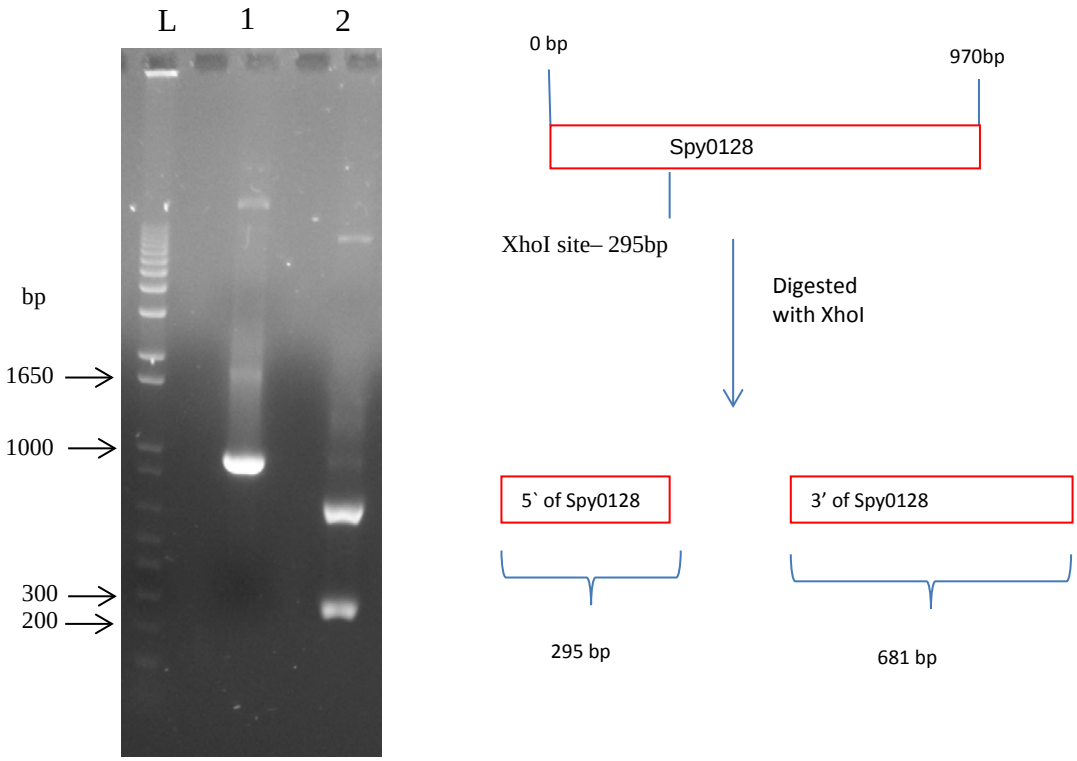

Figure 3.18 Confirming the presence of the XhoI site between the β_D and β_E strands of Spy0128

The *spy0128* gene was PCR amplified from pLZ12-Km2:P23R_PilM1_β_D_XhoI using the Spy0128 fw and rv primers and digested overnight with XhoI. Schematic diagram on the right shows the location of the XhoI site and the expected sizes of the digested PCR product. The image on the left features 1% agarose gel electrophoresis. Lane L: the 1 kb molecular weight marker. Lane 1: undigested *spy0128* gene. Lane 2: *spy0128* gene digested overnight with XhoI.

The pLZ12-Km2:P23R_PilM1_β_D_XhoI plasmid was electroporated into *L. lactis* and Western blots of the cell wall extracts were analysed with rabbit anti-Spy0128 antiserum to determine the effect replacing the loop region had on the surface polymerisation of pili. Unlike the other loop regions, the replacement of the β_D-β_E loop region in itself is enough to abrogate pilus polymerisation, indicated by the absence of the laddering pattern in the immunoblot (figure 3.19).

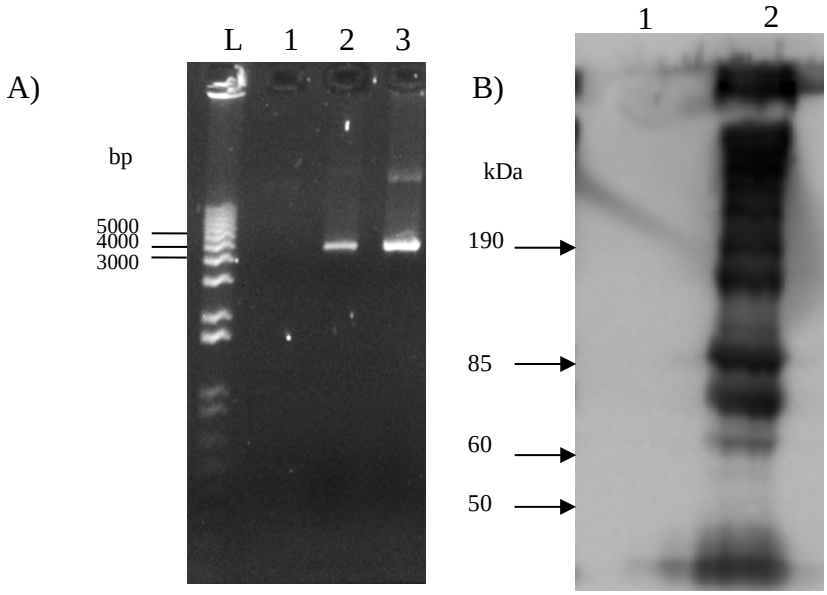

Figure 3.19 Screening for an *L. lactis* colony containing the pLZ12-Km2:P23R_PilM1_β_D_XhoI plasmid and Western blot analyses of the positive colony.

A) The Spy0125 fw and Spy0130 rv primers were used to select an *L. lactis* colony containing the pLZ12-Km2:P23R_PilM1_ β_D_XhoI plasmid. Lane L: the 1 kb molecular weight marker. Lane 1: the negative control (*E. coli* DH5α containing pLZ12-Km2:P23R). Lane 2: *L. lactis*:pLZ12-Km2:P23R_PilM1_β_D_XhoI. Lane 3: the positive control (*L. lactis* containing pLZ12-km2:P23R_PilM1).

B) Representative Western blot, out of three independent experiments, of cell wall extracts analysed with rabbit anti-spy0128 antiserum. Lane 1: *L. lactis*:pLZ12-Km2:P23R_ PilM1_β_D_XhoI. Lane 2: the positive control (*L. lactis*:pLZ12-Km2:P23R_PilM1). No 'laddering' pattern is observed in the cell wall extract from *L. lactis*: pLZ12-Km2:P23R_PilM1_β_D_XhoI.

3.2.6 Replacing the β_E-β_F loop region of Spy0128 with the $OVA_{323-339}$ peptide has no deleterious effect on surface pilus polymerisation

3.2.6.1 Replacing the β_E-β_F loop region with a XhoI site

Since the β_3-β_4 loop region may be important for the homopolymerisation of Spy0128 subunits, the fifth loop region selected to be replaced with the $OVA_{323-339}$ peptide was between the β_E and β_F strands of Spy0128. An 18 bp sequence encoding for the β_E-β_F loop region was replaced with a XhoI restriction enzyme site by PCR and the resulting plasmid, pLZ12-Km2:P23R_PilM1_ β_E _XhoI, was transformed into *E. coli* DH5α. The correct insertion of the XhoI site and verified by the presence of two bands at ~ 600 and 850 bp when the PCR amplified *spy0128* gene was digested overnight with XhoI and visualised on an agarose gel (figure 3.20)

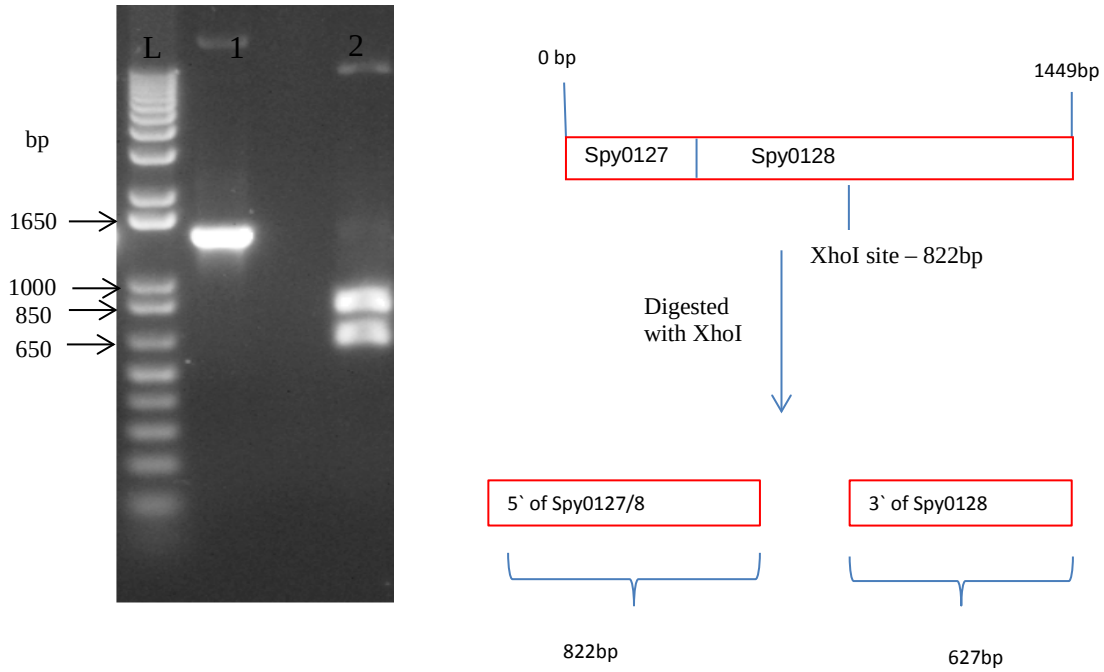

Figure 3.20 Confirming the presence of the XhoI site between the β_E and β_F strands of Spy0128

The *spy0128* gene fragment was PCR amplified from pLZ12-Km2:P23R_ PilM1_ β_E _XhoI using the Spy0127 fw and Spy0128 rv primers and digested overnight with XhoI. Schematic diagram on the right shows the location of the XhoI site and the expected sizes of the digested PCR product. The image on the left features 1% agarose gel electrophoresis. Lane L: the 1 kb molecular weight marker. Lane 1: undigested *spy0128* gene. Lane 2: *spy0128* gene digested overnight with XhoI.

To determine if replacing the β_E-β_F loop region with a XhoI site affects pilus polymerisation, the pLZ12-Km2:P23R_PilM1_β_E _XhoI plasmid was electroporated into *L. lactis* and the cell wall extract was analysed by Western blot. Rabbit anti-Spy0128 antiserum recognised a ladder of high molecular weight bands, indicating that the pilus assembly on the surface of *L. lactis* was not disrupted (figure 3.21).

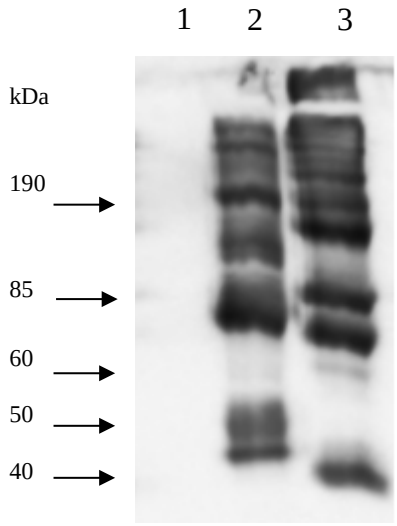

Figure 3.21 Western blot analyses of pLZ12-Km2:P23R_PilM1_β_E_XhoI expressed in *L. lactis*

Cell wall extracts analysed by Western blot with rabbit anti-Spy0128 antiserum. Lane 1: the negative control (*L. lactis*:pLZ12-Km2:P23R). Lane 2: *L. lactis*:pLZ12-Km2:P23R_PilM1_β_E _XhoI. Lane 3: the positive control (*L. lactis*:pLZ12-Km2:P23R_PilM1). High molecular weight laddering pattern was visible in the cell wall extract from *L. lactis*:pLZ12-Km2:P23R_PilM1_β_E_XhoI.

3.2.6.2 Engineering the OVA$_{323\text{-}339}$ peptide between the β_E and β_F strands of Spy0128

Due to the fact that replacing the β_E-β_F loop region with an XhoI site had no adverse impact on surface pilus assembly, the *ova*$_{323\text{-}339}$ DNA sequence was cloned into that XhoI site and the resulting plasmid, pLZ12-Km2:P23R_PilM1_β_E_*ova*$_{323\text{-}339}$, was transformed into *E. coli* DH5α. Following confirmation of a positive colony using the OVA fw and Spy0128 rv primers, the plasmid was extracted from the DH5α and electroporated into *L. lactis* (figure 3.22).

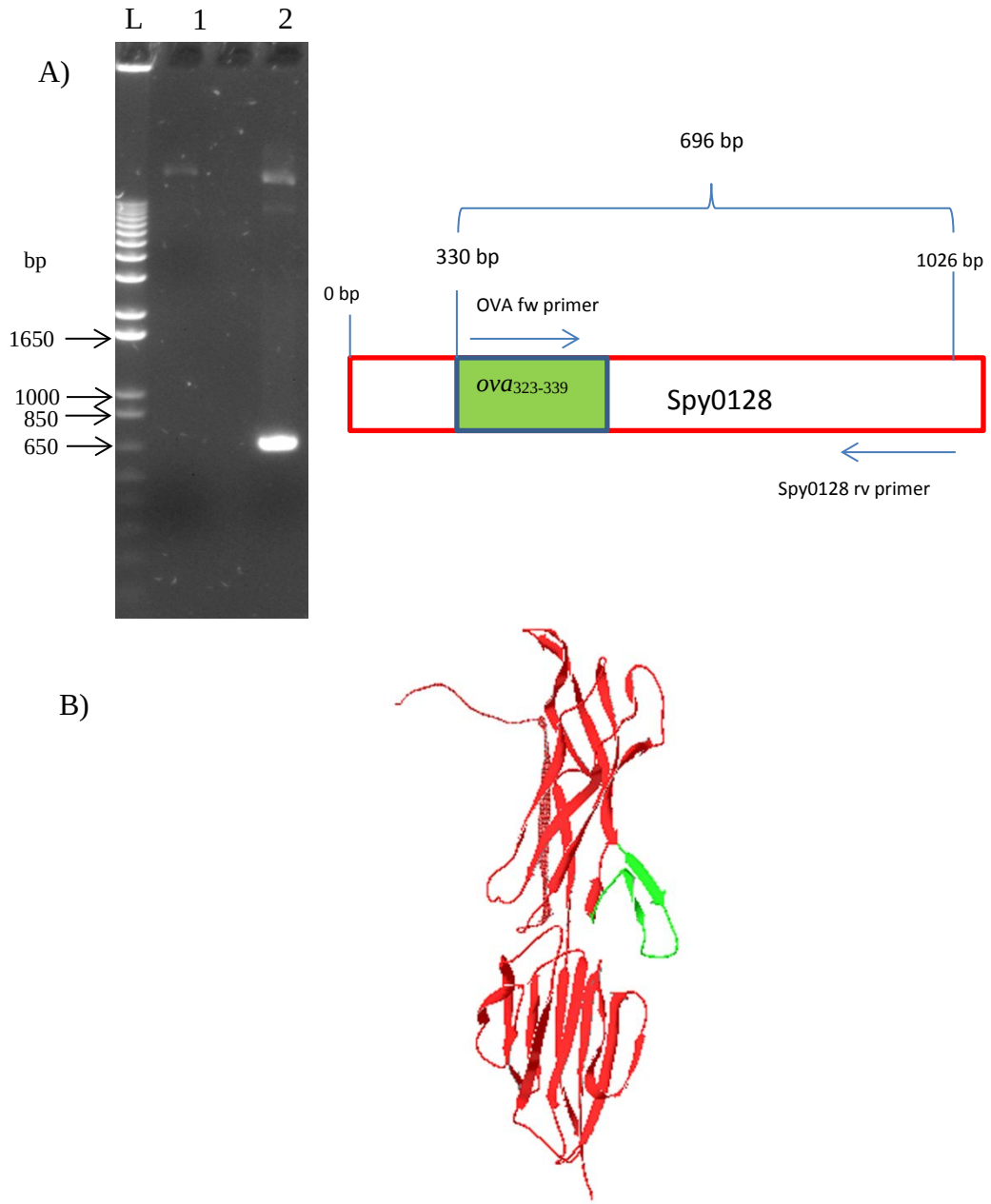

Figure 3.22 The pLZ12-Km2:P23R_PilM1_β_E_*ova*$_{323-339}$ plasmid was successfully electroporated into *L. lactis*

A) The OVA fw and Spy0128 rv primers were used to select an *L. lactis* colony containing with the pLZ12-Km2:P23R_PilM1_β_E_*ova*$_{323-339}$ plasmid. Schematic diagram on the right shows primer binding sites and the expected size of the PCR product if positive. The image on the left features 1% agarose gel electrophoresis. Lane L: the 1 kb molecular weight marker. Lane 1: the negative control (*L .lactis*:pLZ12-Km2:P23R_PilM1). Lane 2: *L. Lactis*:pLZ12-Km2:P23R_PilM1_β_E _*ova*$_{323-339}$.

B) Computer generated structure, using the SWISS-MODEL web server, showing the OVA$_{323-339}$ peptide (in green) between the β_E and β_F strands of Spy0128.

To determine if the integration of the $OVA_{323-339}$ peptide within the Spy0128 subunit affects the surface polymerisation of the pilus, a cell wall extract from *L. Lactis*:pLZ12-Km2:P23R_PilM1_β_E_*ova*$_{323-339}$ was analysed by Western blot with rabbit anti-Spy0128 antiserum. The results indicate that replacing the β_E-β_F loop region with the $OVA_{323-339}$ peptide does not disrupt the polymerisation of the pilus. The anti-Spy0128 antiserum recognised a ladder of high molecular weight bands characteristic of pilus formation and the pattern is similar to that from the cell wall extract of *L. lactis* expressing wild-type pili (figure 3.23).

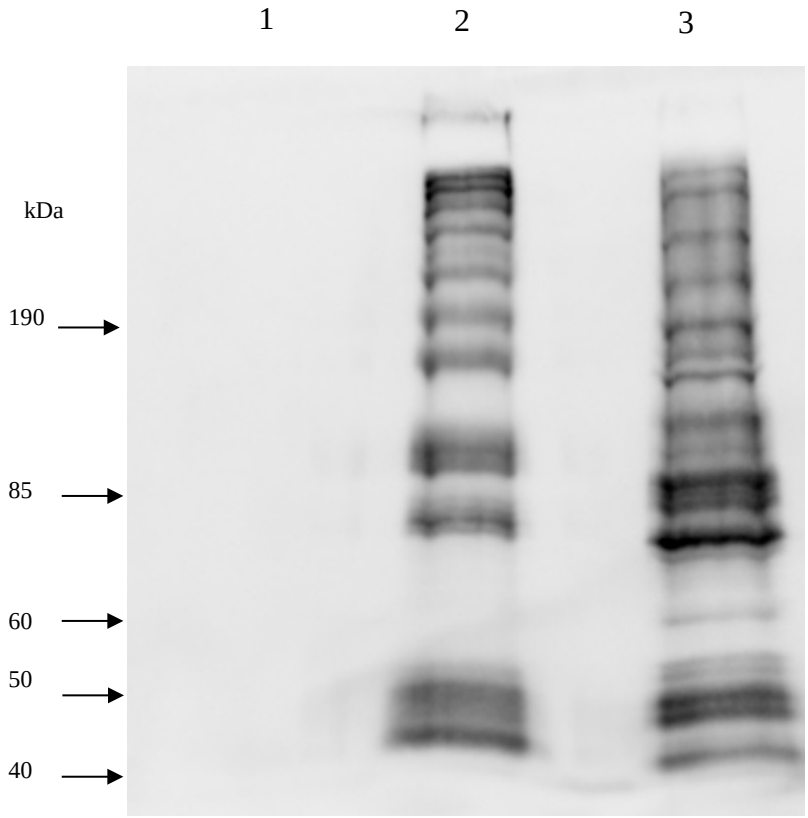

Figure 3.23 Western blot analyses of pLZ12-Km2:P23R_PilM1_β_E _*ova*$_{323-339}$ expressed in *L. lactis*

Cell wall extracts analysed by Western blot with rabbit anti-Spy0128 antiserum. Lane 1: the negative control (*L. Lactis*:pLZ12-Km2:P23R). Lane 2: *L. Lactis*:pLZ12-Km2:P23R_PilM1_β_E _*ova*$_{323-339}$. Lane 3: the positive control (*L. Lactis*:pLZ12-Km2:P23R_PilM1). High molecular weight laddering pattern was visible in the cell wall extract from *L. Lactis*:pLZ12-Km2:P23R_PilM1_β_E _*ova*$_{323-339.}$

Flow cytometry was performed, using mouse antiserum specific for ovalbumin, to confirm the presence of the $OVA_{323-339}$ peptide on the surface of *L. lactis*. For the flow cytometry assay,

Pilvax and *L. lactis* expressing wild type pilus were initially incubated with anti-ovalbumin antiserum. Then, after washing, the two strains were incubated with FITC tagged goat anti-mouse antibodies. If the OVA peptide is integrated within Pilvax, both the anti-OVA antibodies and the FITC tagged antibodies will bind, resulting in a fluorescent shift over the background when detected by flow cytometry. As shown in figure 3.24, the right shift to higher fluorescence values observed for *L. Lactis*:pLZ12-Km2:P23R _PilM1_ β_E _$ova_{323-339}$ (green histogram) confirmed that the peptide was present and exposed on the outer side of the *L. lactis* cell wall. The presence of two peaks in the histogram is probably due to the fact that the recombinant *L. lactis* express varying numbers OVA peptide within their pili. Each pilus shaft can consist of 50-100 Spy0128 subunits, so some *L. lactis* will express more OVA peptide within their pili leading to a greater fluorescent shift than that obtained from other recombinant *L. lactis*. *L. lactis* expressing wild type pilus (red histogram) did not contain OVA peptide, hence the antibodies were unable to bind and thus only exhibited background levels of fluorescence as expected.

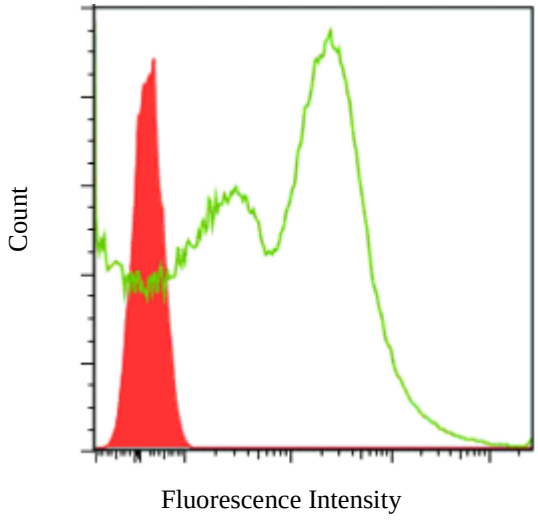

Figure 3.24 Expression of the $OVA_{323-339}$ peptide on the surface of *L. Lactis*:pLZ12-Km2:P23R _PilM1_ β_E _ $ova_{323-339}$ was confirmed by flow cytometry

Flow cytometry analyses of *L. Lactis*:pLZ12-Km2:P23R_PilM1_β_E _$ova_{323-339}$ (*green void histogram*) and *L. Lactis:*pLZ12-Km2:P23R_PilM1 (*full red histogram)* with mouse anti-ovalbumin antiserum.

To confirm the presence of the $OVA_{323-339}$ peptide in the pilus shaft itself, the TCA precipitated cell wall extract from *L. Lactis*:pLZ12-Km2:P23R _PilM1_β_E _$ova_{323-339}$ was analysed by

Western blot with mouse anti-ovalbumin antiserum. The antiserum recognised a ladder of high-molecular-weight bands and this indicates that the $OVA_{323-339}$ peptide was incorporated into the Spy0128 subunit, resulting in the multimeric presentation of the peptide on the surface of *L. lactis*. This result is further confirmed by the absence of bands in the cell wall extract from *L. lactis* expressing wild-type pili and also the presence of a single band at around 45 kDa for the positive control which consisted of ovalbumin protein (figure 3.25).

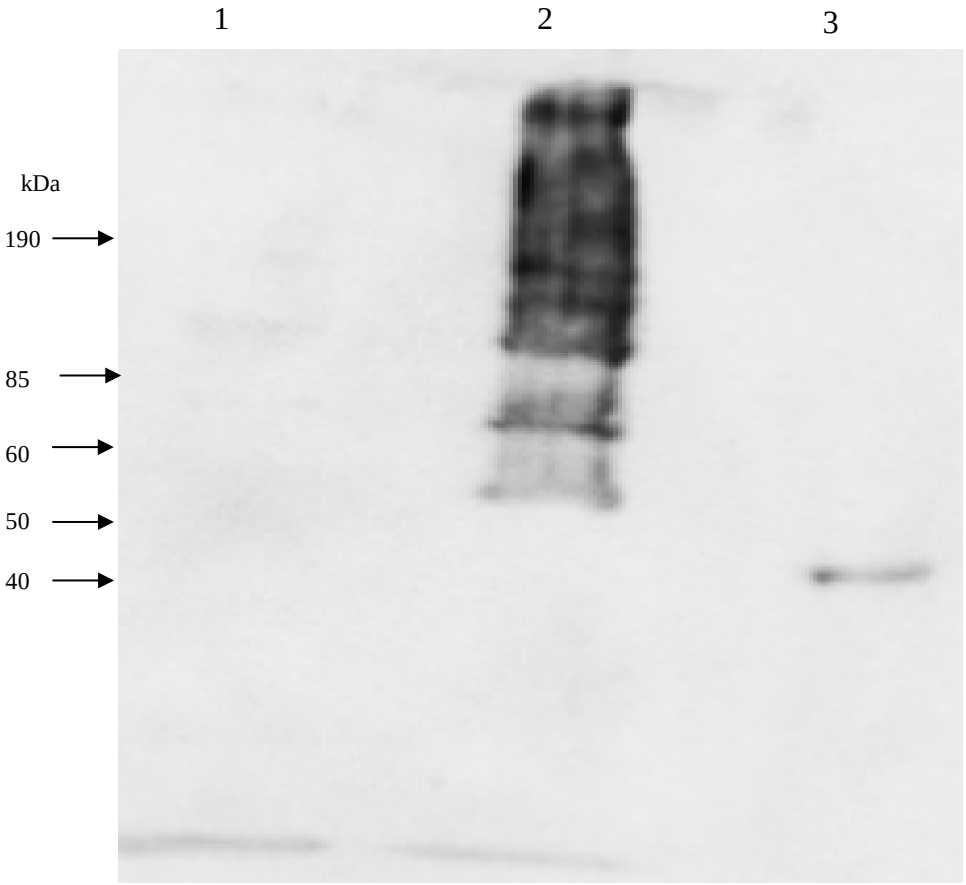

Figure 3.25 The $OVA_{323-339}$ peptide is incorporated into assembled pilus structures on the surface of *L. lactis*

Western blot analyses of cell wall extracts with mouse anti-ovalbumin antiserum. Lane 1: Negative control (cell wall extract from *L. lactis*:pLZ12-Km2:P23R_PilM1). Lane 2: cell wall extract from *L. Lactis*:pLZ12-Km2:P23R_PilM1_β_E_$ova_{323-339}$. Lane 3: Positive control (ovalbumin protein).

3.3 Summary

Five loop regions of Spy0128 were investigated as potential sites which could be replaced with the model $OVA_{323-339}$ peptide and the results are summarised in table 3.2.

Table 3.2 Summary of the Western blot results

Loop Region	Pilus expression after replacing the loop region with a XhoI site	Pilus expression after engineering the $OVA_{323-339}$ peptide into the XhoI site
β_B-β_{C1}		
β_2-β_3		

β_3-β_4		
β_D-β_E		
β_E-β_F	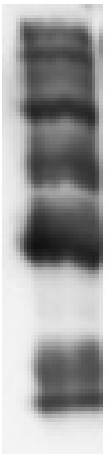	

The initial step of engineering the $OVA_{323-339}$ peptide into a loop region involved replacing the loop region DNA sequence with a XhoI site. Replacing the β_D-$\beta_E$loop region with a XhoI site eliminated the homopolymerisation of the Spy0128 subunits. Following replacement of the loop region, the plasmid was not sequenced due to the large size of the pilus operon. It is, therefore, possible that a mutation somewhere along the pilus operon may cause the abrogation of pilus polymerisation. Another possibility is that deletion of the loop region affected the covalent cross-linking between Spy0128 subunits, thus preventing the shaft of the pilus being formed. Of the remaining loop region sequences replaced with a XhoI site, none resulted in abrogation of pilus polymerisation on the bacterial surface, which enabled the cloning of the *ova*$_{323-339}$ DNA sequence into each of the XhoI sites.

Replacing the β_3-$\beta_4$loop region with the $OVA_{323-339}$ peptide prevented the shaft of the pilus being formed, which suggests that the covalent cross-linking between Spy0128 subunits is affected by the peptide. Replacing the β_B-β_{C1}or β_2-β_3 loop regions with the $OVA_{323-339}$ peptide also affected pilus polymerisation. Although, in contrast to the β_3-β_4 loop region where polymerisation of the pilus shaft was eliminated, the Western blot analyses revealed that shorter forms of the polymeric pilus structures were being assembled. However, for the use of the pilus as a peptide delivery system, long pili are needed for effective multimeric presentation, thus these two loop regions were deemed to be inadequate for that purpose.

Out of the five loop regions investigated, the β_E-β_F loop region was the only site which could be replaced with the $OVA_{323-339}$ peptide without interfering with pilin folding and pilus assembly on the cell surface. Western blot analyses, with anti-Spy0128 antiserum, of a cell wall extract from *L. lactis* expressing $OVA_{323-339}$ peptide-linked pili revealed a ladder of high molecular weight polymers that is characteristic of pilus formation (Mora, et al., 2005). The expression of the $OVA_{323-339}$ peptide within the pilus structure was confirmed by Western blot analyses and flow cytometry. Flow cytometry analyses showed that anti-ovalbumin antiserum specifically bound to the *L. lactis* expressing the peptide-linked pilus. Western blot analyses of a cell wall

extract from the recombinant *L. lactis* using anti-ovalbumin antiserum revealed a laddering pattern which confirms the fact that the peptide has been integrated within the Spy0128 subunit, resulting in the multimeric presentation of the peptide on the surface of *L. lactis*.

Chapter 4

Intranasal immunisation of mice with OVA-Pilvax elicits a mucosal and systemic antibody response

4.1 Introduction

Most licensed vaccines are administered parenterally and are generally poor at eliciting mucosal immune responses. However, mucosal surfaces represent an entry site of many pathogens, so vaccines that can induce protective mucosal immune responses are needed. Vaccine candidate antigens can be delivered to mucosal sites through the use of live bacterial vectors, such as attenuated pathogenic microorganisms. More recently, the food grade bacteria *L. lactis* has been recognised as a promising antigen delivery vehicle for the development of live mucosal vaccines, with numerous studies showing that *L. lactis* can be used to effectively deliver antigens to mucosal sites (Wells & Mercenier, 2008).

Expressing peptides within the GAS pilus structure on the surface of *L. lactis* (Pilvax) may yield a new strategy for peptide delivery by mucosal vaccination. As discussed in chapter three, the β_E-β_F loop region of the Spy0128 pilin subunit was replaced with the $OVA_{323-339}$ peptide and the peptide-linked pilus was expressed on the surface of *L. lactis* to create OVA-Pilvax. Therefore, to examine the potential of using Pilvax as a peptide delivery system, the aim of this chapter was to investigate the immune responses generated to the model peptide in mice intranasally inoculated with OVA-Pilvax.

4.2 Results

4.2.1 Expressing the M1 pilus on the surface of *L. lactis* does not aid bacterial survival following intranasal immunisation

Prolonged antigen exposure is often beneficial for a vaccine (Bachmann, et al., 2006). Due to the adhesive nature of the pilus, it was hypothesised that expressing the peptide-linked pilus on *L. lactis* may aid in bacterial survival and, hence, prolong peptide exposure. To determine if the pilus will aid bacterial survival, three BALB/c mice were intranasally administered with a bioluminescent *L. lactis* strain expressing the serotype M1 GAS pilus and firefly luciferase (*L. Lactis:*pLZ12-Km2:P23R_FFluc_PilM1), kindly obtained from Dr. Jaceyln Loh (University of Auckland, New Zealand), and the clearance of *L. Lactis:*pLZ12-Km2:P23R_FFluc_PilM1 was monitored by reading the bioluminescent signal. Three mice were chosen for each sample group as funding restrictions meant that using a larger sample size of mice was not feasible. A bioluminescent signal was observed in the nasal cavity of all three mice 30 minutes after intranasal administration and imaging also demonstrated the dissemination of bacteria into the lungs of two of the three mice. However, a luminescent signal was not detected in the lungs 6 hours after administration and the signal dissipated to background levels in all three mice 24 hours after administration. Mice were also immunised with a control *L. lactis* strain expressing firefly luciferase (*L. Lactis:*pLZ12-Km2:P23R_FFluc), kindly obtained from Dr. Jaceyln Loh, to determine if the pilus delays the clearance of *L. lactis.* The luminescent signal from *L. Lactis:*pLZ12-Km2:P23R_FFluc dissipated to background levels 24 hours after administration, indicating that both strains were cleared within a similar time frame (figure 4.1).

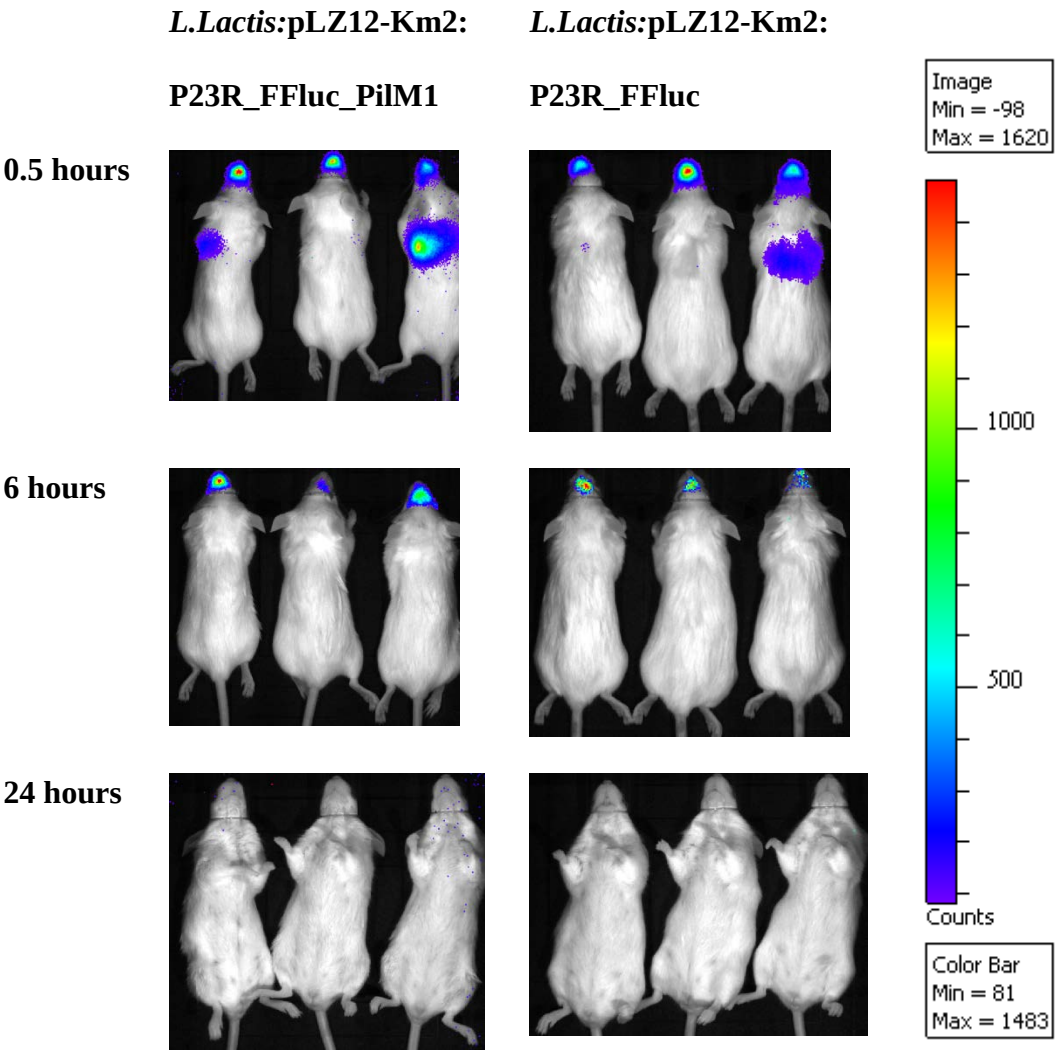

Figure 4.1 Bioluminescence imaging of bacterial distribution after intranasal inoculation with bioluminescent *L. Lactis:*pLZ12-Km2:P23R_FFluc_PilM1 or *L. Lactis:*pLZ12-Km2:P23R_FFluc

$1x10^9$ CFU of *L. Lactis:*pLZ12-Km2:P23R_FFn_PilM1 or *L. Lactis:*pLZ12-Km2:P23R_FFn were administered intranasally to female BALB/c mice (n = 3) in 50 µl of PBS. Images were acquired using an IVIS spectrum system and are displayed as images of peak bioluminescence, with variations in the colour representing light intensity at a given location. Red represents the most intense light emission while blue corresponds to the weakest emission. The colour bar indicates relative signal intensity (as photons s^{-1} cm^2 sr^{-1}).

4.2.2 Ovalbumin-specific antibody responses elicited in mice immunised with OVA-Pilvax

The delivery of peptides using Pilvax may provide a new strategy for mucosal vaccination. A similar delivery system to Pilvax has been developed by Quigley *et al* using the tip of the T3 pilus as a carrier of vaccine antigens (UPTOP delivery system) and they have successfully shown proof of concept, so the immmunisation schedule and also the format to display ELISA results were based on the work undertaken by Quigley *et al* (Quigley, et al., 2010).

To determine if OVA-Pilvax can elicit an ovalbumin (OVA)-specific systemic and mucosal immune response, BALB/c mice were immunised intranasally three times at two week intervals with 25 µl of OVA-Pilvax ($1x10^9$ CFU per mouse) and the immune response was compared to the response from negative control mice similarly immunised with *L. Lactis* expressing the wild-type pilus (*L. lactis*:pLZ12-Km2:P23R_PilM1). Alternatively, mice were also intranasally immunised three times with 25 µg of $OVA_{323-339}$ peptide mixed with 2 µg of cholera toxin B ($OVA_{323-339}$-CTB), in a 25µl dose, as a positive control.

A decrease in body weight of mice is an early predictor of morbidity. Under the animal ethical guidelines of the University of Auckland, weight loss exceeding 20% of baseline bodyweight or weight loss of 15% or more over 24 hours was deemed a humane endpoint for the experiment. Weight-loss was not observed in mice immunised with OVA-Pilvax when monitored one week after each immunisation, nor were any other untoward behavioural effects observed post-immunisation. This indicates that OVA-Pilvax is safe to use in mice at this dose.

The dot blot system is a simple and fast assay that can obtain results with a similar sensitivity to ELISAs; hence it was initially used to assess the induction of an OVA-specific IgG response in the serum from mice following intranasal immunisation (Vera-Cabrera, et al., 1999). Interestingly, a chemiluminescent signal was only produced when OVA protein was blotted with pooled serum from mice immunised with OVA-Pilvax and detected using Goat anti-mouse IgG-HRP, while no signal was produced with pooled serum from mice immunised with $OVA_{323-339}$-

CTB or *L. lactis* expressing wild-type pilus(figure 3.2). This suggests that OVA-specific IgG antibodies were only elicited in mice immunised with OVA-Pilvax.

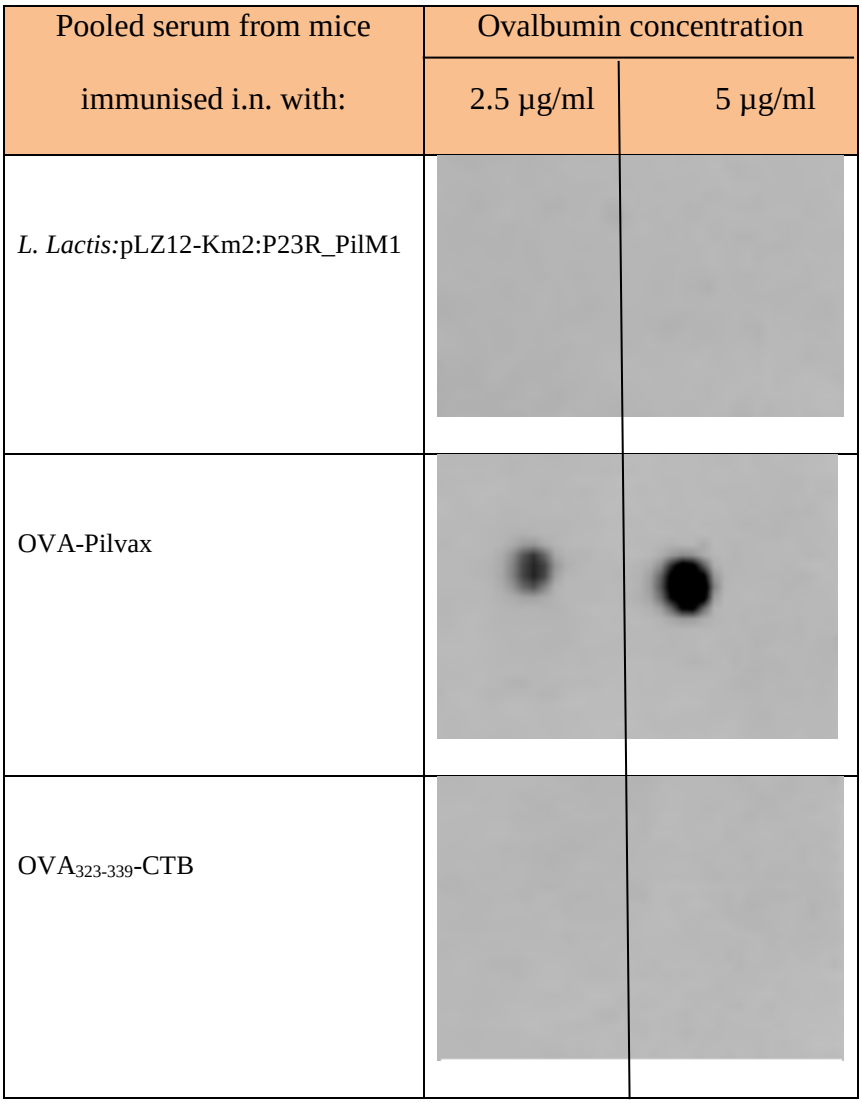

Figure 4.2 Dot blot assay indicating the presence of anti-OVA IgG antibodies in the serum of mice immunised with OVA-Pilvax

Ovalbumin (2.5 and 5 µg/ml) was spotted onto a nitrocellulose membrane and blotted with pooled serum from mice immunised with either OVA-Pilvax, *L. Lactis*:pLZ12-Km2:P23R_PilM1, or $OVA_{323-339}$-CTB. Pooled serum was tested at a 1:100 dilution and the signals were detected by chemiluminescence using peroxidase-conjugated anti-mouse IgG and ECL Western blotting detection reagents.

The predominant Ig isotype in mucosal secretions is IgA (Macpherson, et al., 2008). To assess the induction of a local mucosal antibody response following intranasal immunisation, the

presence of OVA-specific IgA in bronchoalveolar lavage fluid (BALF) from immunised mice was determined by using an ELISA with immobilised OVA. In the group of mice immunised with OVA-Pilvax, an IgA response to OVA was only detected in two of the five mice, with the response being approximately three times and eight times higher than the background response (which was the response generated from negative control mice immunised with *L. lactis* expressing wild-type pilus). In addition, only background activity was found in mice immunised with $OVA_{323-339}$-CTB (figure 4.3).

To explain the variability in the production of anti-OVA IgG antibodies in mice immunised with OVA-Pilvax, the OVA-specific IgG response was compared to the Spy0128-specific IgG response in each individual mice immunised with OVA-Pilvax. The results indicated that the mice which had a low response towards Spy0128 had a low response towards OVA, which is expected as the $OVA_{323-339}$ peptide is integrated into the Spy0128 subunit (figure 4.4). Spy0128 is known to be highly immunogenic, (Manetti, et al., 2007), so the variability in the anti-Spy0128 antibody responses elicited in mice immunised with OVA-Pilvax may be a result of the volume of the inoculum used. A volume of 25 µl was used for immunisation and, in certain mice, this may not allow sufficient OVA-Pilvaxto be deposited into the nasal cavity to induce an antibody response. Thus, the experiment was repeated with mice being immunised with a larger dose of OVA-Pilvax. A study by Shin *et al* investigating the effectiveness of an inactivated swine-origin influenza A/H1N1 virus vaccine suggested that vaccine doses of 50 µl administered intranasally can still insufficient to induce an adequate immune response in the mice (Shin, et al., 2015). However, due to concerns about the adverse effects a dose higher than 50 µl would have on the health of immunised mice, the experiment was repeated with mice being immunised with a 50 µl dose of OVA-Pilvax, with the immunisation timetable being increased by a week in an attempt to reduce variability in the antibody responses.

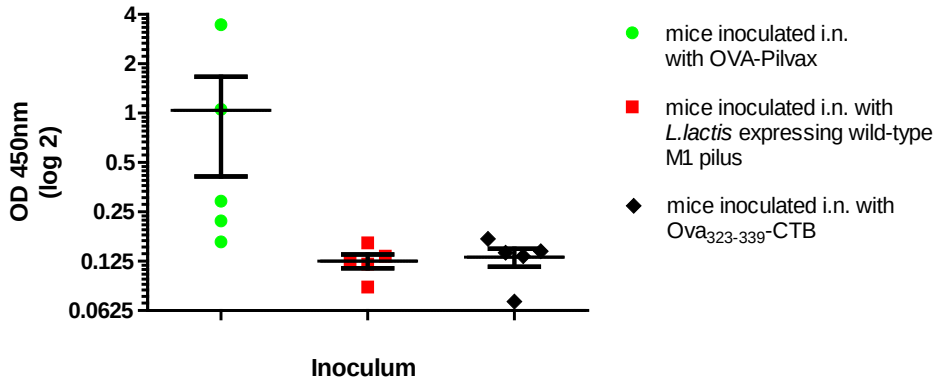

Figure 4.3 OVA-specific IgA antibody responses in bronchoalveolar lavage fluid from immunised BALB/c mice

OVA-specific IgA in BALF collected 7 days after the third immunisation from mice inoculated i.n. with OVA-Pilvax (●, n=5), *L. Lactis:*pLZ12-Km2:P23R_PilM1 (■, n=5), or OVA $_{323-339}$-CTB (◆, n=5). The IgA response was determined in undiluted samples from individual mice by ELISA performed in triplicate and the data is from a single experiment. Each point represents a single mouse with the mean and standard error of the mean for each group represented as bars

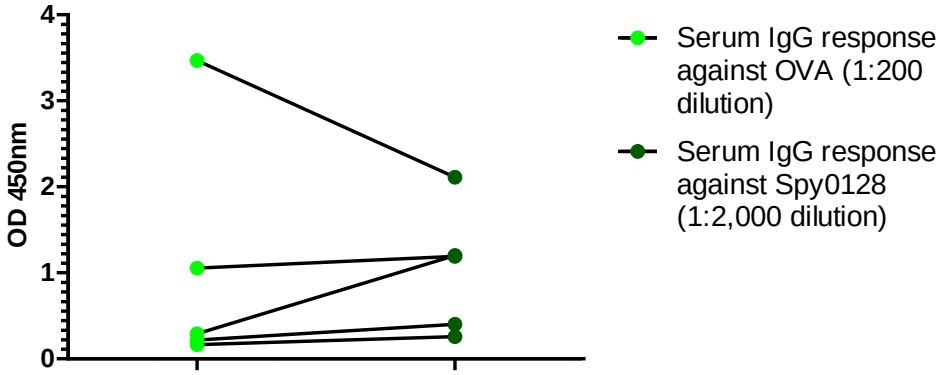

Figure 4.4 Comparing the OVA-specific IgG response to the Spy0128-specific IgG response from individual mice immunised with OVA-Pilvax

The average OVA-specific IgG response in serum (diluted 1:200) was compared to the average Spy0128-specific response in serum (diluted 1:2,000) from each OVA-Pilvax immunised mouse. The IgG responses were determined by ELISA performed in triplicate. Data is from a single experiment (n= 5 mice in total).

4.2.3 New protocol for vaccine administration

Due to the variability in the antibody responses from mice immunised with 25 µl of OVA-Pilvax, a new vaccine administration protocol was selected. Mice were immunised intranasally four times at two-week intervals with 50 µl of OVA-Pilvax ($1x10^9$ CFU per mouse) and the immune response against OVA was compared to the immune response from negative control mice similarly immunised with *L. lactis* expressing wild-type pilus (*L. lactis*:pLZ12-Km2:P23R_PilM1). Since immunising mice with 25 µg of $OVA_{323-339}$ mixed with 2 µg of CTB did not produce an antibody response against OVA, mice were immunised intranasally four times with 50 µg of $OVA_{323-339}$ mixed with 10 µg of CTB in a 50 µl dose. Alternatively, mice were subcutaneously immunised four times at two-week intervals with 50 µg of $OVA_{323-339}$ emulsified 1:1 in Incomplete Freud's Adjuvant to compare the antibody responses generated by parenteral immunisation as opposed to intranasal immunisation.

In order to allow a comparison of the mucosal antibody response elicited by Pilvax to the response from the UPTOP vaccine carrier developed by Quigley *et al*, the same format to display the ELISA results was used, whereby optical density was used to show the induction of an OVA-specific IgA response in mucosal secretions (Quigley, et al., 2010). However, a number of publications proving the effectiveness of *L. lactis* carrying vaccine antigens to elicit a protective immune response display the antigen-specific serum IgG response as endpoint antibody titres, a good example being the study by Hannify *et al* investigating the mucosal delivery of a pneumococcal vaccine using *L. lactis* which afforded protection against respiratory infection (Hanniffy, et al., 2007). Therefore the ELISA data of the OVA-specific serum IgG responses elicited by OVA-Pilvax were displayed using a comparable format (endpoint antibody titres). The size of the mouse group used in the experiments done by Quigley *et al* to show proof of concept for UPTOP consisted of 10 mice, so a similar sample number, 12, was used in the experiments to show proof of concept for Pilvax (Quigley, et al., 2010).

4.2.4 Elicitation of systemic antibody responses in mice after intranasal immunisation

4.2.4.1 The Spy0128-specific serum IgG responses

Initially, the serum IgG response to recombinant Spy0128 protein was assessed by using an ELISA, as an internal control to determine if immunisation with OVA-Pilvax was successful. Anti-Spy0128 antibodies were detected in the serum of all mice immunised with OVA-Pilvax and *L. lactis* expressing wild type pili. The average endpoint titres were 1:36,000 and 1:39,000, respectively. Only background activity was found in serum from the two groups of mice immunised with $OVA_{323-339}$-peptide as expected (figure 4.5).

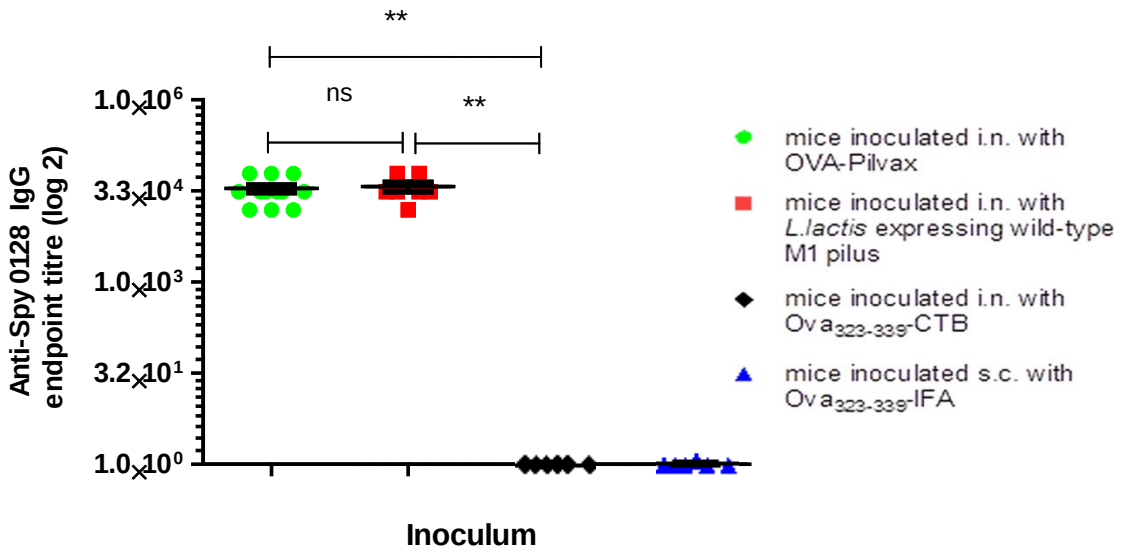

Figure 4.5 Spy0128-specific IgG antibody responses in serum from immunised BALB/c mice

Sera were collected from mice 7 days after the fourth immunisation and the Spy0128-specific IgG antibody titres were determined by ELISA performed in triplicate. Serum samples were taken from mice inoculated i.n. OVA-Pilvax (●, n=12), *L. Lactis:*pLZ12-Km2: P23R_PilM1 (■, n=7), $OVA_{323-339}$-CTB (◆, n=7), or subcutaneously with $OVA_{323-339}$-IFA (▲, n=7). The average titre for individual mice is shown and the data are combined from two independent experiments. The mean and standard error of the mean for each group are represented as bars. Statistical differences were determined using one-way ANOVA with Bonferroni post-hoc test (**P < 0.05; ns = non-significant difference)

4.2.4.2 The OVA-specific serum IgG responses

To assess the induction of a systemic antibody response following intranasal immunisation, the presence of OVA-specific IgG in the serum was determined by using an ELISA with immobilised OVA. Anti-OVA antibodies were detected in ten of the twelve OVA-Pilvax immunised mice and all of the mice subcutaneously immunised with $OVA_{323-339}$-IFA. The average endpoint titre of OVA-specific IgG in the serum samples from OVA-Pilvax immunised mice was approximately 1:7,000. Serum from mice immunised subcutaneously with $OVA_{323-339}$-IFA displayed a significantly higher average endpoint titre of approximately 1:26,000. Only background activity was found in serum from mice immunised with *L. lactis* expressing the wild-type pilus or $OVA_{323-339}$-CTB (figure 4.6).

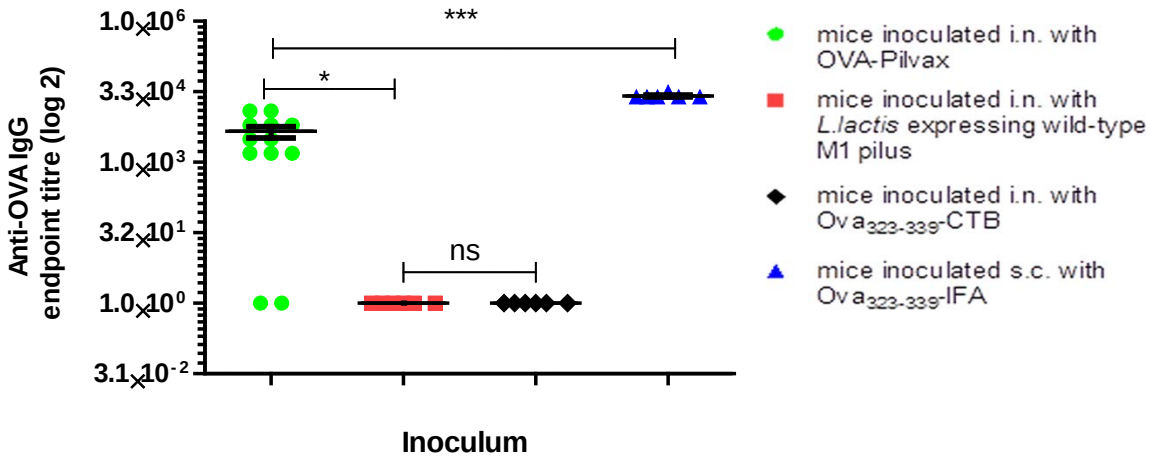

Figure 4.6 OVA-specific IgG antibody responses in serum from immunised BALB/c mice

Sera were collected from mice 7 days after the fourth immunisation and the OVA-specific IgG antibody titres were determined by ELISA performed in triplicate Serum samples were taken from mice inoculated i.n. OVA-Pilvax (●, n=12), *L. Lactis:*pLZ12-Km2: P23R_PilM1 (■, n=7), $OVA_{323-339}$-CTB (◆, n=7), or subcutaneously with $OVA_{323-339}$-IFA (▲, n=7). The average titre for individual mice is shown and the data are combined from two independent experiments. The mean and standard error of the mean for each group are represented as bars.Statistical differences were determined using one-way ANOVA with Bonferroni post-hoc test (*P < 0.05; ***P < 0.001; ns = non-significant difference).

4.2.4.3 Variability in the OVA-specific IgG serum response in mice immunised with OVA-Pilvax

The OVA-specific IgG serum response in a group of mice immunised with OVA-Pilvax shows that, despite increasing the volume of immunisation to 50ul, there is a still a variable antibody response towards OVA between the individual mice in the group. The IgG response in serum (diluted 1:200) increases between the first and second booster immunisations of OVA-Pilvax or $OVA_{323-339}$-IFA emulsion. However, after the fourth booster immunisation, while all the mice immunised with the positive control of $OVA_{323-339}$-IFA had a strong OVA-specific IgG response, there was no noticeable production of OVA-specific IgG in two of the OVA-Pilvax immunised mice and the response in the rest of the mice ranged from two to ten times higher than the background response (the same as in pre-immune serum) (figure 4.7).

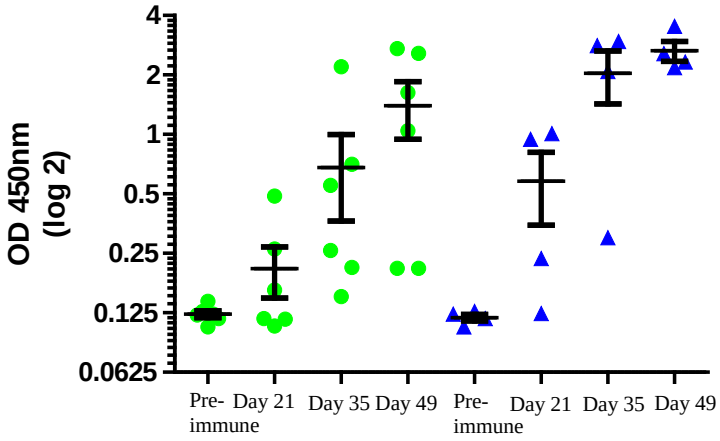

Figure 4.7 OVA-specific IgG responses in serum samples from individual mice taken 1 week after each booster immunisation

OVA-specific IgG in serum collected one week after each booster immunisation from mice inoculated i.n. with OVA-Pilvax (●, n=6) or subcutaneously with $OVA_{323-339}$-IFA(▲, n=4). The IgG response was determined in serum samples (diluted 1:200) from individual mice by ELISA performed once. Each data point represents a single mouse with the mean and standard error of the mean for each group represented as bars.

To explain the variability in the production of anti-OVA IgG antibodies in mice immunised with OVA-Pilvax, from two independent experiments, the OVA-specific IgG response was compared to the Spy0128-specific IgG response in serum from immunised mice. The results indicate that high anti-Spy0128 IgG absorbance levels trended well with high anti-OVA IgG absorbance levels when comparing individual mice which is expected as the $OVA_{323-339}$ peptide is integrated into the Spy0128 subunit (figure 4.8).

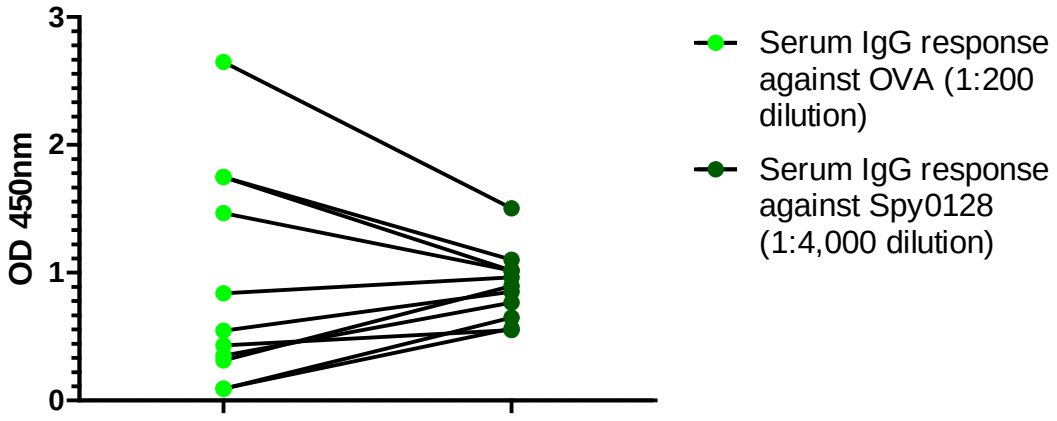

Figure 4.8 Comparing the OVA-specific IgG response to the Spy0128-specific IgG response from individual mice immunised with OVA-Pilvax

The average OVA-specific IgG response in serum (diluted 1:200) was compared to the average Spy0128-specific response in serum (diluted 1:4,000) from each OVA-Pilvax immunised mouse. The IgG responses were determined by ELISA performed in triplicate. Data are combined from two independent experiments (n= 12 mice in total).

4.2.4.4 Determination of IgG subclasses in immunised mouse serum

Levels of OVA-specific IgG1 and IgG2a subclasses in the serum were determined by ELISA using isotope-specific secondary antibodies to investigate the effect that Pilvax and the vaccination route has on T helper subset responses. A Th1 response results in IgG2a synthesis and a Th2 reponse results in IgG1 synthesis. Mice subcutaneously immunised with $OVA_{323-339}$-IFA elicited a dominant OVA-specific IgG1 response, the average endpoint titre being approximately 1:9,000. However, Immunising mice with OVA-Pilvax elicited OVA-specific antibodies of both isotypes, IgG1 and IgG2a, the average endpoint titres being 1:1,600 and 1:4000 respectively (figure 4.9).

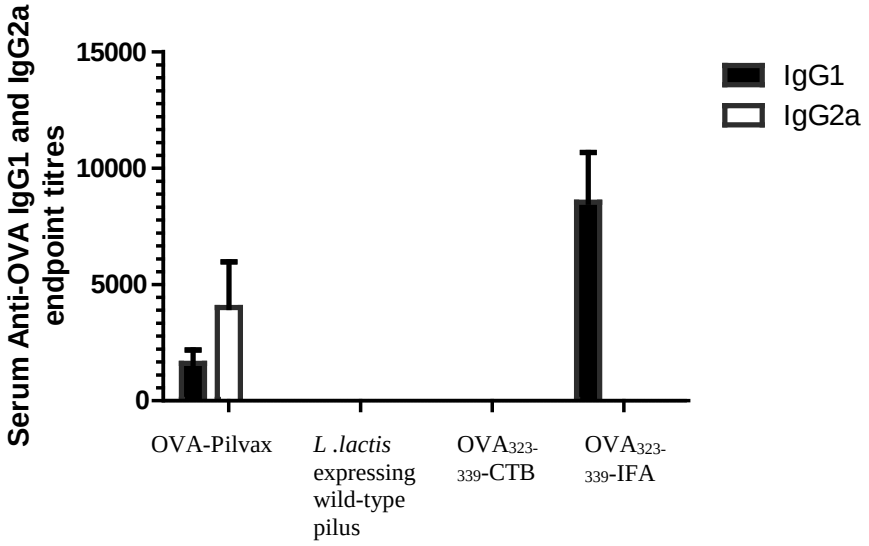

Figure 4.9 OVA-specific IgG1 and IgG2a antibody responses in serum from immunised BALB/c mice

The OVA-specific IgG1 and IgG2a antibody titres in serum samples collected 7 days after the fourth immunisation. Serum samples were taken from mice inoculated i.n. with OVA-Pilvax (n=12), *L. Lactis:*pLZ12-Km2:P23R_PilM (n=7), or $OVA_{323-339}$-CTB (n=7), or subcutaneously with $OVA_{323-339}$-IFA (n=7). The average serum IgG1 and IgG2a antibody titres are shown, with the standard error of the mean indicated, and the data are combined from two independent experiments.

4.2.4.5 The OVA-specific serum IgA responses

While the induction of IgA antibodies is mainly important for mucosal defense against pathogens, it would be interesting to determine if IgA antibodies are present in the serum as well following intranasal immunisation with Pilvax. Therefore, a simple ELISA was undertaken using serum samples from immunised mice, diluted 1:200, to determine the presence of OVA-specific IgA antibodies in the serum. A measurable reaction with OVA was only demonstrated in mice immunised with OVA-Pilvax. The average IgA response to OVA in serum was approximately two times higher than the background response from mice immunised with *L. Lactis:*pLZ12-Km2: P23R_PilM1 (figure 4.10).

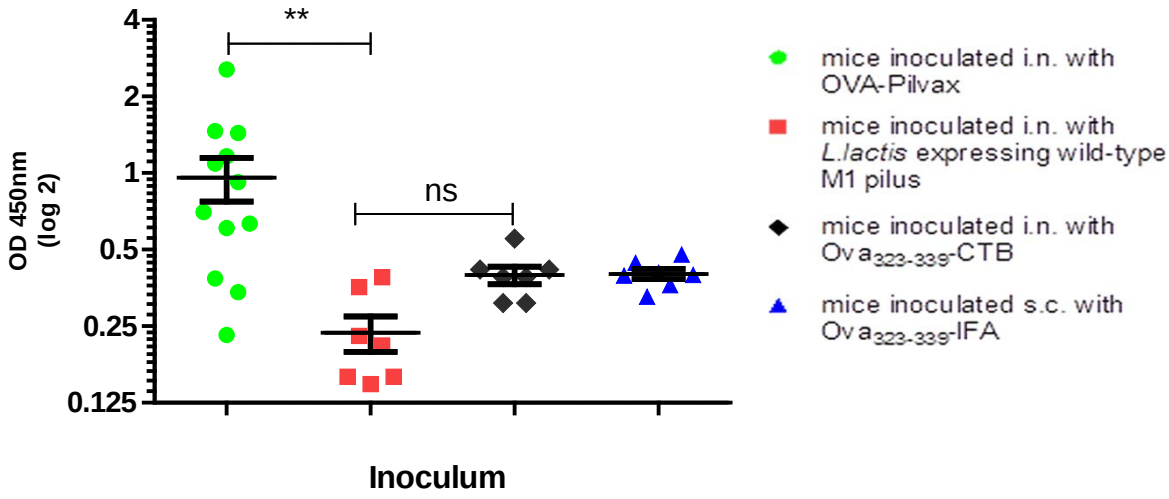

Figure 4.10 OVA-specific IgA antibody responses in serum from immunised BALB/c mice

OVA-specific IgA in serum collected 7 days after the fourth immunisation from mice inoculated i.n. with OVA-Pilvax (●, n=12), *L. Lactis:*pLZ12-Km2:P23R_PilM1 (■, n=7), or $OVA_{323-339}$-CTB (◆, n=7),or subcutaneously with $OVA_{323-339}$-IFA (▲, n=7). The IgA response was determined in serum samples (diluted 1:200) from individual mice by ELISA performed in triplicate and the data are combined from two independent experiments. Each point represents a single mouse with the mean and standard error of the mean for each group represented as bars. Statistical differences were determined using one-way ANOVA with Bonferroni post-hoc test (** $P < 0.01$; ns = non-significant difference).

4.2.4.6 Antigen-specific splenocyte proliferation following administration of OVA-Pilvax

Since OVA-Pilvax induced OVA-specific antibodies of both isotypes, IgG1 and IgG2a, indicating a mixed Th1/Th2 immune response, the ability of splenocytes from immunised mice to proliferate following *ex vivo* restimulation was investigated. Splenocytes from three individual mice which responded to OVA-Pilvax were isolated and restimulated with ovalbumin protein. In addition, splenocytes from three individual mice immunised with each of the control vaccine formulation were also restimulated. All isolated splenocytes were also restimulated with recombinant Toxic shock syndrome toxin 1 (TSST-1) protein, kindly obtained from Dr. Ries Langley (University of Auckland, New Zealand), as a positive control. Proliferation was quantified by the addition of [^{3}H] thymidine for the final 16 hours of the 72 hour culture period.

The splenocytes from all the mice immunised with each of the four different vaccine formulations demonstrated proliferation following *ex vivo* restimulation with 2 µg/ml of TSST-1. However, the splenocytes from mice immunised with OVA-Pilvax failed to proliferate following *ex vivo* restimulation with OVA. The thymidine uptake at the highest OVA concentration of 100 µg/ml was similar to the uptake observed in restimulated splenocytes from negative control mice immunised with *L. lactis* expressing wild-type pilus. In contrast, mice immunised with $OVA_{323-339}$-IFA demonstrated a significant increase in proliferation following restimulation with 100 µg/ml of OVA (figure 4.11).

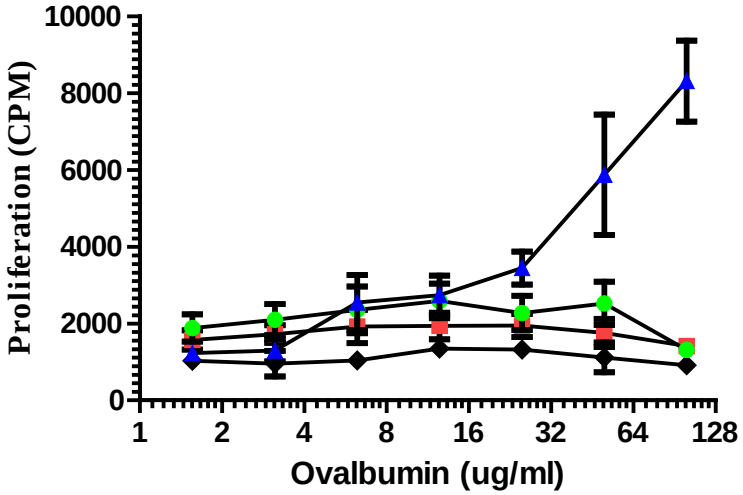

Figure 4.11 splenocytes from mice immunised with OVA-Pilvax failed to proliferate following *ex vivo* restimulation

Murine splenocytes from BALB/c mice inoculated i.n. with OVA-Pilvax (●, n=3), *L. Lactis:*pLZ12-Km2:P23R_PilM1 (■, n=3), or $OVA_{323-339}$-CTB (◆, n=3), or subcutaneously with $OVA_{323-339}$-IFA (▲, n=3) were cultured with graded doses of ovalbumin for 3 days and proliferation was quantified by uptake of tritiated thymidine over the final 16 hours of the culture period. Murine data are the mean and standard error of the mean from a single experiment.

4.2.5 Elicitation of mucosal antibody responses in mice after intranasal immunisation

4.2.5.1 The OVA-specific BALF IgA responses

To assess the elicitation of a local mucosal antibody response following intranasal immunisation, the presence of OVA-specific IgA in BALF from immunised mice was determined by using an ELISA with immobilised OVA. A measurable reaction with OVA was only demonstrated in mice immunised with OVA-Pilvax. Anti-OVA IgA antibodies were detected in ten of the twelve OVA-Pilvax immunised mice. The average IgA response to OVA was approximately seven times higher than the background response (the response from the negative control mice inoculated with *L. lactis* expressing wild-type pilus) and, in the two mice that responded best to OVA-Pilvax, the OVA-IgA endpoint titre in BALF was 1:16. Only background activity was found in BALF from mice immunised with $OVA_{323-339}$-CTB or

$OVA_{323-339}$-IFA (figure 4.12). Therefore, immunisation with OVA-Pilvax elicited a specific IgA response to OVA in the mucosal secretions.

When assessing the OVA-specific IgG response in BALF, the strongest reaction with OVA was noted in mice immunised subcutaneously with $OVA_{323-339}$-IFA, the response being two times higher than the response from mice immunised with OVA-Pilvax (figure 4.13).

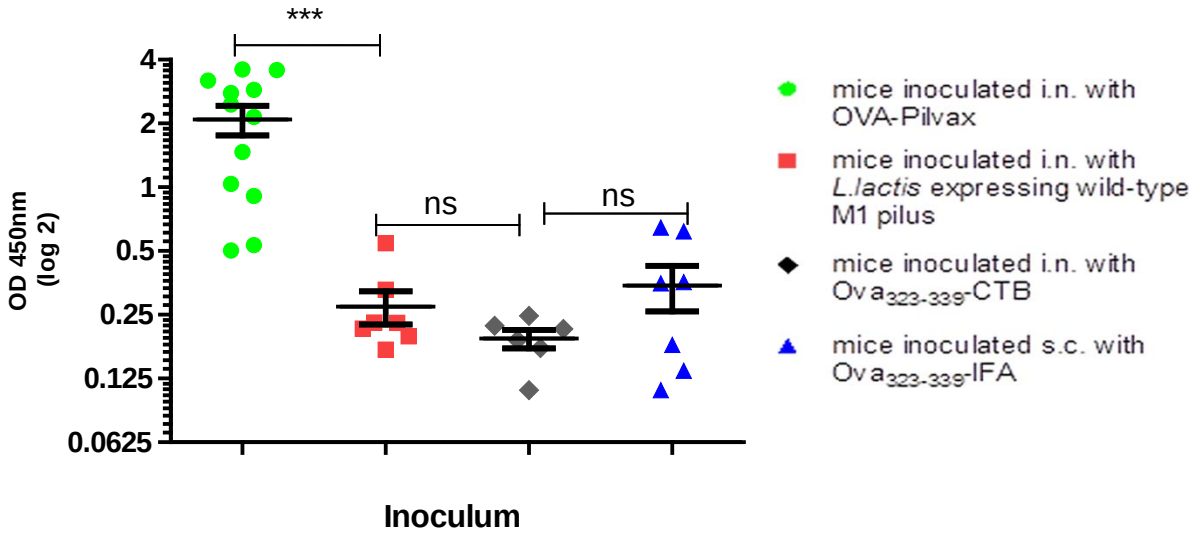

Figure 4.12 OVA-specific IgA antibody responses in bronchoalveolar lavage fluid from immunised BALB/c mice

OVA-specific IgA in BALF collected 7 days after the fourth immunisation from mice inoculated i.n. with OVA-Pilvax (●, n=12), *L. Lactis:*pLZ12-Km2:P23R_PilM1 (■, n=7), or $OVA_{323-339}$-CTB (◆, n=7), or subcutaneously with $OVA_{323-339}$-IFA (▲, n=7). The IgA response was determined in undiluted samples from individual mice by ELISA performed in triplicate and the data are combined from two independent experiments. Each point represents a single mouse with the mean and standard error of the mean for each group represented as bars. Statistical differences were determined using one-way ANOVA with Bonferroni post-hoc test (*** $P < 0.001$; ns = non-significant difference).

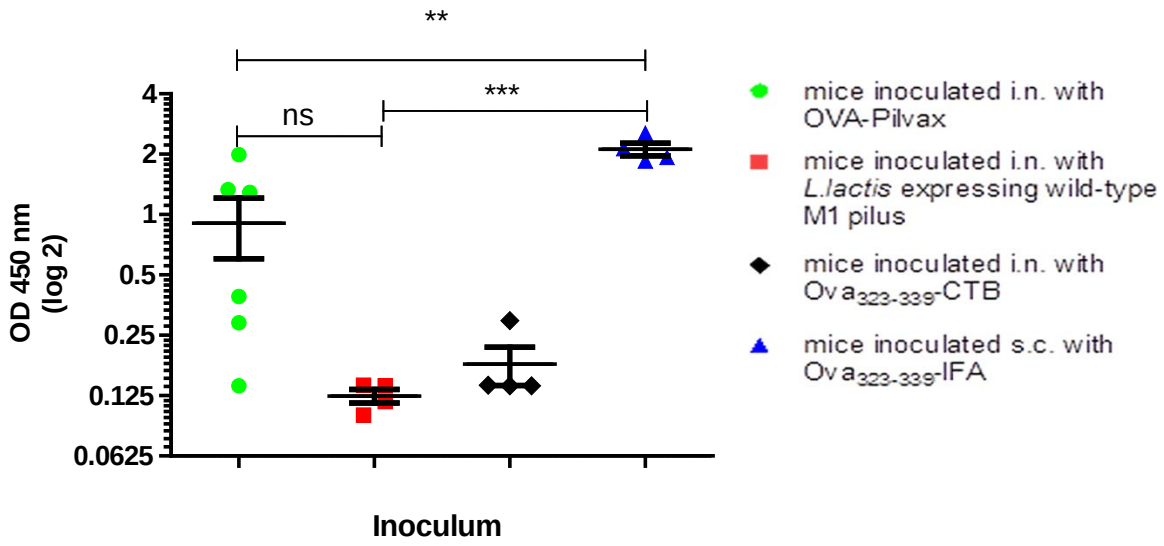

Figure 4.13 OVA-specific IgG antibody responses in bronchoalveolar lavage fluid from immunised BALB/c mice

OVA-specific IgG in BALF collected 7 days after the fourth immunisation from mice inoculated i.n. with OVA-Pilvax (, n=6), *L. Lactis*:pLZ12-Km2:P23R_PilM1(, n=4), or $OVA_{323-339}$-CTB (◆, n=4), or subcutaneously with $OVA_{323-339}$-IFA(, n=4). The IgA response was determined in undiluted samples from individual mice by ELISA performed once. Each data point represents a single mouse with the mean and standard error of the mean for each group represented as bars. Statistical differences were determined using one-way ANOVA with Bonferroni post-hoc test (*** $P < 0.05$; ns = non-significant difference)

4.2.5.2 The OVA-specific salivary IgA responses

The presence of IgA antibodies in the saliva has been shown to have a role in preventing infection by certain pathogens. Studies undertaken by Park *et al* have demonstrated that more than 70% of adults have measurable secretory immunoglobulin A (IgA) in their saliva, directed at the surface-bound C5a peptidase of GAS. In contrast, only 1 in 10 children under the age of 10 years were observed to have anti-SCPA antibodies in their saliva. These findings suggested that anti-SCPA antibodies could account for the lower incidence of disease and carriage of GAS in adults relative to children (Park & Cleary, 2005). Therefor the ability of Pilvax to elicit salivary antibodies against the OVA peptide was investigated. The presence of OVA-specific IgA in saliva from immunised mice was also detected by an ELISA with immobilised OVA. A measurable reaction with OVA was only demonstrated in mice immunised with OVA-Pilvax.

The average IgA response to OVA in undiluted saliva samples was at least 3 times higher than the response from mice immunised with the control vaccine formulations (figure 4.14).

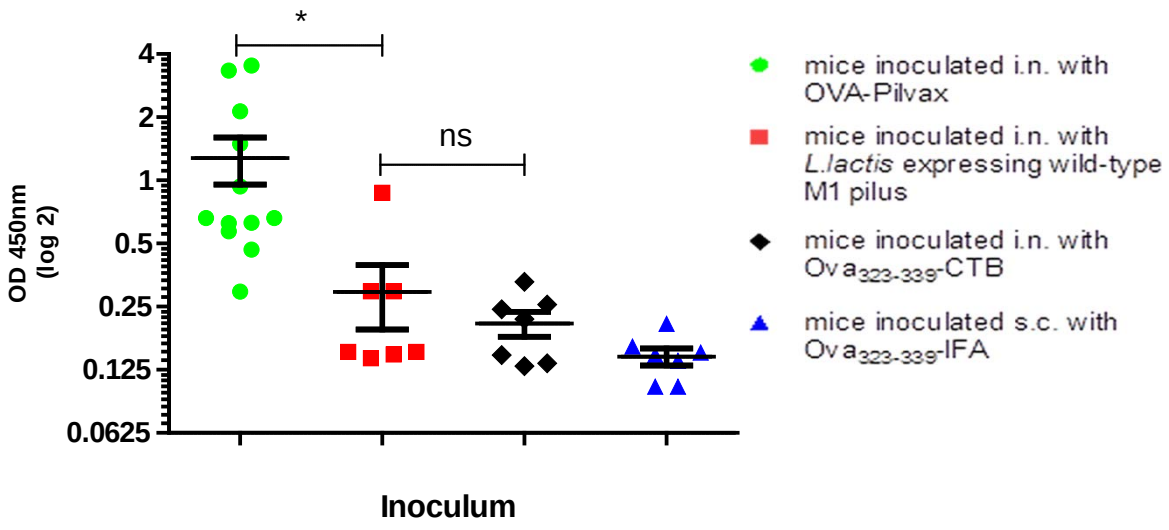

Figure 4.14 OVA-specific IgA antibody responses in saliva samples from immunised BALB/c mice

OVA-specific IgA in saliva samples collected 7 days after the fourth immunisation from mice inoculated i.n. with OVA-Pilvax (, n=12), *L. Lactis*:pLZ12-Km2:P23R_PilM1(, n=7), or $OVA_{323-339}$-CTB (, n=7), or subcutaneously with $OVA_{323-339}$-IFA(, n=7). The IgA response was determined in undiluted samples from individual mice by ELISA performed once. Each data point represents a single mouse with the mean and standard error of the mean for each group represented as bars. Statistical differences were determined using one-way ANOVA with Bonferroni post-hoc test (* $P < 0.05$; ns = non-significant difference).

4.3 Summary

Mucosal administration of OVA-Pilvax resulted in a detectable OVA-specific IgA response in BALF and salivary samples from immunised mice. This result suggests that Pilvax is able to generate mucosal immune responses against selected small peptides. In addition to the detectable IgA response, an IgG response to OVA was also detected in the serum of immunised mice. Therefore, Pilvax can elicit a systemic immune response which is promising as the serum antibodies can contribute to mucosal immunity (Roche, et al., 2015).

The isotype of the antigen-specific antibodies produced is an indicator of the type of immune response generated. Immunisation with OVA-Pilvax induced OVA-specific antibodies of both isotypes IgG1 and IgG2a, but a higher titre of IgG2a antibodies was induced following immunisation which suggests that the adaptive T-cell response to the OVA-Pilvax could be predominantly T helper 1 type. However, despite the elicitation of T cell-dependent anti-OVA IgG1 and IgG2a responses, splenocytes harvested from mice immunised with OVA-Pilvax failed to proliferate when restimulated with OVA.

The mucosal and systemic antibody responses elicited in OVA-Pilvax immunised mice was also variable, with an antibody response to OVA undetectable in some of the immunised mice. When the OVA-specific IgG response was compared to the Spy0128-specific IgG response from the same mouse, high anti-Spy0128 IgG levels trended well with high anti-OVA IgG levels. Since Syp0128 is known to be highly immunogenic, the likely reason that some mice had undetectable levels of anti-OVA IgG was likely because they received a lower dose of the vaccine.

In summary, mucosal administration of OVA-Pilvax induced a detectable OVA-specific IgA and IgG response. These results suggest that Pilvax may be a promising strategy to use for the safe and effective delivery of selected small peptides to mucosal sites.

Chapter 5

Delivering a conformationally restricted peptide to mucosal sites using Pilvax

5.1 Introduction

GAS is a human pathogen whose primary route of colonisation is through the mucosal epithelium of the pharynx (Walker, et al., 2014). A surface protein of GAS that is essential for its virulence is the M-protein. The protein is a key virulence factor involved in immune evasion and it is also highly antigenic (Metzgar & Zampolli, 2011; J. H. Robinson & Kehoe, 1992). It has therefore been investigated as a vaccine target.

The M-protein is a α-helical protein and over 80 different serotypes of M-protein are known. The primary structure of the protein, from the N- to the C- terminus, consists of three repetitive domains (A, B, and C), with a fourth proline/glycine-rich region associated with the cell membrane (Fischetti, 1989). It is the hypervariable N-terminus that defines the *emm* genotype and also the serotype (Whatmore, et al., 1994). The sequence variability that occurs between different GAS M proteins has made it difficult to create a broad-based vaccine against GAS. Furthermore, B cell epitopes, primarily in the B-repeat region, have been identified that are cross-reactive with human heart tissue, joint, kidney, and brain (Bronze & Dale, 1993; Froude, et al., 1989; J. H. Robinson & Kehoe, 1992). Therefore, a vaccine based purely on the variable region of the M-protein will only protect against specific GAS strains and could possibly induce autoimmunity. To overcome these problems, vaccines containing epitopes from the amino terminal region of multiple M-protein serotypes have been created. One example is the 26-valent

vaccine containing M peptides from serotypes of GAS representing the majority of infections in the USA and Canada. This vaccine was found to be safe and immunogenic in adult volunteers (McNeil, et al., 2005).

Although the amino terminus of the M-protein is highly polymorphic, the C-region is conserved in different GAS strains that have been studied (Fischetti, 1989), and has also been targeted for vaccine development. One promising vaccine candidate peptide derived from the carboxy-terminal C-repeat region of the M-protein is the J14 peptide. The J14 peptide consists of a fourteen amino acid minimal B cell epitope from the C-repeat region, J14-i, flanked by sequences derived from the GCN4 leucine zipper DNA-binding protein of yeast which maintains the α-helical secondary structure of the epitope (Relf, et al., 1996). However, the J14 peptide is poorly immunogenic by itself and requires co-administration with an effective adjuvant. One adjuvant that has been used successfully to overcome the immunological non-responsiveness of J14 is a lipopeptide construct containing the universal T cell epitope P25 (sequence, GKLIPNASLIENCTKAEL) and a self-adjuvanting lipid moiety. Intranasally immunising mice with J14 attached to the lipopeptide construct protected mice from lethal respiratory GAS challenge. In addition, the vaccine was capable of inducing J14-specific mucosal IgA antibodies, which coincided with reduced throat colonisation after respiratory GAS challenge (Batzloff, et al., 2006).

J14 is a conformationally restricted peptide, requiring presentation as a coiled-coil to induce a protective immune response (Relf, et al., 1996), and so is different from the $OVA_{323-339}$ peptide described in the previous chapters. Furthermore, it is a “real” vaccine target and it is poorly immunogenic, requiring co-administration with an adjuvant. Therefore, the J14 peptide was selected to be engineered into Pilvax, to investigate if Pilvax can be used to deliver a conformation-dependent peptide to mucosal sites.

5.2 Results

5.2.1 Expression and purification of recombinant J14 peptide for use in mouse immunisations and immunological assays

5.2.1.1 Purification of recombinant J14 peptide using the pET system

The J14 peptide, required for immunising mice, was purified using the pET expression system. A pET32a-3C vector containing the J14 DNA sequence was kindly obtained from Dr. Thomas Proft (University of Auckland, New Zealand) and transformed into AD494(DE3)pLysS *E. coli*. Protein expression was induced for 4 hours at 30 ^{o}C. The pET expression system produces the peptide as a Thioredoxin fusion protein, which was purified using Profinity IMAC Ni-Charged Resin. Step-wise elution with imidazole of the ~30 kDa protein was performed and visualised by SDS-PAGE (figure 5.1).

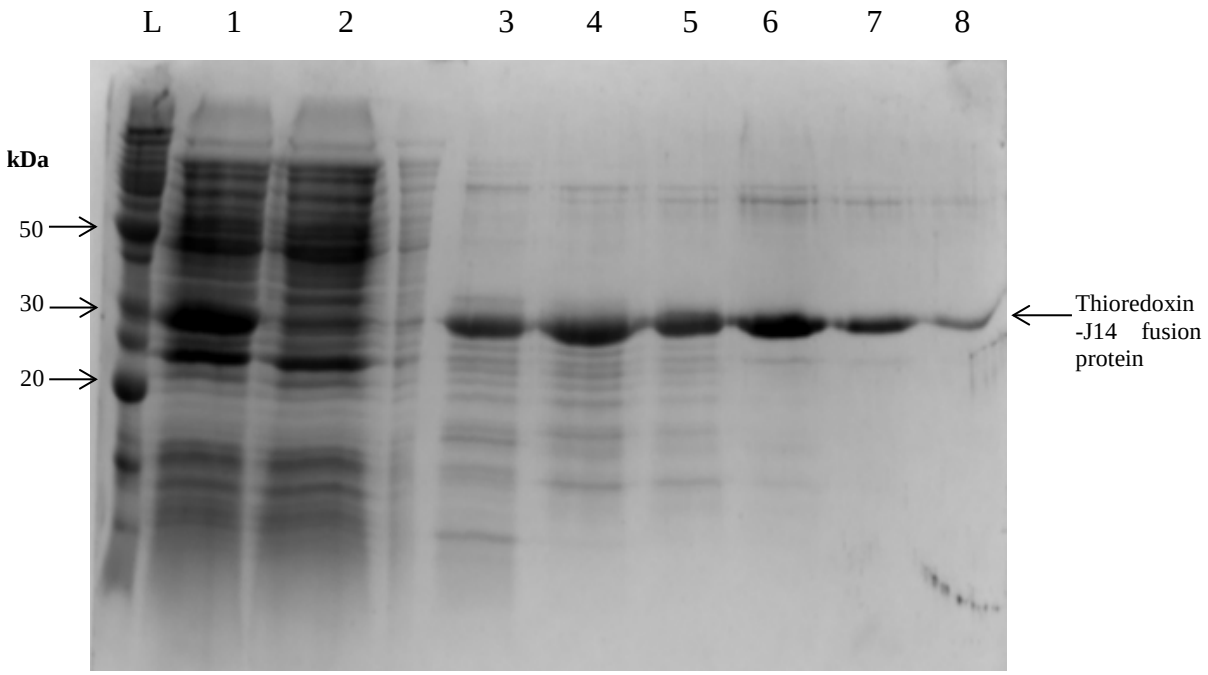

Figure 5.1 Purification of the J14 peptide expressed using the pET system

Thioredoxin-tagged J14 was expressed and purified as described under section 2.7.1. The following fractions were analysed by electrophoresis through a 15% SDS-PAGE gel, followed by staining with Coomassie blue. Lane 1, bacterial cell lysate after sonication. Lane 2, column flow through. Lane 3, 10 mM imidazole elution. Lane 4, 20 mM imidazole elution. Lane 5, 40 mM imidazole elution. Lane 6, 80 mM imidazole elution. Lane 7, 100 mM imidazole elution. Lane 8, 150 mM imidazole elution. The position and sizes (kDa) of the Benchmark protein ladder (L) is indicated.

The fractions eluted with 80 mM, 100 mM, and 150 mM imidazole were pooled together and concentrated on a Vivaspin concentrator. The concentrated Thioredoxin-J14 was then dialysed in PBS overnight and stored for use in immunising mice (figure 5.2).

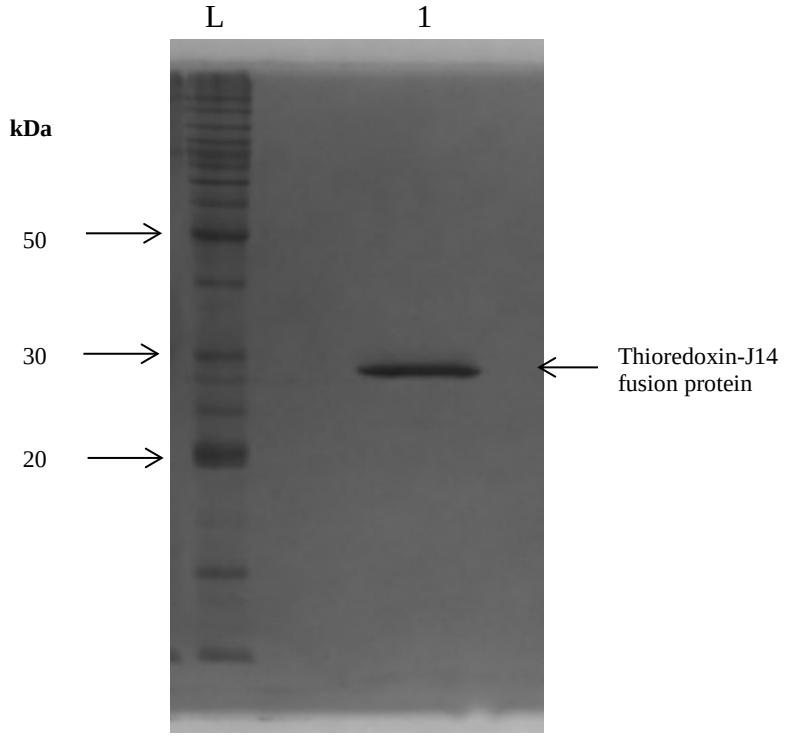

Figure 5.2 Concentrated Thioredoxin-J14 recombinant protein

The Thioredoxin-J14 fusion protein, eluted with 80 mM, 100 mM, and 150 mM of imidazole, was concentrated using a Vivaspin concentrator (molecular weight cut-off, 5,000). The concentrated protein was analysed by electrophoresis through a 15% SDS-PAGE gel, followed by staining with Coomassie blue. Lane L, the Benchmark protein ladder. Lane 1, concentrated Thioredoxin-J14.

5.2.1.2 Purification of recombinant J14 using the pGEX system

The Thioredoxin tag was not cleaved from J14 after purification using the pET system. This prevents the use of Thioredoxin-J14 in any of the ELISAs to test whether a J14-specific antibody response has been elicited in mice immunised with the fusion protein, as any antibodies elicited against the Thioredoxin tag may give a false positive result. Therefore, the J14 peptide was also purified using the Glutathione S-transferase (GST) fusion protein expression system. The pGEX system expresses the desired protein as a fusion with the 26 kDa GST at its N-terminus. The GST gene is under the control of the tac promoter which is inducible by IPTG. A pGEX vector containing the J14 DNA sequence was kindly obtained from Dr. Thomas Proft (University of Auckland, New Zealand) and transformed into AD494(DE3)pLysS *E. coli*. Protein expression was induced during the log-phase of growth, for 4 hours at 30 ^{o}C. The fusion protein was purified from the bacterial lysate by affinity chromatography using GSH sepharose and eluted using

glutathione. After purification, the fusion protein represented the major Coomassie brilliant blue staining band as shown in the SDS–PAGE gel (figure 5.3).

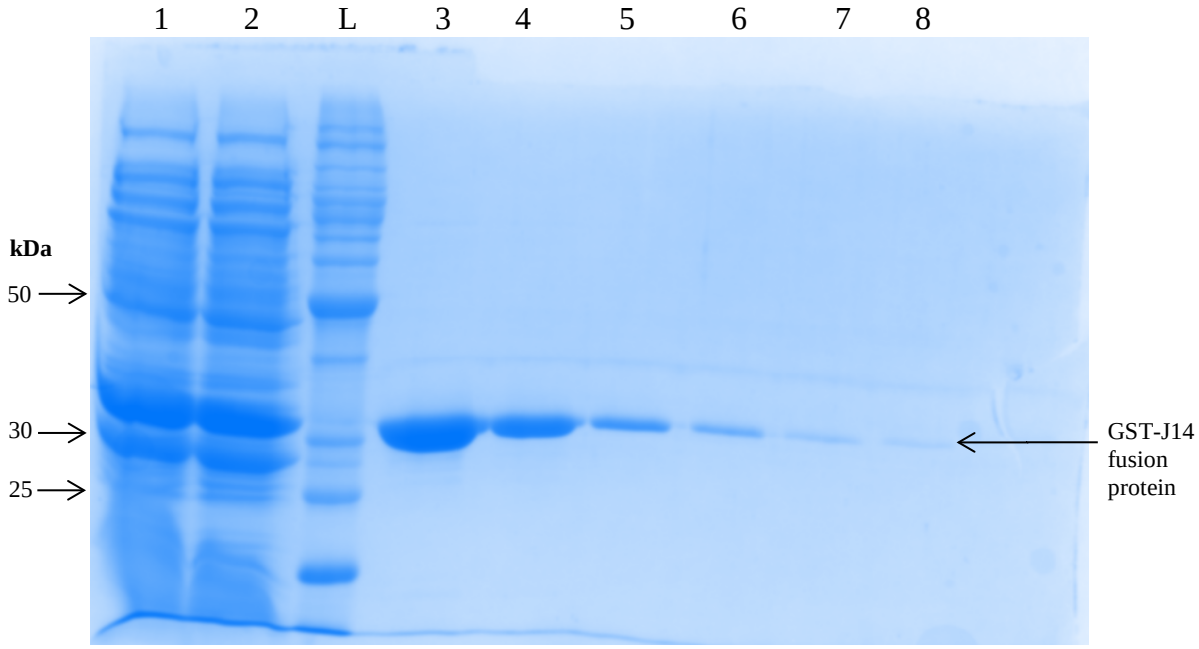

Figure 5.3 Purification of J14 peptide expressed using the pGEX system

Growth of cell cultures and purification of fusion proteins was as described under section 2.7.1 and samples were analysed by electrophoresis through a 15% SDS-PAGE gel, followed by staining with Coomassie blue. Lane 1, bacterial cell lysate after sonication. Lane 2, column flow through. Lanes 3-8, eluted fractions. The position and sizes (kDa) of the Benchmark protein ladder (L) is indicated.

5.2.2 Creating J14-Pilvax by replacing the β_E-β_F loop region of Spy0128 with the J14 peptide

The results from chapter three showed that replacing the β_E-β_F loop region of Spy0128 with the $OVA_{323-339}$ peptide did not disrupt pilus polymerisation on the surface of *L. lactis*. Therefore, the J14 peptide was also engineered between the β_E and β_F strands of Spy0128. A pBC vector containing the J14 DNA sequence flanked by a XhoI and a SalI restriction enzyme site was kindly obtained from Dr. Thomas Proft (University of Auckland, New Zealand). The pBC:J14 plasmid was digested with XhoI/SalI and the excised J14 DNA sequence was ligated into the

XhoI digested pLZ12-Km2:P23R_PilM1_β_E_XhoI plasmid. The resulting plasmid, pLZ12-Km2:P23R_PilM1_β_E_J14, was transformed into *E. coli* DH5α and a positive colony was selected using the J14 fw and Spy0128 rw primers. Afterwards, the pLZ12-Km2:P23R_PilM1_β_E_J14 plasmid was extracted from DH5α and electroporated into *L. lactis* to create J14-Pilvax (figure 5.4).

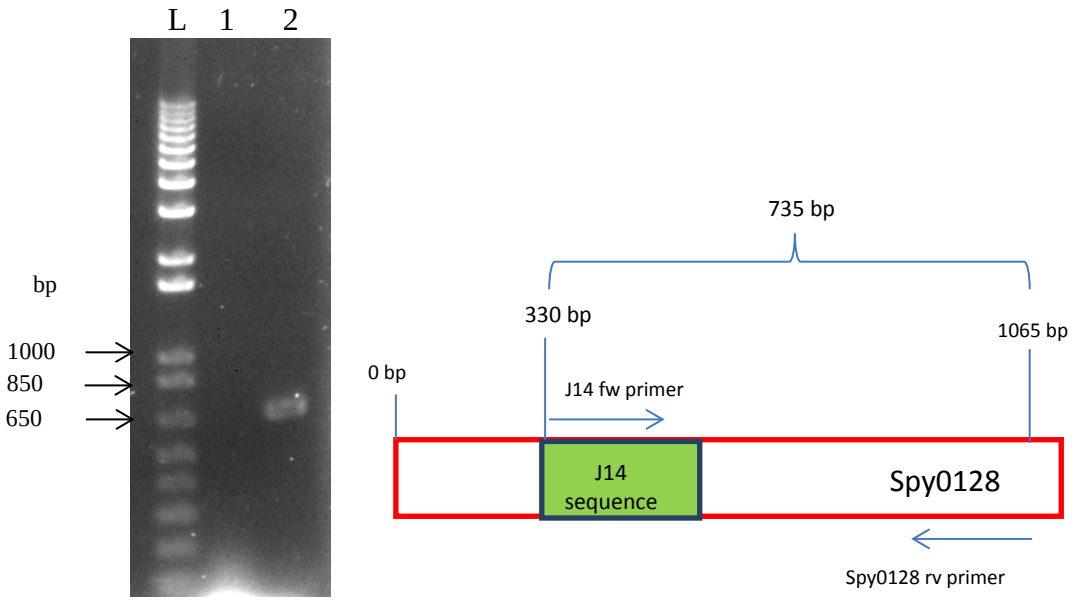

Figure 5.4 The pLZ12-Km2:P23R_PilM1_β_E_J14 plasmid was successfully electroporated into *L. lactis*

J14 fw and Spy0128 rv primers were used to select an *L. lactis* colony containing the pLZ12-Km2: P23R_PilM1_β_E_J14. Schematic diagram on the right shows primer binding sites and the expected size of the PCR product if positive. Image on the left features the 1% agarose gel electrophoresis. Lane L: the 1 kb molecular weight marker. Lane 1: the negative control (*L. lactis*:pLZ12-Km2:P23R_PilM1 plasmid). Lane 2: *L. lactis*:pLZ12-Km2:P23R_PilM1_β_E_J14.

To determine if replacing the β_E-β_F loop region with the J14 peptide disrupts the polymerisation of the pilus on the surface of *L. lactis*, a cell wall extract from J14-Pilvax was analysed by Western blot with rabbit antiserum specific for Spy0128. In the extract, a ladder of high-molecular-mass bands, typically associated with pilus formation, was visible and the pattern formed was comparable to that from the cell wall extract of *L. Lactis* expressing wild-type M1 pilus. In contrast, no bands were visible in the extract from *L. Lactis* containing the empty vector pLZ12-Km2:P23R as expected (figure 5.5). To confirm the integration of the J14 peptide into the backbone pilus fibre itself, the TCA precipitated cell wall extract from J14-Pilvax was analysed by Western blot with mouse antiserum specific for J14. The anti-J14 antiserum recognised a laddering pattern of high-molecular-weight bands and this indicates that the J14 peptide was integrated into the Spy0128 subunit, resulting in the multimeric presentation of the peptide on the surface of *L. lactis*. No bands were visible in the extract from *L. Lactis* expressing wild-type M1 pilus as expected (figure 5.6).

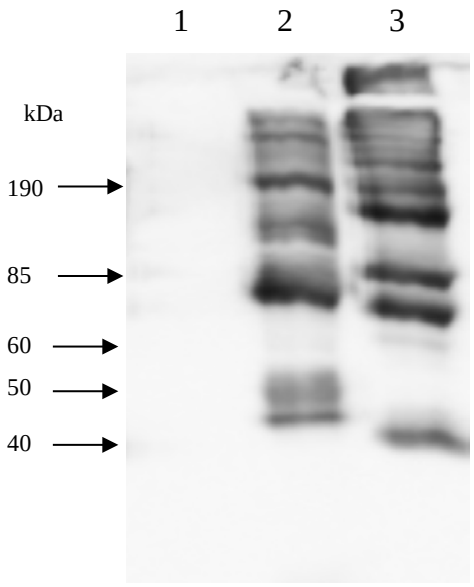

Figure 5.5 Engineering the J14 peptide between the β_E and β_F strands of Spy0128 has no deleterious effect on pilus polymerisation on the surface of *L. lactis*

Cell wall extracts analysed by Western blot with rabbit anti-Spy0128 antiserum. Lane 1: the negative control (*L. lactis*:pLZ12-Km2:P23R). Lane 2: J14-Pilvax. Lane 3: the positive control (*L. lactis*: pLZ12-Km2:P23R_PilM1). A high molecular weight laddering pattern is observed in the cell wall extract from J14-Pilvax, inferring that engineering the J14 peptide into Spy0128 does not impair pilus polymerisation on the surface of *L. lactis.*

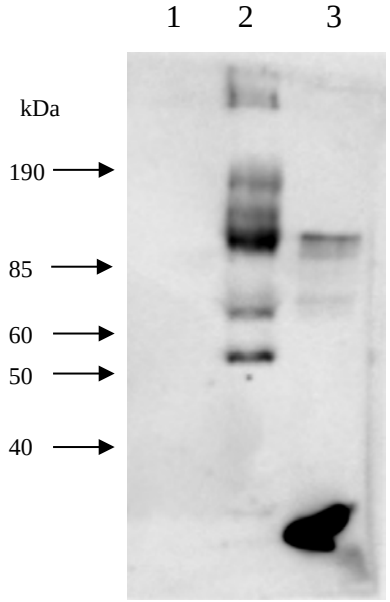

Figure 5.6 The J14 peptide is surface exposed and incorporated into the Spy0128 pilin polymers in *L. lactis*

TCA precipitated cell wall extracts analysed by Western blot with mouse anti-J14 antiserum. Lane 1: the negative control (*L. lactis*:pLZ12-Km2:P23R_PilM1). Lane 2: J14-Pilvax. Lane 3: the positive control (recombinant GST-J14).

5.2.3 Investigation of immune responses in J14-Pilvax immunised mice

The ability of J14-Pilvax to induce J14-specific immune responses was investigated in FVB/n mice. This mouse strain was chosen because previous studies by Alam, *et al.* had determined that FVB/n mice were the most appropriate mouse strain for the development of a GAS nasopharyngeal colonisation model (Alam, et al., 2013). Further studies to test if J14-Pilvax would be protective against GAS challenge would, therefore, likely utilise this mouse strain. To determine if J14-Pilvax can elicit a J14-specific antibody response, mice were immunised intranasally with 50 µl of J14-Pilvax ($1x10^9$ CFU/mouse) at two-week intervals for a total of four immunisations. Mice were similarly immunised with *L. lactis* expressing wild-type M1 pilus (*L. lactis:* pLZ12-Km2:P23R_PilM1) as a negative control. For the positive control, mice were subcutaneously immunised with four doses of Thioredoxin-J14 emulsified 1:1 in Incomplete Freund's adjuvant.

The J14 peptide requires presentation as a coiled coil to generate an immune response. However, when engineered into the loop region of the pilus, there is a strong possibility that the structure of the peptide can be disrupted and a strong immune response to the peptide would not be generated in mice immunised with J14-PIlvax (personal communication with Dr. Paul Young). Therefore, taking due consideration of the animal ethics policies, only a small pilot mouse study was initially undertaken, with five to six mice per sample group, to determine if J14-Pilvax can elicit a J14-specific immune response.

5.2.3.1 The Spy0128-specific serum IgG response following intranasal immunisation

To determine if J14-Pilvax was successfully administered, the serum IgG antibody response to the Spy0128 subunit was examined by using an ELISA with immobilised Spy0128 protein. Anti-Spy0128 antibodies were detected in the serum of all the mice immunised with J14-Pilvax. The average endpoint IgG titre (day 49) was 1:80,000. All mice immunised with *L. lactis* expressing wild-type pilus also gave a serum anti-Spy0128 IgG response, the average endpoint

IgG titre being 1:64,000. Only background activity was found in serum from mice immunised with Thioredoxin-J14-IFA emulsion as expected (figure 5.7).

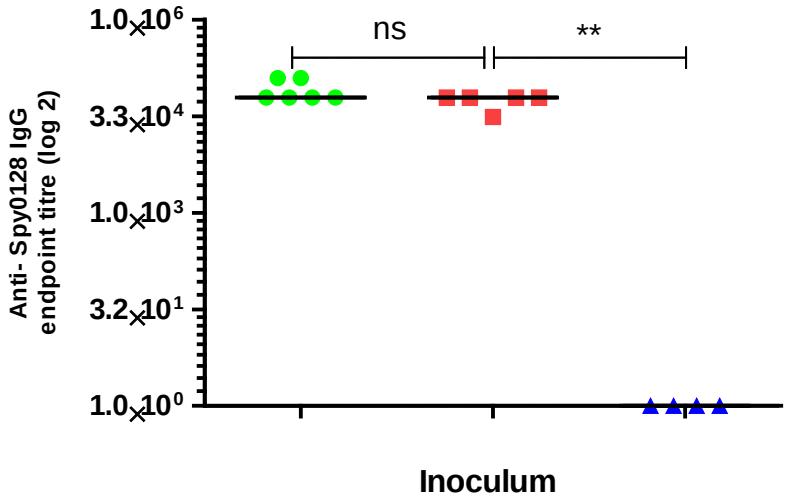

Figure 5.7 Spy0128-specific serum IgG antibody responses in immunised FVB/n mice

Sera were collected from mice 7 days after the fourth immunisation and the IgG antibody titres were determined by ELISA performed in triplicate. Serum samples were taken from mice inoculated i.n. with J14-Pilvax (●, n=6), or *L. lactis:*pLZ12-Km2:P23R_PilM1 (■, n=5), or subcutaneously with Thioredoxin-J14-IFA (▲, n=4). The average titre for individual mice is shown and the data is from a single experiment. The mean and standard error of the mean for each group are represented as bars. Statistical differences were determined using one-way ANOVA with Bonferroni post-hoc test (** $P < 0.01$; ns = non-significant difference).

5.2.3.2 J14-specific mucosal IgA antibody responses following intranasal immunisation

To assess the induction of local mucosal immunity in mice following intranasal immunisation, IgA responses were measured in BALF and saliva samples collected 7 days after the fourth immunisation.

The J14-specific IgA response in undiluted BALF was measured by using an ELISA with immobilised GST-J14. An IgA response to J14 was detected in 4 of the 6 mice immunised with

J14-Pilvax, with the response being at least two times higher than the background response (which was the response generated from the negative control mice immunised with *L. lactis* expressing wild-type M1 pilus). Furthermore, only background activity was found in BALF from mice immunised with the Thioredoxin-J14-IFA emulsion (figure 5.8).

The presence of J14-specific IgA antibodies in undiluted saliva from immunised mice was also measured by ELISA with immobilised GST-J14. However, no IgA responses were detected in the mice immunised with J14-Pilvax or the Thioredoxin-J14-IFA emulsion, with the responses being similar to the background response from the negative control mice (figure 5.9).

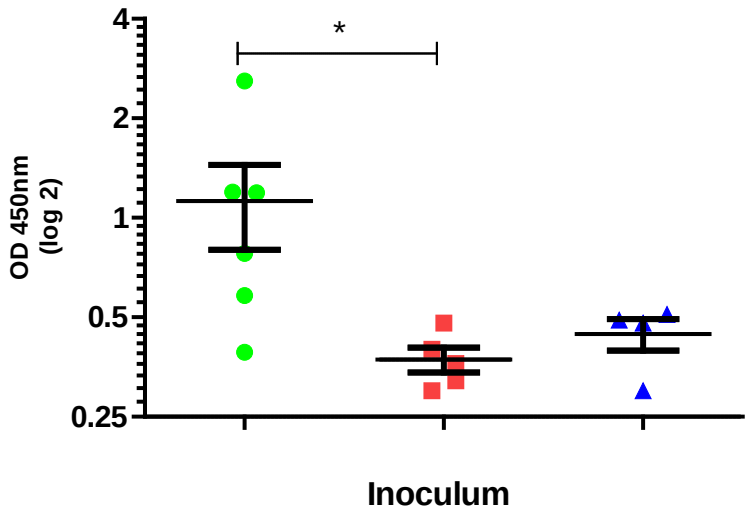

Figure 5.8 J14-specific IgA antibody responses in bronchoalveolar lavage fluid from immunised FVB/n mice

J14-specific IgA in BALF collected 7 days after the fourth immunisation from mice inoculated i.n. with J14-Pilvax (●, n=6), or *L. lactis*:pLZ12-Km2:P23R_PilM1 (■, n=5), or subcutaneously with Thioredoxin-J14-IFA (▲, n=4). The IgA response was determined in undiluted samples from individual mice by ELISA performed in triplicate and the data is from a single experiment. Each point represents a single mouse with the mean and standard error of the mean for each group represented as bars. The statistical significance between mice immunised with J14-Pilvax and the negative control group (*L. lactis*:pLZ12-Km2:P23R_PilM1) was determined by using the Student unpaired *t* test (* $P < 0.05$).

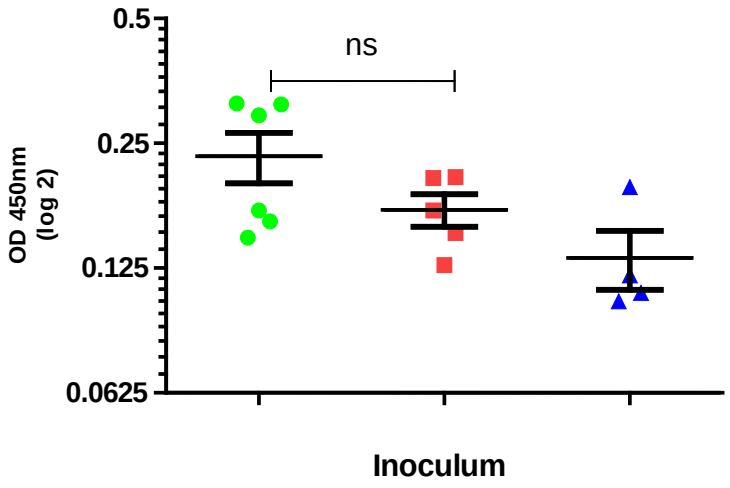

Figure 5.9 J14-specific IgA antibody responses in saliva from immunised FVB/n mice

J14-specific IgA in saliva collected 7 days after the fourth immunisation from mice inoculated i.n. with J14-Pilvax (●, n=6), or *L. lactis:*pLZ12-Km2:P23R_PilM1 (■, n=5), or subcutaneously with Thioredoxin-J14-IFA (▲, n=4). The IgA response was determined in undiluted samples from individual mice by ELISA performed once and the data is from a single experiment. Each point represents a single mouse with the mean and standard error of the mean for each group represented as bars. The statistical significance between mice immunised with J14-Pilvax and the negative control group (*L. lactis:*pLZ12-Km2:P23R_PilM1) was determined by using the Student unpaired *t* test (ns = non-significant difference).

5.2.3.3 J14-specific serum IgG antibody response following intranasal immunisation

To assess the induction of a systemic antibody response following intranasal immunisation, the presence of J14-specific IgG in the serum was determined by using an ELISA with immobilised GST-J14. The pre-immune serum was initially tested and an IgG response to J14 was not detected in any of the mice used in the study. Following subcutaneous immunisation of mice with Thioredoxin-J14-IFA, a strong reaction with the immobilised GST-J14 was observed in serum samples from all five of the immunised mice. The average endpoint titre of the J14-specific IgG in the serum samples was 1:64,000. In the case of mice immunised with J14-Pilvax, a J14-specific serum IgG response was only observed in four of the six mice and the mice responded poorly to J14-Pilvax. The average endpoint titre in the serum samples was 1:3,200. Only background activity was found in the serum samples from negative control mice immunised with *L. lactis* expressing wild-type pilus as expected (figure 5.10).

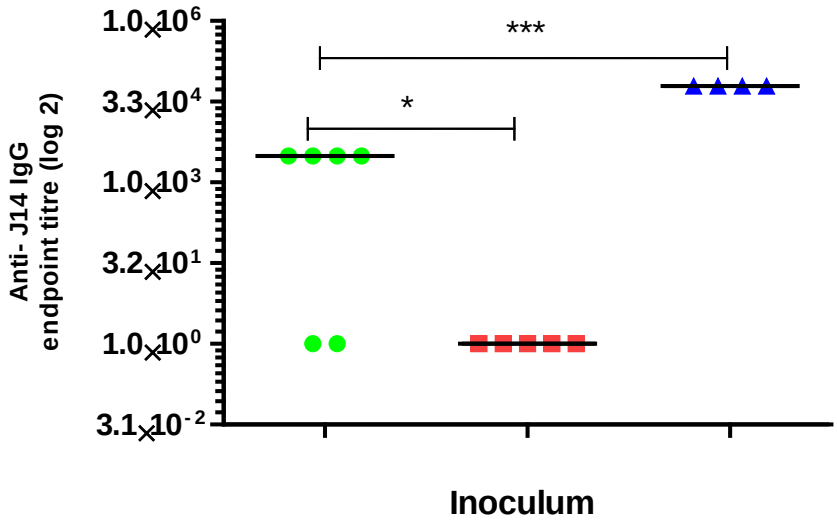

Figure 5.10 J14-specific serum IgG antibody responses in immunised FVB/n mice

Sera were collected from mice 7 days after the fourth immunisation and the J14-specific IgG antibody titres were determined by ELISA performed in triplicate. Serum samples were taken from mice inoculated i.n. with J14-Pilvax (●, n=6), or *L. lactis*:pLZ12-Km2:P23R_PilM1 (■, n=5), or subcutaneously with Thioredoxin-J14-IFA (▲, n=4). The average titre for individual mice is shown and the data is from a single experiment. The mean and standard error of the mean for each group are represented as bars. Statistical differences were determined using one-way ANOVA with Bonferroni post-hoc test (*** $P < 0.001$; * $P < 0.05$).

5.2.3.4 Analysing the binding of J14-specific IgG in the sera from immunised mice to whole GAS using flow cytometry

To investigate if the J14-specific antibodies elicited by J14-Pilvax can bind to the surface of whole GAS, the pilus knockout strain of GAS (SF370 ΔPilM1) was subjected to flow cytometry after staining with antiserum from the mouse that had the best response to J14-Pilvax or the control vaccine formulations. SF370 ΔPilM1, kindly obtained from Dr. Jacelyn Loh (University of Auckland), was used to exclude the binding of antibodies specific for Spy0128. For the flow cytometry assay, serum from the mouse immunised with J14-Pilvax, *L. lactis* expressing wild

type pilus, or Thioredoxin-J14-IFA was initially incubated with SF370 ΔPilM1. Then, after washing, the three samples were incubated with FITC tagged goat anti-mouse antibodies. If the serum produced in the mice can bind M-protein expressed on SF370 ΔPilM1, the FITC tagged antibodies will also bind, resulting in a fluorescent shift over the background when detected by flow cytometry. Following flow cytometry, a fluorescence shift over the background was not observed when using antiserum from the mouse that responded to J14-Pilvax, which suggests that the J14-specific antibodies elicited by J14-Pilvax were unable to bind to M-protein expressed on SF370 ΔPilM1. The serum from the mouse that responded to Thioredoxin-J14-IFA bound to SF370 ΔPilM1, resulting in a fluorescence shift over the background, as expected (figure 5.11).

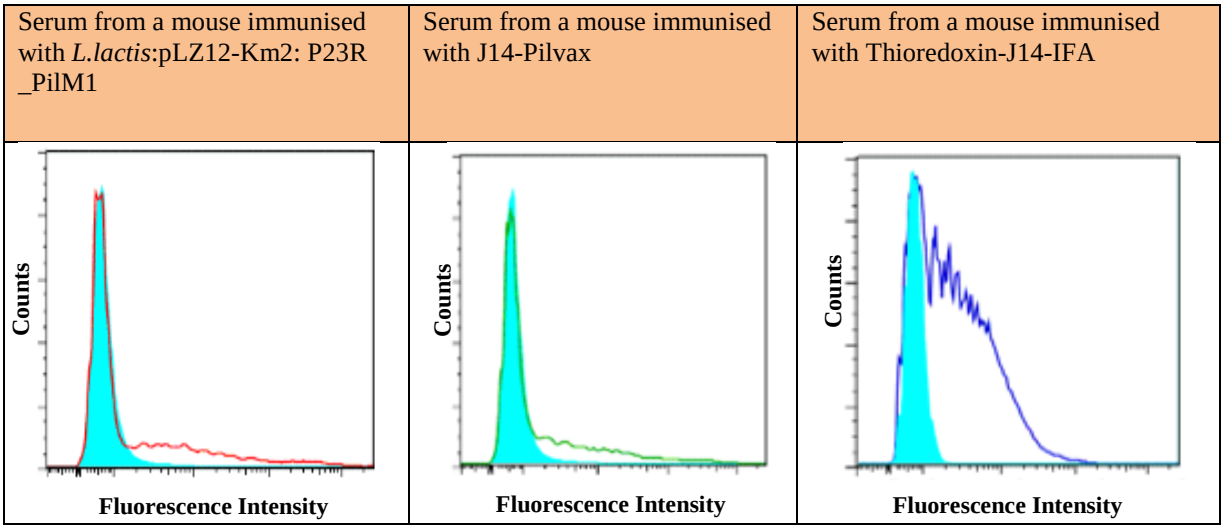

Figure 5.11 The J14-specific serum IgG antibodies elicited in a mouse immunised with J14-Pilvax cannot bind to the surface of GAS SF370 ΔPilM1

Flow cytometry analyses of GAS SF370 ΔPilM1 strain stained with antiserum from a mouse immunised i.n. with J14-Pilvax, or *L. lactis*:pLZ12-Km2:P23R_PilM1, or subcutaneously with Thioredoxin-J14-IFA (*void histograms)*, compared with incubation only with secondary antibody *(blue full histogram).*

5.2.3.5 Binding of J14-specific antibodies from immunised mice to recombinant M-protein.

The inability of the J14-specific antibodies from the J14-Pilvax immunised mouse to bind to SF370 ΔPilM1 may be due to the fact that the immune response against J14-Pilvax was not strong enough and the antibody titre against J14 was too low. Another possibility is that antibodies elicited against the pilus-linked J14 cannot recognise the native M-protein from which the J14 peptide is derived. To determine if the J14-specific antibodies could bind to the M-protein, an ELISA with immobilised recombinant M-protein, kindly provided by Dr. Jacelyn Loh (University of Auckland, New Zealand), was performed using the mucosal secretions and serum from the immunised mice.

Binding of the J14-specific IgA antibodies, in undiluted BALF and saliva samples, to recombinant M-protein was initially assessed. A measurable reaction with immobilised M-protein was not observed in any of the mice immunised with J14-Pilvax. The IgA response to M-protein in undiluted BALF and saliva was similar to the back-ground response (the response from mice immunised with the negative control *L. lactis* expressing wild-type pilus). In addition, only background activity was found in BALF from mice immunised with Thioredoxin-J14-IFA emulsion (figure 5.12 and 5.13).

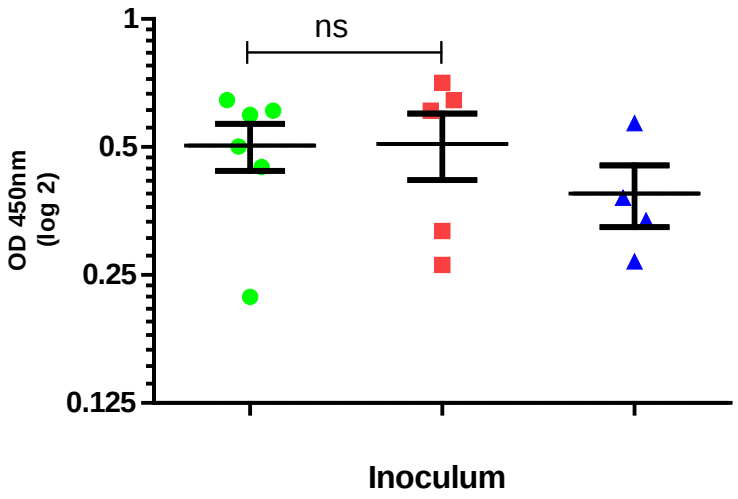

Figure 5.12 M-protein specific IgA antibody responses in bronchoalveolar lavage fluid from immunised FVB/n mice

M-protein specific IgA responses in BALF collected 7 days after the fourth immunisation from mice inoculated i.n. with J14-Pilvax (●, n=6), or *L. lactis*:pLZ12-Km2:P23R_PilM1(■, n=5), or subcutaneously with Thioredoxin-J14-IFA (▲, n=4). The IgA response was determined in undiluted samples from individual mice by ELISA performed in triplicate and the data is from a single experiment. Each point represents a single mouse with the mean and standard error of the mean for each group represented as bars. The statistical significance between mice immunised with J14-Pilvax and the negative control group (*L. Lactis:*pLZ12-Km2:P23R_PilM1) was determined by using the Student unpaired *t* test (ns = non-significant difference).

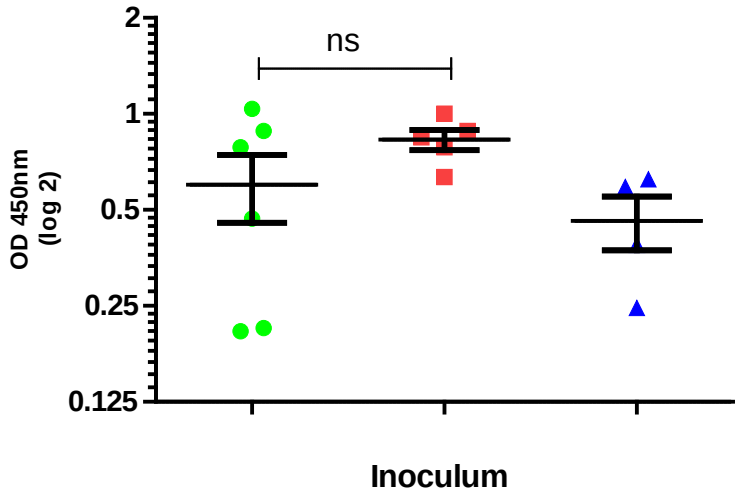

Figure 5.13 M-protein specific IgA antibody responses in saliva from immunised FVB/n mice

M-protein specific IgA responses in saliva collected 7 days after the fourth immunisation from mice inoculated i.n. with J14-Pilvax (●, n=6), or *L. lactis*:pLZ12-Km2:P23R_PilM1(■, n=5), or subcutaneously with Thioredoxin-J14-IFA (▲, n=4). The IgA response was determined in undiluted samples from individual mice by ELISA performed once and the data is from a single experiment. Each point represents a single mouse with the mean and standard error of the mean for each group represented as bars. The statistical significance between mice immunised with J14-Pilvax and the negative control group (*L. Lactis:*pLZ12-Km2:P23R_PilM1) was determined by using the Student unpaired *t* test (ns = non-significant difference).

The ability of J14-specific IgG antibodies, in the serum of immunised mice to bind to recombinant M-protein was also assessed by using an ELISA. A measurable reaction with immobilised M-protein was not observed from any of the mice immunised with J14-Pilvax. The IgG response to M-protein in the serum from mice immunised with J14-Pilvax was similar to that of the background response from the negative control mice. However, a strong reaction was seen in serum samples from mice subcutaneously immunised with the Thioredoxin-J14-IFA emulsion, with the response being at least 6 times higher than background in all mice (figure 5.14). This was expected as a study by Batzloff *et al* showed that the conformation of the J14 peptide is not affected when it is attached to a carrier protein using only one terminus, as was the case when J14 is attached to Thioredoxin (Batzloff, et al., 2006).

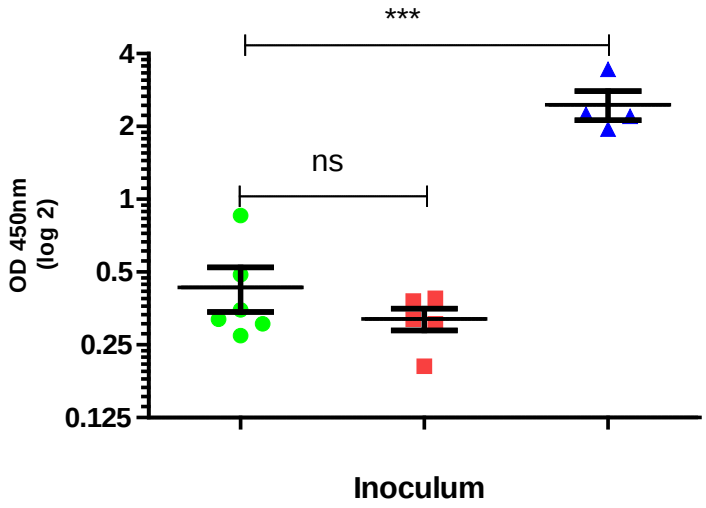

Figure 5.14 M-protein specific IgG antibody responses in serum from immunised FVB/n mice

M-protein specific IgG responses in serum collected 7 days after the fourth immunisation from mice inoculated i.n. with J14-Pilvax (●, n=6), or *L. lactis*:pLZ12-Km2:P23R_PilM1(■, n=5), or subcutaneously with Thioredoxin-J14-IFA (▲, n=4). The IgG responses were determined in serum samples, diluted 1:50, from individual mice by ELISA performed in triplicate and the data is from a single experiment. Each point represents a single mouse with the mean and standard error of the mean for each group represented as bars. Statistical differences were determined using one-way ANOVA with Bonferroni post-hoc test (*** $P < 0.001$; ns = non-significant difference).

The inability of the J14-specific antibodies elicited in mice immunised with J14-Pilvax to recognise and bind the native M-protein was also confirmed using a dot blot assay. Pooled antiserum from mice immunised with J14-Pilvax or *L.lactis* expressing wild-type pilus failed to bind to the M-protein**.** In contrast, Pooled antiserum from mice immunised with the Thioredoxin-J14-IFA emulsion bound to M-protein, producing a chemiluminescent signal (figure 5.15).

Pooled serum from mice:	Recombinant M-protein (5 µg/ml)
Immunised i.n. with *L. lactis*:pLZ12-Km2: P23R_PilM1	
Immunised i.n. with J14-Pilvax	
Immunised subQ with Thioredoxin-J14-IFA	

Figure 5.15 Dot-blot analyses to determine the binding of the J14-specific IgG antibodies in the serum from immunised mice to recombinant M-protein

M protein (5 µg/ml) was spotted onto a nitrocellulose membrane and blotted with pooled serum from mice immunised i.n. with J14-Pilvax, or *L.lactis*:pLZ12-Km2:P23R_PilM1, or subcutaneously with Thioredoxin-J14-IFA. Pooled serum was tested at a 1:100 dilution and the signals were detected by chemiluminescence using peroxidase-conjugated anti-mouse IgG and ECL Western blotting detection reagents. The assay indicates that the anti-J14 IgG antibodies elicited in mice immunised with J14-Pilvax cannot bind to recombinant M-protein.

The ELISA and dot blot results indicate that the J14-specific antibodies elicited in mice immunised with J14-Pivax cannot recognise and bind the native M-protein from which the J14 peptide is derived. This may be due to the inability of the J14 peptide to fold correctly into its native alpha-helical form when engineered into the β_E-β_F loop region of Spy0128 (personal communication with Dr. Paul Young, University of Auckland, New Zealand). To determine if

this result was due to that specific loop region, another loop region was sought to be replaced with the J14 peptide. After analysing the crystal structure of Spy0128, the β_9-β_{10} loop region was selected as a potential site (personal communication with Dr. Paul Young, University of Auckland, New Zealand). Numerous attempts to replace the β_9-β_{10} loop region with the $OVA_{323-339}$ peptide proved unsuccessful. Therefore, the J14 peptide was also used to show proof of concept that the β_9-β_{10} loop region of Spy0128 can be replaced a peptide without disrupting the polymerisation of the pilus on the surface of *L. lactis* (figure 5.16).

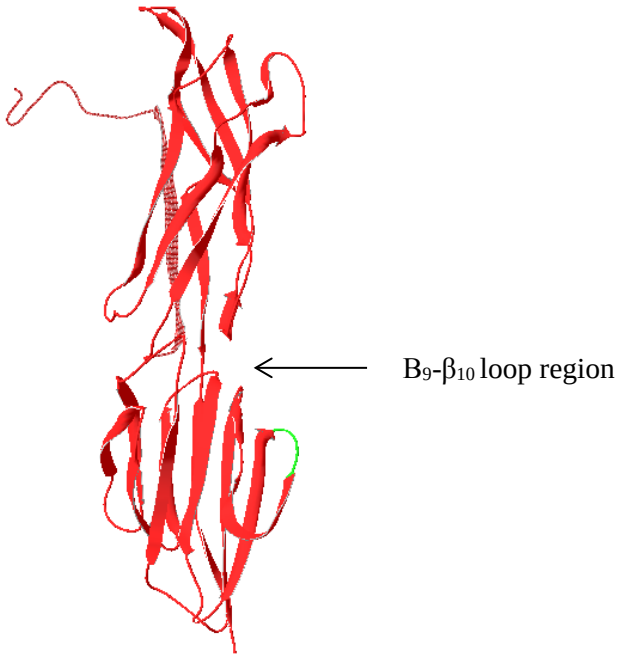

Figure 5.16 The β_9-β_{10} loop region of Spy0128

Computer generated structure, using the SWISS-MODEL web server, showing the β_9-β_{10} loop region (in green) selected to be replaced with the J14 peptide.

5.2.4 Creating β_9-J14-Pilvax by replacing the β_9-β_{10} loop region of Spy0128 with the J14 peptide

5.2.4.1 Replacing the loop region with an XhoI site

To replace the β_9-β_{10} loop region of Spy0128 with an XhoI site, the entire pLZ12-Km2: P23R_PilM1 (-XhoI) plasmid was PCR amplified with the Spy0128_β_9-Xho fw and rv primers. The resulting plasmid, pLZ12-Km2:P23R_PilM1_β_9_XhoI, was transformed into *E.coli* DH5α. A positive colony was selected by PCR using Spy0125 fw and Spy0130 rw primers to ensure the entire pilus operon was present in the plasmid. To confirm the presence of the XhoI site between the two β strands, the *spy0128* gene was PCR amplified using the Spy0127 fw and Spy0128 rw primers and digested overnight with XhoI. After visualising the digested and undigested *spy0128* gene on an agarose gel, the presence of two bands at ~ 1300 and 150 bp confirms that the XhoI site is at the correct position (figure 5.17).

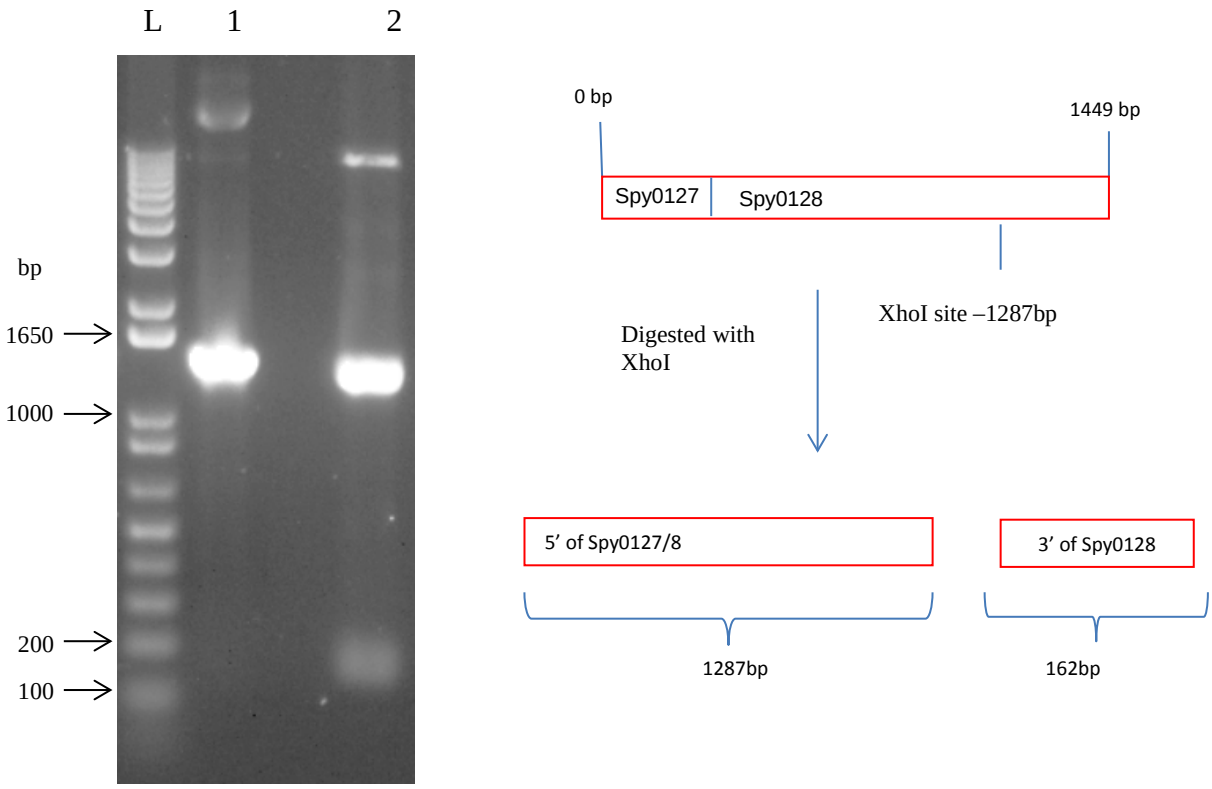

Figure 5.17 Confirming the presence of the XhoI site between the β_9 and β_{10} strands of Spy0128

The *spy0128* gene fragment was PCR amplified from pLZ12-Km2:P23R_PilM1_β_9_XhoI using Spy0127 fw and Spy0128 rv primers and digested overnight with XhoI. Schematic diagram on the right shows the location of the XhoI site and the expected sizes of the digested PCR product. Image on the left features the 1% agarose gel electrophoresis. Lane L: the 1 kb molecular weight marker. Lane 1: undigested *spy0128* gene. Lane 2: *spy0128* gene digested overnight with XhoI.

5.2.4.2 Engineering the J14 peptide into the XhoI site between the β_9 and β_{10} strands

To engineer the J14 peptide into the XhoI site between the β_9 and β_{10} strands, the XhoI/SalI digested J14 DNA sequence from a pBC:J14 plasmid was cloned directly into the XhoI digested pLZ12-Km2:P23R_PilM1_β_9_XhoI plasmid. The resulting plasmid, pLZ12-Km2: P23R_PilM1_β_9_J14, was transformed into *E. coli* DH5α and a positive colony was selected using the J14 fw and Spy0128 rw primers. Afterwards, the pLZ12-Km2 P23R: PilM1_β_9_J14 plasmid was extracted from DH5α and electroporated into *L. lactis* to create β_9-J14-Pilvax (figure 5.18).

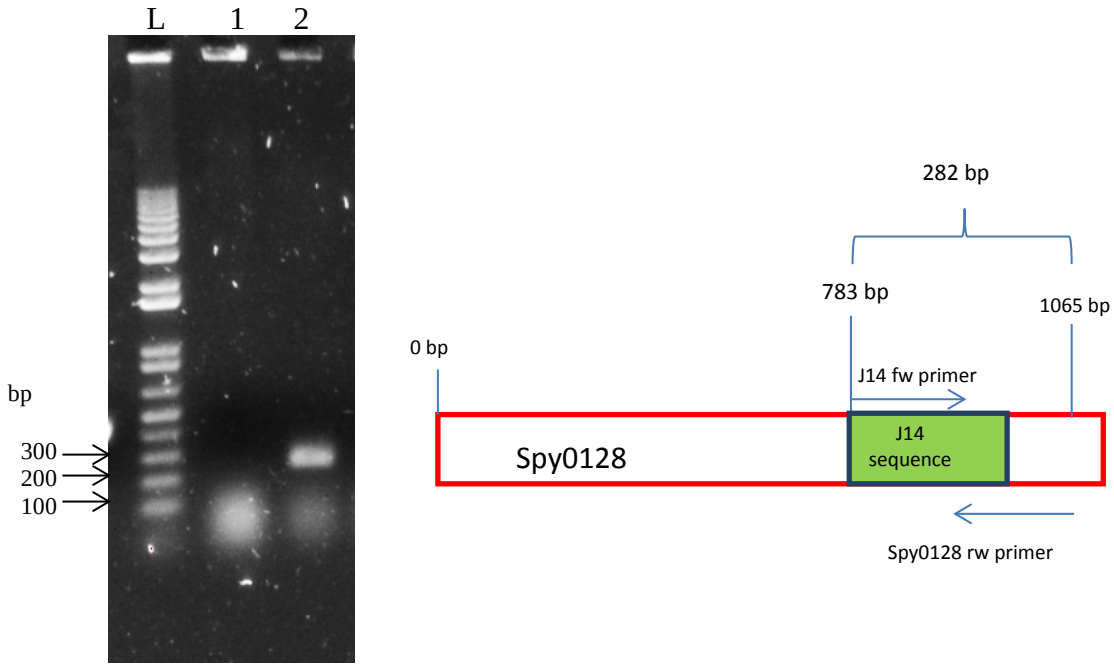

Figure 5.18 The pLZ12-Km2:P23R_PilM1_ β_9_J14 plasmid was successfully electroporated into *L. lactis*

J14 fw and Spy0128 rv primers were used to select an *L. lactis* colony containing the pLZ12-Km2: P23R_PilM1_β_9_J14. Schematic diagram on the right shows primer binding sites and the expected size of the PCR product if positive. Image on the left features the 1% agarose gel electrophoresis. Lane L: the 1 kb molecular weight marker. Lane 1: the negative control (*L. lactis*:pLZ12-Km2:P23R_PilM1 plasmid). Lane 2: *L. lactis*:pLZ12-Km2:P23R_PilM1_β_9_J14.

To determine if engineering the J14 peptide into the loop region affects the polymerisation of the pilus, a cell wall extract from β_9-J14-Pilvax was analysed by Western blot with rabbit antiserum specific for Spy0128. The cell wall extract displayed the typical ladder pattern associated with pilus formation and the pattern is similar to that observed in the extract from *L. lactis* expressing wild-type pilus. To confirm the presence of the J14 peptide within the pilus structure, the TCA precipitated cell wall extract from β_9-J14-Pilvax was analysed by Western blot with mouse antiserum specific for J14. Again a ladder pattern was visible which can only result if the J14 peptide has been incorporated into the Spy0128 subunit (figure 5.19). Therefore, the β_9-β_{10} loop region was successfully replaced with the J14 peptide without disrupting the polymerisation of the pilus on the surface of *L. lactis*.

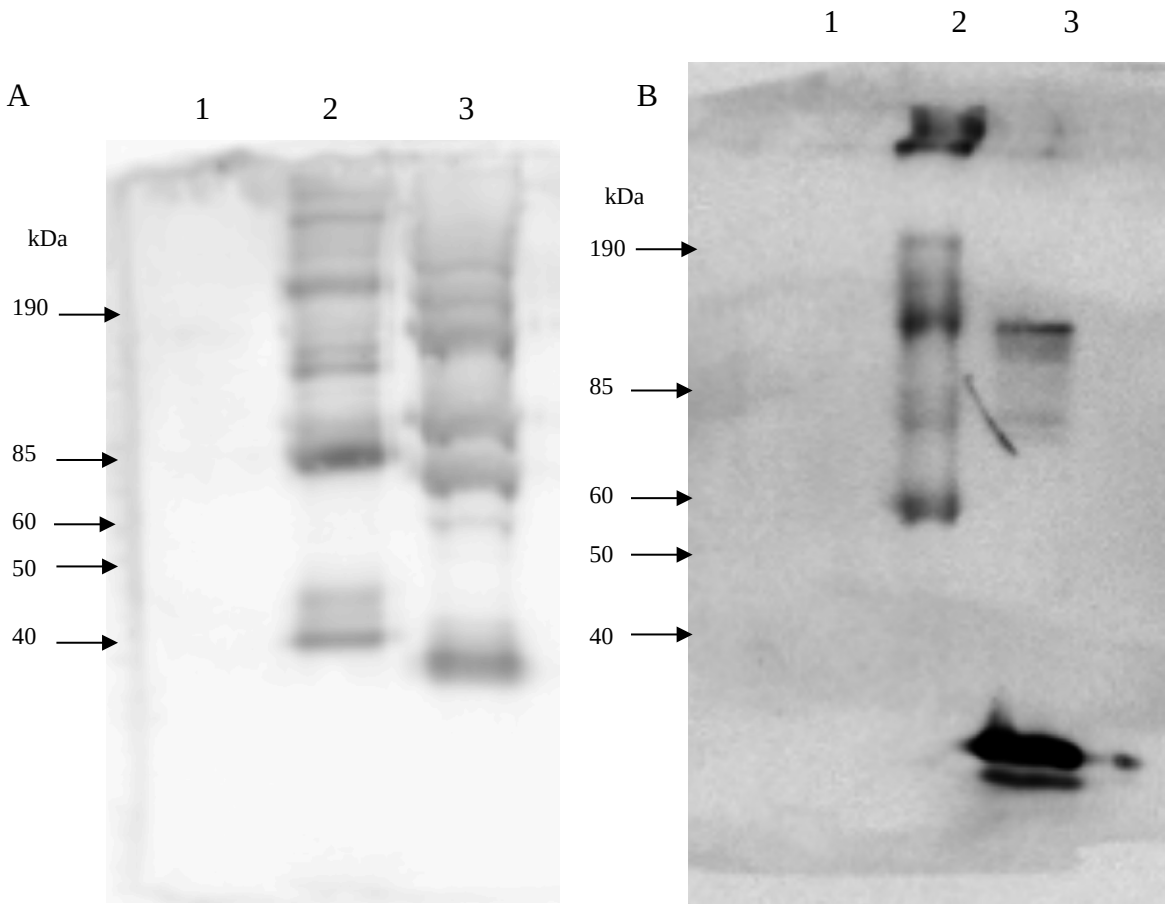

Figure 5.19 Western blot analyses of pLZ12-Km2:P23R_PilM1_β_9_J14 expressed in *L. lactis*

A) Cell wall extracts analysed by Western blot with rabbit anti-spy0128 antiserum. Lane 1: the negative control (*L. lactis*:pLZ12-Km2:P23R). Lane 2: β_9-J14-Pilvax. Lane 3: the positive control (*L. lactis*:pLZ12-Km2:P23R_PilM1). A high molecular weight laddering pattern is observed in the cell wall extract from *L. lactis*:pLZ12-Km2:P23R_PilM1_β_9_J14, inferring that engineering the J14 peptide into Spy0128 does not impair pilus polymerisation on the surface of *L. lactis.*

B) Cell wall extracts analysed by Western blot with mouse anti-J14 antiserum. Lane 1: Negative control (*L. lactis*:pLZ12-Km2:P23R_PilM1). Lane 2: β_9-J14-Pilvax. Lane 3: Positive control (recombinant GST- J14).

5.2.4.3 The J14-specific antibodies elicited by β_9-J14-Pilvax cannot bind to M-protein

A small pilot study was undertaken to determine if immunising FVB/n mice with β_9-J14-Pilvax can elicit a J14-specific immune response. Mice were immunised intranasally with 50 µl of β_9-J14-Pilvax ($1x10^9$ CFU/mouse) at two-week intervals for a total of four immunisations. Mice were similarly immunised with *L. lactis* expressing wild-type M1 pilus (*L. lactis:*pLZ12-Km2:P23R_PilM1) as a negative control. For the positive control, mice were subcutaneously immunised with four doses of a Thioredoxin-J14 emulsified 1:1 in Incomplete Freund's adjuvant. The presence of J14-specific IgG antibodies in the serum samples from immunised mice was determined by using an ELISA with immobilised GST-J14 protein. IgG responses to J14 was detected in two out of the five mice immunised with β_9-J14-Pilvax and all of the mice subcutaneously immunised with the Thioredoxin-J14-IFA emulsion. The average J14-specific IgG endpoint titre in the serum from mice immunised with β_9-J14-Pilvax was approximately 1:2,500. In the mice subcutaneously immunised with Thioredoxin-J14-IFA emulsion, the average endpoint titre was significantly higher reaching approximately 1:85,000. Only background activity was found in the serum from negative control mice immunised *L. lactis* expressing the wild-type pilus as expected (figure 5.20).

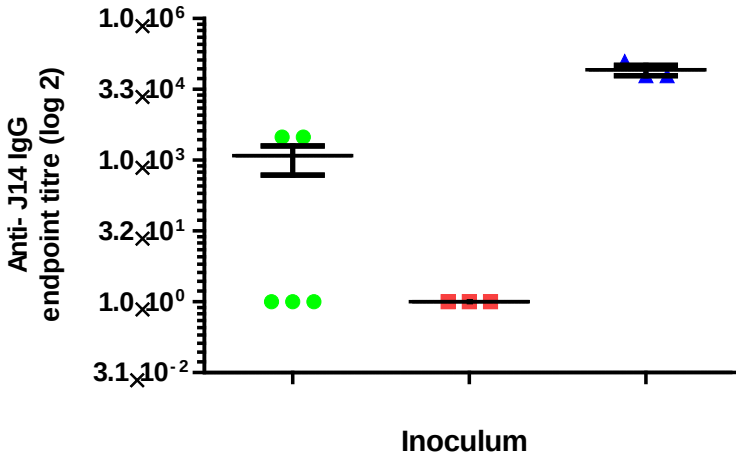

Figure 5.20 J14-specific serum IgG antibody responses in immunised FVB/n mice

Sera were collected from mice 7 days after the fourth immunisation and the J14-specific IgG antibody titres were determined by ELISA performed in triplicate. Serum samples were taken from mice inoculated i.n. with β_9-J14-Pilvax (●, n=5), or *L. lactis*:pLZ12-Km2:P23R_PilM1 (■, n=3), or subcutaneously with Thioredoxin-J14-IFA (▲, n=3). The data is from a single experiment and the average endpoint titre for individual mice is shown. The mean and standard error of the mean for each group are represented as bars.

The ability of J14-specific IgG antibodies in the serum of mice immunised with J14-Pilvax to bind recombinant M-protein was assessed by using an ELISA with immobilised M-protein. A reaction with immobilised M-protein was not observed from any of the mice immunised with β_9-J14-Pilvax. The IgG response to M-protein was similar to the back-ground response from negative control mice immunised with *L. lactis* expressing wild-type pilus. However, a strong reaction with M-protein was noted in serum samples from mice subcutaneously immunised with the Thioredoxin-J14-IFA emulsion, with the response being at least 6 times higher than background in all mice (figure 5.21).

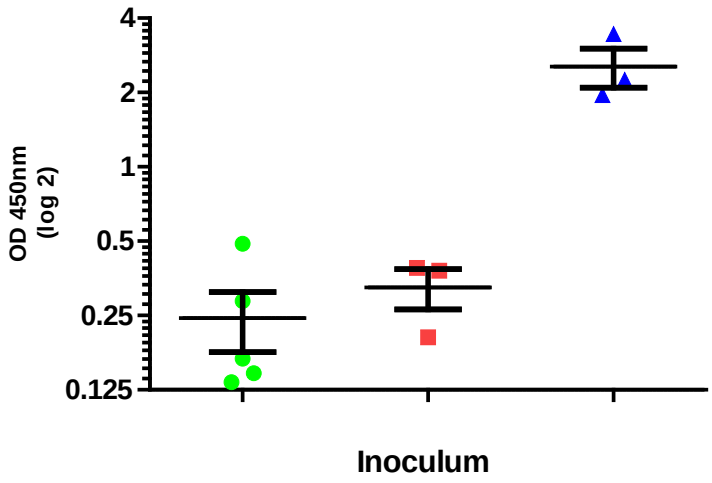

Figure 5.21 M-protein specific serum IgG antibody responses in immunised FVB/n mice

M-protein specific IgG responses in serum collected 7 days after the fourth immunisation from mice inoculated i.n. with β_9-J14-Pilvax (●, n=5), or *L. lactis*:pLZ12-Km2:P23R_PilM1(■, n=3), or subcutaneously with Thioredoxin-J14-IFA (▲, n=3). The IgG responses were determined in serum samples, diluted 1:50, from individual mice by ELISA performed in triplicate and the data is from a single experiment. Each point represents a single mouse with the mean and standard error of the mean for each group represented as bars.

5.3 Summary

The aim of this chapter was to determine if Pilvax could be used to deliver the conformation-dependent J14 peptide to mucosal sites. The β_E-β_F loop region of Spy0128 was replaced with the J14 peptide and the J14-linked pilus was expressed on the surface of *L. lactis* to create J14-Pilvax. Western blots of the cell wall extract from J14-Pilvax, reacted with rabbit anti-Spy0128 antiserum or mouse anti-J14 antiserum, both displayed a ladder pattern of high molecular weight bands, which indicates that the J14 peptide was successfully engineered into the Spy0128 subunit and pilus polymerisation on the surface of *L. lactis* was not disrupted by the peptide.

Intranasal immunisation of a cohort of FVB/n mice with J14-Pilvax elicited a strong Spy0128-specific serum IgG response in all the immunised mice. However, the J14-specific serum IgG response was variable, with anti-J14 antibodies only being detected in some of the immunised

mice. Furthermore, the J14-specific serum IgG endpoint titre from the mice that responded to J14-Pilvax was significantly lower than the endpoint titre from mice subcutaneously immunised with the Thioredoxin-J14-IFA emulsion. This suggests that the J14-Pilvax was not very effective in eliciting a serum IgG antibody response against the J14 peptide when delivered through the i.n. route. However, intranasal administration of J14-Pilvax resulted in a detectable J14-specific IgA response in the BALF of immunised mice which suggests that this delivery system can trigger a mucosal antibody response towards J14, at least in the upper respiratory tract.

To determine if the J14-specific antibodies elicited by J14-Pilvax could recognise whole GAS, the pilus knockout strain of GAS (SF370 ΔPilM1) was used, which would exclude the binding of pilus-specific antibodies in the serum. Flow cytometry analyses could not detect any binding of serum from J14-Pilvax immunised mice to SF370 ΔPilM1. ELISAs and a dot blot assay, with immobilised recombinant M-protein, indicated that the inability of the J14-immune mouse serum bind to SF370 ΔPilM1 was likely due to the fact that the J14-specific antibodies elicited by J14-Pilvax cannot recognise the native M-protein on the surface of SF370 ΔPilM1. This suggested that the J14 peptide did not form the appropriate structural epitope when integrated into the pilus structure.

To determine if this effect was a result of where the peptide was integrated, another loop region was sought to be replaced with the J14 peptide. The β_9-β_{10} loop region from the C-terminal domain of Spy0128 was selected. The β_9-β_{10} loop region was successfully replaced with the J14 peptide and Western blot analyses indicated that the J14 peptide was successfully integrated within the pilus structure and pilus polymerisation on the surface of *L. lactis* was not disrupted by the peptide. Intranasally immunising mice with β_9-J14-Pilvax elicited a weak serum anti-J14 IgG response in some of the immunised mice. However, the J14-specific antibodies were again unable to recognise and bind the native M-protein.

Therefore, the fact that both J14-Pilvax and β_9-J14-Pilvax were unable to elicit antibodies in immunised mice that could bind the M-protein suggests that the conformation of the J14 peptide is disrupted when it is integrated into the Spy0128 subunit. These results highlight a limitation of using Pilvax to deliver peptides that are conformation dependent.

Chapter 6

Engineering the J14 peptide into the N-terminus of Spy0128

6.1 Introduction

Immunising mice with J14-Pilvax elicited J14-specific antibodies that were unable to recognise and bind the native M-protein from which it is derived, as discussed in chapter five. It was hypothesised that this may be due to the disruption to the α-helical conformation of the J14 peptide when it is integrated into the Spy0128 subunit. However, immunising mice with recombinant J14 which had a Thioredoxin tag attached at its N-terminus elicited J14-specific antibodies which could recognise the native M-protein. Furthermore, immunising mice with J14 peptide synthesised with a lipopeptide adjuvant attached to its N-terminus protected mice from lethal respiratory GAS challenge (Batzloff, et al., 2006). These results suggest that the J14 peptide can maintain its conformation when it is attached to a carrier protein using one terminus, with the other terminus left unattached. According to the crystallographic data, the N-terminus of Spy0128 forms an exposed region extending to the side of the pilus fibre. Therefore, engineering the J14 peptide into the N-terminus will leave one terminus of the peptide unattached and this may allow the peptide to maintain its α-helical conformation (figure 6.1). The aim of this chapter was to investigate if Pilvax can be used to deliver the conformation-dependent J14 peptide to mucosal sites, by engineering J14 into the N-terminus of the Spy0128 pilin subunit.

Figure 6.1 The J14 peptide integrated at the N-terminus of Spy0128

Computer generated structural model, using the SWISS-MODEL server, depicting the J14 peptide (green) integrated at the N-terminus of Spy0128. Engineering the J14 peptide into the N-terminus of Spy0128 will leave one terminus of the peptide unattached and this may allow the peptide to maintain its α-helical conformation.

6.2 Results

6.2.1 Engineering the J14 peptide into the N-terminus of Spy0128

6.2.1.1 Inserting an XhoI site at the N29 position of Spy0128

Spy0128 is expressed as a precursor protein that contains an N-terminal secretion sequence. Computer predictions using Signal P had revealed a putative signal peptide cleavage site between amino acid position 23 and 24. Signal P prediction has shown that an insertion after amino acid position 29 (asparagine) does not interfere with the signal peptidase recognition site and cleavage probability. Therefore, to avoid the cleavage and release of J14, the peptide was inserted at position 29 in the N-terminus of Spy0128.

To insert an XhoI site at the N29 position of Spy0128, the entire pLZ12-Km2:P23R_PilM1 (-XhoI) plasmid was PCR amplified with the Spy0128_N29-Xho fw and rv primers, digested with XhoI, and ligated. The resulting plasmid, pLZ12-Km2:P23R_PilM1_N29_XhoI, was transformed into *E. coli* DH5α. A positive colony was selected by PCR using the Spy0125 fw and Spy0130 rw primers to ensure the entire pilus operon was present in the plasmid. To confirm the presence of the XhoI site at the N29 position, the *spy0128* gene was PCR amplified using the Spy0127 fw and Spy0128 rw primers and digested overnight with XhoI. After visualising the digested and undigested *spy0128* gene on an agarose gel, the presence of two bands at ~ 550 and 850 bp confirms that the XhoI site is at the correct position (figure 6.2).

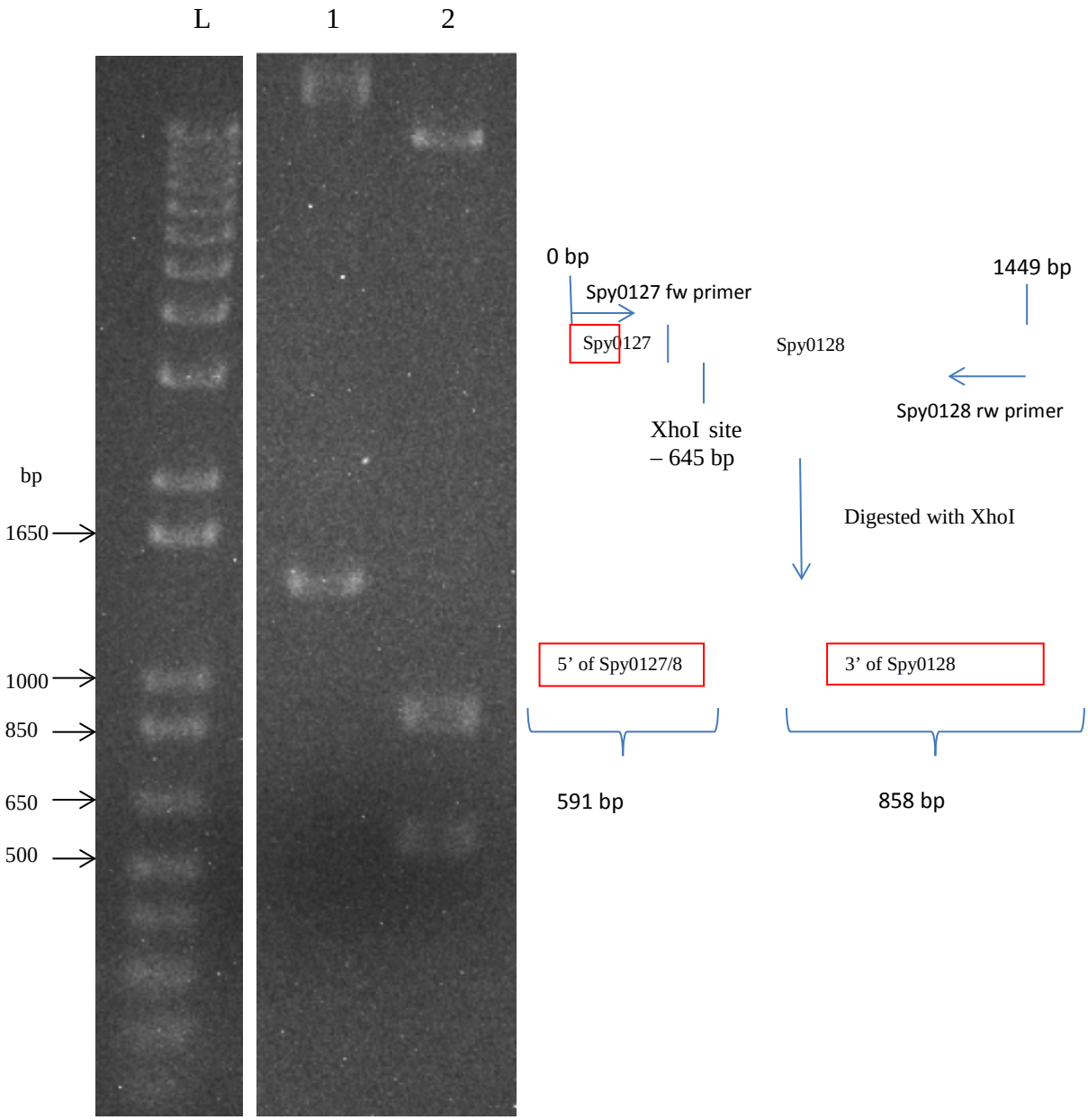

Figure 6.2 Confirming the presence of the XhoI site at the N29 position of Spy0128

The *spy0128* gene was PCR amplified from pLZ12-Km2:P23R_PilM1_N29_XhoI using the Spy0127 fw and Spy0128 rv primers and digested overnight with XhoI. Schematic diagram on the right shows the location of the XhoI site and the expected sizes of the digested PCR product. Image on the left features the 1% agarose gel electrophoresis. Lane L: the 1 kb molecular weight marker. Lane 1: undigested *spy0128* gene. Lane 2: *spy0128* gene digested overnight with XhoI.

To determine if the addition of the XhoI site at position N29 impairs polymerisation of the pilus on the surface of *L. lactis*, the pLZ12-Km2:P23_PilM1_N29_XhoI plasmid was electroporated into *L. lactis* and cell wall extracts were analysed by Western blot with rabbit antiserum specific for Spy0128. In the extract, high molecular weight bands, characteristic of pilus formation, were

visible and the pattern formed was comparable to that observed in a cell wall extract from *L. Lactis* expressing the wild type pilus. In contrast, no bands were visible in the extract from *L. Lactis* containing the empty vector pLZ12-Km2:P23R as expected (figure 6.3).

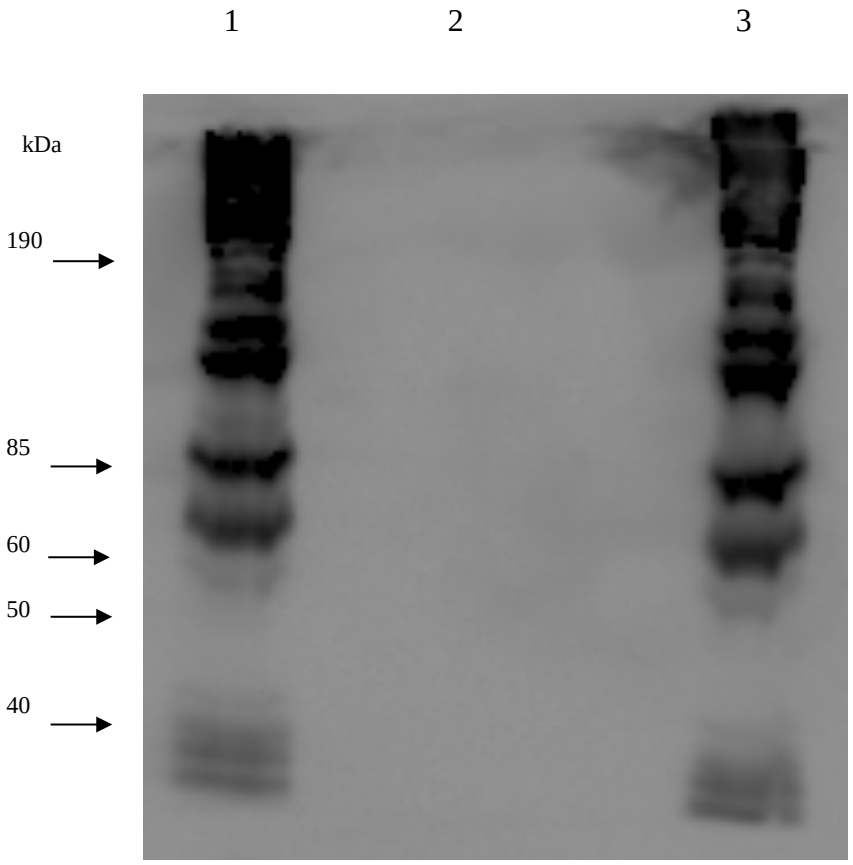

Figure 6.3 Western blot analyses of pLZ12-Km2:P23R_PilM1_N29_XhoI expressed in *L. lactis*

Cell wall extracts analysed by Western blot using rabbit anti-spy0128 antiserum. Lane 1: *L. lactis*: pLZ12-Km2:P23R_PilM1_N29_XhoI. Lane 2: the negative control (*L.lactis*:pLZ12-Km2:P23R). Lane 3: the positive control (*L. lactis*:pLZ12-Km2:P23R_PilM1). A high molecular weight laddering pattern is observed in the cell wall extract from both *L. lactis*: pLZ12-Km2:P23R_PilM1_N29_XhoI and the positive control.

6.2.1.2 Engineering the J14 peptide into the XhoI site

To engineer the J14 peptide into the XhoI site at the N29 position of Spy0128, the XhoI/SalI digested J14 DNA sequence from a pBC:J14 plasmid was cloned directly into the XhoI digested pLZ12-Km2:P23R_PilM1_N29_XhoI plasmid. The resulting plasmid, pLZ12-

Km2:P23R_PilM1_N29_J14, was transformed into *E. coli* DH5α and a positive colony was selected using the J14 fw and Spy0128 rw primers. Afterwards, the pLZ12-Km2:P23R_ PilM1_N29_J14 plasmid was extracted from DH5α and electroporated into *L. lactis* to create NTN-J14-Pilvax (figure 6.4).

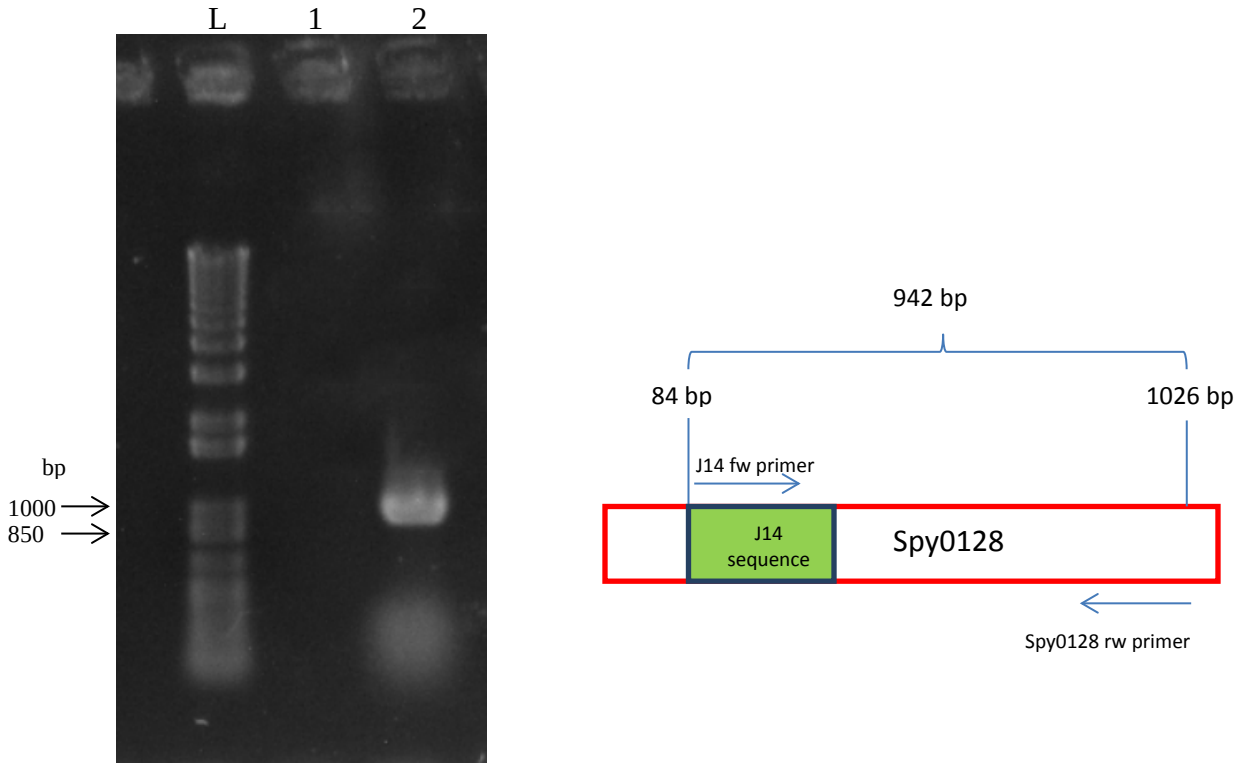

Figure 6.4 The pLZ12-Km2:P23R_PilM1_N29_J14 plasmid was successfully electroporated into *L. lactis*

J14 fw and Spy0128 rv primers were used to select an *L. lactis* colony containing the pLZ12-Km2:P23R_PilM1_N29_J14 plasmid. Schematic diagram on the right shows primer binding sites and the expected size of the PCR product if positive. Image on the left features 1% agarose gel electrophoresis. Lane L: the 1 kb molecular weight marker. Lane 1: the negative control (*L. lactis*: pLZ12-Km2: P23R_PilM1 plasmid). Lane 2: *L. lactis*:pLZ12-Km2:P23R_PilM1_N29_J14.

6.2.1.3 Engineering the J14 peptide into the N29 site affects the cell surface pilus expression

Western blot analyses of the cell wall extract from NTN-J14-Pilvax, using rabbit antiserum specific for Spy0128, revealed certain high molecular weight bands, but a complete laddering pattern, as seen in the cell wall extract from *L. Lactis* expressing the wild type pilus, was absent. This indicates that the J14 peptide is interfering with pilus polymerisation on the surface of *L. lactis*. (figure 6.5).

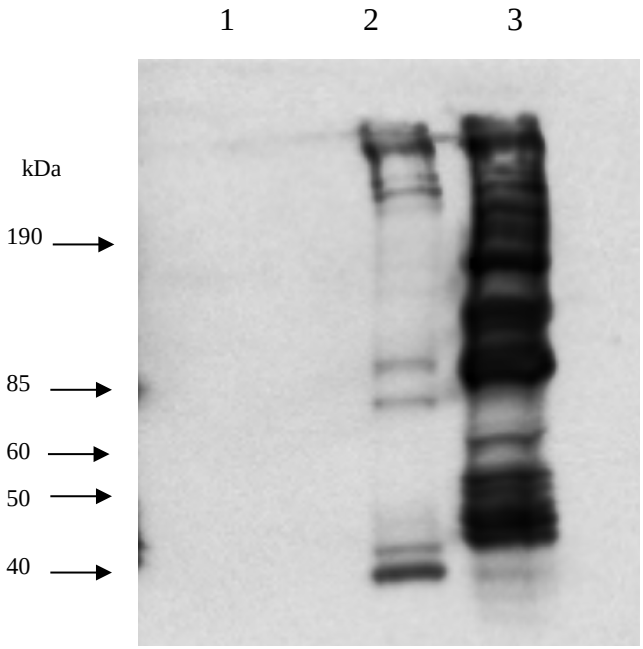

Figure 6.5 Engineering the J14 peptide into the N-terminus of Spy0128 interferes with pilus polymerisation on the surface of *L.lactis*

Cell wall extracts were analysed by Western blot using rabbit anti-spy0128 antiserum. Lane 1: the negative control (*L. lactis*:pLZ12-Km2:P23R). Lane 2: NTN-J14-Pilvax. Lane 3: the positive control (*L. lactis*:pLZ12-Km2:P23R_PilM1).

To verify that the cell surface pilus expression was affected by integrating J14 into the N-terminus of Spy0128, bacteria, stained with anti-M1 pilus antiserum were subjected to flow cytometry. For the flow cytometry assay, Pilvax, *L. lactis* expressing wild type pilus, and *L. lactis* containing the empty vector pLZ12-Km2:P23R, were initially incubated with antiserum against the M1 pilus. Then, after washing, the three strains were incubated with FITC tagged goat anti-mouse antibodies. If the strains express pili, both the anti-M1 pilus antibodies and the FITC tagged antibodies will bind, resulting in a fluorescent shift over the background when detected by flow cytometry. As shown in figure 5.6, while the antiserum specifically bound to both NTN-J14-Pilvax (green histogram) and *L. lactis* expressing wild-type pilus (red histogram), the fluorescence shift over the background observed for NTN-J14-Pilvax was lower than that observed for *L. lactis* expressing wild-type pilus. This suggests that NTN-J14-Pilvax is expressing less pili than *L. lactis* expressing wild-type pilus. *L. lactis* containing the empty vector pLZ12-Km2:P23R (blue histogram) does not express pili and thus exhibited background levels of fluorescence as expected (figure 6.6).

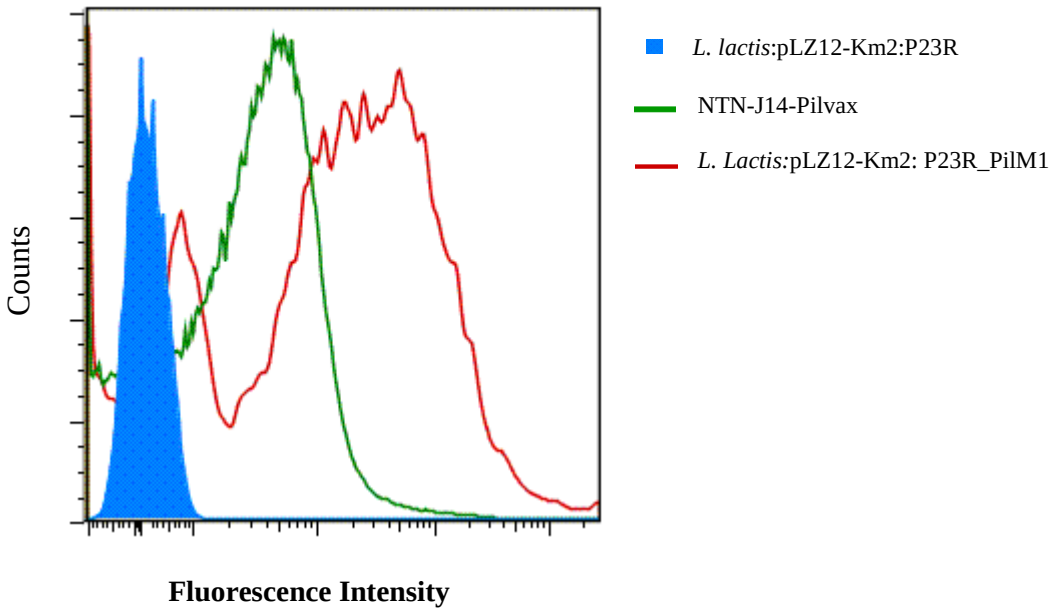

Figure 6.6 Engineering the J14 peptide into the N-terminus of Spy0128 reduces the amount of pilus expressed on the cell surface

Flow cytometry analyses of NTN-J14-Pilvax (*green void histogram*), *L. Lactis:*pLZ12-Km2: P23R_PilM1 (*red void histogram)*, or *L. lactis*:pLZ12-Km2:P23R *(full blue histogram)* stained with serum from a mouse immunised with *L. Lactis:*pLZ12-Km2:P23R_PilM1. Staining of NTN-J14-Pilvax with the antiserum was reduced when compared to staining of *L. lactis* expressing wild-type pilus. This suggests that fewer pili are being expressed on the surface of NTN-J14-Pilvax.

Since pilus polymerisation was not completely eliminated in NTN-J14-Pilvax, flow cytometry was performed, using mouse antiserum specific for J14, to determine the presence of the J14 peptide on the surface of the recombinant *L. lactis*. As shown in figure 6.7, the anti-J14 antiserum specifically bound to NTN-J14-Pilvax (green histogram), with a fluorescence shift over the background being observed, and this confirmed that the J14 peptide was present and exposed on the outer side of the *L. lactis* cell wall. *L. lactis* expressing wild-type pilus (red histogram) exhibited only background levels of fluorescence as expected.

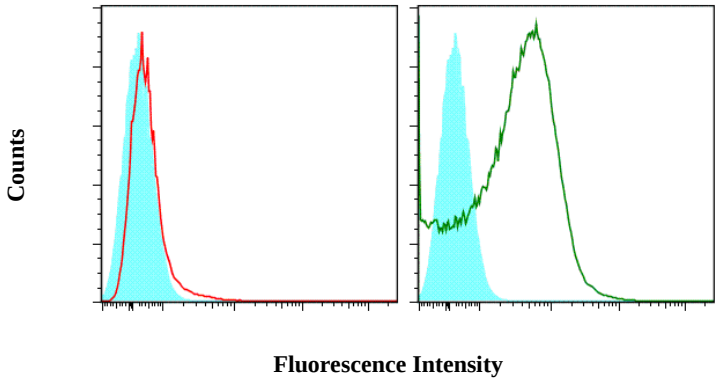

Figure 6.7 Mouse anti-J14 antiserum can bind to NTN-J14-Pilvax

Flow cytometry analyses of J14 expression on the surface of NTN-J14-Pilvax (*green void histogram*) and *L. Lactis:*pLZ12-Km2:P23R_PilM1 (*red void histogram),* compared with incubation only with secondary antibody *(full light blue histogram).*

To determine if the J14 peptide was expressed within the pilus structure, the TCA precipitated cell wall extract from NTN-J14-Pilvax was analysed with mouse antiserum specific for J14. The antiserum recognised a strong band corresponding to the J14 peptide at a molecular weight greater than 190 kDa, which correlates well with the size of the bands observed in the cell wall extract analysed with anti-Spy0128 antibodies (figure 6.8).

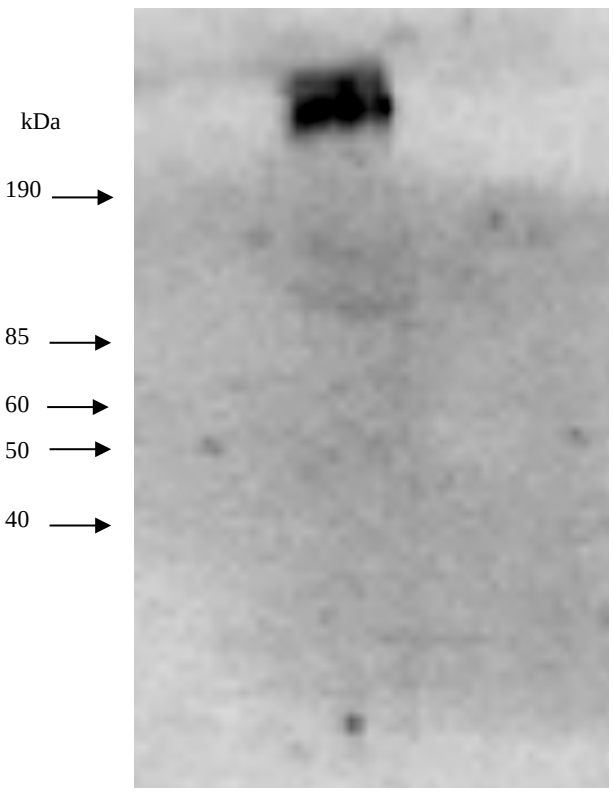

Figure 6.8 The J14 peptide is only integrated into longer forms of the polymeric structure

TCA precipitated cell wall extracts were analysed by western blot using mouse anti-J14 antiserum. Lane 1: NTN-J14-Pilvax. Lane 2: the negative control (*L.lactis*: pLZ12-Km2:P23R_PilM1).

6.2.2 Intranasally immunising mice with NTN-J14-Pilvax

Since flow cytometry and Western blot analyses indicated the presence of the J14 peptide on the surface of NTN-J14-Pilvax, a small pilot study was undertaken to determine if NTN-J14-Pilvax can elicit a J14-specific immune response. CD1 mice were used for the pilot study as all the FVB/n mice housed in the animal unit became infected with S. aureus and had to be culled. CD1 mice were immunised intranasally with 50 µl of NTN-J14-Pilvax ($1x10^9$ CFU per mouse) at two-week intervals for a total of four immunisations. Mice were similarly immunised with *L. lactis* expressing wild-type pilus (*L.lactis*:pLZ12-Km2:P23R_PilM1) as a negative control. For the positive control, mice were subcutaneously immunised with four doses of a Thioredoxin-J14-IFA emulsion.

6.2.2.1 The Spy0128-specific serum IgG responses

The serum IgG response to the Spy0128 subunit was evaluated by ELISA with immobilised Spy0128 protein. An IgG response to Spy0128 was detected in three of the five mice immunised with NTN-J14-Pilvax and all the mice immunised with *L. lactis* expressing wild-type pilus. The average end-point titres (day 49) were approximately 1:12,800 and 1:106,000 respectively. Only background activity was found in the serum from mice immunised with the Thioredoxin-J14-IFA emulsion as expected (figure 6.9).

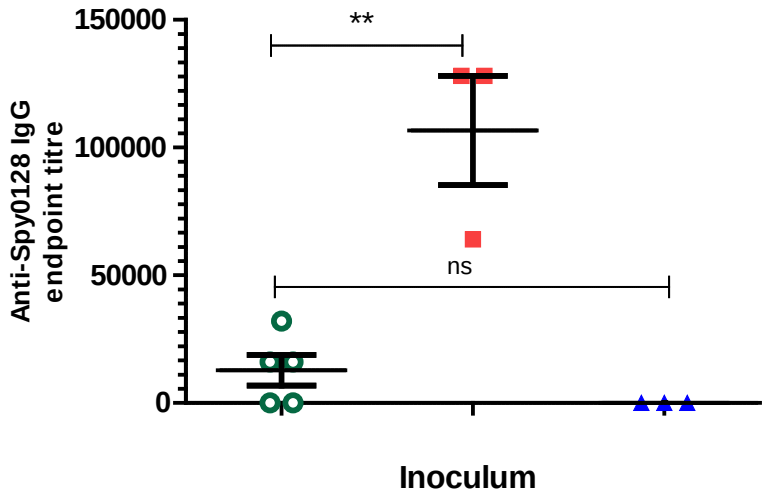

Figure 6.9 The Spy0128-specific serum IgG antibody responses in immunised CD1 mice.

Sera were collected from mice 7 days after the fourth immunisation and the Spy0128-specific IgG antibody titres were determined by ELISA performed in triplicate. Serum samples were taken from mice inoculated i.n. with NTN-J14-Pilvax (✿, n=5), or *L. Lactis:*pLZ12-Km2:P23R_PilM1 (■, n=3), or subcutaneously with Thioredoxin-J14-IFA (▲, n=3). The average titre for individual mice is shown and the data is from a single experiment. The mean and standard error of the mean for each group are represented as bars. Statistical differences were determined using one-way ANOVA with Bonferroni post-hoc test (**P < 0.05, ns = non-significant difference).

6.2.2.2 The J14-specific BALF IgA responses

To assess the elicitation of a local mucosal antibody response following intranasal immunisation, the presence of J14-specific IgA in undiluted BALF from immunised mice was determined by using an ELISA with immobilised GST-J14. IgA responses to J14 were not detected in any of the mice immunised with NTN-J14-Pilvax or the Thioredoxin-J14-IFA emulsion, with the response being similar to the background response in the negative control mice immunised with *L. lactis* expressing wild-type pilus (figure 6.10).

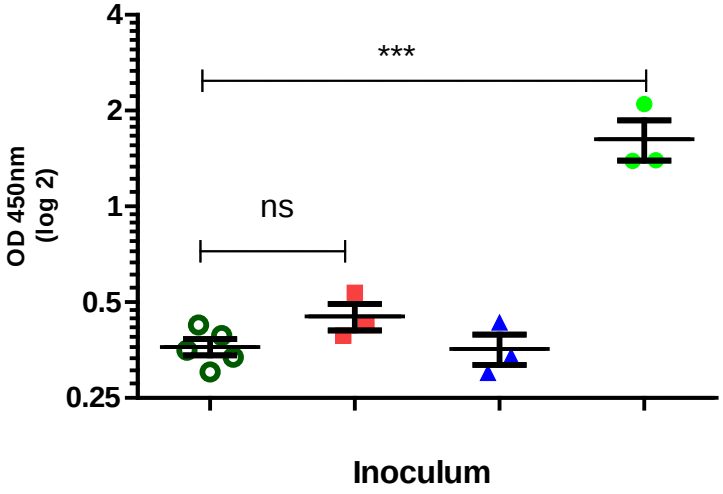

Figure 6.10 J14-specific IgA antibody responses in bronchoalveolar lavage fluid from immunised CD1 mice

J14-specific IgA responses in BALF collected 7 days after the fourth immunisation from mice inoculated i.n. with NTN-J14-Pilvax (○, n=5), or *L. Lactis*:pLZ12-Km2:P23R_PilM1 (■, n=3), or subcutaneously with Thioredoxin-J14-IFA (▲, n=3). The IgA response was determined in undiluted samples from individual mice by ELISA performed in triplicate and the data is from a single experiment. Each point represents a single mouse with the mean and standard error of the mean for each group represented as bars. BALF from J14-Pilvax immunised FVB/n mice (●, n=3) that produced a mucosal immune response were used as an ELISA positive control. Statistical differences were determined using one-way ANOVA with Bonferroni post-hoc test (*** $P < 0.05$; ns = non-significant difference).

6.2.2.3 The J14-specific serum IgG responses

To assess the induction of a systemic antibody response following intranasal immunisation, the presence of J14-specific IgG in serum from immunised mice was determined by using an ELISA with immobilised GST-J14. While a measurable reaction with GST-J14 was demonstrated in all of the mice immunised with the Thioredoxin-J14-IFA emulsion, no measurable reaction was demonstrated in any of the mice immunised with NTN-J14-Pilvax, with the IgG response to J14 being similar to the background response detected in the negative control mice (figure 6.11).

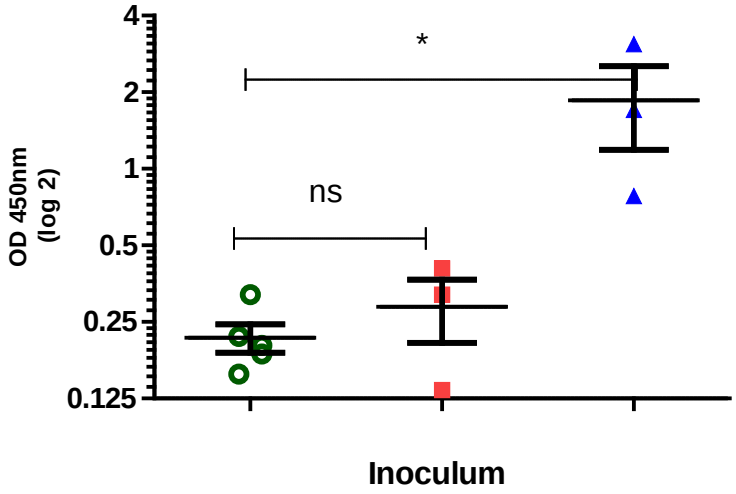

Figure 6.11 The J14-specific IgG antibody responses in serum from immunised CD1 mice.

J14-specific IgG responses in serum collected 7 days after the fourth immunisation from mice inoculated i.n. with NTN-J14-Pilvax (✪, n=5), or *L. Lactis:*pLZ12-Km2:P23R_PilM1 (■, n=3), or subcutaneously with Thioredoxin-J14-IFA (▲, n=3). The IgG response was determined in serum samples, diluted 1:50, from individual mice by ELISA performed in triplicate and the data is from a single experiment. Each point represents a single mouse with the mean and standard error of the mean for each group represented as bars.Statistical differences were determined using one-way ANOVA with Bonferroni post-hoc test (*P < 0.05; ns = non-significant difference).

6.3 Summary

The N-terminus of Spy0128 was selected as a potential site where the J14 peptide could be integrated into without disrupting its α-helical conformation. Inserting an XhoI site at the N29 position of the N-terminus did not affect pilus polymerisation on the surface of *L. lactis*. Therefore, the J14 peptide was engineered into the XhoI site to create NTN-J14-Pilvax. In Western blots of the cell wall extract from NTN-J14-Pilvax, analysed with rabbit anti-Spy0128 antiserum, an overall reduction in the amount of pilus was detected, with mainly high molecular bands observed. The reduction in pilus expression was confirmed by flow cytometry. However, flow cytometry analyses of NTN-J14-Pilvax, using mouse anti-J14 antiserum, indicated the presence of the J14 peptide on the cell surface. When a Western blot of the TCA precipitated cell wall extract from NTN-J14-Pilvax was incubated with mouse anti-J14antiserum, high molecular weight bands greater than 190kDa were observed, which suggests that only long pili containing the J14 peptide were assembled on the surface of *L. lactis*.

Immunisation of mice with NTN-J14-Pilvax did not produce any measurable antibody response against the J14 peptide. The antibody response to Spy0128 was also not present or weak compared to the control. These results suggest that the amount of pilus expressing J14 on the surface of *L.lactis* was insufficient to trigger an immune response in mice and, therefore, NTN-J14-Pilvax is ineffective as a mucosal vaccine delivery system of the J14 peptide.

Chapter 7

Discussion

7.1 Introduction

The aim of this thesis was to develop a novel peptide delivery system (Pilvax), by expressing peptides within the GAS pilus structure on the surface of *L. Lactis.* The serotype M1 pilus of GAS consists of 50-100 protease-resistant Spy0128 pilin subunits that are covalently linked by isopeptide bond formation (Kang, et al., 2007; Linke, et al., 2010). The homopolymerisation of Spy0128 subunits to form the pilus shaft enables the potential use of the pilus as an amplified vaccine peptide carrier. Genetic engineering of a peptide into the Spy0128 subunit will result in the expression of up to 100 repeated copies of the peptide along the pilus extension and thousands of copies across the surface of the bacterium. It was hypothesised that the multimeric presentation of a poorly immunogenic peptide within the pilus structure would likely increase its immunogenicity. The complete M1 GAS pilus structure can be expressed and assembled on the surface of *L. lactis*, a non-pathogenic relative of GAS. *L. lactis* has been recognised as an effective immunomodulator and promising antigen delivery vehicle, having been used to deliver numerous vaccine candidate antigens to both mucosal and systemic sites (Wells & Mercenier, 2008).

7.2 Risk assessment of using the M1 pilus of GAS as a vaccine carrier

There are no published reports of the M1 pilus generating autoimmune responses. However, experiments have shown that antibodies against the M1 pilus does not cross react with human heart extract (personal communication with Dr. Moreland, University of Auckland). This is not

surprising as autoantibody generating epitopes of GAS have been mapped to the M-protein and the GlcNAc found in the group A antigen. The alpha helical structure of the M-protein is similar to alpha helical coiled coil proteins found in humans, such myosin, keratin, vimentin, or laminin, and it is this molecular mimicry that is responsible for the generation of cross-reactive antibodies between GAS and human tissue (Massilamany, et al., 2014). The shaft of the M1 GAS pilus consists of irregular all-β structures that are modified variants of the immunoglobulin fold (Kang, et al., 2007), therefore, molecular mimicry with the alpha helical human proteins should not occur.

GAS is also known to internalise into epithelial cells and if this occurs with Pilvax it would be hidden from the immune system and the response elicited by any vaccine antigen carried by Pilvax would be abrogated. However, in GAS, it is the interaction of GAS fibronectin-binding protein (SfbI F1) with fibronectin on epithelial cells that triggers bacterial internalisation. Blocking of the SfbI adhesion, by either antibodies against the whole protein or antibodies against the fibronectin-binding domains of SfbI, prevents GAS internalisation. Entry of serotype M1 GAS into host cells also depends on binding of the host fibronectin by the bacterial M1 protein. Deletion of both the N-terminal A and B repeat regions of M1 abrogates fibronectin binding and intracellular invasion (Passàli, et al., 2007). Therefore, the absence of these proteins on Pilvax should mean that it cannot internalise into host epithelial cells.

The Spy0125 protein on the tip of the pilus shares strucutural homologies with both collagen-binding and fibronectin-binding proteins from other GAS strains (Ferretti, et al., 2001). In addition, the serotype M1 GAS strain has been shown to bind type I (though not type IV) collagen (Kreikemeyer, et al., 2005). This raised the possibility the Spy0125 protein might act as an adhesin for either fibronectin or collagen. The pilus tip adhesion of Group B Streptococcus (GBS), PilA, has been shown to bind collagen and contribute to GBS adherence to blood-brain barrier (BBB) endothelium and efficient penetration of the BBB (Banerjee, et al., 2011). Hence, the collagen binding properties of Spy0125 may be a risk to using Pilvax as a vaccine peptide carrier.

However, there are no published reports on the ability for the M1 pilus to bind to the BBB. Furthermore, it has been shown that the adhesion by the M1 pilus is tissue specific. Pili were essential for adhesion of M1 GAS strain to tonsil, primary keratinocytes and HaCaT cells, which represent tissues from the two main sites of GAS infections in humans, the skin and oropharynx. In contrast, they played little or no role in adhesion to either a cervical cancer cell line HEp-2 or a human alveolar cancer cell line A549, which are far less likely to mimic the types of squamous epithelia colonized by GAS (Abbot, et al., 2007). Therefore, adhesion of Pilvax will likely be limited to the squamous epithelia of the oropharynx following intranasal immunisation. In this site, damage to the epithelium would be required to expose collagen and, in the case of tonsil, type IV collagen from basement membranes is likely to be exposed more readily than type 1 collagen (Abbot, et al., 2007). So, the collagen binding properties of the Spy0125 should not pose a risk in Pilvax. Furthermore, a study has shown that pre-incubation of wild-type SF370 with either fibronectin, type I collagen, type IV collagen, or fibronectin and collagen combined, had no significant effect on adhesion to tonsil epithelium or HaCaT cells. These findings indicate that pilus mediated adhesion is neither dependant on, nor inhibited by, fibronectin, type I or type IV collagen, and this suggests it is unlikely to involve direct interaction with these host proteins (Abbot, et al., 2007).

7.3 Replacing selected loop regions of Spy0128 with the $OVA_{323-339}$ peptide

After analysing the crystal structure of Spy0128, five loop regions connecting the β strands of Spy0128 were initially selected as potential sites for peptide insertion. Out of the five loop regions investigated, only the β_E-β_F loop region could be replaced with the model foreign peptide, $OVA_{323-339}$, without disrupting the polymerisation of the pilus shaft on the surface of *L. lactis*.

Replacing the β_D-β_E loop region with an XhoI site, to enable the insertion of the $OVA_{323-339}$ peptide between the two β strands, abolished pilus polymerisation on the surface of *L. lactis*. This suggests that replacing the loop region probably interferes with the isopeptide bond formation between the Spy0128 subunits. However, following replacement of the loop region, the plasmid was not sequenced due to the large size of the pilus operon and the cost it would incur. Therefore, it is possible that a mutation somewhere along the pilus operon may cause the abrogation of pilus polymerisation. Replacing any of the remaining loop regions with an XhoI site did not affect pilus polymerisation on the surface of *L. lactis* and so the $OVA_{323-339}$ peptide was genetically engineered into each site.

Engineering the $OVA_{323-339}$ peptide between the β_B and β_{C1}, β_2 and β_3, or β_3 and β_4 strands of Spy0128 affected pilus polymerisation to varying degrees. Engineering the peptide between the β_3 and β_4 strands eliminated pilus assembly on the surface of *L. lactis*, which suggests that the peptide is preventing the covalent cross-linking between the Spy0128 subunits. Engineering the peptide between the β_B and β_{C1} or the β_2 and β_3 strands did not interfere with the formation of the shorter forms of the polymeric structure; however, the formation of long pili was disrupted. Since short pili were formed, the peptide is probably not interfering with the cross-linking of Spy0128 subunits. Therefore, the sortase mediated attachment of long pili to the surface of *L. Lactis* may be impeded by the peptide. For the use of the pilus as a carrier of poorly immunogenic vaccine peptides, long pili would be likely needed for effective multimeric presentation. Thus, these two loop regions were deemed to be inadequate for that purpose.

Since engineering the peptide between the β_B and β_{C1} or the $\beta_2$and β_3 strands did not interfere with the cross-linking of Spy0128 subunits, fully formed pili containing the peptide may be present in the supernatant. When Smith *et al* was investigating the functions of the cell wall linker Spy0130, they found that Spy0130 deletion mutants did contain pili in the culture supernatants (Smith, et al., 2010).

However, for Pilvax, the goal was to find a loop region where adding the peptide did not affect pilus assembly on the cell surface and thereby allow the pilus peptide construct to be attached to the cell wall of *L. lactis* for immunisation. The main reason for this is that studies have shown that immunisation with *L. lactis* containing a cell wall attached antigen generates a stronger antibody response than when the antigen is secreted by *L. lactis*. In a study where the TTFC was engineered into *L. lactis*, either attached to the cell wall or secreted, the cell wall anchored form was significantly more immunogenic. Protective antibodies were also more readily elicited when the TTFC was anchored into the cell membrane (Norton, et al., 1996). A similar result was obtained in a study using *L. lactis* expressing E7 antigen of HPV, either secreted or attached to the cell wall. Splenocytes from mice immunized with *L. lactis* expressing the cell wall anchored E7 and re-stimulated *in vitro* produced higher IL-2 and IFN-γ than those obtained from mice immunised with *L. lactis* secreting E7 (Bermudez-Humaran, et al., 2004). This was attributed either to a better accessibility to the immune system when the antigen is exposed at the bacterial surface or to some adjuvant properties of the LAB vector itself. Also, the transient nature of *L. lactis*, it is cleared very rapidly following inoculation, may contribute to the reduced immunogenicity of the secreted form. Therefore, since anchoring peptides to the cell wall of *L. lactis* produces the strongest immune response against the peptide, the ability of Pilvax secreting pilus-peptide constructs to stimulate an immune response was not investigated.

Engineering the $OVA_{323-339}$ peptide between the β_E and β_F strands of Spy0128 did not interfere with pilin folding and pilus assembly on the surface of *L. lactis*. A ladder pattern of high molecular mass products, characteristic of pilus formation (Mora, et al., 2005), was visible in a Western blot of a cell wall extract from the modified *L. lactis* analysed with anti-Spy0128 antiserum. A ladder pattern was also visible in a cell wall extract analysed with anti-ovalbumin antiserum. This indicates that the $OVA_{323-339}$ peptide has been integrated into the Spy0128 subunit, resulting in the multimeric presentation of the peptide on the surface of *L. lactis*.

The OVA peptide was only shown to be integrated in the pilus structure above 69 kDa, while bands representing the Spy0128 subunit were shown at 40 kDa and above. Theoretically the OVA peptide should be detected at 40 kDa as the peptide is integrated within the Spy0128 subunit, so, the fact that it is not seen at 40 kDa is most likely a sensitivity issue with the Western Blot assay itself. The Spy0128 bands at 40 kDa represent the smallest pilus structures, so the least amount of OVA peptide is integrated into these pili and is likely too low to be detected by the assay. Immunogold electron microscopy to detect the OVA peptide may be used to determine if the peptide is present within the smallest pilus structures and also gain an idea of the amount of peptide expressed on the surface of *L. lactis*.

Flow cytometry, using anti-ovalbumin antiserum, also verified that the peptide was present and exposed on the surface of *L. lactis*. For the flow cytometry assay, Pilvax and *L. lactis* expressing wild type pilus were initially incubated with anti-ovalbumin antiserum. Then, after washing, the two strains were incubated with FITC tagged goat anti-mouse antibodies. If the OVA peptide is integrated within Pilvax, both the anti-OVA antibodies and the FITC tagged antibodies will bind, resulting in a fluorescent shift over the background when detected by flow cytometry. This fluorescent shift was present following flow cytometry analysis of Pilvax which verified that the OVA peptide was present and exposed on the cell surface of Pilvax. *L. lactis* expressing wild type pilus did not contain OVA peptide, hence the antibodies were unable to bind and thus only background fluorescence was present.

Thus, OVA-Pilvax was successfully developed by replacing the β_E-β_F loop region of Spy0128 with the $OVA_{323-339}$ peptide and expressing the peptide-linked pilus on the surface of *L. lactis.*

7.4 Competing delivery systems which use surface proteins for foreign antigen expression

In Pilvax, the peptide was incorporated into the loop region of the pilus and a similar method has been used previously to create a peptide delivery system using VLPs. Sadeyen *et al*

engineered a peptide of the hepatitis B virus core antigen into six different surface loops of HPV16 L1 VLPs. With the exception of the one C-terminal insertion loop, all resulting chimeras were able to induce antigen-specific antibodies in mice. The antigenicity and immunogenicity of some of these VLPs were reduced compared to the levels observed with wild-type VLPs. All were nevertheless able to induce neutralizing antibodies (Sadeyen, et al., 2003).

A pilus based vaccine protein carrier has also been developed by Quigley et al called UPTOP (unhindered presentation on tips of pili). The C-terminal of the tip protein CPA of the T3 pilus of GAS was used as a fusion site for foreign protein and the pilus-protein construct was expressed on *L. lactis*. To show proof of concept the *E. coli* maltose binding protein (MBP) was fused to the CPA. Binding of the recombinant lactococcus to amylase resin indicated that the MBP retains its activity as that requires correct folding of the protein. Immunising mice with UPTOP generated both a systemic and mucosal antibody response against the MBP protein, thus showing proof of concept for the delivery system (Quigley, et al,. 2010). The advantage of the UPTOP system is that it can present whole proteins containing multiple epitopes and the structure of the protein is not affected. Although the disadvantage, compared to Pilvax, is that there is no amplification of the protein as only a single copy of the protein would be presented on the tip of the pilus. However, while this system is used to deliver proteins, Quigley *et al* have indicated that a peptide has also successfully been engineered into the T3 pilus shaft (B. R. Quigley, Z. Eichenbaum, and J. R. Scott, unpublished results), thus possibly enabling the creation of a carrier system for simultaneous delivery of peptides and proteins.

The UPTOP carrier system elicited both a systemic and mucosal immune response against the displayed protein so the ability of OVA-Pilvax to elicit a similar immune response was investigated. In order to allow a comparison of the ELISA results from mice immunised with OVA-Pilvax with those from the UPTOP study, the same format to display results was used, whereby optical density was used to display the OVA-specific IgA responses. The cohort of

mice in the experiments done by Quigley *et al* to show proof of concept for UPTOP consisted of 10 mice, so a similar sample number, 12, was used in the experiments to show proof of concept for Pilvax (Quigley, et al,. 2010).

7.5 Elicitation of mucosal and systemic antibody responses in OVA-Pilvax immunised BALB/c mice

The 323-339 region of OVA was reported to be a T cell epitope for BALB/c mice (Yang & Mine, 2009). The $OVA_{323-339}$ peptide has also been shown to be a B cell epitope in BALB/c mice (Radcliff, et al., 2012). Therefore, BALB/c mice were chosen as the mouse strain to investigate if Pilvax can effectively present the $OVA_{323-339}$peptide and trigger a mucosal and systemic immune response. The induction of IgA antibodies is required for an effective mucosal immune response. IgA antibodies can a form a barrier at the mucosal surface by promoting the entrapment of pathogens and preventing direct contact of pathogens with the mucosal surface. Secretory IgA can also bind to bacterial adhesins that mediate epithelial attachment (Hutchings, et al., 2004; Lamm, 1997). The protection provided by IgA is especially important in areas that cannot be accessed effectively by serum IgG antibodies. Intranasal administration of OVA-Pilvax resulted in a detectable OVA-specific IgA response in the serum, lung lavages and saliva of immunised mice. These results suggest that Pilvax is able to generate mucosal immune responses against selected small peptides. The average IgA response to OVA in mice immunised with OVA-pilvax was approximately seven times greater than the background response. This was higher than the IgA response to the MBP protein seen in mice immunised by the UPTOP vaccine carrier, the response being only three times higher. In Pilvax, there is multimeric presentation of the peptide which is not present in the UPTOP vaccine carrier and this may be the reason for the higher response.

The OVA-specific IgA antibody responses in mucosal secretions were tested using undiluted samples and presented as the direct O.D. compared with a control. A disadvantage of this

approach is that the data has a large quantitative uncertainty since the relationship between O.D. and antibody concentration is highly non-linear. In addition the O.D. values could be changed by a number of factors (e.g., time of incubation, type of antigen, species of animal, etc) (Miura, et al., 2008). However, the purpose of this study was to show proof of concept that Pilvax can elicit an antibody response against the peptide it carriers and so presenting the data as direct O.D. is sufficient. When experiments are done to determine if Pilvax carrying a vaccine antigen can generate a protective immune response, presenting the results as direct O.D. would probably be insufficient and using protein concentrations should be considered.

In the OVA-Pilvax immunised mice that had a detectable OVA-specific IgA response, a serum IgG response to OVA was also detected. This is promising as serum IgG can aide in the mucosal defence, especially in the lower respiratory and in the genitourinary pathways which are permeable to serum antibody (Holmgren & Czerkinsky, 2005). In addition, the serum antibody response can also prevent the spread of invasive pathogens within the body.

However, the OVA-specific serum IgG antibody titre elicited by OVA-Pilvax was significantly lower than the titre induced by subcutaneous immunisation with $OVA_{323-339}$ emulsified 1:1 in IFA. The end-point titre in mice immunised with OVA-Pilvax was approximately 1:7,000 compared to a titre of approximately 1:26,000 induced by $OVA_{323-339}$-IFA. The difference in the route of immunisation may explain this result. Furthermore, IFA is also a water-oil emulsion that forms a depot allowing the slow release of the antigen (Freund 1956). Since the bioluminescent imaging results from chapter 2 suggests that OVA-Pilvax will likely be cleared one day after immunisation, the prolonged presentation of the $OVA_{323-339}$ peptide to mice immunised with $OVA_{323-339}$-IFA may be a reason a higher titre was elicited compared to the mice immunised intranasally with OVA-Pilvax.

While immunising mice with $OVA_{323-339}$-IFA generated a serum IgG response against OVA, the formulation did not induce an OVA-specific IgA response in the serum, lung lavages or saliva of immunised mice, confirming previous studies showing injected vaccines to be poor

inducers of mucosal immunity (Mannam, et al., 2004, Hanniffy et al., 2007). In a study investigating the novel *L. lactis*-conserved C-repeat region vaccine (LL-CRR), made from *L. lactis* expressing the CRR of M protein from *S. pyogenes* serotype 6, mice vaccinated intranasally produced CRR-specific salivary IgA and serum IgG. However, subcutaneously vaccinated mice did not produce a CRR-specific salivary IgA response. Following intranasal challenge with *S. pyogenes* M serotype 14, mice vaccinated nasally were significantly protected against pharyngeal infection while subcutaneous vaccination did not protect mice against infection. The results from the study suggested that CRR-specific salivary IgA was both necessary and sufficient to prevent pharyngeal infection with *S. pyogenes* (Mannam, et al., 2004). An intranasal vaccine *of L. lactis* intracellularly producing pneumococcal surface protein (PspA) also afforded better protection against respiratory challenge with pneumococcus than did vaccination with purified antigen injected with alum (Hanniffy, et al., 2007). Therefore, the advantage of using Pilvax, compared to subcutaneous inoculations of a peptide emulsified in an adjuvant, is its ability to elicit a mucosal IgA antibody response, which has been shown to be important in preventing infection with mucosal pathogens.

$OVA_{323-339}$-IFA cannot be introduced intranasally so another control was used consisting of $OVA_{323-339}$ mixed with cholera toxin B-subunit (CTB), which is a potent mucosal adjuvant (Moschos, et al., 2004). Control mice immunised with the soluble peptide and CTB did not generate specific Ig responses. These results highlight the poor immunogenicity of the $OVA_{323-339}$ peptide and also provide evidence for the fact that Pilvax can increase the immunogenicity of a peptide it carries. One method to increase the immunogenicity of the $OVA_{323-339}$ peptide would have been to conjugate the peptide to the CTB adjuvant. However the fact that $OVA_{323-339}$-IFA positive control elicited OVA-specific IgG antibodies meant that the failure of the $OVA_{323-339}$-CTB control was not a limiting factor in the study.

However, in the cohort of mice intranasally administered with OVA-Pilvax, an OVA-specific antibody response was only detected in some of the immunised mice. The remaining mice had

a weak response or did not respond at all. Imaging of mice administered with a bioluminescent *L. lactis* strain expressing the wild-type GAS pilus, at the same dose used for immunisation with OVA-Pilvax, revealed that the bacteria were either deposited in the lungs or restricted to the nasal cavity and upper respiratory tract. This indicates that the delivery of a vaccine to mice by intranasal immunisation can be variable, which may cause a variable antibody response in the immunised cohort.

In light of the variable antibody response generated in mice immunised with OVA-Pilvax, the observed serum IgG response to the Spy0128 pilin subunit was also tested. This provided an internal control to determine if delivery of the vaccine was adequate, as it is known that intranasal delivery of *L. lactis* expressing the pilus alone generates antibody titres against Spy0128 above 1:100,000 in CD1 mice (personal communication with Dr. Jacelyn Loh). While all the OVA-Pilvax immunised mice had a detectable response to Spy0128, the antibody titres ranged from 1:16,000 to 1:64,000. High anti-Spy0128 IgG levels trended well with high anti-OVA IgG levels when comparing individual mice. This suggests that the likely reason that some mice had undetectable levels of anti-OVA IgG was because they received a lower dose of the vaccine. The Spy0128-specific antibody titres generated were lower than those generated in the mouse experiments by Dr. Jacelyn Loh but this is likely due to the different strain of mice being used.

The isotype of the antigen-specific antibodies produced is an indicator of the type of immune response generated. In mice, IgG1 is associated with a Th2-like response, while a Th1 response promotes the induction of IgG2a antibodies (Germann, et al., 1995). Immunising mice with OVA-Pilvax elicited OVA-specific antibodies of both isotypes, IgG1and IgG2a, which suggests that a mixed Th1-Th2 type immune response was induced. However in the mice that responded best to OVA-Pilvax, the ratio of the titre of IgG2a:IgG1was at 4. This suggests that the adaptive T-cell response to the $OVA_{323-339}$ could be a predominantly Th1 type. Th1 cells, which produce interferon (IFN)-γ, interleukin (IL)-2 and tumor necrosis factor (TNF)-

β, promote a cellular immune response including macrophage activation and T-cell cytotoxicity. BALB/c mice typically exhibit a Th2 response (Fukushima, et al., 2006), as was seen in mice immunised subcutaneously with $OVA_{323-339}$:IFA, which suggests that Pilvax contributes to the skewing of the immune response towards a Th1 response.

A similar shift towards a Th1 immune response was also seen in the live *L. lactis* vaccine against *S. pneumoniae*. Intranasal administration of live *L. lactis* expressing PspA elicited similar PspA-specific IgG1:IgG2a titres while immunisation with recombinant PspA/alum induced antigen-specific antibodies primarily of the IgG_1 isotype. Therefore, this indicates that the lactococcal vaccine shifted the immune response towards Th1, which was also characterised by the lower levels of antibodies in the serum. From the study on the live *L. lactis* vaccine against *S. Pneumonia*, the elicitation of IgG2a antibodies is likely to afford greater protection at the mucosal surface than a predominantly IgG1 response (Hanniffy, et al., 2007).

Although T cell-dependent anti-OVA IgG1 and IgG2a responses were induced, splenocytes harvested from mice immunised with OVA-Pilvax failed to proliferate following restimulation with ovalbumin. One possible explanation is that, since only a single OVA epitope is presented by OVA-Pilvax and a mixed Th1-Th2 type immune response is induced, the population of T-cells in immunised mice with sufficient avidity to the $OVA_{323-339}$ peptide may be small. Therefore, following re-stimulation, the amount of T-cell proliferation is likely too low to be detected (personal communication with Dr. Fiona Radcliffe, University of Auckland, New Zealand). The fact that ovalbumin protein was used as a stimulus may also be a reason for stimulation failure. However, the prohibitive expense involved in buying OVA peptide meant stimulation with peptide was not feasible so this may need to be investigated at a later date. The failure of the T cell proliferation assay also meant that cytokine production resulting from immunisation with Pilvax was not tested.

7.6 Other immunological assays that should be investigated for further development of Pilvax

One possibility with mutimeric presentation of peptides such as in Pilvax is that they can cause clustering of B cell receptors, allowing B cells to be activated in a T cell independent manner. Although a problem with this is that memory B cells are not formed when this happens (Haniuda, et al., 2011). CD4+ T cells in mice immunised with OVA-Pilvax could be depleted and the antibody response analysed to determine if this occurs.

T cell activation and function in lymphocytes from BAL fluid, ezymatically digested lungs and draining lymph nodes can also be analysed. CD4 and 8 T cells can be enriched using magnetic bead separation and activation assessed by flow cytometry measuring CD69, CD44, CD25, CD62L and CD127 expression on T cells. Cytokine production in mucosal secretions could also be analysed.

The activation of pulmonary dendritic cells, following intranasal immunisation with Pilvax, can also be determined using flow cytometry. $CD3^{-}CD19^{-}F480^{-}CD103^{-}$ live cells can be gated for $MHCII^{+}CD11c^{+}$ expression to identify DCs and these cells can be analysed for CD86 expression to determine activation following immunisation with Pilvax.

7.7 Possible methods to achieve a better and broader immune response to Pilvax

7.7.1 Modifying/adapting the immunisation timetable

The easiest way to modify the immunisation schedule to try and increase the immune response to Pilvax would be increase the number of bacteria administered per dose. In an *L. lactis*-based GBS vaccine, for example, mice were immunized with 10^{11} CFU/dose, 100 times the dose used in this study, without adverse effects (Buccato, et al., 2006).

Lactococcus also has numerous promoters which can cause different levels of gene expression. Finding the strongest promoter may allow an increase in the number of pili expressed on the cell surface which in turn would increase the number of peptide and lead to a stronger immune response. One expression system that can be investigated is the nisin-inducible expression (NICE) system. The NICE system was successfully used to express many proteins, both homologous and heterologous on the cell surface of *L. lactis* with gene expression reaching as high as 50% of total protein in some cases (Morello, et al., 2008).

The frequency of administration of the vaccine could also be improved. This may not be possible in parenteral administered vaccine which require needles and trained health professional. However, intranasal immunisation with Pilvax does not require trained professionals so the frequency of administration could easily be increased.

The possibility of prime boosting could also be investigated. This strategy involves priming the immune system to a target antigen delivered by one vector, such as a VLP carrying the vaccine antigen or Pilvax, and then selectively boosting with the other vector. Such strategies have shown to generate high levels of T-cell memory in animal models. This is because the first vector would drive the expansion of antigen specific T cells and vector specific T cells. Subsequent boosting with the second vector drives the expansion of antigen specific memory T cells and vector specific naïve T cells. This results in both a synergistic expansion of T cells specific for the target antigen and selection of T cells that have greater avidity for the antigen. The powers of prime boosts strategies in eliciting protective cellular immunity to a variety of pathogens have been shown. One example is the combination of subcutaneous Bacillus Calmette-Guerin (BCG) priming vaccine followed by the mucosal HBHA+CT vaccine as a booster, which significantly enhanced protective immunity against pulmonary *M. tuberculosis* infection (Dalmia & Ramsay, 2012).

It is also possible that immune response to Pilvax can be improved by administering *L. lactis* expressing IL-12 in conjunction with Pilvax. The effectiveness of this strategy has been shown

in a study using *L. lactis* expressing the E7 antigen of HPV. An antigen-specific cellular response elicited by the recombinant *L. lactis* strain displaying a cell wall-anchored E7 antigen was dramatically increased by co-administration with an *L. lactis* strain secreting IL-12 protein. Higher E7-specific IgG and IgA antibodies were also produced (Bermudez-Humaran, et al., 2003).

7.7.2 Increasing local persistence

Increasing Lactococcus persistence may not be needed to achieve a better immune response. In a direct comparison of *L. plantarum* expressing TTFC, which can persist in the gut, and *L. lactis* expressing TTFC, which cannot, that used repeated bacterial doses to immunise mice by the intragastric route, there was no overriding advantage in using LAB that could persist to elicit an antibody response to TTFC (Wells & Mercenier, 2008). This finding suggests that persistence of the LAB vaccine vector is not the only factor that affects induction of a systemic response to the expressed antigen. Furthermore, there are numerous examples of L. lactis expressing foreign antigens generating protective immune responses following intransal immunisation despite its rapid clearance after inoculation (Wells & Mercenier, 2008).

However, it has been observed that long-lived memory CD8+ T cells are programmed by prolonged antigen exposure (Bachmann, et al., 2006). So improving the persistence of Pilvax may be advantageous in certain situations such as developing a cancer vaccine.

It may be difficult to achieve persistence of Pilvax following immunisation due to the high antigenicity of the pilus of GAS. It has been shown that pilus expression by GAS actually blunts GAS virulence, a result of its high antigenicity. In a subcutaneous injection model where GAS M1T1 produces necrotising lesions, compared to the WT GAS parent strain, the isogenic pilus deleted mutant (ΔPil) produced significantly larger lesions by day 2 and day 3 post-infection. When GAS pneumonia was established in mice by intranasal inoculation and lungs harvested at 24 or 48 hours, significantly more bacteria were recovered from lungs of mice infected with the GAS ΔPil mutant than the WT parent strain at either time point. By 48 hours, markedly more

severe pneumonia with dense neutrophilic infiltration was evident in the ΔPil-infected mice. When GAS sepsis was modeled by injecting the bacteria intravenously and monitoring mortality, the ΔPil mutant GAS demonstrated more rapid kinetics of lethality (Crotty Alexander, et al., 2010).

In human whole blood killing assays, the ΔPil mutant had a 50% increase in blood survival compared with WT GAS parent strain. Survival was reduced toward WT levels in the ΔPil + Pil complemented mutant. Neutrophils infected with the WT GAS strain was shown to release ~35% more IL-8 than those infected with the isogenic ΔPil mutant and pilus expression was also shown to increase neutrophil extracellular trap production and the entrapment of GAS within these structures (Crotty Alexander, et al., 2010).

Due to the high antigenicity of the pilus, the most probable way to increase persistence would be to change the fluid in which Pilvax is delivered through the incorporation of a mucoadhesive adjuvant. One adjuvant that can be investigated is chitosan. It is an adjuvant that has been known to enhance the bioavailability of the antigens due to a mucoadhesive property. The efficacy of chitosan as an adjuvant has been displayed in a series of studies. A clinical study where diphtheria vaccine was administered with chitosan, the presence of chitosan increased the antigen specific IgA response 10-fold. A second clinical study using chitosan and norovirus VLP also showed the effectiveness of chitosan, whereby the duration, and severity, of acute gastoenteristis caused by norovirus was significantly reduced in patients receiving the chitosan-VLP (Smith, et al., 2014).

Therefore, if the immune response elicited by Pilvax alone is not sufficient to provide protection, there are numerous options that can be investigated to try and achieve a better immune response. However, Pilvax is able to generate mucosal immune responses against the $OVA_{323-339}$ peptide. Therefore, it is a promising strategy which may be used to develop vaccines for protection against mucosal pathogens. To further investigate the possibilty of using Pilvax to deliver different peptides, the ability of this peptide delivery strategy todeliver a structural epitope to

mucosal sites was investigated. The antigen chosen was the J14 peptide, a chimeric peptide derived from the carboxy-terminal C-repeat region of GAS M-protein. The J14 peptide contains a conformationally restricted B cell epitope, J14-i, flanked by sequences derived from the GCN4 leucine zipper DNA-binding protein of yeast to maintain the original coiled-coil structure of the epitope (Relf, et al., 1996).

7.8 Engineering the J14 peptide into Pilvax

The β_E-β_F loop region was successfully replaced with the J14 peptide to create J14-Pilvax. Replacing the β_E-β_F loop region with the J14 peptide did not interfere with pilin folding and pilus assembly on the surface of *L. lactis*. A ladder pattern of high molecular weight polymers, characteristic of pilus formation, was visible in a Western blot of a cell wall extract from J14-Pilvax analysed with anti-Spy0128 antiserum and the presence of a ladder of high molecular weight bands in an extract analysed with anti-J14 antiserum indicates that the J14 peptide has been integrated into the Spy0128 subunit. The J14 peptide is bigger than the $OVA_{323-339}$ peptide and this shows the versatility of using Pilvax to deliver peptides of different length to mucosal sites.

7.9 Antibody responses elicited by J14-Pilvax in immunised mice

Intranasal administration of J14-Pilvax resulted in a detectable J14-specific IgA response in the lung lavages of immunised FVB/n mice, although the response was variable, with only 4 out of the 6 immunised mice responding. However, unlike OVA-Pilvax which elicited OVA-specific salivary IgA, a J14-specific IgA response was not detected in the saliva of mice after immunisation with J14-Pilvax. When the J14-specific serum IgG response was analysed, only a weak reaction with recombinant J14 was noted in serum samples from mice immunised with J14-Pilvax. The average end-point titre was 1:3,200, which was significantly lower that the titre elicited by subcutaneous immunisation with thioredoxin-J14-IFA. These results suggest that Pilvax is not very effective at presenting the J14 peptide to trigger an immune response.

Since a strong IgG response to the Spy0128 pilin was detected in the serum of all the mice immunised with J14-Pilvax, the average end-point titre being 1:80,000, the poor response to the J14 peptide is not due to unsuccessful administration of J14-Pilvax. One possible reason for the loss of antigenicity of the J14 peptide when delivered using Pilvax is that the conformation of the peptide is disrupted when it is engineered into Spy0128.

The M-protein is known to be a coiled coil and Relf *et al*. found that the peptide encompassing the minimal B cell epitope, J14-i, needed to be folded into a coiled coil structure for use as a vaccine antigen. To achieve this, the J14 sequence was displayed within a larger peptide derived from the sequence of the GCN4 leucine zipper DBA binding protein of yeast to preserve the helical structure. The resulting chimeric peptide, J14, contained the necessary conformation to elicit protective immune responses (Relf, et al., 1996).

However, when the J14 peptide is engineered between the β_E and β_F strands of Spy0128 it is locked, with both the N- and C- termini joined to a β-strand, and it was hypothesised that this prevents the J14 peptide from forming the α-helical secondary structure (personal communication with Dr. Paul Young, University of Auckland, New Zealand).

Flow cytometry analyses could not detect any binding of the J14-specific serum IgG antibodies, elicited by J14-Pilvax, to SF370 ΔPilM1 indicating that the IgG antibodies could not recognise the M-protein on the surface of SF370 ΔPilM1. An ELISA and dot blot assay with recombinant M-protein confirmed that the J14-specific IgG antibodies could not bind to the M-protein and this suggests that the J14 peptide did not form the appropriate structural epitope when integrated into the pilus.

To gain further evidence to the hypothesis that engineering the J14 peptide into a loop region will disrupt the α-helical conformation of the peptide, a new loop region of Spy0128, the β_9-β_{10} loop region, was replaced with the J14 peptide. Replacing the loop region did not disrupt pilus

polymerisation on the surface of *L. lactis* and the J14 was shown to be incorporated into the Spy0128 subunit by Western blot analyses.

Numerous attempts replace the β_9-β_{10} loop region with the $OVA_{323-339}$ peptide proved unsuccessful, so the J14 peptide was also used to show proof of concept that selected peptides can be engineered between β_9 and β_{10} strands of Spy0128 without disrupting pilus assembly on the surface of *L. lactis*. The fact that the β_9-β_{10} loop region can also be replaced with a peptide may provide an opportunity for multiple epitopes to be engineered within one pilus structure.

Immunising mice with β_9-J14-Pilvax elicited a J14-specific mucosal IgA antibody response and a weak serum IgG response in some of the immunised mice. However, the J14-specific antibodies were again unable to recognise and bind the native M-protein.

Therefore, the fact that both J14-Pilvax and β_9-J14-Pilvax were unable to elicit antibodies in immunised mice that could bind the native M-protein suggests that the conformation of the peptide is disrupted when engineered into a loop region of the Spy0128 pilin and this highlights a limitation of using Pilvax to deliver peptides that are conformationally restricted.

7.10 Engineering the J14 peptide into the N-terminal of Spy0128

Previous studies using J14 as a vaccine peptide have shown that when an adjuvant is attached to the J14 peptide using only one terminus, with the other terminus left unattached, the conformation of the peptide is not disrupted and immunising mice with the vaccine elicits a protective immune response against GAS infection (Batzloff, et al., 2006; Zaman, et al., 2012). According to the crystallographic data, the N-terminus of Spy0128 forms an exposed region extending to the side of the pilus fibre. Therefore, it was hypothesised that if the J14 peptide was engineered into the N-terminus of Spy0128, leaving one terminus of the peptide unattached, the peptide may be able to maintain its alpha-helical conformation while expressed within the pilus structure.

The J14 peptide was successfully engineered into the N-terminal of Spy0128 and expressed on the surface of *L. lactis* to create NTN-J14-Pilvax. Unfortunately, engineering the peptide into the N-terminus impedes pilus polymerisation on the surface of *L. lactis*. In a Western blot of a cell wall extract from NTN-J14-Pilvax, antiserum specific for the Spy0128 protein detected an atypical laddering pattern. While certain high molecular bands of lower intensity were observed, the complete ladder pattern, as seen in the cell wall extract from *L. lactis* expressing wild-type pilus, was not detected. To confirm the Western blot result, the surface expression of pilus protein in NTN-J14-Pilvax was analysed by flow cytometry using serum from a mouse immunised with *L. lactis* expressing wild-type M1 pilus. Staining of NTN-J14-Pilvax with the antiserum was reduced compared to *L. lactis* expressing wild-type pilus, which suggests that less pili are being expressed on the surface of NTN-J14-Pilvax.

However, flow cytometry using anti-J14 antiserum indicated that the J14 peptide was present and exposedon the surface of NTN-J14-Pilvax. When a cell wall extract from NTN-J14-Pilvax was analysed with anti-J14 antiserum, high molecular weight bands greater than 190 kDa were observed, which suggests that only long pili containing the J14 peptide can be successfully assembled on the surface of *L.lactis*. Therefore, while the peptide is not interfering with the polymerisation of the Spy0128 subunits, it probably prevents sortase mediated the attachment of the pilus to the cell wall of *L. lactis* if the length of the pilus is not sufficiently long enough.

Immunising mice with NTN-J14-Pilvax did not elicit a mucosal or systemic immune response to the J14 peptide. The Spy0128-specific serum IgG titre elicited by NTN-J14-Pilvax was significantly lower than the titre elicited by *L. lactis* expressing wild-type pili. This is in line with the results from the Western blot and flow cytometry analyses of NTN-J14-Pilvax which suggested that the amount of pilus expressed on the surface of *L. lactis* was reduced. NTN-J14-Pilvax was unable to elicit an IgG or IgA response to J14, which suggests that the amount of J14 expressed on the surface of *L. lactis* is insufficient to induce an effective immune response.

Therefore, these results suggest that the N-terminus of Spy0128 is not a suitable site in which to express peptides. However further investigation is necessary to determine if peptides smaller than J14 can be engineered into the N-terminus of Spy0128 without affecting pilus polymerisation.

7.11 Concluding Remarks

This thesis shows that two loop regions of the Spy0128 pilin subunit can be utilised as integration sites for certain small peptides and the peptide linked pilus can be expressed on the surface of *L. lactis* to create a novel peptide delivery strategy, Pilvax. Intranasal administration of mice with Pilvax carrying a model peptide, $OVA_{323-339}$, induced a detectable OVA-specific IgA and IgG antibody response. However, engineering the conformationally restricted J14 peptide into Pilvax likely disrupted the α-helical structure of the peptide. Therefore, Pilvax may provide an alternative strategy to allow safe and effective delivery of vaccine peptides to mucosal sites, but may be limited to conformation-independent peptides.

7.12 Future directions

Despite the limitation of using Pilvax with a conformation dependent peptide such as J14, the carrier system merits further investigation. Since immunising mice with OVA-Pilvax elicited an OVA-specific mucosal antibody response, the ability of Pilvax carrying a non-structural vaccine peptide to generate protective immunity should be investigated.

There are databases, containing lists of antigenic epitopes from pathogenic microorganisms or cancer, from which an appropriate peptide could be selected. One promising vaccine peptide against *Mycobacterium tuberculosis* (Mtb) that may be used is the CD4 epitope: I-A(b) Mtb antigen 85B precursor $peptide_{280-294}$. Extensively drug-resistant Mtb strains are an increasing problem in many countries, so a vaccine to prevent Mtb infection is highly desirable (Lange, et al., 2010). Miki *et al* has shown that intravenous vaccination of BALB/c mice with a recombinant attenuated *Listeria monocytogenes* strain carrying an expression plasmid for

Ag85B induced a protective immune response comparable to that induced by a live *Mycobacterium bovis* BCG vaccine (Miki, et al., 2004). Therefore, the ablilty of Pilvax carrying the Ag85B peptide to elicit a protective immune response should be investigated.

The GAS pilus was expressed on *L. lactis* using the pLZ12 plasmid which also encodes an antibiotic resistant marker. Strains expressing such plasmids cannot be introduced into humans due to safety issues such as the possible transfer of antibiotic resistance genes to other bacteria. However, a biocontainable strain of *L. lactis* has been created by Steidler *et al*. by replacing the chromosomal thymidylate synthase (*thyA*) gene with a gene of interest (Steidler, et al., 2003). Therefore, when using Pilvax to test the vaccine candidate antigen from Mtb, the possibility of integrating the pilus gene cluster into the chromosome of *L. lactis*, by replacing the *thyA* gene, should also be investigated.

Oral immunisation with a fusion protein consisting of antigen 85 complex B (Ag85B) and early secretory antigen target 6 (ESAT-6) in combination with an adjuvant also protected mice against Aerosol Infection with *Mtb* (Doherty, et al., 2002). Since both the β_E-β_F and β_9-β_{10} loop regions were successfully replaced with a peptide, Pilvax expressing a combination of Ag85B and ESAT-6 using both integration sites can also be investigated for its ability to elicit a protective immune response against Mtb infection.

Bibliography

Abbot, E. L., Smith, W. D., Siou, G. P., Chiriboga, C., Smith, R. J., Wilson, J. A., et al. (2007). Pili mediate specific adhesion of Streptococcus pyogenes to human tonsil and skin. *Cell Microbiol, 9*(7), 1822-1833.

Akira, S., & Takeda, K. (2004). Toll-like receptor signalling. *Nat Rev Immunol, 4*(7), 499-511.

Akira, S., Uematsu, S., & Takeuchi, O. (2006). Pathogen recognition and innate immunity. *Cell, 124*(4), 783-801.

Alam, F. M., Turner, C. E., Smith, K., Wiles, S., & Sriskandan, S. (2013). Inactivation of the CovR/S virulence regulator impairs infection in an improved murine model of Streptococcus pyogenes naso-pharyngeal infection. *PLoS One, 8*(4), p. e61655.

Allison, A. C., & Gregoriadis, G. (1974). Liposomes as immunological adjuvants. *Nature, 252*(5480), 252-252.

Alpar, H. O., Bowen, J. C., & Brown, M. R. W. (1992). Effectiveness of liposomes as adjuvants of orally and nasally administered tetanus toxoid. *Int. J. Pharm., 88*(1–3), 335-344.

Amidi, M., van Helden, M. J., Tabataei, N. R., de Goede, A. L., Schouten, M., de Bot, V., et al. (2012). Induction of humoral and cellular immune responses by antigen-expressing immunostimulatory liposomes. *J Control Release, 164*(3), 323-330.

Audibert, F., Chedid, L., Lefrancier, P., & Choay, J. (1976). Distinctive adjuvanticity of synthetic analogs of mycobacterial water-soluble components. *Cell Immunol, 21*(2), 243-249.

Audibert, F. M., & Lise, L. D. (1993). Adjuvants: current status, clinical perspectives and future prospects. *Immunol Today, 14*(6), 281-284.

Bachmann, M. F., Beerli, R. R., Agnellini, P., Wolint, P., Schwarz, K., & Oxenius, A. (2006). Long-lived memory CD8+ T cells are programmed by prolonged antigen exposure and low levels of cellular activation. *Eur. J. Immunol., 36*(4), 842-854.

Bahey-El-Din, M., Casey, P. G., Griffin, B. T., & Gahan, C. G. (2008). Lactococcus lactis-expressing listeriolysin O (LLO) provides protection and specific CD8(+) T cells against Listeria monocytogenes in the murine infection model. *Vaccine, 26*(41), 5304-5314.

Baird, R. W., Bronze, M. S., Kraus, W., Hill, H. R., Veasey, L. G., & Dale, J. B. (1991). Epitopes of group A streptococcal M protein shared with antigens of articular cartilage and synovium. *J. Immunol., 146*(9), 3132-3137.

Banerjee, A., Kim, B. J., Carmona, E. M., Cutting, A. S., Gurney, M. A., Carlos, C., et al. (2011). Bacterial Pili exploit integrin machinery to promote immune activation and efficient blood-brain barrier penetration. *Nat. Commun., 2*, 462.

Batzloff, M. R., Hartas, J., Zeng, W., Jackson, D. C., & Good, M. F. (2006). Intranasal vaccination with a lipopeptide containing a conformationally constrained conserved minimal peptide, a universal T cell epitope, and a self-adjuvanting lipid protects mice from group A streptococcus challenge and reduces throat colonization. *J. Infect. Dis., 194*(3), 325-330.

Baylor, N. W., Egan, W., & Richman, P. (2002). Aluminum salts in vaccines-US perspective. *Vaccine, 20 Suppl 3*, S18-23.

Bermudez-Humaran, L. G., Cortes-Perez, N. G., Le Loir, Y., Alcocer-Gonzalez, J. M., Tamez-Guerra, R. S., de Oca-Luna, R. M., et al. (2004). An inducible surface presentation system improves cellular immunity against human papillomavirus type 16 E7 antigen in mice after nasal administration with recombinant lactococci. *J. Med. Microbiol., 53*(Pt 5), 427-433.

Bermudez-Humaran, L. G., Cortes-Perez, N. G., Lefevre, F., Guimaraes, V., Rabot, S., Alcocer-Gonzalez, J. M., et al. (2005). A novel mucosal vaccine based on live Lactococci expressing E7 antigen and IL-12 induces systemic and mucosal immune responses and protects mice against human papillomavirus type 16-induced tumors. *J. Immunol., 175*(11), 7297-7302.

Bermudez-Humaran, L. G., Kharrat, P., Chatel, J. M., & Langella, P. (2011). Lactococci and lactobacilli as mucosal delivery vectors for therapeutic proteins and DNA vaccines. *Microb. Cell Fact., 30*(10), 1475-2859.

Bermudez-Humaran, L. G., Langella, P., Cortes-Perez, N. G., Gruss, A., Tamez-Guerra, R. S., Oliveira, S. C., et al. (2003). Intranasal immunization with recombinant Lactococcus lactis secreting murine interleukin-12 enhances antigen-specific Th1 cytokine production. *Infect. Immun., 71*(4), 1887-1896.

Bermudez-Humaran, L. G., Langella, P., Miyoshi, A., Gruss, A., Guerra, R. T., Montes de Oca-Luna, R., et al. (2002). Production of human papillomavirus type 16 E7 protein in Lactococcus lactis. *Appl. Environ. Microbiol., 68*(2), 917-922.

Bernhardt, S. L., Gjertsen, M. K., Trachsel, S., Moller, M., Eriksen, J. A., Meo, M., et al. (2006). Telomerase peptide vaccination of patients with non-resectable pancreatic cancer: a dose escalating phase I//II study. *Br. J. Cancer, 95*(11), 1474-1482.

Bessen, D. E. (2009). Population biology of the human restricted pathogen, Streptococcus pyogenes. *Infect. Genet. Evol., 9*(4), 581-593.

Bessen, D. E., & Kalia, A. (2002). Genomic localization of a T serotype locus to a recombinatorial zone encoding extracellular matrix-binding proteins in Streptococcus pyogenes. *Infect. Immun., 70*(3), 1159-1167.

Betancourt, A. A., Delgado, C. A., Estevez, Z. C., Martinez, J. C., Rios, G. V., Aureoles-Rosello, S. R., et al. (2007). Phase I clinical trial in healthy adults of a nasal vaccine candidate containing recombinant hepatitis B surface and core antigens. *Int. J. Infect. Dis., 11*(5), 394-401.

Bhattacharya, S. (2008). The World Health Organization and global smallpox eradication. *J. Epidemiol. Community Health., 62*(10), 909-912.

Black, M., Trent, A., Tirrell, M., & Olive, C. (2010). Advances in the design and delivery of peptide subunit vaccines with a focus on Toll-like receptor agonists. *Expert Rev. Vaccines., 9*(2), 157-173.

Boisgerault, F., Rueda, P., Sun, C. M., Hervas-Stubbs, S., Rojas, M., & Leclerc, C. (2005). Cross-priming of T cell responses by synthetic microspheres carrying a CD8+ T cell epitope requires an adjuvant signal. *J. Immunol., 174*(6), 3432-3439.

Bordet, A. L., Michenet, P., Cohen, C., Arbion, F., Ekindi, N., Bonneau, C., et al. (2001). [Post-vaccination granuloma due to aluminium hydroxide]. *Ann. Pathol., 21*(2), 149-152.

Braat, H., Rottiers, P., Hommes, D. W., Huyghebaert, N., Remaut, E., Remon, J. P., et al. (2006). A phase I trial with transgenic bacteria expressing interleukin-10 in Crohn's disease. *Clin. Gastroenterol Hepatol., 4*(6), 754-759.

Bramwell, V. W., & Perrie, Y. (2005). Particulate delivery systems for vaccines. *Crit Rev Ther Drug Carrier Syst., 22*(2), 151-214.

Bronze, M. S., & Dale, J. B. (1993). Epitopes of streptococcal M proteins that evoke antibodies that cross-react with human brain. *J. Immunol., 151*(5), 2820-2828.

Brunsvig, P., Aamdal, S., Gjertsen, M., Kvalheim, G., Markowski-Grimsrud, C., Sve, I., et al. (2006). Telomerase peptide vaccination: a phase I/II study in patients with non-small cell lung cancer. *Cancer Immunol. Immunother., 55*(12), 1553-1564.

Buccato, S., Maione, D., Rinaudo, C. D., Volpini, G., Taddei, A. R., Rosini, R., et al. (2006). Use of Lactococcus lactis expressing pili from group B Streptococcus as a broad-coverage vaccine against streptococcal disease. *J. Infect. Dis., 194*(3), 331-340.

Byington, C. L., Yvonne A. Maldonado, Y. A., Elizabeth D. Barnett, E. D., Davies, H. D., Kathryn M. Edwards, K. M., Mary Anne Jackson, M. A., et al. (2015). Recommended Childhood and Adolescent Immunization Schedule-United States, 2015. *Pediatrics, 135*(2),

Calmette, A. (1931). Preventive Vaccination Against Tuberculosis with BCG. *J. R. Soc. Med., 24*(11), 1481-1490.

Carapetis, J. R., Steer, A. C., Mulholland, E. K., & Weber, M. (2005). The global burden of group A streptococcal diseases. *Lancet Infect. Dis., 5*(11), 685-694.

Casalta, E., & Montel, M. C. (2008). Safety assessment of dairy microorganisms: the Lactococcus genus. *Int. J. Food Microbiol., 126*(3), 271-273.

Celis, E. (2002). Getting peptide vaccines to work: just a matter of quality control? *J. Clin. Invest., 110*(12), 1765-1768.

Chaplin, D. D. (2010). Overview of the immune response. *J. Allergy Clin. Immunol., 125*(2 Suppl 2), S3-23.

Charpilienne, A., Nejmeddine, M., Berois, M., Parez, N., Neumann, E., Hewat, E., et al. (2001). Individual rotavirus-like particles containing 120 molecules of fluorescent protein are visible in living cells. *J Biol Chem, 276*(31), 29361-29367.

Cheun, H. I., Kawamoto, K., Hiramatsu, M., Tamaoki, H., Shirahata, T., Igimi, S., et al. (2004). Protective immunity of SpaA-antigen producing Lactococcus lactis against Erysipelothrix rhusiopathiae infection. *J. Appl. Microbiol.*, *96*(6), 1347-1353.

Cody, C. L., Baraff, L. J., Cherry, J. D., Marcy, S. M., & Manclark, C. R. (1981). Nature and rates of adverse reactions associated with DTP and DT immunizations in infants and children. *Pediatrics*, *68*(5), 650-660.

Cohen, S., Yoshioka, T., Lucarelli, M., Hwang, L. H., & Langer, R. (1991). Controlled delivery systems for proteins based on poly(lactic/glycolic acid) microspheres. *Pharm. Res.*, *8*(6), 713-720.

Cortes-Perez, N. G., Bermudez-Humaran, L. G., Le Loir, Y., Rodriguez-Padilla, C., Gruss, A., Saucedo-Cardenas, O., et al. (2003). Mice immunization with live lactococci displaying a surface anchored HPV-16 E7 oncoprotein. *FEMS Microbiol. Lett.*, *229*(1), 37-42.

Crotty Alexander, L. E., Maisey, H. C., Timmer, A. M., Rooijakkers, S. H., Gallo, R. L., von Kockritz-Blickwede, M., et al. (2010). M1T1 group A streptococcal pili promote epithelial colonization but diminish systemic virulence through neutrophil extracellular entrapment. *J Mol Med (Berl)*, *88*(4), 371-381.

Cunningham, M. W. (2000). Pathogenesis of group A streptococcal infections. *Clin Microbiol Rev*, *13*(3), 470-511.

Czerkinsky, C., Anjuere, F., McGhee, J. R., George-Chandy, A., Holmgren, J., Kieny, M. P., et al. (1999). Mucosal immunity and tolerance: relevance to vaccine development. *Immunol Rev*, *170*, 197-222.

Dale, J. B., & Beachey, E. H. (1982). Protective antigenic determinant of streptococcal M protein shared with sarcolemmal membrane protein of human heart. *J Exp Med*, *156*(4), 1165-1176.

Dalmia, N., & Ramsay, A. J. (2012). Prime-boost approaches to tuberculosis vaccine development. *Expert Rev. Vaccines., 11*(10), 1221-1233.

Dalsgaard, K. (1974). Saponin adjuvants. 3. Isolation of a substance from Quillaja saponaria Molina with adjuvant activity in food-and-mouth disease vaccines. *Arch Gesamte Virusforsch, 44*(3), 243-254.

Daniel, C., Sebbane, F., Poiret, S., Goudercourt, D., Dewulf, J., Mullet, C., et al. (2009). Protection against Yersinia pseudotuberculosis infection conferred by a Lactococcus lactis mucosal delivery vector secreting LcrV. *Vaccine, 27*(8), 1141-1144.

Davidson, N. J., Leach, M. W., Fort, M. M., Thompson-Snipes, L., Kuhn, R., Muller, W., et al. (1996). T helper cell 1-type CD4+ T cells, but not B cells, mediate colitis in interleukin 10-deficient mice. *J Exp Med, 184*(1), 241-251.

de Vos, W. M. (1999). Gene expression systems for lactic acid bacteria. *Curr Opin Microbiol, 2*(3), 289-295.

Decker, M. D., Edwards, K. M., Steinhoff, M. C., Rennels, M. B., Pichichero, M. E., Englund, J. A., et al. (1995). Comparison of 13 acellular pertussis vaccines: adverse reactions. *Pediatrics, 96*(3 Pt 2), 557-566.

Diminsky, D., Moav, N., Gorecki, M., & Barenholz, Y. (1999). Physical, chemical and immunological stability of CHO-derived hepatitis B surface antigen (HBsAg) particles. *Vaccine, 18*(1-2), 3-17.

Doherty, T. M., Olsen, A. W., van Pinxteren, L., & Andersen, P. (2002). Oral Vaccination with Subunit Vaccines Protects Animals against Aerosol Infection with Mycobacterium tuberculosis. *Infect Immun, 70*(6), 3111-3121.

Douce, G., Turcotte, C., Cropley, I., Roberts, M., Pizza, M., Domenghini, M., et al. (1995). Mutants of Escherichia coli heat-labile toxin lacking ADP-ribosyltransferase activity act as nontoxic, mucosal adjuvants. *Proc. Natl. Acad. Sci. USA, 92*(5), 1644-1648.

Duguid, J. P., Smith, I. W., Dempster, G., & Edmunds, P. N. (1955). Non-flagellar filamentous appendages (fimbriae) and haemagglutinating activity in Bacterium coli. *J Pathol Bacteriol, 70*(2), 335-348.

Edelman, R. (1980). Vaccine adjuvants. *Rev Infect Dis, 2*(3), 370-383.

Ehreth, J. (2003). The value of vaccination: a global perspective. *Vaccine, 21*(27-30), 4105-4117.

Eldridge, J. H., Staas, J. K., Meulbroek, J. A., McGhee, J. R., Tice, T. R., & Gilley, R. M. (1991). Biodegradable microspheres as a vaccine delivery system. *Mol Immunol, 28*(3), 287-294.

Ellis, R. W. (1999). New technologies for making vaccines. *Vaccine, 17*(13–14), 1596-1604.

Esparza, I., & Kissel, T. (1992). Parameters affecting the immunogenicity of microencapsulated tetanus toxoid. *Vaccine, 10*(10), 714-720.

Falugi, F., Zingaretti, C., Pinto, V., Mariani, M., Amodeo, L., Manetti, A. G., et al. (2008). Sequence variation in group A Streptococcus pili and association of pilus backbone types with lancefield T serotypes. *J Infect Dis, 198*(12), 1834-1841.

Fang, J.-H., & Hora, M. (2000). The Adjuvant MF59: A 10-Year Perspective Gary Ott, Ramachandran Radhakrishnan. In D. O'Hagan (Ed.), *Vaccine Adjuvants* (Vol. 42, pp. 211-228): Springer New York.

Felnerova, D., Viret, J. F., Gluck, R., & Moser, C. (2004). Liposomes and virosomes as delivery systems for antigens, nucleic acids and drugs. *Curr Opin Biotechnol, 15*(6), 518-529.

Ferretti, J. J., McShan, W. M., Ajdic, D., Savic, D. J., Savic, G., Lyon, K., et al. (2001). Complete genome sequence of an M1 strain of Streptococcus pyogenes. *Proc. Natl. Acad. Sci. USA, 98*(8), 4658-4663.

Fischetti, V. A. (1989). Streptococcal M protein: molecular design and biological behavior. *Clin. Microbiol. Rev., 2*(3), 285-314.

Foged, C., Hansen, J., & Agger, E. M. (2012). License to kill: Formulation requirements for optimal priming of CD8(+) CTL responses with particulate vaccine delivery systems. *Eur J Pharm Sci, 45*(4), 482-491.

Freund, J. (1956). The mode of action of immunologic adjuvants. *Bibl Tuberc, 10*, 130-148.

Frossard, C. P., Steidler, L., & Eigenmann, P. A. (2007). Oral administration of an IL-10-secreting Lactococcus lactis strain prevents food-induced IgE sensitization. *J. Allergy Clin. Immunol., 119*(4), 952-959.

Froude, J., Gibofsky, A., Buskirk, D. R., Khanna, A., & Zabriskie, J. B. (1989). Cross-reactivity between streptococcus and human tissue: a model of molecular mimicry and autoimmunity. *Curr Top Microbiol Immunol, 145*, 5-26.

Fukushima, A., Yamaguchi, T., Ishida, W., Fukata, K., Taniguchi, T., Liu, F. T., et al. (2006). Genetic background determines susceptibility to experimental immune-mediated blepharoconjunctivitis: comparison of Balb/c and C57BL/6 mice. *Exp Eye Res, 82*(2), 210-218.

Furione, M., Guillot, S., Otelea, D., Balanant, J., Candrea, A., & Crainic, R. (1993). Polioviruses with natural recombinant genomes isolated from vaccine-associated paralytic poliomyelitis. *Virology, 196*(1), 199-208.

Garcea, R. L., & Gissmann, L. (2004). Virus-like particles as vaccines and vessels for the delivery of small molecules. *Curr Opin Biotechnol, 15*(6), 513-517.

Georgescu, M. M., Balanant, J., Macadam, A., Otelea, D., Combiescu, M., Combiescu, A. A., et al. (1997). Evolution of the Sabin type 1 poliovirus in humans: characterization of strains isolated from patients with vaccine-associated paralytic poliomyelitis. *J Virol, 71*(10), 7758-7768.

Germann, T., Bongartz, M., Dlugonska, H., Hess, H., Schmitt, E., Kolbe, L., et al. (1995). Interleukin-12 profoundly up-regulates the synthesis of antigen-specific complement-fixing IgG2a, IgG2b and IgG3 antibody subclasses in vivo. *Eur. J. Immunol, 25*(3), 823-829.

Gilbert, C., Robinson, K., Le Page, R. W., & Wells, J. M. (2000). Heterologous expression of an immunogenic pneumococcal type 3 capsular polysaccharide in Lactococcus lactis. *Infect Immun, 68*(6), 3251-3260.

Glenny, A. T., & Barr, M. (1931). The precipitation of diphtheria toxoid by potash alum. *Pathol., 34*(2), 131-138.

Grangette, C., Muller-Alouf, H., Geoffroy, M., Goudercourt, D., Turneer, M., & Mercenier, A. (2002). Protection against tetanus toxin after intragastric administration of two recombinant lactic acid bacteria: impact of strain viability and in vivo persistence. *Vaccine, 20*(27-28), 3304-3309.

Greco, D., Salmaso, S., Mastrantonio, P., Giuliano, M., Tozzi, A. E., Anemona, A., et al. (1996). A controlled trial of two acellular vaccines and one whole-cell vaccine against pertussis. Progetto Pertosse Working Group. *N Engl J Med, 334*(6), 341-348.

Gruzza, M., Fons, M., Ouriet, M. F., Duval-Iflah, Y., & Ducluzeau, R. (1994). Study of gene transfer in vitro and in the digestive tract of gnotobiotic mice from Lactococcus lactis strains to various strains belonging to human intestinal flora. *Microb Releases, 2*(4), 183-189.

Gupta, R. K., & Relyveld, E. H. (1991). Adverse reactions after injection of adsorbed diphtheria-pertussis-tetanus (DPT) vaccine are not due only to pertussis organisms or pertussis components in the vaccine. *Vaccine, 9*(10), 699-702.

Gupta, R. K., Relyveld, E. H., Lindblad, E. B., Bizzini, B., Ben-Efraim, S., & Gupta, C. K. (1993). Adjuvants — a balance between toxicity and adjuvanticity. *Vaccine, 11*(3), 293-306.

Hammarlund, E., Lewis, M. W., Hansen, S. G., Strelow, L. I., Nelson, J. A., Sexton, G. J., et al. (2003). Duration of antiviral immunity after smallpox vaccination. *Nat Med, 9*(9), 1131-1137.

Haniuda, K., Nojima, T., Ohyama, K., & Kitamura, D. (2011). Tolerance induction of IgG+ memory B cells by T cell-independent type II antigens. *J Immunol, 186*(10), 5620-5628.

Hanniffy, S. B., Carter, A. T., Hitchin, E., & Wells, J. M. (2007). Mucosal delivery of a pneumococcal vaccine using Lactococcus lactis affords protection against respiratory infection. *J Infect Dis, 195*(2), 185-193.

Heath, T. D., Edwards, D. C., & Ryman, B. E. (1976). The adjuvant properties of liposomes. *Biochem Soc Trans, 4*(1), 129-133.

Holmgren, J., & Czerkinsky, C. (2005). Mucosal immunity and vaccines. *Nat Med, 11*(4 Suppl), S45-53.

Hu, C. X., Xu, Z. R., Li, W. F., Niu, D., Lu, P., & Fu, L. L. (2009). Secretory expression of K88 (F4) fimbrial adhesin FaeG by recombinant Lactococcus lactis for oral vaccination and its protective immune response in mice. *Biotechnol Lett, 31*(7), 991-997.

Hutchings, A. B., Helander, A., Silvey, K. J., Chandran, K., Lucas, W. T., Nibert, M. L., et al. (2004). Secretory immunoglobulin A antibodies against the sigma1 outer capsid protein of reovirus type 1 Lang prevent infection of mouse Peyer's patches. *J Virol, 78*(2), 947-957.

Johnson, A. G., Gaines, S., & Landy, M. (1956). Studies on the O antigen of Salmonella typhosa. V. Enhancement of antibody response to protein antigens by the purified lipopolysaccharide. *J Exp Med, 103*(2), 225-246.

Jon, O., Fen, Y., & Kemp, B. C. (2010). A synthetic peptide vaccine directed against the 2ß2-2ß3 loop of domain 2 of protective antigen protects rabbits from inhalation anthrax. *J Immunol, 185*(6), 3661-3668.

Kang, H. J., Coulibaly, F., Clow, F., Proft, T., & Baker, E. N. (2007). Stabilizing isopeptide bonds revealed in gram-positive bacterial pilus structure. *Science, 318*(5856), 1625-1628.

Katre, N. (2004). Liposome-based depot injection technologies. *Am. j. drug deliv. ther., 2*(4), 213-227.

Kaufmann, S. H. (2007). The contribution of immunology to the rational design of novel antibacterial vaccines. *Nat Rev Microbiol, 5*(7), 491-504.

Kensil, C. R. (1996). Saponins as vaccine adjuvants. *Crit Rev Ther Drug Carrier Syst, 13*(1-2), 1-55.

Kieronczyk, A., Skeie, S., Langsrud, T., & Yvon, M. (2003). Cooperation between Lactococcus lactis and nonstarter lactobacilli in the formation of cheese aroma from amino acids. *Appl Environ Microbiol, 69*(2), 734-739.

Kim, S. J., Lee, J. Y., Jun, D. Y., Song, J. Y., Lee, W. K., Cho, M. J., et al. (2009). Oral administration of Lactococcus lactis expressing Helicobacter pylori Cag7-ct383 protein induces systemic anti-Cag7 immune response in mice. *FEMS Immunol Med Microbiol, 57*(3), 257-268.

Kimoto, H., Mizumachi, K., Okamoto, T., & Kurisaki, J. (2004). New Lactococcus strain with immunomodulatory activity: enhancement of Th1-type immune response. *Microbiol Immunol, 48*(2), 75-82.

Kolesanova, E. F., Sanzhakov, M. A., & Kharybin, O. N. (2013). Development of the Schedule for Multiple Parallel "Difficult" Peptide Synthesis on Pins. *Int J Pept, 2013*, 9 pages.

Kotani, S., Watanabe, Y., Shimono, T., Narita, T., & Kato, K. (1975). Immunoadjuvant activities of cell walls, their water-soluble fractions and peptidoglycan subunits, prepared from various gram-positive bacteria, and of synthetic n-acetylmuramyl peptides. *Z Immunitatsforsch Exp Klin Immunol, 149*(2-4), 302-319.

Koutsky, L. A., Ault, K. A., Wheeler, C. M., Brown, D. R., Barr, E., Alvarez, F. B., et al. (2002). A Controlled Trial of a Human Papillomavirus Type 16 Vaccine. *N. Engl. J. Med., 347*(21), 1645-1651.

Kramp, W. J., Six, H. R., & Kasel, J. A. (1982). Postimmunization Clearance of Liposome Entrapped Adenovirus Type 5 Hexon. *Exp. Biol. Med., 169*(1), 135-139.

Kratovac, Z., Manoharan, A., Luo, F., Lizano, S., & Bessen, D. E. (2007). Population genetics and linkage analysis of loci within the FCT region of Streptococcus pyogenes. *J Bacteriol, 189*(4), 1299-1310.

Kreikemeyer, B., Nakata, M., Oehmcke, S., Gschwendtner, C., Normann, J., & Podbielski, A. (2005). Streptococcus pyogenes collagen type I-binding Cpa surface protein. Expression profile, binding characteristics, biological functions, and potential clinical impact. *J. Biol. Chem, 280*(39), 33228-33239.

Kuno-Sakai, H., & Kimura, M. (2004). Safety and efficacy of acellular pertussis vaccine in Japan, evaluated by 23 years of its use for routine immunization. *Pediatr Int, 46*(6), 650-655.

Kyte, J., Trachsel, S., Risberg, B., thor Straten, P., Lislerud, K., & Gaudernack, G. (2009). Unconventional cytokine profiles and development of T cell memory in long-term survivors after cancer vaccination. *Cancer Immunol. Immunother., 58*(10), 1609-1626.

Lamm, M. E. (1997). Interaction of antigens and antibodies at mucosal surfaces. *Annu Rev Microbiol, 51*, 311-340.

Lancefield, R. C. (1933). A SEROLOGICAL DIFFERENTIATION OF HUMAN AND OTHER GROUPS OF HEMOLYTIC STREPTOCOCCI. *J. Exp. Med., 57*(4), 571-595.

Lancefield, R. C. (1940). Type-Specific Antigens, M and T, of Matt and Glossy Variants of Group a Hemolytic Streptococci. *J. Exp. Med., 71*(4), 521-537.

Lange, C., Yew, W. W., Migliori, G. B., & Raviglione, M. (2010). The European Respiratory Journal targets tuberculosis. *Eur. Respir. J., 36*(4), 714-715.

Lechmann, M., Murata, K., Satoi, J., Vergalla, J., Baumert, T. F., & Liang, T. J. (2001). Hepatitis C virus-like particles induce virus-specific humoral and cellular immune responses in mice. *Hepatology, 34*(2), 417-423.

Lee, J. L., Naguwa, S. M., Cheema, G. S., & Gershwin, M. E. (2009). Acute rheumatic fever and its consequences: a persistent threat to developing nations in the 21st century. *Autoimmun Rev, 9*(2), 117-123.

Lee, M. H., Roussel, Y., Wilks, M., & Tabaqchali, S. (2001). Expression of Helicobacter pylori urease subunit B gene in Lactococcus lactis MG1363 and its use as a vaccine delivery system against H. pylori infection in mice. *Vaccine, 19*(28-29), 3927-3935.

Levine, M. M., & Sztein, M. B. (2004). Vaccine development strategies for improving immunization: the role of modern immunology. *Nat Immunol, 5*(5), 460-464.

Li, W., Joshi, M., Singhania, S., Ramsey, K., & Murthy, A. (2014). Peptide Vaccine: Progress and Challenges. *Vaccines, 2*(3), 515.

Lieberman, J. (2010). Anatomy of a murder: how cytotoxic T cells and NK cells are activated, develop, and eliminate their targets. *Immunol Rev, 235*(1), 5-9.

Linke, C. (2010). *Structural characterisation of adhesins from the human pathogen Streptococcus pyogenes*. University of Auckland, Auckland.

Linke, C., Young, P. G., Kang, H. J., Bunker, R. D., Middleditch, M. J., Caradoc-Davies, T. T., et al. (2010). Crystal structure of the minor pilin FctB reveals determinants of Group A streptococcal pilus anchoring. *J Biol Chem, 285*(26), 20381-20389.

Liu, Y., McNevin, J., Zhao, H., Tebit, D. M., Troyer, R. M., McSweyn, M., et al. (2007). Evolution of human immunodeficiency virus type 1 cytotoxic T-lymphocyte epitopes: fitness-balanced escape. *J Virol, 81*(22), 12179-12188.

Luan, J., Zhuang, Z., Liu, Y., Yun, K., Chen, M., & Wang, P. G. (2010). Expression of EspA in Lactococcus lactis NZ9000 and the detection of its immune effect in vivo and vitro. *Immunopharmacol Immunotoxicol, 32*(1), 133-140.

Macpherson, A. J., McCoy, K. D., Johansen, F. E., & Brandtzaeg, P. (2008). The immune geography of IgA induction and function. *Mucosal Immunol, 1*(1), 11-22.

Manetti, A. G., Zingaretti, C., Falugi, F., Capo, S., Bombaci, M., Bagnoli, F., et al. (2007). Streptococcus pyogenes pili promote pharyngeal cell adhesion and biofilm formation. *Mol. Microbiol., 64*(4), 968-983.

Mannam, P., Jones, K. F., & Geller, B. L. (2004). Mucosal vaccine made from live, recombinant Lactococcus lactis protects mice against pharyngeal infection with Streptococcus pyogenes. *Infect Immun, 72*(6), 3444-3450.

Marrack, P., McKee, A. S., & Munks, M. W. (2009). Towards an understanding of the adjuvant action of aluminium. *Nat. Rev. Immunol., 9*(4), 287-293.

Marshall, C. S., Cheng, A. C., Markey, P. G., Towers, R. J., Richardson, L. J., Fagan, P. K., et al. (2011). Acute post-streptococcal glomerulonephritis in the Northern Territory of Australia: a review of 16 years data and comparison with the literature. *Am J Trop Med Hyg, 85*(4), 703-710.

Marx, P. A., Compans, R. W., Gettie, A., Staas, J. K., Gilley, R. M., Mulligan, M. J., et al. (1993). Protection against vaginal SIV transmission with microencapsulated vaccine. *Science, 260* (5112), 1323-1327.

Massilamany, C., Huber, S. A., Cunningham, M. W., & Reddy, J. (2014). Relevance of molecular mimicry in the mediation of infectious myocarditis. *J. Cardiovasc. Transl. Res., 7*(2), 165-171.

McCarty, M. (1956). Variation in the group-specific carbohydrate of group A streptococci. II. Studies on the chemical basis for serological specificity of the carbohydrates. *J Exp Med, 104*(5), 629-643.

McElrath, M. J. (1995). Selection of potent immunological adjuvants for vaccine construction. *Semin Cancer Biol., 6*(6), 375-385.

McHeyzer-Williams, M., Okitsu, S., Wang, N., & McHeyzer-Williams, L. (2012). Molecular programming of B cell memory [10.1038/nri3128]. *Nat Rev Immunol, 12*(1), 24-34.

McNeil, S. A., Halperin, S. A., Langley, J. M., Smith, B., Warren, A., Sharratt, G. P., et al. (2005). Safety and immunogenicity of 26-valent group a streptococcus vaccine in healthy adult volunteers. *Clin Infect Dis, 41*(8), 1114-1122.

Medina, M., Villena, J., Vintini, E., Hebert, E. M., Raya, R., & Alvarez, S. (2008). Nasal immunization with Lactococcus lactis expressing the pneumococcal protective protein A induces protective immunity in mice. *Infect Immun, 76*(6), 2696-2705.

Metzgar, D., & Zampolli, A. (2011). The M protein of group A Streptococcus is a key virulence factor and a clinically relevant strain identification marker. *Virulence, 2*(5), 402-412.

Miki, K., Nagata, T., Tanaka, T., Kim, Y. H., Uchijima, M., Ohara, N., et al. (2004). Induction of protective cellular immunity against Mycobacterium tuberculosis by recombinant attenuated self-destructing Listeria monocytogenes strains harboring eukaryotic expression plasmids for antigen 85 complex and MPB/MPT51. *Infect Immun, 72*(4), 2014-2021.

Milne, R. J., Lennon, D. R., Stewart, J. M., Vander Hoorn, S., & Scuffham, P. A. (2012). Incidence of acute rheumatic fever in New Zealand children and youth. *J Paediatr Child Health, 48*(8), 685-691.

Miura, K., Orcutt, A. C., Muratova, O. V., Miller, L. H., Saul, A., & Long, C. A. (2008). Development and characterization of a standardized ELISA including a reference serum on each plate to detect antibodies induced by experimental malaria vaccines. *Vaccine, 26*(2), 193-200.

Mogensen, T. H. (2009). Pathogen recognition and inflammatory signaling in innate immune defenses. *Clin Microbiol Rev, 22*(2), 240-273.

Moingeon, P., de Taisne, C., & Almond, J. (2002). Delivery technologies for human vaccines. *Br Med Bull, 62*, 29-44.

Moorthy, G., & Ramasamy, R. (2007). Mucosal immunisation of mice with malaria protein on lactic acid bacterial cell walls. *Vaccine, 25*(18), 3636-3645.

Mora, M., Bensi, G., Capo, S., Falugi, F., Zingaretti, C., Manetti, A. G., et al. (2005). Group A Streptococcus produce pilus-like structures containing protective antigens and Lancefield T antigens. *Proc Natl Acad Sci U S A, 102*(43), 15641-15646.

Morello, E., Bermudez-Humaran, L. G., Llull, D., Sole, V., Miraglio, N., Langella, P., et al. (2008). Lactococcus lactis, an efficient cell factory for recombinant protein production and secretion. *J Mol Microbiol Biotechnol, 14*(1-3), 48-58.

Morris, W., Steinhoff, M. C., & Russell, P. K. (1994). Potential of polymer microencapsulation technology for vaccine innovation. *Vaccine, 12*(1), 5-11.

Moschos, S. A., Bramwell, V. W., Somavarapu, S., & Alpar, H. O. (2004). Adjuvant synergy: The effects of nasal coadministration of adjuvants. *Immunol Cell Biol, 82*(6), 628-637.

Murray, R., Cohen, P., & Hardegree, M. C. (1972). Mineral oil adjuvants: biological and chemical studies. *Ann Allergy, 30*(3), 146-151.

Nardin, E. (2010). The past decade in malaria synthetic peptide vaccine clinical trials. *Hum Vaccin, 6*(1), 27-38.

Neurath, M. F., Finotto, S., & Glimcher, L. H. (2002). The role of Th1/Th2 polarization in mucosal immunity. *Nat. Med, 8*(6), 567-573.

Niers, L. E., Hoekstra, M. O., Timmerman, H. M., van Uden, N. O., de Graaf, P. M., Smits, H. H., et al. (2007). Selection of probiotic bacteria for prevention of allergic diseases: immunomodulation of neonatal dendritic cells. *Clin Exp Immunol, 149*(2), 344-352.

Nkowane, B. M., Wassilak, S. G., Orenstein, W. A., Bart, K. J., Schonberger, L. B., Hinman, A. R., et al. (1987). Vaccine-associated paralytic poliomyelitis. United States: 1973 through 1984. *Jama, 257*(10), 1335-1340.

Norton, P. M., Brown, H. W., Wells, J. M., Macpherson, A. M., Wilson, P. W., & Le Page, R. W. (1996). Factors affecting the immunogenicity of tetanus toxin fragment C expressed in Lactococcus lactis. *FEMS IMMUNOL MED MIC, 14*(2-3), 167-177.

Norton, P. M., Wells, J. M., Brown, H. W., Macpherson, A. M., & Le Page, R. W. (1997). Protection against tetanus toxin in mice nasally immunized with recombinant Lactococcus lactis expressing tetanus toxin fragment C. *Vaccine*, *15*(6-7), 616-619.

O'Hagan, D. T., & De Gregorio, E. (2009). The path to a successful vaccine adjuvant--'the long and winding road'. *Drug Discov Today, 14*(11-12), 541-551.

Ott, G., Barchfeld, G. L., Chernoff, D., Radhakrishnan, R., van Hoogevest, P., & Van Nest, G. (1995). MF59. Design and evaluation of a safe and potent adjuvant for human vaccines. *Pharm Biotechnol, 6*, 277-296.

Park, H. S., & Cleary, P. P. (2005). Active and passive intranasal immunizations with streptococcal surface protein C5a peptidase prevent infection of murine nasal mucosa-associated lymphoid tissue, a functional homologue of human tonsils. *Infect Immun, 73*(12), 7878-7886.

Passàli, D., Lauriello, M., Passàli, G. C., Passàli, F. M., & Bellussi, L. (2007). Group A Streptococcus and its antibiotic resistance. *Acta Otorhinolaryngol Ital., 27*(1), 27-32.

Paul, W. E., & Zhu, J. (2010). How are T(H)2-type immune responses initiated and amplified? *Nat. Rev. Immunol., 10*(4), 225-235.

Pavan, S., Desreumaux, P., & Mercenier, A. (2003). Use of mouse models to evaluate the persistence, safety, and immune modulation capacities of lactic acid bacteria. *Clin Diagn Lab Immunol, 10*(4), 696-701.

Pei, H., Liu, J., Cheng, Y., Sun, C., Wang, C., Lu, Y., et al. (2005). Expression of SARS-coronavirus nucleocapsid protein in Escherichia coli and Lactococcus lactis for serodiagnosis and mucosal vaccination. *Appl Microbiol Biotechnol, 68*(2), 220-227.

Perez-Casal, J., Caparon, M. G., & Scott, J. R. (1991). Mry, a trans-acting positive regulator of the M protein gene of Streptococcus pyogenes with similarity to the receptor proteins of two-component regulatory systems. *J Bacteriol., 173*(8), 2617-2624.

Perez, C. A., Eichwald, C., Burrone, O., & Mendoza, D. (2005). Rotavirus vp7 antigen produced by Lactococcus lactis induces neutralizing antibodies in mice. *J Appl Microbiol, 99*(5), 1158-1164.

Pichichero, M. E. (1996). Acellular pertussis vaccines. Towards an improved safety profile. *Drug Saf, 15*(5), 311-324.

Pichichero, M. E. (1998). Group A beta-hemolytic streptococcal infections. *Pediatr Rev, 19*(9), 291-302.

Pichichero, M. E., Edwards, K. M., Anderson, E. L., Rennels, M. B., Englund, J. A., Yerg, D. E., et al. (2000). Safety and immunogenicity of six acellular pertussis vaccines and one whole-cell pertussis vaccine given as a fifth dose in four- to six-year-old children. *Pediatrics, 105*(1):e11.

Plotkin, S. (2014). History of vaccination. *Proc. Natl. Acad. Sci. USA, 111*(34), 12283-12287.

Plotkin, S. A. (2005). Vaccines: past, present and future. *Nat Med,* 11(4 Suppl):S5-11.

Podbielski, A., Melzer, B., & Lutticken, R. (1991). Application of the polymerase chain reaction to study the M protein(-like) gene family in beta-hemolytic streptococci. *Med Microbiol Immunol, 180*(4), 213-227.

Pontes, D. S., Dorella, F. A., Ribeiro, L. A., Miyoshi, A., Le Loir, Y., Gruss, A., et al. (2003). Induction of partial protection in mice after oral administration of Lactococcus lactis producing Brucella abortus L7/L12 antigen. *J Drug Target, 11*(8-10), 489-493.

Potter, M., & Boyce, C. R. (1962). Induction of Plasma-Cell Neoplasms in Strain BALB/c Mice with Mineral Oil and Mineral Oil Adjuvants [10.1038/1931086a0]. *Nature, 193*(4820), 1086-1087.

Proft, T., & Baker, E. N. (2009). Pili in Gram-negative and Gram-positive bacteria-structure, assembly and their role in disease. *Cell Mol Life Sci, 66*(4), 613-635.

Purcell, A. W., Zeng, W., Mifsud, N. A., Ely, L. K., Macdonald, W. A., & Jackson, D. C. (2003). Dissecting the role of peptides in the immune response: theory, practice and the application to vaccine design. *J. Pept. Sci., 9*(5), 255-281.

Quigley, B. R., Hatkoff, M., Thanassi, D. G., Ouattara, M., Eichenbaum, Z., & Scott, J. R. (2010). A foreign protein incorporated on the Tip of T3 pili in Lactococcus lactis elicits systemic and mucosal immunity. *Infect Immun, 78*(3), 1294-1303.

Radcliff, F. J., Loh, J. M., Ha, B., Schuhbauer, D., McCluskey, J., & Fraser, J. D. (2012). Antigen targeting to major histocompatibility complex class II with streptococcal mitogenic exotoxin Z-2 M1, a superantigen-based vaccine carrier. *Clin Vaccine Immunol, 19*(4), 574-586.

Ramasamy, R., Yasawardena, S., Zomer, A., Venema, G., Kok, J., & Leenhouts, K. (2006). Immunogenicity of a malaria parasite antigen displayed by Lactococcus lactis in oral immunisations. *Vaccine, 24*(18), 3900-3908.

Reed, S. G., Orr, M. T., & Fox, C. B. (2013). Key roles of adjuvants in modern vaccines. *Nat Med, 19*(12), 1597-1608.

Relf, W. A., Cooper, J., Brandt, E. R., Hayman, W. A., Anders, R. F., Pruksakorn, S., et al. (1996). Mapping a conserved conformational epitope from the M protein of group A streptococci. *J Pept Res., 9*(1), 12-20.

Rietschel, E., Wollenweber, H.-W., Zähringer, U., & Lüderitz, O. (1982). Lipid A, the lipid component of bacterial lipopolysaccharides: Relation of chemical structure to biological activity. *Wien Klin Wochenschr, 60*(14), 705-709.

Robinson, J. H., & Kehoe, M. A. (1992). Group A streptococcal M proteins: virulence factors and protective antigens. *Immunol Today, 13*(9), 362-367.

Robinson, K., Chamberlain, L. M., Schofield, K. M., Wells, J. M., & Le Page, R. W. (1997). Oral vaccination of mice against tetanus with recombinant Lactococcus lactis. *Nat Biotechnol, 15*(7), 653-657.

Roche, A. M., Richard, A. L., Rahkola, J. T., Janoff, E. N., & Weiser, J. N. (2015). Antibody blocks acquisition of bacterial colonization through agglutination [Article]. *Mucosal Immunol, 8*(1), 176-185.

Romagnani, S. (1992). Induction of TH1 and TH2 responses: a key role for the 'natural' immune response? *Immunol Today, 13*(10), 379-381.

Sadeyen, J. R., Tourne, S., Shkreli, M., Sizaret, P. Y., & Coursaget, P. (2003). Insertion of a foreign sequence on capsid surface loops of human papillomavirus type 16 virus-like particles reduces their capacity to induce neutralizing antibodies and delineates a conformational neutralizing epitope. *Virology, 309*(1), 32-40.

Scavone, P., Miyoshi, A., Rial, A., Chabalgoity, A., Langella, P., Azevedo, V., et al. (2007). Intranasal immunisation with recombinant Lactococcus lactis displaying either anchored or secreted forms of Proteus mirabilis MrpA fimbrial protein confers specific immune response and induces a significant reduction of kidney bacterial colonisation in mice. *Microbes Infect, 9*(7), 821-828.

Sevil Domenech, V. E., Panthel, K., Meinel, K. M., Winter, S. E., & Russmann, H. (2007). Pre-existing anti-Salmonella vector immunity prevents the development of protective antigen-specific CD8 T-cell frequencies against murine listeriosis. *Microbes Infect, 9*(12-13), 1447-1453.

Shek, P. N., Yung, B. Y., & Stanacev, N. Z. (1983). Comparison between multilamellar and unilamellar liposomes in enhancing antibody formation. *Immunology, 49*(1), 37-44.

Shin, J. H., Park, J. K., Lee, D. H., Quan, F. S., Song, C. S., & Kim, Y. C. (2015). Microneedle Vaccination Elicits Superior Protection and Antibody Response over Intranasal Vaccination against Swine-Origin Influenza A (H1N1) in Mice. *PLoS One, 10*(6), e0130684.

Shive, M. S., & Anderson, J. M. (1997). Biodegradation and biocompatibility of PLA and PLGA microspheres. *Adv Drug Deliv Rev, 28*(1), 5-24.

Shulman, S. T., & Tanz, R. R. (2010). Group A streptococcal pharyngitis and immune-mediated complications: from diagnosis to management. *Expert Rev Anti Infect Ther, 8*(2), 137-150.

Sim, A. C., Lin, W., Tan, G. K., Sim, M. S., Chow, V. T., & Alonso, S. (2008). Induction of neutralizing antibodies against dengue virus type 2 upon mucosal administration of a recombinant *Lactococcus lactis* strain expressing envelope domain III antigen. *Vaccine, 26*(9), 1145-1154.

Sjolander, A., Cox, J. C., & Barr, I. G. (1998). ISCOMs: an adjuvant with multiple functions. *J Leukoc Biol, 64*(6), 713-723.

Smith, A., Perelman, M., & Hinchcliffe, M. (2014). Chitosan: a promising safe and immune-enhancing adjuvant for intranasal vaccines. *Hum Vaccin Immunother, 10*(3), 797-807.

Smith, W. D., Pointon, J. A., Abbot, E., Kang, H. J., Baker, E. N., Hirst, B. H., et al. (2010). Roles of minor pilin subunits Spy0125 and Spy0130 in the serotype M1 Streptococcus pyogenes strain SF370. *J Bacteriol, 192*(18), 4651-4659.

Solares, A. M., Baladron, I., Ramos, T., Valenzuela, C., Borbon, Z., Fanjull, S., et al. (2011). Safety and Immunogenicity of a Human Papillomavirus Peptide Vaccine (CIGB-228) in Women with High-Grade Cervical Intraepithelial Neoplasia: First-in-Human, Proof-of-Concept Trial. *ISRN Obstet. Gynecol. 2011*, 2011:292951.

Stanekova, Z., Kiraly, J., Stropkovska, A., Mikuskova, T., Mucha, V., Kostolansky, F., et al. (2011). Heterosubtypic protective immunity against influenza A virus induced by fusion peptide of the hemagglutinin in comparison to ectodomain of M2 protein. *Acta Virol, 55*(1), 61-67.

Steer, A. C., Law, I., Matatolu, L., Beall, B. W., & Carapetis, J. R. (2009). Global emm type distribution of group A streptococci: systematic review and implications for vaccine development. *Lancet Infect Dis, 9*(10), 611-616.

Steidler, L., Hans, W., Schotte, L., Neirynck, S., Obermeier, F., Falk, W., et al. (2000). Treatment of murine colitis by Lactococcus lactis secreting interleukin-10. *Science, 289*(5483), 1352-1355.

Steidler, L., Neirynck, S., Huyghebaert, N., Snoeck, V., Vermeire, A., Goddeeris, B., et al. (2003). Biological containment of genetically modified Lactococcus lactis for intestinal delivery of human interleukin 10. *Nat Biotechnol, 21*(7), 785-789.

Sutter, R. W., Prevots, D. R., & Cochi, S. L. (2000). Poliovirus vaccines. Progress toward global poliomyelitis eradication and changing routine immunization recommendations in the United States. *Pediatr Clin North Am, 47*(2), 287-308.

Suzuki, C., Kimoto-Nira, H., Kobayashi, M., Nomura, M., Sasaki, K., & Mizumachi, K. (2008). Immunomodulatory and cytotoxic effects of various Lactococcus strains on the murine macrophage cell line J774.1. *Int J Food Microbiol, 123*(1-2), 159-165.

Szmuness, W., Stevens, C. E., Harley, E. J., Zang, E. A., Oleszko, W. R., William, D. C., et al. (1980). Hepatitis B Vaccine. *N. Engl. J. Med, 303*(15), 833-841.

Tabata, Y., & Ikada, Y. (1988). Macrophage phagocytosis of biodegradable microspheres composed of L-lactic acid/glycolic acid homo- and copolymers. *J Biomed Mater Res, 22*(10), 837-858.

Ton-That, H., & Schneewind, O. (2003). Assembly of pili on the surface of Corynebacterium diphtheriae. *Mol Microbiol, 50*(4), 1429-1438.

Trombetta, E. S., & Mellman, I. (2005). Cell biology of antigen processing in vitro and in vivo. *Annu Rev Immunol, 23*, 975-1028.

Trunz, B. B., Fine, P., & Dye, C. (2006). Effect of BCG vaccination on childhood tuberculous meningitis and miliary tuberculosis worldwide: a meta-analysis and assessment of cost-effectiveness. *Lancet, 367*(9517), 1173-1180.

Tsunetsugu-Yokota, Y., Morikawa, Y., Isogai, M., Kawana-Tachikawa, A., Odawara, T., Nakamura, T., et al. (2003). Yeast-derived human immunodeficiency virus type 1 p55(gag) virus-like particles activate dendritic cells (DCs) and induce perforin expression in Gag-specific CD8(+) T cells by cross-presentation of DCs. *J Virol, 77*(19), 10250-10259.

Uchida, K., Akashi, K., Motoshima, H., Urashima, T., Arai, I., & Saito, T. (2009). Microbiota analysis of Caspian Sea yogurt, a ropy fermented milk circulated in Japan. *Anim Sci J, 80*(2), 187-192.

Ulanova, M., Tarkowski, A., Hahn-Zoric, M., & Hanson, L. A. (2001). The Common vaccine adjuvant aluminum hydroxide up-regulates accessory properties of human monocytes via an interleukin-4-dependent mechanism. *Infect Immun, 69*(2), 1151-1159.

Valenzuela, P., Medina, A., Rutter, W. J., Ammerer, G., & Hall, B. D. (1982). Synthesis and assembly of hepatitis B virus surface antigen particles in yeast [10.1038/298347a0]. *Nature, 298*(5872), 347-350.

Vera-Cabrera, L., Rendon, A., Diaz-Rodriguez, M., Handzel, V., & Laszlo, A. (1999). Dot blot assay for detection of antidiacyltrehalose antibodies in tuberculous patients. *Clin Diagn Lab Immunol., 6*(5), 686-689.

Vesa, T., Pochart, P., & Marteau, P. (2000). Pharmacokinetics of Lactobacillus plantarum NCIMB 8826, Lactobacillus fermentum KLD, and Lactococcus lactis MG 1363 in the human gastrointestinal tract. *Aliment Pharmacol Ther, 14*(6), 823-828.

Villena, J., Medina, M., Vintini, E., & Alvarez, S. (2008). Stimulation of respiratory immunity by oral administration of Lactococcus lactis. *Can J Microbiol, 54*(8), 630-638.

Vogel, F. R. (1998). Adjuvants in perspective. *Dev Biol Stand, 92*, 241-248.

Vogel, F. R., & Powell, M. F. (1995). A compendium of vaccine adjuvants and excipients. *Pharm Biotechnol, 6*, 141-228.

Walker, M. J., Barnett, T. C., McArthur, J. D., Cole, J. N., Gillen, C. M., Henningham, A., et al. (2014). Disease manifestations and pathogenic mechanisms of Group A Streptococcus. *Clin Microbiol Rev, 27*(2), 264-301.

Wells, J. M., & Mercenier, A. (2008). Mucosal delivery of therapeutic and prophylactic molecules using lactic acid bacteria. *Nat Rev Microbiol, 6*(5), 349-362.

Wells, J. M., Wilson, P. W., Norton, P. M., Gasson, M. J., & Le Page, R. W. (1993). Lactococcus lactis: high-level expression of tetanus toxin fragment C and protection against lethal challenge. *Mol Microbiol, 8*(6), 1155-1162.

Whatmore, A. M., Kapur, V., Sullivan, D. J., Musser, J. M., & Kehoe, M. A. (1994). Non-congruent relationships between variation in emm gene sequences and the population genetic structure of group A streptococci. *Mol Microbiol, 14*(4), 619-631.

Williamson, D. A., Moreland, N. J., Carter, P., Upton, A., Morgan, J., Proft, T., et al. (2014). Molecular epidemiology of group A streptococcus from pharyngeal isolates in Auckland, New Zealand, 2013. *N. Z. Med. J., 127*(1388), 55-60.

Wilson, M. E., Chen, L. H., & Barnett, E. D. (2004). Yellow Fever Immunizations: Indications and Risks. *Curr Infect Dis Rep, 6*(1), 34-42.

Xin, K. Q., Hoshino, Y., Toda, Y., Igimi, S., Kojima, Y., Jounai, N., et al. (2003). Immunogenicity and protective efficacy of orally administered recombinant Lactococcus lactis expressing surface-bound HIV Env. *Blood, 102*(1), 223-228.

Yam, K. K., Pouliot, P., N'Diaye M. M., Fournier, S., Olivier, M., & Cousineau, B. (2008). Innate inflammatory responses to the Gram-positive bacterium *Lactococcus lactis*. *Vaccine, 26*(22), 2689-2699.

Yanagawa, R., & Otsuki, K. (1970). Some properties of the pili of Corynebacterium renale. *J Bacteriol, 101*(3), 1063-1069.

Yang, M., & Mine, Y. (2009). Novel T-cell epitopes of ovalbumin in BALB/c mouse: potential for peptide-immunotherapy. *Biochem Biophys Res Commun, 378*(2), 203-208.

Young, P. G., Proft, T., Harris, P. W., Brimble, M. A., & Baker, E. N. (2014). Structure and activity of Streptococcus pyogenes SipA: a signal peptidase-like protein essential for pilus polymerisation. *PLoS One, 9*(6), p. e99135

Yuki, Y., & Kiyono, H. (2003). New generation of mucosal adjuvants for the induction of protective immunity. *Rev Med Virol., 13*(5), 293-310.

Yuki, Y., & Kiyono, H. (2009). Mucosal vaccines: novel advances in technology and delivery. *Expert Rev Vaccines, 8*(8), 1083-1097.

Zaman, M., Abdel-Aal, A. B., Fujita, Y., Phillipps, K. S., Batzloff, M. R., Good, M. F., et al. (2012). Immunological evaluation of lipopeptide group A streptococcus (GAS) vaccine: structure-activity relationship. *PLoS One, 7*(1), 12.

Zhang, Z. H., Jiang, P. H., Li, N. J., Shi, M., & Huang, W. (2005). Oral vaccination of mice against rodent malaria with recombinant Lactococcus lactis expressing MSP-1(19). *World J Gastroenterol, 11*(44), 6975-6980.